

This file is part of the following work:

Whalen, Casey (2021) *Characterizing the bacterial community associated with the model alcyoniid Lobophytum pauciflorum*. PhD Thesis, James Cook University.

Access to this file is available from:

<https://doi.org/10.25903/rp59%2Dq233>

Copyright © 2021 Casey Whalen.

The author has certified to JCU that they have made a reasonable effort to gain permission and acknowledge the owners of any third party copyright material included in this document. If you believe that this is not the case, please email

researchonline@jcu.edu.au

Characterizing the Bacterial Community Associated with the Model Alcyoniid *Lobophytum pauciflorum*

Casey Whalen

A dissertation submitted for the degree of

Doctor of Philosophy (PhD)

In Medical and Molecular Biology

James Cook University

College of Public Health, Veterinary and Medical Sciences

May 2021



Acknowledgement of Contribution by Others

I would first like to thank my family for their support throughout this process, and my fellow PhD students who suffered in the fish bowl next to me: Chloe Boote, Ramona Brunner, Beatriz Diaz-Guijarro, Mila Grinblat, Legana Fingerhut, Felicity Kuek, Bruna Pereira Luz, and Jia Zhang. I am also grateful to our post-docs, Dr. Aurelie Moya and Dr. Natalia Andrade-Rodriguez for their time and energy shepherding us through the process. Dr. Roger Huerlimann also went above and beyond in his attentiveness during sequencing prep and analysis, thank you and everybody else who assisted with labwork and analysis. I would not have had samples to sequence if it were not for the amazing team in the field at OIRS, thank you Marta, Bryn and Jimmy for helping us through the long nights of coral spawning. I also want to thank Chris Bligh, without whom our lab would likely be in ruins. I also want to thank Paul O'Brien and Wiebke Wessels for the use of their data for comparative analyses in chapters 2 and 5. Finally I would like to express my gratitude to the Australian Institute of Research Centre of Excellence for Coral Reef Research for this opportunity which would not have been possible without my supervisors, Dr. David Bourne, Dr. Ira Cooke and Dr. David Miller. Thank you DB, especially, for putting the extra time and effort toward seeing this project through to completion.

Research funding:

- James Cook University, Townsville, AU
- Australian Research Council – Centre of Excellence for Coral Reef Studies, Townsville, AU

Supervisory panel\Editing and revision:

- Dr. David Bourne^{3,4}
- Dr. Ira Cooke¹
- Dr. David Miller^{1,2}

Experimental design:

- Dr. David Bourne^{3,4}
- Dr. Aurelie Moya^{1,2}
- Dr. Wiebke Wessels^{1,2}

Volunteers in the field:

- Brayden Cockerell¹
- Lily Donnelly¹

Labwork and bioinformatics:

- Dr. Natalia Andrade-Rodriguez^{1,2}
- Dr. Ira Cooke¹
- Dr. Roger Huerlimann³
- Sandra Infante Villamil³

¹College of Public Health, Medicine and Veterinary Studies - James Cook University, Townsville, Australia

²Australian Research Council – Centre of Excellence for Coral Reef Studies, Townsville, Australia

³College of Science and Engineering, James Cook University, Townsville, Australia

⁴Australian Institute of Marine Sciences, Townsville, Australia

Abstract

The microbiome associated with all Metazoa is an integral component supporting host health and physiology. In Cnidaria, microbial symbionts have been associated with metabolic and signalling pathways and host resilience to disease and environmental change. The rapid decline of coral reefs in recent decades due to disease and climate change resulting from anthropogenic activity has led to an increased research focus on characterizing the bacterial communities associated with coral hosts. Many knowledge gaps remain in the field of cnidarian microbiology, however, especially regarding the Octocorallia. This study characterizes the bacterial community associated with *Lobophytum pauciflorum* in mature colonies (Chapter 2), explores this bacterial diversity across inner tissue, outer tissue and mucus layers as microhabitats (Chapter 3) and follows the bacterial diversity through larval development (Chapter 4). The final data chapter compares bacterial community dynamics with host gene expression (Chapter 5) at 9 time points between fertilization and competency.

The soft leather coral *L. pauciflorum*, family Alcyoniidae, is common in shallow tropical reefs along the Great Barrier Reef, Australia. Agreeing with previous studies on coral-associated Bacteria, the microbiome of *L. pauciflorum* appears to comprise conserved core sequences as well as a more diverse, variable fraction. The core community was dominated by sequences aligning to *Parendoziomonas haliclona* and *Endoziomonas* spp. but some variability in bacterial community diversity was also observed between colonies. The bacterial community associated with *L. pauciflorum* was compared with those of other Octocorallia hosts (*Briareum*, *Cladiella*, *Clavularia*, *Pinnigorgia*, *Sarcophyton*, *Sinularia*, *Xenia*), which showed similarity in their association with Endoziomonadaceae. The results show that *L. pauciflorum* hosts a species-specific bacterial community that has both similarities and differences to those of other octocorallian hosts.

The mucus, tissue and skeleton form distinct microhabitats in Scleractinia, but the anatomical differences between Scleractinia and Octocorallia suggest that these taxa could potentially have very different bacterial community structures. Chapter 3 characterized the Bacteria associated with inner tissue, outer tissue and mucus layers as three potentially distinct microhabitats in *L. pauciflorum*. The microbiome of the mucus layer was clearly distinct and more diverse than those of the tissue layers, and was dominated by Cyanobacteria, Francisellaceae, Planctomycetes and Verrucomicrobia. The tissue layers hosted similar communities, dominated by Endoziomonadaceae and other common coral-associated taxa such as Shewinellaceae and Terasakiellaceae. Putative functional analysis suggested that the bacteria associated with tissues and mucus in *L. pauciflorum* perform distinct functions in the holobiont. Due to the importance of the compartmentalization of Bacteria to host physiology in other Cnidaria, additional studies are recommended to examine the potential for

localisation of bacterial communities in distinct microhabitats of soft coral through microscopic and imaging approaches.

Little is known about the onset and establishment of bacteria on developing coral larvae and no studies have investigated bacterial community development in octocoral larvae. To begin this investigation, chapter 4 analyzed the bacteria associated with *L. pauciflorum* larvae at 9 time points between 6 and 210 hours post-fertilization (hpf). At least 2 stages of community succession were apparent, an “early” stage (6 – 48 hpf) and a “late” stage (72-210 hpf), and by 210 hpf all larvae expressed competency and showed a distinct microbial community. The early stage was dominated by Alteromonadaceae and Pseudoalteromonadaceae, both of which have demonstrated antimicrobial properties and have been detected in association with scleractinian larvae. The late stage was dominated by Sphingomonadaceae, Comamonadaceae and Burkholderiaceae, taxa also commonly associated with corals. Francisellaceae become dominant at the transition point between the early and late stages (i.e. the sample points before and after 48 hpf) though were in low relative abundance or absent from samples taken before 36 hpf or after 72 hpf. By 210 hpf, common *L. pauciflorum* associates were detected including the families Endozoicomonadaceae and Shewinellaceae. The results of this study show that there is a complex pattern of community succession in developing soft coral larvae. Future studies should test whether this pattern of succession is repeatable in Alcyoniidae, and how it is influenced by environmental stressors expected in the near future.

The observed change in community structure indicates a response to post-gastrulation physiological factors or, potentially, the expression of antimicrobial peptides (AMPs) as the larvae develops. The potential for AMP mediation of the bacterial community development on *L. pauciflorum* larvae, as observed in *Hydra*, was explored through host transcriptomics and bioinformatics (Chapter 5). A previous study in our lab (Wessels 2016) produced *de novo* assembled transcriptomes of *L. pauciflorum* larvae sampled at 6 time points between fertilization and competency (16, 27, 36, 48, 96 and 193 hpf). The larval transcriptomes were analyzed in Chapter 5 of this study, scanned for candidate AMPs with the R package AMPiR and aligned to known Cnidarian antimicrobial proteins obtained from GenBank (search terms: “defensin”, “Kazal-type” and “antimicrobial peptide”; source organism: “Cnidaria”). The R package mFuzz was then used to cluster homologs by differential expression profile. The results of these analyses suggest that *L. pauciflorum* may produce homologs of the known cnidarian antimicrobial peptides aurelin, hydramacin and periculin, and Kazal-domain containing proteins. While diverse, Kazal-type proteins can also exhibit antibacterial activity through serine protease inhibition in animal hosts such as *Hydra*. The differential expression pattern of most predicted and known AMP and Kazal-type homologs, was distinct between samples before 48 hpf and after 72 hpf, consistent with the observed shift from “early”- to “late”-stage bacterial communities

(Chapter 4). While physiological developments such as gastrulation probably also play a role in the patterns observed in bacterial community composition and transcriptomics, this study indicates that antimicrobial peptides – some of which are shared among other cnidarian taxa – may help shape the onset and development of the bacterial community in *L. pauciflorum* larvae.

The comprehensive set of data chapters associated with this doctoral dissertation describes a complex community of bacteria as it develops from fertilization through to larval competency, in mature healthy adult colonies, and within 3 microhabitats in *L. pauciflorum*. As an emerging model alcyoniid for genomics and transcriptomics, the work described in this dissertation provides further context for *L. pauciflorum* as a model organism for the study of soft coral-associated bacteria. Future studies must address the function of the associated bacteria in the holobiont, and this is especially important for commonly reported strains such as *Endozoicomonas* spp. and *Vibrio* spp. These functional attributes likely include nutrient exchange with the host and establishing molecular mechanisms of information exchange between host and symbiont. To this end it is also important that studies further explore the biological role of antimicrobial peptides in soft corals and in coral larvae rather than just pharmaceutical application. For coral reef conservation to succeed, the host-symbiont interplay must be elucidated as it may underpin the resilience of corals to changing environmental conditions.

Table of Contents

List of Tables	xi
List of Figures	xii
Chapter 1: The coral holobiont	1
1.1 The microbiome	2
1.2 Cnidaria as hosts	3
1.2.1 Model Cnidaria – the <i>Hydrozoa</i>	3
1.3 The coral holobiont	4
1.3.1 Coral-associated microbiota	4
1.3.2 Coral-associated Bacteria	5
1.3.3 Factors shaping the coral holobiont	5
1.3.3.1 Internal factors influencing holobiont structure	5
1.3.3.2 External factors influencing holobiont structure	7
1.3.4 Bacteria associated with Scleractinia	8
1.3.4.1 The role of the coral mucus layer	8
1.3.4.2 Coral tissue as a microhabitat	9
1.3.4.3 Coral skeleton as a microhabitat	9
1.3.5 Bacteria associated with Octocorallia	10
1.4 Objectives	10
1.6 Structure of dissertation	11
Chapter 2: Bacterial Diversity Associated with the Soft Leather Coral <i>Lobophytum pauciflorum</i>	13
2.1 Introduction	14
2.2 Methods	16
2.2.1 Sample collection	16
2.2.2 DNA isolation and amplification	16
2.2.3 Next-generation sequencing of 16S rRNA	17
2.2.4 16S rRNA gene sequence analysis	17
2.2.5 Comparison with other available datasets	19
2.3 Results	20
2.3.1 Alpha diversity in <i>L. pauciflorum</i>	20
2.3.2 Composition of the 16S rRNA gene community in <i>L. pauciflorum</i>	20
2.3.3 Ubiquitously distributed ASVs recovered from <i>L. pauciflorum</i>	22
2.3.4 Comparison with other available datasets	25
2.3.5 Endozoicomonadaceae	29
2.3.6 Spirochaetaceae	31

2.4	Discussion	32
2.4.1	The bacterial community of <i>L. pauciflorum</i>	32
2.4.2	Variability between colonies of <i>L. pauciflorum</i>	34
2.4.3	Conclusion	36
Chapter 3: Bacterial communities in microhabitats of the Alcyoniidae <i>Lobophytum pauciflorum</i>		37
3.1	Introduction	38
3.2	Methods	41
3.2.1	Sample collection	41
3.2.2	Sample preparation for histology	41
3.2.3	DNA isolation and 16S rRNA gene amplification	41
3.2.4	Next-generation sequencing of 16S rRNA	42
3.2.5	Bioinformatics	42
3.3	Results	43
3.3.1	Histology	43
3.3.2	Alpha and beta diversity	44
3.3.3	Bacterial community composition of host microhabitats	46
3.3.4	Phylogeny of Endozoicomonadaceae	50
3.3.5	Putative biological characteristics associated with distinct microhabitats	50
3.4	Discussion	52
3.4.1	The mucus layer hosts a distinct community of associated bacteria	54
3.4.2	The tissue layers host similar bacterial communities	55
3.4.3	Putative biological characteristics associated with distinct microhabitats	56
3.4.4	Conclusion	57
Chapter 4: <i>Lobophytum pauciflorum</i> larva-associated bacteria from fertilization to competency		59
4.1	Introduction	60
4.2	Methods	62
4.2.1	Spawning of <i>L. pauciflorum</i>	62
4.2.2	Sample collection	63
4.2.3	DNA isolation and amplification	64
4.2.4	16S rRNA gene sequencing	65
4.2.5	Analysis of 16S rRNA gene sequences communities	65
4.3	Results	66
4.3.1	16S rRNA gene sequencing and data processing	66
4.3.2	Bacterial community composition during the first 210 hours of life	66
4.3.3	Stages of community succession	69
4.3.4	Alignment to BLAST hits	71

4.3.5	Analysis of a contaminated blank	72
4.4	Discussion	73
4.4.1	Phases of community development	73
I	Early Stage	73
II	Early stage – transition	74
III	Late Stage – 72 hpf to 210 hpf	75
IV	Competency – by 210 hpf	76
4.4.2	Conclusion	76
Chapter 5: Differential expression of genes encoding AMP and Kazal-domain proteins may influence bacterial community development in <i>L. pauciflorum</i> larvae		78
5.1	Introduction	79
5.2	Methods	81
5.2.1	Acquisition of available transcript data	81
5.2.2	Read alignment and quantification	82
5.2.3	Predictive package AMPiR	83
5.2.4	Cnidarian AMP homology	83
5.3	Results	83
5.3.1	Sequencing and assembly	83
5.3.2	AMPiR predicted AMPs	85
5.3.3	Homology of cnidarian AMPs and defensins from literature	86
5.3.3.1	Protein homologs in <i>L. pauciflorum</i>	86
5.3.3.2	Nucleotide sequence homologs in <i>L. pauciflorum</i>	89
5.3.4	Differential expression of homologs in <i>L. pauciflorum</i> larvae	90
5.4	Discussion	92
5.4.1	AMPs in <i>L. pauciflorum</i> predicted by AMPiR	93
5.4.2	Candidate homologs of antimicrobial peptides	94
5.4.3	Kazal-type protein homologs	94
5.4.4	Differential expression in <i>L. pauciflorum</i> larvae	95
5.4.5	Conclusion	96
Chapter 6: Development and structure of the bacterial community associated with the soft leather coral <i>Lobophytum pauciflorum</i>		97
6.1	The holobiont <i>L. pauciflorum</i> : community structure	98
6.1.1	Bacteria associated with soft corals	98
6.1.2	The baseline community of <i>L. pauciflorum</i> is flexible	99
6.1.2.1	The Endozoicomonadaceae-Spirochaetaceae dynamic in <i>L. pauciflorum</i>	99
6.1.2.2	High flexibility in the coral holobiont	101

6.2	Bacterial community development in larvae	103
6.3	<i>L. pauciflorum</i> as a model Alconiid	105
6.4	Final Conclusions	106
Appendix		108
Appendix A: Phylogenetic relationships between host Octocorallia used in this study (Chapter 2)		108
Appendix B: Putative identification of unclassified ASVs via NCBI BLAST (Chapter 2)		110
Appendix C: Decontamination of 16S community data with the R package microDecon (Chapter 4)		114
References		120

List of Tables

Table 2.1: Summary of Diversity indices from the <i>Lobophytum pauciflorum</i> 16S rRNA sequenced dataset	20
Table 2.2: Ubiquitous amplicon sequence variants (ASVs) recovered from <i>Lobophytum pauciflorum</i>	23
Table 2.3: Alpha diversity metrics and dominant bacterial families in each host genus.	27
Table 3.1: The number of samples across colonies and microhabitats	44
Table 4.1: List of samples collected and processed for 16S rRNA gene amplification, sequencing and analysis	64
Table 5.1: Summary of BLAST hits received between <i>Lobophytum pauciflorum</i> genes and known AMP and Kazal-type genes from NCBI	86
Table 5.2: BLASTn results (e^{-50}) of AMP and Kazal-type homologs in <i>Lobophytum pauciflorum</i>	88
Table 6.1: Overview of the current understanding of the timing of bacterial community onset and succession	104
Table Appendix 1: Basic local alignment search tool (BLAST) results	111
Table Appendix 2: Samples of developing <i>Lobophytum pauciflorum</i> larvae collected at each time point	114
Table Appendix 3: Analysis of significant extrinsic variables influencing community composition in developing larvae.	116
Table Appendix 4: Results of analysis of similarity (ANOSIM)	116

List of Figures

Figure 2.1: Bacterial community composition and diversity between 7 colonies of <i>Lobophytum pauciflorum</i>	21
Figure 2.2: Bayesian distances between core amplicon sequence variants (ASVs) in <i>Lobophytum pauciflorum</i> and Endozoicomnadaceae type strains.....	24
Figure 2.3: Bayesian phylogenetic tree of type strains and core amplicon sequence variants (ASVs) affiliated with Endozoicomnadaceae.....	26
Figure 2.4: Non-metric multi-dimensional scaling (NMDS) plot built on bacterial community composition of Octocorallia.....	28
Figure 2.5: Bayesian phylogenetic tree of Endozoicomnadaceae-affiliated	29
Figure 2.6: Bayesian phylogenetic tree Spirochaetes-affiliated ASVs	32
Figure 3.1: Image of inner and outer tissue layers in <i>Lobophytum pauciflorum</i> cross-section.....	40
Figure 3.2: Histology of inner and outer tissue layers in <i>Lobophytum pauciflorum</i>	44
Figure 3.3: Count of ASVs specific to and shared between microhabitats in <i>Lobophytum pauciflorum</i>	45
Figure 3.4: Faith’s Phylogenetic Diversity (PD) (left) and Pielou’s Evenness (right)	45
Figure 3.5: Non-metric multi-dimensional scaling (NMDS) plot of Bray-Curtis dissimilarity showing distinct community composition in each of the three microhabitats sampled.....	46
Figure 3.6: Relative abundance of sequences affiliated with Bacterial taxa at phylum (A) and family (B) level	47
Figure 3.7: Phylogentic tree displaying the 29 Endozoicomnadaceae-affiliated sequences.....	49
Figure 3.8: Putative metabolic pathways affiliated with sequences recovered from Inner tissue, outer tissue and mucus layers.....	51
Figure 3.9: Putative biological parameters and preferences of 16S communities in each microhabitat	52
Figure 3.10: Summary of 16S community taxonomic affiliation and inferred biological characteristics	53
Figure 4.1: Modes of reproduction in corals showing pelagic and benthic stages of development	61
Figure 4.2: <i>Lobophytum pauciflorum</i> larvae photographed under a dissection microscope at each timepoint sampled.....	63
Figure 4.3: Faith’s phylogenetic diversity index.....	65
Figure 4.4: Most prominent bacterial families affiliated with sequences recovered from larvae	67
Figure 4.5: Stages of Community Succession showing mean relative abundance of sequences between early (14 to 48 hours post-fertilization [hpf]) and late (72 to 210 hpf) communities.....	69
Figure 4.6: Non-metric multi-dimensional scaling (NMDS) plot of all samples analysed including the blank, displayed with color representing the amplification run (A, B or C).....	72

Figure 5.1: Timeline of samples (analyzed here) collected for 16S rRNA gene analysis (green) (chapter 4) and transcriptomics (blue) (Wessels <i>et al.</i> 2016) throughout the development of <i>Lobophytum pauciflorum</i> larvae	82
Figure 5.2: Differential expression of <i>L. pauciflorum</i> transcripts	84
Figure 5.3: Differential expression of <i>Lobophytum pauciflorum</i> genes predicted at 99% AMP or higher	85
Figure 5.4: Differential expression of AMP protein homologs in developing <i>Lobophytum pauciflorum</i> larvae.....	89
Figure 5.5: Differential expression of Kazal-type homologs of nucleotide sequences.....	90
Figure 5.6: Differential expression of antimicrobial peptide nucleotide homologs to Cnidarian antimicrobial peptides (e^{-5}) in <i>Lobophytum pauciflorum</i> larvae.....	91
Figure 5.7: Differential expression of antimicrobial peptide and Kazal-type nucleotide sequence homologs (e^{-50}) differentially expressed in <i>Lobophytum pauciflorum</i> larvae.....	92
Figure 5.8: Composition of the bacterial community during larval development in <i>Lobophytum pauciflorum</i>	93
Figure 6.1: The baseline community of <i>Lobophytum pauciflorum</i>	100
Figure 6.2: Bacterial community of early and late stage larvae and the adult microhabitats in the mucus layer, outer tissue and inner tissue of <i>Lobophytum pauciflorum</i>	105
Figure Appendix 1: MUSCLE alignment of sequences corresponding to the <i>msh1</i> gene	108
Figure Appendix 2: Phylogenetic tree depicting the relationship between host species.....	109
Figure Appendix 3: Distribution of sequences associated with the respective families in NCBI BLAST	112
Figure Appendix 4: Composition of the 16S rRNA gene community.....	113
Figure Appendix 5: NMDS of all samples - including blankA -	115
Figure Appendix 6: Bacteria driving the dissimilarity between samples and clusters.....	118
Figure Appendix 7: community composition of each sample.....	119

“The microbiota functions as an extra organ, to which the host has outsourced numerous crucial metabolic, nutritional, and protective functions.”

-Bevins and Salzman (2011)



Lobophytum pauciflorum "The devil's hand coral" - Orpheus Island, Queensland Australia 2017.

Chapter 1: The coral holobiont

1.1 The microbiome

All metazoan organisms host an assortment of microbes including Archaea, Bacteria, Eukarya, Fungi, protists and viruses (Gilbert *et al.* 2012; McFall-Ngai *et al.* 2013). This community, along with its genetic information and functions, is collectively referred to as a host-associated microbiome (examiner 1 ref; Berg *et al.* 2020). While originally portrayed as a source of disease, it has become apparent that the microbiome provides a number of beneficial services to metazoan hosts (O'Hara and Shanahan 2006; Fraune and Bosch 2010). Host physiology depends on associated microbes for metabolite production and the regulation of signalling pathways (Lee and Hase 2014). The identification and characterization of pathogens in human-associated microbiota has also helped to understand medical conditions such as obesity, gastrovascular and cardiovascular diseases (Hattori and Taylor 2009; Lee and Hase 2014). Next-generation whole-genome sequencing, metagenomics, metabarcoding and advanced bioinformatics approaches have made possible more in-depth studies of host-symbiont interactions on a molecular level (Medina and Sachs 2010; Porter and Hajibabaei 2018). As a result, studying the host-associated microbiome has become a primary research focus among multiple disciplines from human medicine to coral reef ecology (Ruby *et al.* 2004; Hattori and Taylor 2009; Bosch and Ngai 2011; McFall-Ngai *et al.* 2013).

The reliance of complex organisms (including humans), on symbiotic microbial consortia has challenged the biological and physiological concept of 'the individual' (Gilbert *et al.* 2012; Rees *et al.* 2018). However, there are many factors that determine the composition and persistence of host-associated microbial consortia. Host phylogeny is an important factor in microbial community composition (Ley *et al.* 2008 a, b) and dictates the microhabitat characteristics available for microbial colonization. To maintain a stable relationship with microbial associates, the host must create a favourable environment to harbor them. A well-studied example of this is in legumes when nitrogen-limitation triggers the formation of root nodules that provide a microhabitat for nitrogen-fixing bacteria to enrich the host's supply (Chen *et al.* 2003). Localized, discriminatory antimicrobial compounds can help proliferate probiotic organisms while inhibiting colonization by others, including those potentially pathogenic to the host (Bevins and Salzman 2011). As associated microbiota also require a reliable source of suitable nutrition, host diet has remained a significant factor shaping the metazoan microbiome throughout evolution (Ley *et al.* 2008 a,b). Bacteria mediate the digestion of lignocellulose in termites, allowing them to eat wood (Brune *et al.* 2010). In a more unusual example, the annelid *Olavius* spp. has lost both mouth and anus and is completely dependent on microbial metabolism to recycle nutrients via a redox pathway (Woyke *et al.* 2016).

1.2 Cnidaria as hosts

1.2.1 Model Cnidaria – the Hydrozoa

The Cnidaria have over 10,000 descended extant species among the classes Anthozoa (including Octocorallia and Scleractinia), Hydrozoa, Scyphozoa and Cubozoa (Valentine 2004). Several model organisms have risen to provide insight into microbial associations with animal hosts. Evolution and development are studied in *Nematostella* spp. while dinoflagellate associations and bleaching are studied in *Aiptasia* spp. (Lehnert *et al.* 2012). From the *Hydras* we have gained a great deal of insight into Cnidaria-Bacteria associations and mediation tactics, some of which are thought to have been conserved throughout the Cnidaria.

Species-specificity (Fraune and Bosch 2007) observed between *Hydra* spp. and the associated bacterial community is shaped and maintained by a distinct, host-specific regime of antimicrobial compounds (Bosch 2012; Franzenberg *et al.* 2013a) including the novel, antimicrobial peptides *Hydramacin-1* (Jung *et al.* 2008), *NDA-1* (Augustin *et al.* 2017) and *Periculin* (Augustin and Bosch 2010). Some antimicrobial compounds are vertically transmitted from the parent to offspring to mediate the colonization of new offspring by bacteria in the environment (Fraune *et al.* 2010; Franzenberg *et al.* 2013). This system allows a repeatable pattern of community succession in larval *Hydra* across generations (Franzenberg *et al.* 2013b).

The bacteria associated with *Hydra* communicate with the host neural net, modulating activity such as spontaneous bodily contractions and feeding behavior (Murillo-Rincon *et al.* 2017; 2018). The bacterial community also plays an important role in innate immunity of the host. Toll-like pattern recognition receptors in the epithelial layer of *Hydra* detect potential pathogens, triggering a signal cascade for the production of antimicrobial peptides (Bosch *et al.* 2009, Bosch 2013). When resident bacteria were removed from the epithelial layer the innate immune system failed and the host was compromised by a fatal fungal infection. A diverse community of epithelium-associated bacteria were therefore required for an effective innate immune response from the host (Fraune *et al.* 2015). As a result of these studies, the innate immune system is now suspected of having arisen for the purpose of mediating and maintaining the associated microbial community rather than strictly as a defence against pathogens (Franzenberg *et al.* 2013, Bosch 2014, Bosch and Rosenstiel 2016). It is hypothesized that this mechanism may be conserved throughout the Cnidaria (Augustin *et al.* 2010, Fraune *et al.* 2015).

1.3 The coral holobiont

1.3.1 Coral-associated microbiota

The microbial community associated with corals is composed of a diverse array of algae, Archaea, Bacteria, Fungi and viruses which are dynamic and distinct from the surrounding environment (Rohwer *et al.* 2001; Knowlton and Rohwer 2003; Kellogg 2004; Littman *et al.* 2011; Kimes *et al.* 2013; Blackall *et al.* 2015). The coral host and its associated microbiota are collectively referred to as the coral holobiont (Knowlton and Rhower 2003). Some host coral species show tolerance to shifts in microbial community structure (Ziegler *et al.* 2019), allowing the holobiont to adapt to changes in the local environment (Ziegler *et al.* 2017). Significant shifts in the environment, however, can negatively impact the microbiome and lead to disease or mortality in the host, such as during coral bleaching (Ritchie and Smith 2004; Brandt *et al.* 2009; Pendleton *et al.* 2016; Hughes *et al.* 2018). Anthropogenic activity also induces shifts in the environment and, thereby, the coral-associated bacterial community that can be detrimental to coral health (Vezzulli *et al.* 2013; Claar *et al.* 2019). The most well-studied component of the holobiont are dinoflagellates in the family Symbiodiniaceae (LaJeunesse *et al.* 2018). These microalgae are prevalent across about half of all coral species (dubbed 'zooxanthellate' corals) and provide the host with a significant source of photosynthetically fixed carbon (Muscatine *et al.* 1981, 1990). During coral bleaching, Symbiodiniaceae disassociate from the host, leaving a deficit of energy which makes recovery under multiple stressors more difficult and often results in mass coral mortality (Loya *et al.* 2001; Pendleton *et al.* 2016; Harrison *et al.* 2019).

Corals – both zooxanthellate and azooxanthellate – also host diverse yet less well-studied consortia of Archaea and Fungi (Kellogg 2004; Sato *et al.* 2013; Li *et al.* 2014; Frade *et al.* 2016). Some Fungi produce antimicrobial compounds which can aid in host defence (Li *et al.* 2014), but some endolithic Fungi can also become opportunistically pathogenic under extreme environmental stress (Golubic *et al.* 2005). It has been suggested that Archaea may be involved in nitrogen cycling within the holobiont (Siboni *et al.* 2008). The archaeal community appears to be more specific to location than to host species (Kellogg *et al.* 2004; Frade *et al.* 2016) and sequences affiliated with opportunistic Archaeota have been recovered from diseased coral tissue (Sato *et al.* 2013). It has been suggested that nitrogen cycled through Archaea and Bacteria may also fuel the coral-Symbiodiniaceae association (Radecker *et al.* 2015). The advancement of next generation sequencing approaches (16S rRNA gene amplicon and metagenomics) has allowed for a more comprehensive understanding of the diversity and potential functions of bacterial communities associated with corals and reefs more broadly (Lozupone and Knight 2008; Robbins *et al.* 2019).

1.3.2 Coral-associated Bacteria

Disease outbreaks in corals facilitated a focus on research into coral-associated bacteria to identify pathogens associated with coral diseases (Sekar *et al.* 2006; Bruck *et al.* 2007; Bourne *et al.* 2009; Kvennefors *et al.* 2010; Kimes *et al.* 2013). It quickly became apparent that some coral-associated bacteria may also have roles beneficial to the host (Rhower *et al.* 2001; Reshef *et al.* 2006; Nissimov *et al.* 2009; Ainsworth *et al.* 2010; Peixoto *et al.* 2017). Corals, like *Hydra*, form species-specific relationships with some associated bacteria that often appear stable over time and space (Rohwer *et al.* 2002; De Castro *et al.* 2010; Kvennefors *et al.* 2010; La Riviere *et al.* 2015; Chu and Vollmer 2016) and have been recovered from Scleractinia and Octocorallia from both shallow and deep-sea host coral species (Bruck *et al.* 2007; Kellogg *et al.* 2019; Zanotti *et al.* 2020). Analysis with fluorescence *in situ* hybridization (FISH) showed endosymbiotic bacteria in coral tissue, further stressing the intimacy of the host-symbiont relationship in corals (Ainsworth *et al.* 2006; Bayer *et al.* 2013 b; La Riviere *et al.* 2016; Wada *et al.* 2016).

1.3.3 Factors shaping the coral holobiont

The microbial consortia associated with corals has been described as several fractions which express differing levels of flexibility and external influence (Hernandez-Agreda *et al.* 2017; van de Water *et al.* 2017). A highly conserved fraction is composed of a small group of organisms in a species-specific relationship with the host and is presumed to be conserved over space and time (Ainsworth *et al.* 2015; Hernandez-Agreda *et al.* 2017). Referred to as the “core” community, conserved symbionts are often presumed play important roles in maintaining holobiont health. Additionally, there are local and widespread fractions which are influenced by factors including nutrient sources and water currents at the respective spatial scales (Hernandez-Agreda *et al.* 2017).

1.3.3.1 Internal factors influencing holobiont structure

Providing a favourable environment for the proliferation of beneficial symbionts and deterring or inhibiting the colonization of undesirable microbes are both required to maintain a stable associated bacterial community. This can be done passively via settlement and competition between resident microbes and environmental colonizers that happens to benefit holobiont stability, or through active targeting of pathogens by the host (Sieber *et al.* 2018). The level of mediation and flexibility varies between host species (Ziegler *et al.* 2019), possibly due either to differences in metabolic pathways within the holobiont or host susceptibility to environmental influences (Meistertzheim *et al.* 2016). The diversity of microhabitats available within the host can therefore have a big impact on the composition and structure of the associated bacterial community.

The reproductive strategy of the host is one factor influencing community succession of bacteria colonizing larvae (Neave *et al.* 2017 b). The process of bacterial community onset and succession in larvae is poorly understood, however, as inconsistencies between coral species and reproductive strategies make it difficult to for generalizations on this topic with the few studies currently available. Brooding corals undergo internal fertilization and release fully developed planulae, while broadcast-spawners release gametes for external fertilization and development in the water column (Harrison *et al.* 1984; Babcock and Heyward 1986). Brooding colonies can impact the microbiome of future generations via vertical transmission, passing bacteria from the parent colony to ensure their assimilation by the offspring (Ceh *et al.* 2013 a; Sharp *et al.* 2012; Leite *et al.* 2017). Broadcast-spawners, however, are thought not to form endosymbiotic associations with bacteria until post metamorphosis (Sharp *et al.* 2010; Damjanovic *et al.* 2020b). It is possible, however, that larvae may still rely on associations with larvae in the mucus at this time (Damjanovic *et al.* 2020b). A different study found that coral larvae take up ^{13}C and ^{15}N stable-isotope labels previously metabolized by associated bacteria (Ceh *et al.* 2013 b). Whether vertical transmission occurs or not, horizontal acquisition is the primary method of bacterial community diversity for developing coral larvae (Aprill *et al.* 2009; Sharp *et al.* 2010; Epstein *et al.* 2019; Damjanovic *et al.* 2020c), highlighting the importance of a healthy environment for the development of the microbial community.

Once a diverse community has developed and formed endosymbiotic associations with the host, the organization of probiotic members and exclusion of pathogens becomes a complex and poorly understood system. One method of maintaining order in a complex system is the provision of distinct microhabitats within the host which provide favourable conditions for different niche communities. This was illustrated above with the specialist root nodules in legumes (Chen *et al.* 2003). Additionally, however, some microhabitats form to fulfill biological requirements of the host, such as the skeleton, tissue and mucus layer in corals, and also host distinct bacterial communities (Bourne *et al.* 2016; Pollock *et al.* 2018). The gastrovascular cavity where coral polyps digest food harbors a distinct assemblage of bacteria, some of which are presumably involved in coral metabolism or nutrition (Agostini *et al.* 2012).

An important mechanism for maintaining homeostasis in the microbial community is the application of discriminatory antimicrobial compounds (AMPs). Coral extracts demonstrate powerful, discriminatory antimicrobial activity against coral pathogens (Gochfeld and Aeby 2008). Coral mucus, especially, has demonstrated high antimicrobial activity and inhibited the growth of coral pathogens (Ritchie *et al.* 2006; Kvennefors *et al.* 2012). Antimicrobial compound production has been shown to increase following mechanical stress (Geffen and Rosenberg 2005), but coral bleaching can significantly decrease antimicrobial activity in coral mucus (Ritchie *et al.* 2006). Some antimicrobial

compounds are produced by other coral-associated bacteria (Nissimov *et al.* 2009; Bharathi *et al.* 2013; Fu *et al.* 2013; Pham *et al.* 2016) and some are produced by the host itself (Vidal-Dupiol *et al.* 2011; Mason *et al.* 2021).

In addition to the production of antimicrobial peptides, “quorum-quenching” also occurs in the coral holobiont. Quorum-quenching is the disruption of quorum-sensing communication pathways between bacterial cells to inhibit their virulence in the host (Miller and Bassler 2001; Tait *et al.* 2010; Goldberg *et al.* 2011, 2013) and fight against active disease (Zimmer *et al.* 2014). The combination of quorum-quenching molecules utilized is specific to host species (Ransome *et al.* 2013; 2014). Evidence also suggests that quorum-quenching, like AMPs, may regulate the resident bacterial community as well as providing a defence mechanism (Zimmer *et al.* 2014).

1.3.3.2 External factors influencing holobiont structure

Regulation of the associated microbiota is a complicated endeavour and many external variables are constantly acting on the community and contributing to variation. In some cases, local environmental factors can be greater drivers of community structure than host species (Littman *et al.* 2009; Silveira *et al.* 2017). Depth has been shown to influence the bacterial community structure between deep (>200 m), mesophotic (30-200 m) and shallow (30 m) corals (Jensen *et al.* 2019; Kellogg *et al.* 2019), but not at smaller scales such as 24-41 m depth (Bayer *et al.* 2013). In the stony coral *Coelastrea aspera*, the age of the colony (as it pertains to colony size) also influenced bacterial community structure (Williams *et al.* 2015). Several studies have reported an influence of seasonality on the bacterial community (Koren and Rosenberg 2006; Kimes *et al.* 2013; Zhang *et al.* 2015), but this was not observed in the Mediterranean species *Corallium rubrum* (van de Water *et al.* 2018). Similarly, no significant shifts were detected between night and day in *Mussismilia braziliensis* (Silveira *et al.* 2017).

As the environment is a significant determining factor of bacterial community structure in corals, shifts in the environment also cause shifts in the composition of the coral-associated bacterial community (Kushmaro *et al.* 1997; Koren and Rosenberg 2006; Rosenberg *et al.* 2007; Littman *et al.* 2011; McDevitt-Irwin *et al.* 2017). The marine environment is currently undergoing significant shifts as a result of climate change and other consequences of anthropogenic activity, resulting in increases in the abundance of pathogens on reefs and compromising holobiont integrity and coral health (Littman *et al.* 2011; Ainsworth *et al.* 2016, Pendleton *et al.* 2016, Hughes *et al.* 2018). Anthropogenic activity and pollution can significantly alter bacterial community structure within the holobiont (Lee *et al.* 2012; Vezzulli *et al.* 2013; Zhang *et al.* 2015; Ziegler *et al.* 2016; Claar *et al.* 2019). Climate-change-, pollution- and overfishing-related stressors inhibit the holobiont’s ability to regulate its community

structure resulting in higher diversity, higher prevalence of opportunists and pathogens in addition to reducing the relative abundance of putatively beneficial bacteria such as *Endozoicomonas* sp. (McDervitt-Irwin *et al.* 2017). Local anthropogenic activity can also increase the abundance of viruses, opportunists and pathogens in the water column overlying coral reefs thereby influencing corals' exposure to harmful microbes (Dinsdale *et al.* 2008; Ziegler *et al.* 2016).

Recent studies have correlated shifts in coral associated bacterial communities with local environmental gradients, suggesting the potential increase of host tolerance to the respective environment is linked to these changes in the microbiome (Epstein *et al.* 2019, Ziegler *et al.* 2019). To explore this concept, coral colonies were reciprocally transplanted between habitats and, over time, the community associated with each colony came to resemble those native to the new environmental conditions (Ziegler *et al.* 2019). In some cases, manipulation of the bacterial community through the addition of putative probiotic strains in aquaria can increase thermal stress tolerance (Rosado *et al.* 2019), though the mechanisms that conferred increased tolerance in the holobiont were not determined. Over time, shifts in the bacterial community structure may help coral holobionts adapt to long term changes in the environment (Rothig *et al.* 2017; Voolstra and Ziegler 2020). While the level of tolerance for shifts in the bacterial community structure varies by host species, some corals have demonstrated high apparent propensity for community flexibility (Rothig *et al.* 2017; Ziegler *et al.* 2017).

1.3.4 *Bacteria associated with Scleractinia*

Scleractinia, the hard corals, secrete a calcified skeletal matrix which accumulates to form the biophysical structures we know as coral reefs. As crucial ecosystem engineers, hard corals have received the majority of resources and attention when it comes to microbiological research. While the skeletal matrix is vast, the living coral polyps lie in a thin layer of tissue on the skeletal surface, covered in a bioactive mucus layer. Each of these layers has been identified as a microhabitat hosting a distinct bacterial community (Bourne *et al.* 2016).

1.3.4.1 *The role of the coral mucus layer*

The coral mucus layer is secreted at the interface between the animal tissue and the surrounding seawater, forming the first line of defence against transient microbes. While many bacteria colonize the mucus layer as a food source (Wild *et al.* 2004), media mimicking coral tissue did not reflect passive colonization patterns in seawater suggesting control mechanisms could be at play (Sweet *et al.* 2011). Corals also periodically shed old mucus and produce new layers, creating a cyclical pattern of succession in the resident bacterial community (Glasl *et al.* 2016). Extracts of coral mucus

are highly enriched in powerful, discriminatory antimicrobial peptides (AMPs) (Ritchie *et al.* 2006, Nissimov *et al.* 2009, Kvennefors *et al.* 2012). Some of this antimicrobial activity has been attributed to other mucus-associated Bacteria, such as *Pseudoalteromonas* spp. and *Roseobacter* sp. (Nissimov *et al.* 2009; Shnit-Orland *et al.* 2012). The mucus layer therefore acts as a physical and biochemical barrier against microbes which could be pathogenic or upset the homeostasis of the associated microbial community while serving as a microhabitat for associated bacteria.

1.3.4.2 Coral tissue as a microhabitat

Tissues host microbial communities that are distinct from those of coral mucus, the skeleton or the surrounding seawater (Ritchie and Smith 2004; Koren and Rosenberg 2006; Sweet *et al.* 2010; Pollock *et al.* 2018). While nutrient transfer between Bacteria and the coral host has not been demonstrated directly, coral-associated bacteria are involved in carbon (Neave *et al.* 2017) nitrogen (Lesser *et al.* 2007) and sulfur (Raina *et al.* 2009; 2013) metabolism and could potentially participate in nutrient recycling in the holobiont (Robbins *et al.* 2019). The gastric cavity – where food is broken down into nutrients by the host - provides a microhabitat to a distinct, prolific community of bacteria in corals (Bourne *et al.* 2016) as well as higher animals (Ley *et al.* 2008), further supporting their likely role in extending metabolic pathways of the holobiont. Symbiodiniaceae are found within the gastrodermal tissue layers of the coral and may receive fixed nitrogen from bacteria, fuelling the photosynthetic carbon supply to the host (Rädecker *et al.* 2015).

1.3.4.3 Coral skeleton as a microhabitat

The microbiome in the coral skeleton is diverse and metabolically active, potentially extending the metabolite pathways of the host (Pernice *et al.* 2020). Endolithic bacteria also take up organic excretions from the coral host (Shashar *et al.* 1994). A study of diseased *Mussismilia* spp. recovered an abundance of sequences from the skeleton commonly associated with healthy corals, suggesting the skeleton may offer refuge to a healthy microbial community when the overlying tissue is diseased (Fernando *et al.* 2015). The endolithic *Ostreobium* sp. was recovered from the skeleton of new polyps within the first week following the onset of calcification (Masse *et al.* 2018) and dominates the skeletal microhabitat in a wide range of mature Scleractinia (Gutner-Hoch and Fine 2011). *Ostreobium* spp. appear to share an intimate relationship with corals, having adjusted their metabolic requirements from the free-living stage to actively participate in carbon and nitrogen cycling as a member of the coral holobiont (Masse *et al.* 2020).

1.3.5 *Bacteria associated with Octocorallia*

Octocorallia, while drawing less research focus than Scleractinia, were found to support similar fish assemblages on coral reefs indicating that Scleractinia do not provide a more favorable habitat for reef residents. Species richness among fish increased in correlation with live cover of Octocorallia, emphasizing the importance of soft coral habitat (Epstein and Kingsford 2019). However, the work on Octocorallia has thus far focused on the abundance of novel AMPs present in tissue and mucus extracts for pharmaceutical purposes (Ibrahim *et al.* 2012; Setyaningsih *et al.* 2012; Harder *et al.* 2003; Huang *et al.* 2015). Strong antimicrobial activity plays an important role in the defense of the holobiont (Kelmen *et al.* 2009, Nunez-Pons *et al.* 2013). The inhibitory activity of AMPs in soft corals is also highly selective. In addition to inhibitory compounds, a study in Gorgonians found an abundance of novel stimulatory compounds suggesting that some host mechanisms may inhibit undesirable colonizers while other mechanisms encourage the proliferation of probiotic members (Hunt *et al.* 2012).

A metastudy of bacterial symbionts on coral reef invertebrates determined that Octocorallia differ from scleractinians in their microbial community structure (O'Brien *et al.* 2020). Characteristics such as microhabitat establishment and larval colonization have not been investigated in soft corals (in contrast to a number of studies on hard corals), however, several studies have characterized the bacterial community associated with various soft coral host species through 16S rRNA profiling. Recent studies have shown that the bacterial communities associated with Octocorallia often show a degree of species-specificity (Gray *et al.* 2011; Holm and Heidelberg 2018) and associated bacterial communities differ between shallow, tropical reefs and cold-water coral communities (Kellogg *et al.* 2019). Tropical communities are often dominated by *Endozoicomonas* spp. (Correa *et al.* 2015; Bayer *et al.* 2013 b; van de Water *et al.* 2018) which may also display host species-specificity (La Riviere *et al.* 2015; van de Water *et al.* 2017). Imaging with fluorescence *in situ* hybridization (FISH) revealed endosymbiotic bacteria (La Riviere 2016), including *Endozoicomonas* spp. (Bayer *et al.* 2013 b), further highlighting a potential intimate association with this family of bacteria. The bacterial communities associated with soft corals are therefore complex and closely associated with the host, though our understanding of this relationship is limited in comparison to other Cnidaria.

1.4 Objectives

The primary objective of this study was to gain a comprehensive understanding of the bacterial community associated with the soft coral *Lobophytum pauciflorum*. The Alcyoniidae *L. pauciflorum* is an emerging model organism for octocoral genomics and transcriptomics, yet we know comparatively little about the microbiome of soft corals when compared to that of hard corals. To

improve the understanding of the microbiome of *Lobophytum pauciflorum* and mechanisms regulating this association, the following objectives were addressed in this study:

- 1. To comprehensively characterize the bacterial community associated with healthy adult colonies of *L. pauciflorum*.** Using 16S rRNA gene amplicon sequencing this study analyzed the structure and phylogeny of the associated bacterial community within and between individual colonies. The *L. pauciflorum*-associated bacterial community was then compared to that of other host Octocorallia to establish distinctions and similarities between soft coral hosts, improve our understanding of soft coral microbiology and serve as a baseline for the following chapters on *L. pauciflorum*-associated bacteria.
- 2. To explore the extent to which the inner tissue, outer tissue and mucus layers of *L. pauciflorum* as microhabitats host distinct bacterial communities.** By characterizing the bacterial communities of the tissue and mucus layers separately I provide the first study of microhabitats within a soft coral host. Microhabitats support niche bacterial communities in other Cnidaria, potentially providing distinct services to the holobiont, but this possibility had not previously been explored in soft corals and therefore constitutes a knowledge gap in coral microbiology.
- 3. To characterize the pattern of bacterial community succession during larval development.** The bacterial community composition at each of 9 time points between fertilization and competency was characterized during the early development of *L. pauciflorum* larvae. Few studies have explored the bacterial community associated with developing coral larvae and none have done so for Octocorallia. This study therefore contributes significantly to an understudied aspect of coral microbiology, thereby addressing a second knowledge gap in the field.
- 4. To identify potential homologs of known antimicrobial peptides that are differentially expressed in *L. pauciflorum* during early development.** Using bioinformatics on the transcriptome of developing larvae, basic local alignment searches identified potential homologs of antimicrobial peptides known from other Cnidaria. This study analyzed the differential expression of these homologs in relation to the timeline of bacterial community succession in developing larvae.

1.6 Structure of dissertation

The research objectives of this dissertation are achieved in chapters 2 to 5, followed by a general discussion (Chapter 6). In Chapter 2 I characterize the bacterial community associated with mature, healthy *L. pauciflorum* colonies by profiling the conserved and variable bacterial members

and investigating variability between colonies and against other host Octocorallia. After characterizing the community of bacteria, phylogenetic analyses focus on sequences affiliated with the families Endozoicomonadaceae and Spirochaetaceae due to their high relative abundance and consistency throughout the dataset as compared to other affiliated taxa. I explore the bacterial community associated with *L. pauciflorum* more deeply in Chapter 3, analyzing a new set of samples separating the inner tissue, outer tissue and mucus layers to test for the presence of microhabitats within Alcyoniidae. Putative functional analysis was also run on the sequences to determine whether various community functional characteristics are predicted to differ between microhabitats. With a better understanding of the baseline bacterial community in healthy, mature colonies of *L. pauciflorum*, Chapter 4 follows succession of the colonizing Bacteria on new *L. pauciflorum* larvae between 6 and 210 hours post-fertilization (hpf). I characterize the bacterial community present at each of 9 developmental time points to better understand how the microbiome develops in coordination with developing larvae. Chapter 5 expands on the study of larval development by identifying homologs of antimicrobial peptides differentially expressed in the larvae and correlating this data with the structure of the associated bacterial community. In Chapter 6 I discuss the findings from Chapters 2 through 5 in the context of *L. pauciflorum* as a host and a model organism for the study of microbiology in soft corals, a vastly understudied aspect of cnidarian microbiology and host-symbiont interactions. This final discussion (Chapter 6) unites all four data chapters into a comprehensive characterization of the bacterial community associated with *L. pauciflorum* as it relates to other coral holobionts.

Chapter 2: Bacterial Diversity Associated with the Soft Leather Coral *Lobophytum pauciflorum*

Abstract

The microbial community associated with corals is composed of a diverse community of resident organisms, some of which are presumed to benefit host fitness via metabolic and antibacterial activity. Shifting environmental conditions can destabilize the host-symbiont association, increasing the risk of disease and mortality, making research in this field more important in the current age of climate change than ever before. This study characterizes the bacterial community associated with the Alcyoniidae *Lobophytum pauciflorum*, a model organism in soft coral 'omics research. The bacterial community associated with *L. pauciflorum* consists of a conserved component dominated by Endozoicomonadaceae as well as a diverse fraction that varies in structure between colonies in the same location, dominated by Spirochaetaceae. We also present here a phylogenetic analysis of the sequences associated with these taxa and a comparison of bacterial community structure with other soft coral hosts (*Cladiella* sp., *Sarcophyton* spp., and *Sinularia* spp. as well as *Briareum* spp., *Clavularia* sp., *Isis hippuris*, *Pinnigorgia* sp., and *Xenia* sp.). Endozoicomonadaceae-affiliated sequences were most abundant in the alcyoniids and *Pinnigorgia* sp. and dominated by sequences aligned with *Parendoziomonas haliclona*. The recovery of Spirochaetaceae-affiliated sequences from coral hosts in literature revealed a pattern of host-symbiont association which, unlike other host-symbiont relationships, does not appear to correlate with host phylogeny. This study provides an important contribution to our understanding of soft coral microbiology and stresses the need to determine symbiont function to effectively interpret the observed host-symbiont affiliations.

2.1 Introduction

Coral reefs are often compared to “oases in a marine desert” for their reputation as hotspots of nutrient cycling and biodiversity in the vast open ocean. However, the changing climate and other consequences of anthropogenic activity have been contributing to ecosystem degradation for decades, threatening the survival of coral reefs as we recognize them today (Richmond 1993; Hoegh-Guldberg *et al.* 2007; D’Angelo and Wiedenmann 2014; Hughes *et al.* 2018). Mass-bleaching events, ocean acidification and environmental degradation leave corals immuno-compromised, increasing the risk of infection and disease (Miller *et al.* 2009).

Disease outbreaks in the Caribbean throughout the 1990’s led to a wave of research into coral pathogens and, thereby, the coral microbiome (Rosenberg and Ben-Haim 2002). The microbiome is attributed with benefiting host physiology (Reshef *et al.* 2006; Fraune *et al.* 2015, Peixoto *et al.* 2017) and can assist in holobiont adaptation to some environmental changes (Voolstra and Ziegler 2020). Some coral-associated bacteria produce discriminatory antimicrobial peptides which could contribute to holobiont defence mechanisms (Ritchie *et al.* 2006). It is thought that the symbionts are also involved in carbon (Tremblay *et al.* 2012), nitrogen (Shashar *et al.* 1994; Radecker *et al.* 2015) and sulfur (Raina *et al.* 2009) cycling though no nutrient exchange with the host has yet been proven. The potential benefits of coral-associated microbiota to the host health and environmental resilience have highlighted coral microbiology as an important research topic in the modern era of climate change and global marine habitat degradation.

The bacterial community associated with corals is considered as 3 fractions. A small component intimately associated with the host is sometimes called the ‘core’ microbiome. The term ‘core’ microbiome was coined in the human microbiome project (Turnbaugh *et al.* 2007) and later applied to the coral holobiont by Ainsworth *et al.* (2015). The relationship between a host and the core microbiota is presumed to be stable over space and time and may therefore be important functional components of the holobiont (Ainsworth *et al.* 2015; Hernandez-Agreda *et al.* 2017). The remaining members of the bacterial community are divided among a diverse fraction influenced by local environmental factors and a larger, highly diverse fraction susceptible to variations in the marine microbial community over space and time (Hernandez-Agreda *et al.* 2017). Some host corals can tolerate higher flexibility within the bacterial community than others (Ziegler 2019), but it is clear that the environment is a major determinant in the composition of coral-associated microbiota.

Research on the coral microbiome has shown that more distantly related host corals harbor more dissimilar bacterial communities, implying some degree of co-evolution between host and symbiont (Rosenberg and Rosenberg 2008; Pollock *et al.* 2018; O’Brien *et al.* 2019, 2020). Consistent

with this theory, the bacterial communities associated with the cnidarian clades Scleractinia and Octocorallia are known to differ in diversity and composition (O'Brien *et al.* 2020). However, while Octocorallia and Scleractinia have been shown to provide equally favorable and important reef habitat (Epstein *et al.* 2019), the majority of coral-symbiont studies have focused on Scleractinia.

To contribute toward a better understanding of the host-bacteria relationships in Octocorallia, this study establishes a baseline for the bacterial community of the soft leather coral (Alcyoniidae) *Lobophytum pauciflorum* (Ehrenberg, 1834), a gonochoric broadcast-spawner that is widely distributed in shallow waters from East Africa to the Coral Sea. At our field study site in the Palm Islands, Queensland, Australia, *L. pauciflorum* is commonly found at around 3-10 m depth (Wessels *et al.* 2017). The lobes form simple, unbranched 'digits' (Fabricius and Alderslade 2001) which can easily be sampled with minimal disturbance to the colony as a whole (Figure 2.1). Modes of reproduction and stages of development are similar to other Alcyoniidae and described in detail in Wessels *et al.* (2016).

The "devil's hand coral" *L. pauciflorum* is emerging as a model organism for the study of molecular mechanisms and interactions in the soft coral family Alcyoniidae (Wessels 2016, Andrade-Rodríguez 2018). Secondary metabolites from *L. pauciflorum* have demonstrated antibacterial properties (Yan *et al.* 2010a, 2010b, Ibrahim *et al.* 2012) and are additionally proposed as a mechanism for interspecies competition for reef space (Andrade-Rodríguez 2018). Transcriptomics analyses suggested that the immune system and nervous system may be interrelated (Andrade-Rodríguez 2018), potentially exemplifying the immuno-compromising effects of climate change if host behaviour or physiology are also compromised. However, transcriptomics and 16S rRNA sequencing showed that the host and a bacterial community remained stable throughout small changes in temperatures (+3.5°C) and pH (-0.2 pH_{NBS}) suggesting that the *L. pauciflorum* holobiont is somewhat resistant to environmental changes (Wessels *et al.* 2017).

The bacterial community of *L. pauciflorum* was dominated by Endozoicomonadaceae and Spirochaetaceae in a study on sex differentiation (Wessels *et al.* 2017). Members of the Endozoicomonadaceae are common symbionts of marine invertebrates (Neave *et al.* 2016; 2017b) and have been documented in a number of gorgonians (Bayer *et al.* 2013; Correa *et al.* 2013; Pike *et al.* 2013; La Riviere *et al.* 2015; Robertson *et al.* 2015; van der Water 2017) and hard corals (Yang *et al.* 2010; Sheu *et al.* 2017; Kvennefors *et al.* 2010). Several species of *Endozoicomonas* have been analysed with whole-genome sequencing, resulting in a better understanding of their metabolic pathways (Sheu *et al.* 2017) and supporting evidence for their potential roles in regulating the microbial community composition and defending the holobiont from pathogens (Neave *et al.* 2014;

2016; Ding *et al.* 2016). Members of the Spirochaetaceae are also common as symbiotic associates of marine invertebrates but have been reported in abundance from only a small number of coral species (Holm and Heidelberg 2016; van de Water *et al.* 2016). Both free-living and symbiotic spirochaetes have been shown to be involved in nitrogen cycling (Lilburn *et al.* 2001).

In this study we provide a robust characterization of the bacterial community associated with *L. pauciflorum* in order to establish a current baseline for healthy, mature colonies. In doing so, we will further explore the relationship between *L. pauciflorum* and Endozoicomonadaceae- and Spirochaetaceae-affiliated symbionts observed in a previous study (Wessels *et al.* 2017). After establishing the baseline community for *L. pauciflorum* we will compare it with those of other soft coral host taxa to determine what characteristics contribute to similarity or dissimilarity between *L. pauciflorum* and other members of Alyconiidae and Octocorallia.

2.2 Methods

2.2.1 Sample collection

Field work was conducted at Orpheus Island Research station (OIRS), James Cook University in October 2016. Samples were collected by SCUBA at approximately 4-6 m depth at Pelorus Island, QLD (18°33'15"S, 146°29'17"E). Tissue samples from 7 visually healthy *Lobophytum pauciflorum* colonies (referred to as colonies I-VII) were collected under the Great Barrier Reef Marine Park Association (GBRMPA) permit number G16/38499.1. From each colony, 3 digits (~3 cm) were collected for 16S rRNA sequencing analysis and an additional digit was collected for histology. Each digit was cut with scissors while wearing gloves and placed into individual, sterile falcon tubes. The tubes were clean, filled with ambient seawater at the time and place of tissue collection. Sample tubes were kept on ice while returning to the station (~30 min) to prevent warming and help slow changes to the associated bacterial community. Tissues were also thoroughly rinsed 3 times with 0.22 µm-filtered seawater immediately on return to the station and placed in new, individual, sterile cryovials for snap-freezing in liquid nitrogen. Samples for sequencing were snap-frozen in liquid Nitrogen and kept at -80°C until DNA was extracted. Histological samples were fixed for 10 hours in 4 % paraformaldehyde in 10 mM phosphate-buffered saline solution and kept in 1:1 solution of 10 mM phosphate-buffered saline and 100% molecular grade ethanol.

2.2.2 DNA isolation and amplification

Total genomic DNA was extracted using the PowerPlant DNA Isolation Kit (QIAGEN) according to manufacturer's instructions. Genomic DNA was extracted from 100 mg of frozen tissue cut from

each digit with a sterile scalpel and weighed while frozen. Tissue sections were cut to include portions from the inner core tissue as well as surface tissue. These precautions were taken to provide continuity between sampled communities and to avoid bias introduced by accidentally sampling specific microhabitats as identified in these sampled regions in Scleractinia (Sweet *et al.* 2010). Tissue was homogenized by re-snap-freezing in liquid nitrogen and crushing under a sterile mortar and pestle, horizontal bead-beat for 5 min before 5 min resting on ice.

The 16S rRNA gene was amplified from genomic DNA extracts with 16S V3/V4 primers 341F and 785R with Illumina adapter overhangs (underlined) (S-D-Bact-0341-b-S-17 “TCGTCGGCAGCGTCAGATGTGTATAAGAGACAGCCTACGGGNGGCWGCAG” and S-D-Bact-0785-a-A-21 “GTCTCGTGGGCTCGGAGATGTGTATAAGAGACAGGACTACHVGGGTATCTAATCC”, respectively) (Klindworth 2013). Reaction conditions were as follows: 30 sec at 98°C, [10 sec at 98°C, 30 sec at 55°C, 25 sec at 72°C]x32 cycles, 5 min at 72°C and infinite hold at 4°C. Reactions contained 1.25 µl genomic DNA, 1.25 µl each of 5 µM forward and reverse primers, 6.25 µl Platinum SuperFi PCR MasterMix (Invitrogen, US). Blanks were included in each run.

2.2.3 Next-generation sequencing of 16S rRNA

The same reaction conditions were used for indexing but with only 8 cycles, with Nextera XT DNA Library Prep Kit (Illumina, USA). Products were cleaned before and after indexing with Sera-Mag Speed Beads (Merk, DE), using a Zephyr G3 NGS Workstation (PerkinElmer, USA) to standardize pipetting. Quantification was carried out on an Enspire Alpha Plate Reader (Perkin Elmer, US) with Quantifluor dsDNA (Promega, USA). Samples were pooled and final libraries normalized to 4 nM, 5 µl from each indexed library so that 6 pM were entered into the sequencing run. Sequencing for 2 x 300 bp reads was done on a 2x300 Cycles V3 Flow Cell for MiSeq (Illumina, USA). The run was spiked with 15% PhiX v3 Control Kit (Illumina, USA) for quality and calibration control.

2.2.4 16S rRNA gene sequence analysis

Raw sequences were sorted and cleaned with QIIME2 (Bolyen *et al.* 2018). After demultiplexing, the dataset was denoised with the quality control plugin DADA2 (Callahan *et al.* 2016). A sampling depth threshold of 18,000 was applied during denoising with DADA2, retaining 342,000 (71 %) sequences in 19 (79 %) samples. After denoising, identical sequences are stacked into amplicon sequence variants (ASVs) representing unique biological units in the absence of accurate taxonomic classification (Porter and Hajibabaei 2018). Taxonomic units were classified with the SILVA 99 % database release 132 (Quast *et al.* 2013). Sequences which did not affiliate with Bacterial clades were removed as they likely represent Archaea, mitochondria and chloroplasts. A minimum read threshold

of 10 was applied to each ASV, retaining 350 ASVs (from initial 901) and 99.5 % of total sequence reads. For visualizing community structure and comparison of relative composition between samples, data was normalized using total sum standardization (TSS) (McKnight 2019). Dominant ASVs and % community contribution in this study are therefore reported in relative abundance by TSS.

Alpha and Beta diversity were calculated with QIIME2; Shannon Index was used for rarefaction diversity and richness, Faith's PD for phylogenetic diversity and Pielou Index for evenness. Community dissimilarity was calculated with Bray-Curtis index to determine distances for PCoA and PERMANOVA analyses. Taxonomy and feature data was imported to R for analysis of bacterial community composition (R Studio Team 2015). The package seqINR was used to work with sequences in fasta format, the package VEGAN was used for community analysis (Oksanen *et al.* 2018) including PERMANOVA and PCoA, and tidyverse and ggplot were used for visualizing bacterial communities.

In addition to the establishing a baseline community for *L. pauciflorum* we will also identify potential members of the core community based on ubiquity among samples. Previous studies have used cut-offs from 30 % (Ainsworth *et al.* 2015) to 50% (Robertson *et al.* 2015; Chu *et al.* 2016) up to 100 % (Lawler *et al.* 2016) distribution across samples to identify members of the core microbiome in coral hosts. In this study, as it is a putative core community without considering space and time, we will identify ASVs distributed across 100% of *L. pauciflorum* samples as well as a looser but still conservative cut-off of 75%.

Unclassified sequences and sequences associated with Endozoicomonadaceae and Spirochaetaceae that were recovered from *L. pauciflorum* were aligned to known bacterial sequences via the basic local alignment search tool (BLAST) at NCBI for further insight into their identity (Altschul 1990; Anjay 2012). Sequence alignments, phylogenetic trees and BLAST searches were conducted using Geneious Prime 2019.2.1 (<http://www.geneious.com>). Phylogenetic trees were built from MAFFT alignments using MrBayes (Huelsenbeck and Ronquist 2001, Ronquist and Huelsenbeck 2003) with 1.1 million iterations. Substitution models for each dataset were predicted by IQTree ModelFinder (Nguyen *et al.* 2015; Kalyaanamoorthy *et al.* 2017), the top results were K80 (Kimura 1980) and Hasegawa-Kishino-Yano 85 (Hasegawa *et al.* 1985) as denoted in the respective trees presented below. For added robustness, tree topology was compared and found to agree with maximum-likelihood trees built according to the same respective substitution models in PhyML package (Guindon *et al.* 2010) and 1,000x bootstrapping replicates to estimate branch uncertainty. The full 16S rRNA gene for type strains were retrieved from NCBI Genbank. Aligned type strains (1,436-1,556 bp) and potential core ASV sequences (440bp) were trimmed include the full respective ASV sequences but remove gaps, resulting in 442 bp aligned region for *L. pauciflorum*-derived

Endozoicomonadaceae sequences and 216 and 215 for Endozoicomonadaceae and Spirochaetaceae ASVs from the multiple-host dataset. All alignments and phylogenetic analyses were performed in Geneious Prime 2019.2.1 with the exception of ModelFinder run on IQTree webserver (Nguyen *et al.* 2015).

2.2.5 Comparison with other available datasets

To provide reference to the bacterial community affiliated with *L. pauciflorum* in the context of other soft coral hosts, the 16S rRNA bacterial community data presented here was compared with that of available additional studies (Wessels *et al.* 2017, O'Brien *et al.* 2020). Octocorallia host taxa from O'Brien *et al.* (2020) include the alcyoniids *Cladiella sp.*, *Sarcophyton spp.*, and *Sinularia spp.* as well as *Briareum spp.*, *Clavularia sp.*, *Isis hippuris*, *Pinnigorgia sp.*, and *Xenia sp.* The phylogenetic relationship of these hosts was explored by aligning the *msh1* gene sequence of each host species, acquired from NCBI Genbank, also via a MAFFT alignment followed by treebuilding with MrBayes in Geneious Prime 2019.2.1 using a HKY substitution model as predicted by IQTree (Nguyen *et al.* 2015) (Appendix B).

The 16S rRNA sequences from host octocorals were compared with the *L. pauciflorum* dataset by merging the raw sequences in QIIME2 and analyzing them together to remove some of the bias in methodology between studies. For denoising the sequences with those from the previous *L. pauciflorum* dataset (Wessels *et al.* 2017), a sampling depth of 18,000 bp retained 684,000 (35.9 %) sequences in 38 (88.4 %) of samples. To denoise the current *L. pauciflorum* dataset with 16S rRNA communities of other octocorallian host taxa, sample depth was set at 13,200 reads, retaining 976,800 (36 %) sequences in 74 (93 %) of samples. In building the dataset from multiple hosts, only *L. pauciflorum* samples from the current study were included as the number of samples and ASVs per sample already greatly outnumbered those for any of the other host taxa incorporated. The 16S rRNA sequences from additional host taxa were amplified with a different set of 16S primers (515F: GTGYCAGCMGCCGCGGTAA, 806R: GGACTACNVGGGTWTCTAAT) (O'Brien *et al.* 2020). All sequences in this analysis were therefore trimmed in QIIME2 to fit the same 230 bp amplicon region (nt 535-765 of the 16S rRNA V4 region). The average length of classified sequences was 219 ± 15 bp. Diversity metrics and statistics of community composition were calculated via the same methodology as above in QIIME2, R and Geneious software. A percentage similarity analysis (SIMPER) was also run to determine which ASVs contribute to the differentiation between host families.

2.3 Results

2.3.1 *Alpha diversity in L. pauciflorum*

The 16S rRNA gene was successfully amplified from genomic DNA extracts of *L. pauciflorum* tissue samples. Sequencing yielded 481,857 sequences with an average read length of 430 ± 25 bp. The sequencing run produced high-quality reads as determined by recovery of 15.8 % PhiX (on 15% initial spike). Alpha rarefaction subsampled at 22,000 reads implied adequate sampling for optimum diversity based on Shannon and Faith's Diversity indices as well as ASV count. After removal of low-read sequences and ASVs not affiliated with Bacteria, 405,857 sequences were analysed. Alpha diversity metrics are summarized in Table 2.1. Phylogenetic diversity relative to colonies was highest in colony I and lowest in colony II, but otherwise similar across the colonies sampled. Evenness was similar between all colonies. Samples were more similar within colonies than between them (PERMANOVA; $p = 0.001$) so replicates were aggregated to represent each colony. In pairwise analysis, none of the colonies were significantly distinct from one another and were therefore pooled for comparison with other host taxa.

2.3.2 *Composition of the 16S rRNA gene community in L. pauciflorum*

Out of the 405,857 sequence reads analysed in the 16S rRNA gene community of *L. pauciflorum*, 313,848 (77.3%) were classified to a phylum with 92,009 (22.7%) left unclassified beyond the kingdom Bacteria. Sequences affiliated with the phyla Proteobacteria were in highest relative abundance (58.9 % of all sequence reads), followed by Spirochaetes (16.6 %) (Figure 2.1).

Table 2.1: Summary of Diversity indices from the *Lobophytum pauciflorum* 16S rRNA sequenced dataset after subsampling and filtering. The number of replicates remaining after data-filtering is listed in column 'n'. The number of reads and amplicon sequence variants (ASVs) per colony, as well as alpha variables Pielou's Evenness index and Faith's Phylogenetic Diversity, are displayed as mean and standard deviation across replicates for respective colonies.

Colony	n	Sequence Reads	ASVs	Pielou's e	Faiths PD
I	2	18,910 \pm 367	86 \pm 32	0.7 \pm 0.05	17.3 \pm 4.3
II	2	20,812 \pm 2,951	34 \pm 16	0.6 \pm 0.02	7.2 \pm 2.5
III	3	24,825 \pm 674	64 \pm 30	0.6 \pm 0.03	12.2 \pm 5
IV	3	24,588 \pm 2,875	47 \pm 5	0.6 \pm 0.03	10.1 \pm 0.9
V	2	20,084 \pm 2,720	70 \pm 9	0.6 \pm 0.06	12.9 \pm 0.4
VI	3	23,398 \pm 2,872	65 \pm 17	0.6 \pm 0.01	10.5 \pm 2.5
VII	2	33,906 \pm 22,756	74 \pm 5	0.5 \pm 0.09	14.2 \pm 1
Total	17	405857	339	0.6 \pm 0.1	11.1 \pm 4.1

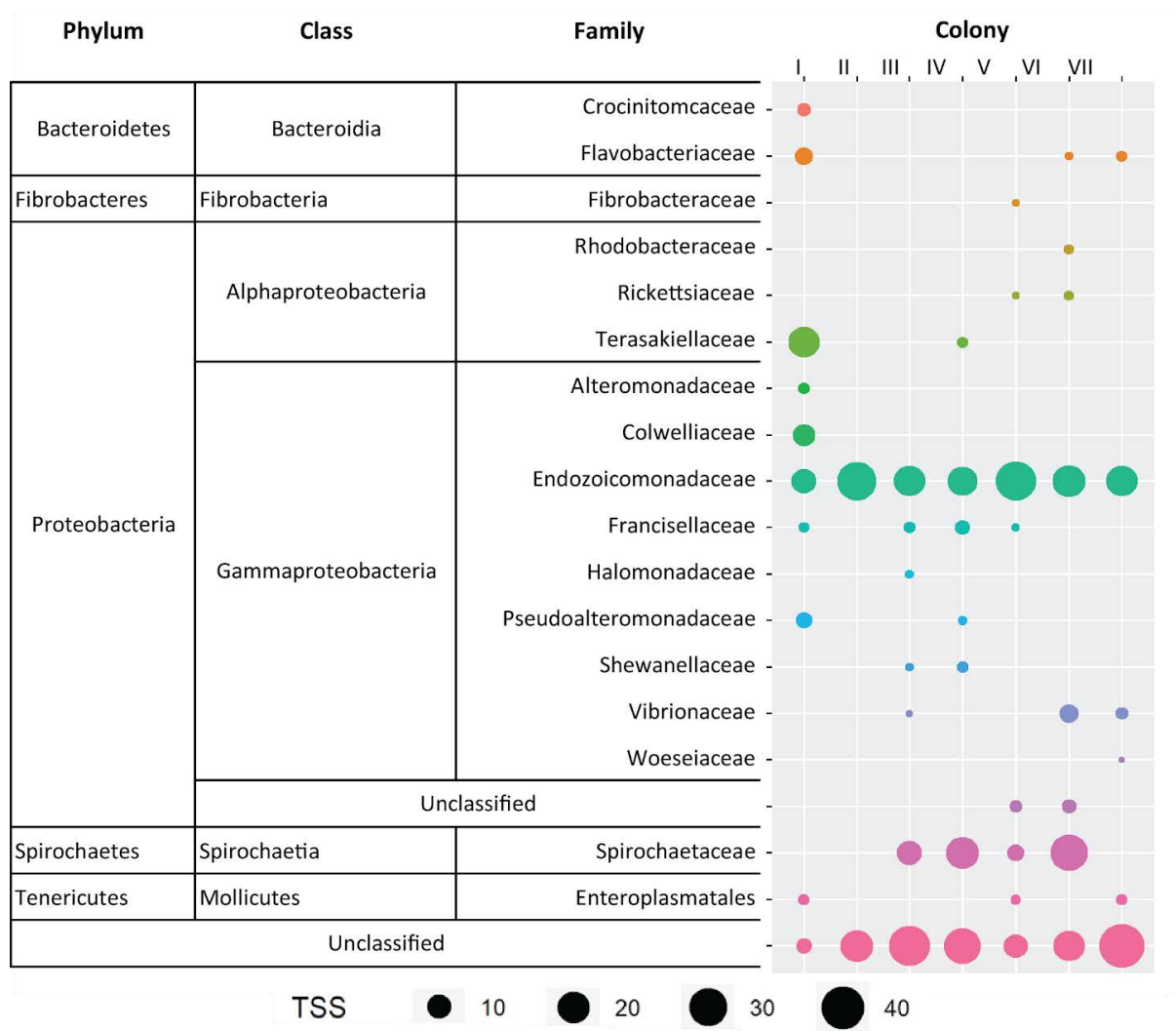


Figure 2.1: Bacterial community composition and diversity between 7 colonies of *Lobophytum pauciflorum* along Y-axis. Point size represents relative abundance of sequences (total standardized sum). Taxa affiliated with less than 0.5 % of sequences were not included.

Proteobacteria-affiliated sequences dominated colonies I, II and V and made up about half of the community in the remaining 4 colonies. Abundant in all replicates in colonies III, IV and VI (16.9 %, 36.9 %, 37.2 %, respectively), Spirochaetes-affiliated sequences were not retrieved from colonies I or II, made up 3.9 % in one replicate from colony V and only 34 reads total were retrieved from colony VII. Cumulatively, sequences affiliated with Proteobacteria and Spirochaetes made up 98.1 % of all successfully classified sequences. The next most abundant phyla affiliated with sequences here were Bacteroidetes (1.1%) and Tenericutes (0.4 %).

Sequences within the Proteobacteria mostly affiliated with the Gammaproteobacteria class (96.2 % of Proteobacteria). Alphaproteobacteria-affiliated sequences were only abundant in colony I

(19 % of community, <2 % in other colonies). At the family level, 93.7 % of Gammaproteobacteria-affiliated sequences across all samples were classified as Endozoicomonadaceae. Other Gammaproteobacteria families which were distributed across colonies but with lower read count include Vibrionaceae (1.5 %), Francisellaceae (1.1 %), Pseudoalteromonadaceae (0.9 %), Colwelliaceae (0.9), Shewinellaceae (0.5 %). The sequences affiliated with Pseudoalteromonadaceae (*Pseudoalteromonas* sp.) and Colwelliaceae (*Thalassotalea* sp.) were also highest in Colony I. Sequences affiliated with Spirochaetes were all classified to the genus *Spirochaeta* in the family Spirochaetaceae. Taken together, the sequences affiliated with the families Endozoicomonadaceae and Spirochaetaceae comprised 69.7 % of all sequences and 90.5 % of classified sequences.

Unclassified sequences input to BLAST comprised 44 distinct ASVs, 34 of which received BLAST hits with significance greater than $1e^{-5}$ (Appendix A). Some of the unclassified sequences were in high relative abundance across the dataset including Lentisphaeraceae (NR_145667.1) (35.9 ± 12.4 %) and Spirochaetaceae (NR_104732.1) (8.6 ± 3.1 %) in colony VII, Kiloniellaceae in colony II (10.75664540) (21.9 %). Sequences recovered in high relative abundance from colony III (27.8 ± 7.3 %) and IV (17.3 ± 12.2 %), in lower abundance from colony VI (10.7 ± 11.8 %) and from 1 sample of colony V (10.0 %) affiliated with Rhodospirillaceae (NR_159190.1) though members of this family were not a prominent component of the *L. pauciflorum* associated bacterial community according to classification with SILVA.

2.3.3 Ubiquitously distributed ASVs recovered from *L. pauciflorum*

A total of 26 ASVs were identified in more than 75% of samples, 15 of which were distributed across 100 % of samples ("core ASVs [1-15]") (Table 2.2). Of the 15 universally distributed ASVs, 14 belonged to the family Endozoicomonadaceae. The ASVs in this group also include the most abundant sequences in the dataset. The consensus identity sequence of the 14 potential core Endozoicomonadaceae-affiliated sequences aligned 98.2% to *Parendozoicomonas haliclona* (NR_157681) and 98.1 % to *Endozoicomonas ascidicola* (NR_146693). Individual BLAST alignments of these 15 ASVs matched most closely to either *Endozoicomonas montiporae* (NR_116609) or *Parendozoicomonas haliclona* (NR_157681) with the exception of core_ASV_15 which aligned most closely to *Endozoicomonas euniceicola* (NR_109684). The dominant Endozoicomonadaceae-affiliated sequences in *L. pauciflorum* from the Wessels (*et al.* 2017) dataset also aligned most closely to *P. haliclona* in BLAST.

Table 2.2: Ubiquitous amplicon sequence variants (ASVs) recovered from *Lobophytum pauciflorum* (>100%; 75 % distribution across samples) may be members of a conserved, 'core' community.

ASV	Sample Distribution	Relative Sequence Abundance	Top BLAST Alignment				
			Grade	NCBI	Family	Organism	Source
core_ASV_01	100%	14.8%	98.9%	NR_157681	Endozoicomnadaceae	Parendoziomonas haliclonae	<i>Haliclona</i> (Sponge)
core_ASV_02	100%	9.6%	99.0%	NR_157681	Endozoicomnadaceae	Parendoziomonas haliclonae	<i>Haliclona</i> (Sponge)
core_ASV_03	100%	7.9%	92.5%	NR_145667	Lentisphaeraceae	Lentisphaerae profundi	Deep seawater (Japan)
core_ASV_04	100%	5.3%	98.8%	NR_157681	Endozoicomnadaceae	Parendoziomonas haliclonae	<i>Haliclona</i> (Sponge)
core_ASV_05	100%	4.0%	98.9%	NR_157681	Endozoicomnadaceae	Parendoziomonas haliclonae	<i>Haliclona</i> (Sponge)
core_ASV_06	100%	2.7%	99.0%	NR_116609	Endozoicomnadaceae	Endozoicomonas montiporae	<i>Montiporae aequituberculata</i> (Hard Coral)
core_ASV_07	100%	2.2%	98.9%	NR_116609	Endozoicomnadaceae	Endozoicomonas montiporae	<i>Montiporae aequituberculata</i> (Coral)
core_ASV_08	100%	2.1%	98.8%	NR_157681	Endozoicomnadaceae	Parendoziomonas haliclonae	<i>Haliclona</i> (Sponge)
core_ASV_09	100%	1.8%	99.3%	NR_116609	Endozoicomnadaceae	Endozoicomonas montiporae	<i>Montiporae aequituberculata</i> (Coral)
core_ASV_10	100%	1.7%	99.0%	NR_116609	Endozoicomnadaceae	Endozoicomonas montiporae	<i>Montiporae aequituberculata</i> (Coral)
core_ASV_11	100%	1.6%	98.6%	NR_157681	Endozoicomnadaceae	Parendoziomonas haliclonae	<i>Haliclona</i> (Sponge)
core_ASV_12	100%	1.5%	99.2%	NR_116609	Endozoicomnadaceae	Endozoicomonas montiporae	<i>Montiporae aequituberculata</i> (Coral)
core_ASV_13	100%	1.5%	99.3%	NR_116609	Endozoicomnadaceae	Endozoicomonas montiporae	<i>Montiporae aequituberculata</i> (Coral)
core_ASV_14	100%	0.3%	98.3%	NR_116609	Endozoicomnadaceae	Endozoicomonas montiporae	<i>Montiporae aequituberculata</i> (Coral)
core_ASV_15	100%	0.2%	97.7%	NR_109684	Endozoicomnadaceae	Endozoicomonas euniceicola	Octocorallia spp.
core_ASV_16	94%	0.7%	99.1%	NR_157681	Endozoicomnadaceae	Parendoziomonas haliclonae	<i>Haliclona</i> (Sponge)
core_ASV_17	94%	0.6%				<i>no match</i>	
core_ASV_18	94%	0.3%	98.8%	NR_157681	Endozoicomnadaceae	Parendoziomonas haliclonae	<i>Haliclona</i> (Sponge)
core_ASV_19	88%	0.2%	99.2%	NR_149235	Halomonadaceae	Halomonas urumqiensis	Saline-Alkaline Lake (China)
core_ASV_20	88%	0.2%	89.6%	NR_149301	Xanthomonadaceae	Luteimonas arsenica	Contaminated Soil (China)
core_ASV_21	82%	0.2%	100.0%	NR_117771	Shewanellaceae	Shewanella sp.	Culture
core_ASV_22	76%	0.6%	98.1%	NR_118553	Francisellaceae	Francisella persica	<i>Argas persicus</i> (Arthropod)
core_ASV_23	76%	0.4%	91.6%	NR_041589	Bacillaceae	Lysinibacillus parvivoronicapiens	Soil (Turkey)
core_ASV_24	76%	0.2%	99.1%	NR_116609	Endozoicomnadaceae	Endozoicomonas montiporae	<i>Montiporae aequituberculata</i> (Coral)
core_ASV_25	76%	0.2%	97.6%	NR_146691	Endozoicomnadaceae	Endozoicomonas ascidiicola	<i>Asciidiella</i> sp. (Coral)
core_ASV_26	76%	0.1%	98.6%	NR_125480	Prochloraceae	Prochlorococcus marinus	Culture

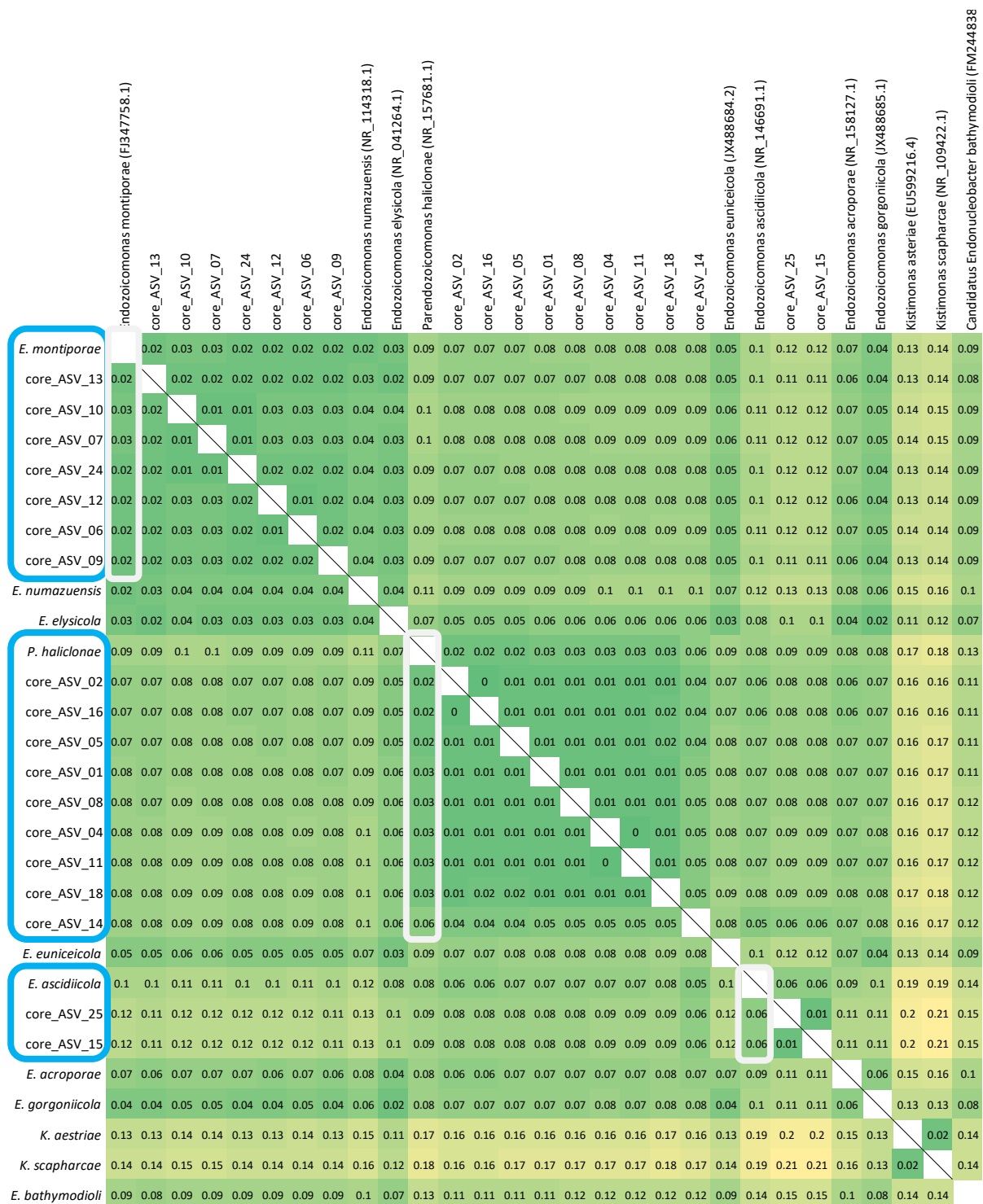


Figure 2.2: Bayesian distances between core amplicon sequence variants (ASVs) in *Lobophytum pauciflorum* and Endozoicomonadaceae type strains for phylogenetic tree building. The 3 ASV clusters are highlighted with their distance to the closest type strain.

The single universally distributed ASV not affiliated with Endozoicomonadaceae, (coreASV_11), was not classified beyond the domain of Bacteria but the closest alignment in BLAST affiliated with an uncultured strain of Lentisphaerae. When the sequence was trimmed to 220 bp and analysed with the larger Octocorallia dataset it was then classified as Lentisphaerae during feature assignment with the SILVA database. This sequence contributed 40.1 % of the community in Colony VII but only 1.9 ± 1.4 % in the rest of the colonies.

In addition to these 15 universally distributed ASVs, 11 other ASVs (core_ASV_[16-26]) were present in all but a few samples and present a much more diverse group of potential core ASVs (Table 2.2). Many were affiliated with Gammaproteobacteria, including 4 more ASVs affiliated with Endozoicomonadaceae (core_ASV_[16,18,24 and 25]) and single ASVs affiliated with each of the families Francisellaceae, Halomonadaceae, Shewinellaceae and Xanthomonadaceae (core_ASV_[22, 19, 21 and 20], respectively). Single ASVs affiliated with two additional phyla, Firmicutes (Family Bacillaceae) and Cyanobacteria (Family Prochloraceae), were also recovered from more than 75 % of samples.

The phylogenetic relationship between the 18 *Endozoicomonas*-affiliated core_ASVs suggests that they are closely related but may represent at least three distinct species (Figure 2.2). The ASVs were primarily assigned to 2 large clades near the type strains for *E. montiporae* (core_ASV_[06,07,09,10,12,13,24]; posterior probability = 0.96) and *P. haliclona* (core_ASV_[01,02,04,05,08,11,14,16,18]; 0.83) (Figure 2.3). The remaining two ASVs (core_ASV_[15,25]) were assigned to their own branch (1.0) closest to the type strain for *E. ascidiicola* (0.59). The ASVs in highest relative abundance in the *L. pauciflorum* 16S community were assigned to *Parendozoicomonas haliclona*.

2.3.4 Comparison with other available datasets

Sequences derived from this study were compared to 16S rRNA community sequences from two additional datasets. First, the dataset was compared with the previous *L. pauciflorum*-derived 16S rRNA gene sequences (data from Wessels *et al.* 2017). Dissimilarity between the datasets was significant (PERMANOVA, $p=0.001$), and they clustered entirely apart in Bray-Curtis and UNIFRAC (unweighted) PCoA. Phylogenetic diversity was 14x higher in the prior dataset than the current study (94.2 ± 29.9 PD and 6.6 ± 2.6 PD, respectively), although mean evenness was the same in both (0.6 ± 0.05 e) (Table 2.3). Alpha rarefaction subsampled at 44,000 reads was sufficient to capture the full diversity present.

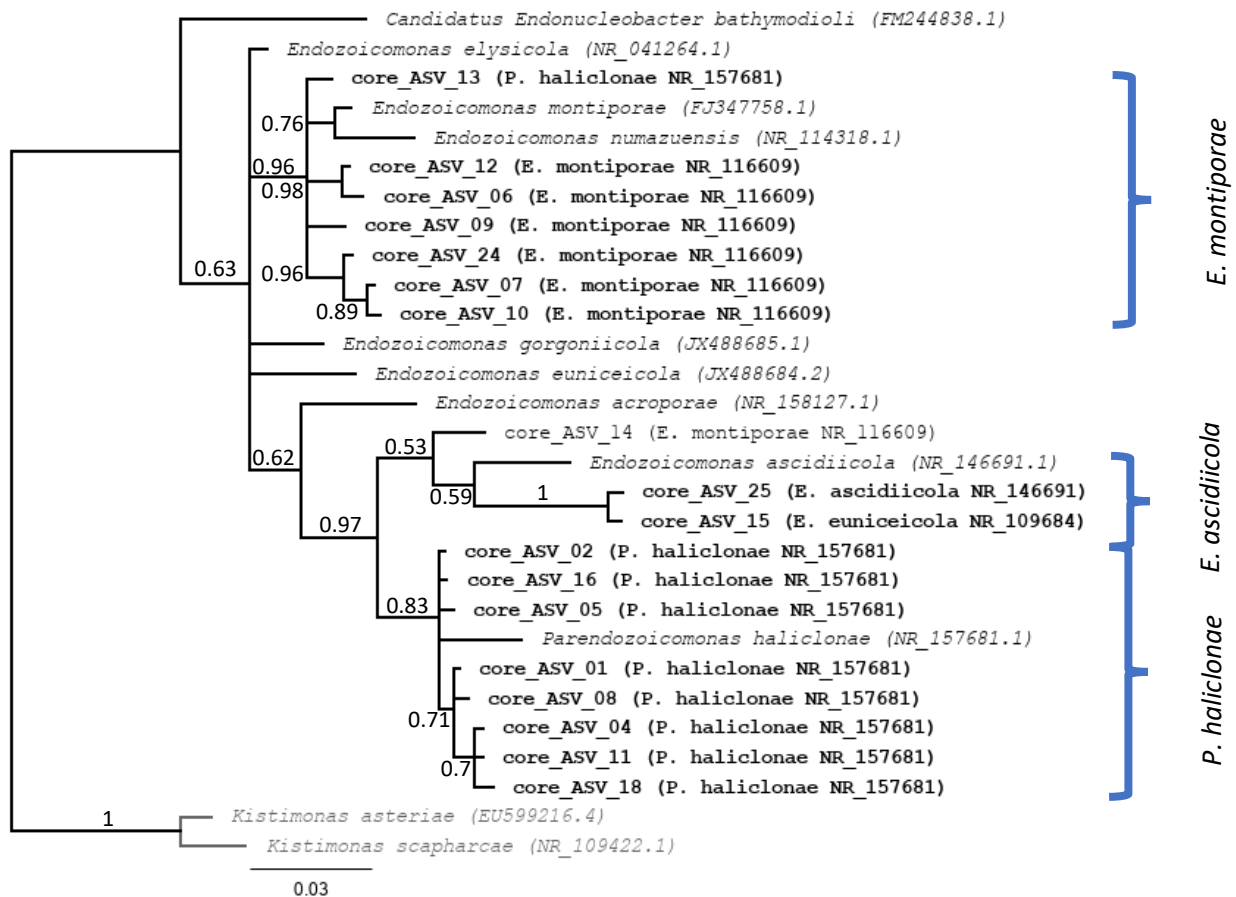


Figure 2.3: Bayesian phylogenetic tree of type strains and core amplicon sequence variants (ASVs) affiliated with Endozoicomonadaceae. The tree was built on a 442 bp aligned region extracted from a MAFFT alignment with Hasegawa-Kishino-Yano '85 (Hasegawa *et al.* 1985) and rooted to the genus *Kistimonas* spp. Type strains are in italic with NCBI accession number in parentheses. Core ASVs from this study are named as such followed by the closest aligned identity match in BLAST in parentheses and are marked in bold.

Despite differences in alpha diversity, both *L. pauciflorum* datasets were dominated by sequences affiliated with Endozoicomonadaceae and Spirochaetaceae. Overall distribution and relative abundance of sequences affiliated with Spirochaetaceae were greater in the prior data and Endozoicomonadaceae in the current study. Spirochaetes dominated 100 % of the colonies sampled in Wessels (*et al.* 2017), but only 43 % of the colonies in the current dataset. Both datasets also had a large, unclassified fraction of the community, 36 % and 22 %, respectively. Sequences affiliated with Spirochaetaceae were dominant in 3 of the 7 colonies in the current study but were dominant in all colonies from the previous study. Unfortunately, only 1 sample was collected from each colony in Wessels *et al.* (2017) making it difficult to explicitly explore intercolonial variability or to parse the influence of time from intercolonial variability to compare the datasets over time.

The 16S rRNA gene community of *L. pauciflorum* (current study) was compared to other soft coral hosts for which data were available to provide context among the Octocorallia (data from O'Brien *et al.* 2020). In Alpha diversity metrics, evenness was similar between host genera, but phylogenetic diversity varied (Table 2.3). The alpha diversity of *L. pauciflorum* was similar to the other alcyoniids, as well as *Pinnigorgia* and *Xenia*. The host genera *Isis*, *Clavularia* and *Briareum* showed 4-, 6- and 7-fold higher diversity than *L. pauciflorum*. *Clavularia* and *Briareum* also displayed over an order

Table 2.3: Alpha diversity metrics and dominant bacterial families in each host genus. Evenness was estimated according to Pielou evenness index and diversity by Faith's phylogenetic diversity index and taking the mean across replicates. The percent community contribution presented for dominant bacterial affiliations were calculated by total sum standardization within each host genus.

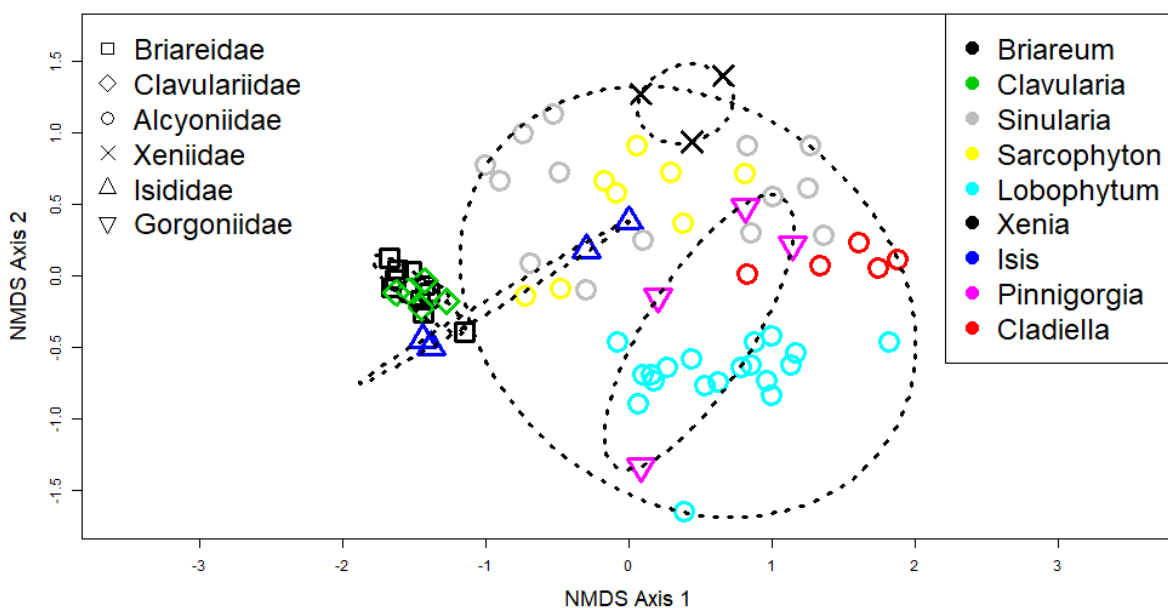
Host Genus	Host Family		Replicates			ASVs	Evenness	Diversity	Dominant Bacterial Families
	Host Family	Replicates	Sequences	ASVs	Evenness				
<i>Lobophytum</i>	Alcyoniidae	19	25505 ± 8704	41.3 ± 18	0.5 ± 0.12	11.4 ± 3.9	Endozoicomnadaeae (57.42 %) Spirochaetaeae (21.2 %)		
<i>Briareum</i>	Briareidae	10	42134 ± 17752	651.3 ± 283	0.7 ± 0.07	77.4 ± 22.3	Unclassified Bacteria (16.2 %) Uncultured Alphaproteobacteria (11.4 %) Endozoicomnadaeae (9.7 %)		
<i>Cladiella</i>	Alcyoniidae	5	24432 ± 5695	25.2 ± 9	0.6 ± 0.06	8.1 ± 1.9	Endozoicomnadaeae (64 %) Entomoplasmatales Incertae Sedis (33.7 %)		
<i>Clavularia</i>	Clavulariidae	5	54961 ± 9665	605.8 ± 77	0.7 ± 0.04	66.1 ± 9.6	Endozoicomnadaeae (19.2 %) Unclassified Bacteria (14.9 %) Uncultured Alphaproteobacteria (10.6 %)		
<i>Isis</i>	Isididae	4	21536 ± 10817	290.5 ± 259	0.6 ± 0.24	42.4 ± 27.5	Rhodobacteraceae (15.1 %) Endozoicomnadaeae (11.3 %) Flavobacteriaceae (10.9 %)		
<i>Pinnigorgia</i>	Gorgoniidae	4	16442 ± 3703	46.5 ± 13	0.4 ± 0.06	13.3 ± 5.4	Endozoicomnadaeae (78.7 %) Unclassified Bacteria (9.2 %)		
<i>Sarcophyton</i>	Alcyoniidae	8	44321 ± 21927	88.6 ± 56	0.5 ± 0.06	19.8 ± 6.5	Endozoicomnadaeae (35.4 %) Unclassified Bacteria (29 %) Spirochaetaeae (16.1 %)		
<i>Sinularia</i>	Alcyoniidae	14	37744 ± 16486	73.9 ± 47	0.4 ± 0.14	15 ± 6.8	Endozoicomnadaeae (59.3 %) Unclassified Bacteria (15.4 %)		
<i>Xenia</i>	Xenidae	3	49588 ± 19244	44 ± 7	0.3 ± 0.12	10.7 ± 0.3	Unclassified Alphaproteobacteria (61 %) Endozoicomnadaeae (29.9 %)		
Total		72	2486545	5819	0.5 ± 0.2	26.9 ± 27.2			

of magnitude more ASVs present in each sample. Alpha rarefaction indicates that read depth and distribution are sufficient to encompass the majority of biological diversity present in the merged dataset, according to Shannon's Diversity Index and total ASV count.

Dissimilarity between the datasets was significant ($p = 0.001$), likely due to methodological differences between studies. A PERMANOVA on host species determined all samples relate better within host genus than between ($p = 0.001$) and were therefore aggregated by host genus for analysis. Furthermore, taxa belonging to the family Alcyoniidae were more similar to each other than to other host taxa ($p = 0.001$) and were therefore analyzed at the family level as well. Representation of the sequence data with NMDS showed that *Lobophytum* samples were not disproportionately distant from other host taxa, being clustered together and nearby other Alcyoniidae (Figure 2.4). The Gorgoniidae sample were widely dispersed but the centroid was very close to that of Alcyoniidae. The families Briareidae and Clavulariidae clustered apart from Alcyoniidae.

There were both similarities and differences between the 16S rRNA community composition of *L. pauciflorum* and the host taxa analysed. All host taxa were dominated by sequences affiliated with Proteobacteria (64.6 ± 17.2 % mean TSS) but only *Lobophytum* and *Sarcophyton* harbor Spirochaetes-affiliated sequences in high relative abundances (21.2 and 16.1 %, respectively; 0-0.4 %

Figure 2.4: Non-metric multi-dimensional scaling (NMDS) plot built on bacterial community composition of Octocorallia. For each sample, the shape designates family level and the color designates genus level phylogeny. Dotted lines show the distribution of samples from the same family. The *Lobophytum pauciflorum* samples (light blue circles) are clustered with other Alcyoniidae (circles).



in the other host genera). Only *L. pauciflorum* hosted sequences affiliated with Lentisphaerae in high relative abundance (8 %, <0.1% in the rest). The greatest contribution to Alcyoniidae differentiation as determined by SIMPER analysis was Endozoicomonadaceae (11.8-26.8 % of contribution). Spirochaetaceae also contributed (4.5-7.5 %) as *Lobophytum* and *Sarcophyton* were the only host genera associated with it and both are alcyoniids. Alphaproteobacteria contributed 6.4 % and 8.4 % of the dissimilarity between Alcyoniidae and Briareidae and Clavulariidae, respectively. Rhodobacteriaceae contributed 6.1 % of the dissimilarity between Alcyoniidae and Isididae. The Mollicutes family Enteroplasmatales contributed 3.4 % and 1.3 % of the dissimilarity between Alcyoniidae and Gorgoniidae and Xenidiidae, respectively.

2.3.5 Endozoicomonadaceae

A total of 69 ASVs (comprising 53.1 % of recovered sequences) affiliated with Endozoicomonadaceae were recovered from *L. pauciflorum* samples collected for this study, including those most abundant and well distributed ASVs. When the *L. pauciflorum* dataset from this study was merged with those from other soft coral hosts, sequences affiliated with Endozoicomonadaceae made

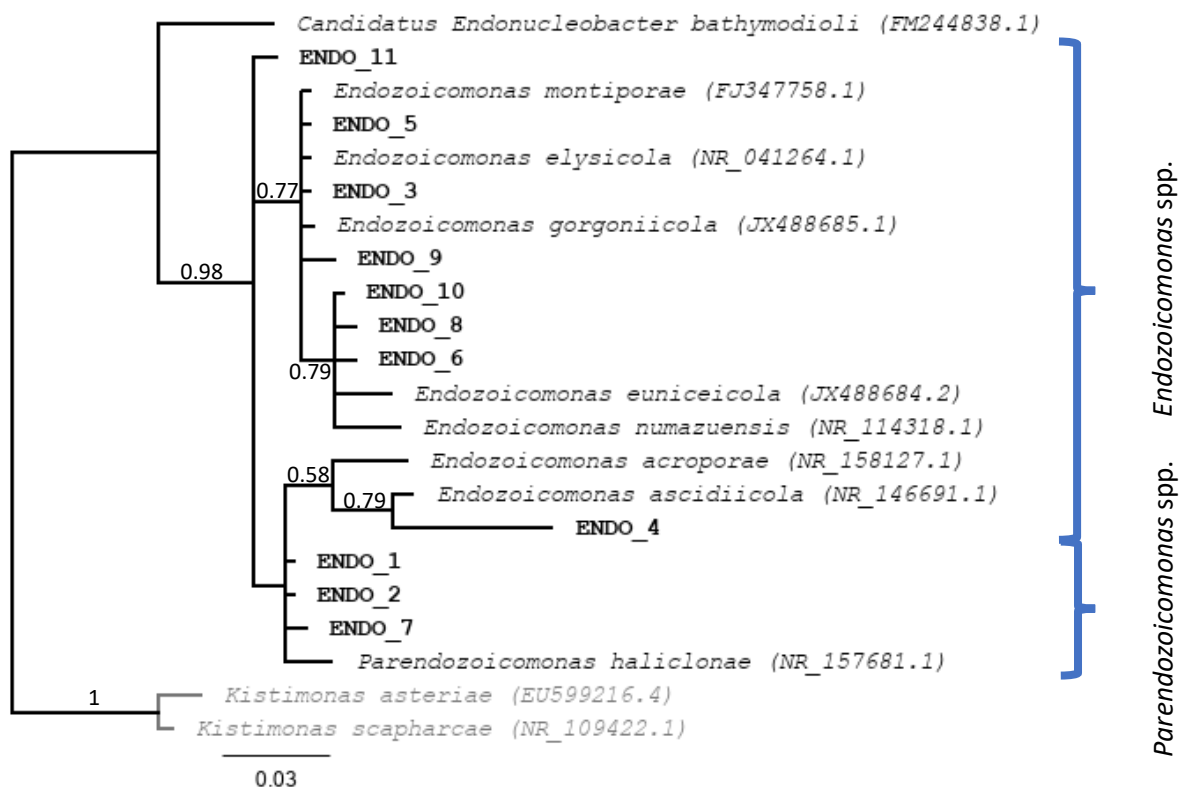


Figure 2.5: Bayesian phylogenetic tree of Endozoicomonadaceae-affiliated ASVs from host Octocorallia (bold) and type strains for common Endozoicomonadaceae genera (italic). The tree was built on a 216 bp region extracted from a MAFFT alignment and used the top IQTree-suggested substitution model Kimura 2-P (Kimura 1980).

Table 2.5: The most dominant ASVs affiliated with Endozoicomonadaceae (ENDO_[1-11]) and Spirochaetaceae (SPIRO_[1-7]) associated with soft coral host taxa. Top BLAST Alignment statistics refer to highest identity match in NCBI BLAST search.

	Total Number of Sequence Reads	Percent of Endozoicomonadaceae-affiliated Reads	Top BLAST Alignment				
			Organism	Source	Grade	NCBI Accession Number	Abundant in Host Genus
ENDOZOICOMONADACEAE - AFFILIATED ASVS							
ENDO_1	389083	39.1 %	<i>Parendoziomonas haliclona</i>	<i>Haliclona</i> (Sponge)	99.3 %	NR_157681	<i>Sarcophyton, Sinularia, Xenia, Cladiella, Clavularia</i>
ENDO_2	187877	18.9 %	<i>Parendoziomonas haliclona</i>	<i>Haliclona</i> (Sponge)	99.4 %	NR_157681	<i>Lobophytum</i>
ENDO_3	61324	6.2 %	<i>Endozoicomonas gorgoniicola</i>	<i>Eunicea fusca</i> (Soft Coral)	99.5 %	JX488684	<i>Sarcophyton, Sinularia, Cladiella</i>
ENDO_4	60060	6 %	<i>Endozoicomonas ascidiicola</i>	<i>Asciidiella</i> sp. (Sea Squirt)	97.9 %	NR_146691	<i>Sinularia</i>
ENDO_5	48278	4.9 %	<i>Endozoicomonas gorgoniicola</i>	<i>Eunicea fusca</i> (Soft Coral)	99.2 %	JX488684	<i>Lobophytum</i>
ENDO_6	41093	4.1 %	<i>Endozoicomonas gorgoniicola</i>	<i>Eunicea fusca</i> (Soft Coral)	99.1 %	JX488684	<i>Briareum, Clavularia</i>
ENDO_7	37675	3.8 %	<i>Parendoziomonas haliclona</i>	<i>Haliclona</i> (Sponge)	99.1 %	NR_157681	<i>Pinnigorgia, Clavularia</i>
ENDO_8	27991	2.8 %	<i>Endozoicomonas euniceicola</i>	<i>Octocorallia</i> spp.	99 %	JX488684	<i>Lobophytum</i>
ENDO_9	18225	1.8 %	<i>Endozoicomonas gorgoniicola</i>	<i>Eunicea fusca</i> (Soft Coral)	99.1 %	JX488684	<i>Cladiella</i>
ENDO_10	15521	1.6 %	<i>Endozoicomonas gorgoniicola</i>	<i>Eunicea fusca</i> (Soft Coral)	99.3 %	JX488684	<i>Sinularia, Cladiella</i>
ENDO_11	14455	1.5 %	<i>Endozoicomonas gorgoniicola</i>	<i>Eunicea fusca</i> (Soft Coral)	98.8 %	JX488684	<i>Briareum</i>
SPIROCHAETACEAE - AFFILIATED ASVS							
SPIRO_1	52494	32.3 %	<i>Spirochaeta cellobiosiphila</i>	<i>Cyanobacterial mat</i>	92%	NR_044505	<i>Lobophytum</i>
SPIRO_2	34816	21.4 %	<i>Alkalispirochaeta americana</i>	Freshwater (California)	91 %	NR_028820	<i>Sarcophyton</i>
SPIRO_3	34211	21 %	<i>Oceanispirochaeta litoralis</i>	<i>Marine mud</i> (Puerto Rico)	92.7	NR_104732	<i>Lobophytum</i>
SPIRO_4	14263	8.8 %	<i>Haloactinopolyspora alba</i>	Saline lake (China)	89.4 %	NR_116875	<i>Sarcophyton</i>
SPIRO_5	8692	5.3 %	<i>Spirochaeta cellobiosiphila</i>	<i>Cyanobacterial mat</i>	91.9 %	NR_044505	<i>Lobophytum</i>
SPIRO_6	8079	5 %	<i>Alkalispirochaeta americana</i>	Freshwater (California)	91 %	NR_028820	<i>Sarcophyton</i>
SPIRO_7	6020	3.7 %	<i>Oceanispirochaeta litoralis</i>	<i>Marine mud</i> (Puerto Rico)	92.7 %	NR_104732	<i>Lobophytum</i>

up 53.4 % relative sequence abundance among all Alcyoniidae, compared with 78.7 % in *Pinnigorgia*

and a mean of only 17.5 ± 9.2 % among other host taxa. The metadataset showed high sequence variability with 94 ASVs affiliated with Endozoicomonadaceae; only 30 ASVs had more than 1,000 reads. The most abundant ASVs were disproportionately enriched, with 11 sequences (each over 12,000 reads) together comprising 94 % of all Endozoicomonadaceae-affiliated reads across all host taxa (Figure 2.5). The 2 most dominant ASVs ENDO_1 (dominant in Lobophytum) and ENDO_2 (dominant in *Cladiella*, *Clavularia*, *Sarcophyton*, *Sinularia* and *Xenia*) were aligned most closely with *P. haliclona* in BLAST (Table 2.5). The other hosts harboured sequences affiliated with *Endozoicomonas* in equal or higher relative abundance than sequences affiliated with *Parendoziomonas*. The genus *Xenia* is the only genus with sequences affiliated with only a single Endozoicomonadaceae-affiliated ASV (coreASV_1), which aligned to *P. haliclona*.

In a Bayesian phylogenetic tree, most of the ASVs are spread across a diverse *Endozoicomonas* assemblage; three ASVs (ENDO_[3,5,9]) grouped with the type strains *E. montiporae*, *E. elysicola* and *E. gorgoniicola* (posterior probability = 0.77), and three (ENDO_[6,8,10]) with *E. euniceicola* and *E. ascidiicola* (0.79). The dominant ASVs ENDO_1 and ENDO_2, along with ENDO_7, were all assigned near *P. haliclona* (0.57). The results of this phylogenetic analysis suggest that the Octocorallia hosts included are associated with a diversity of *Endozoicomonas* species but that a strain closely related to *P. haliclona* dominates the Endozoicomonadaceae-affiliated community in the Alcyoniidae, especially in *L. pauciflorum* and the gorgonian *Pinnigorgia* spp.

2.3.6 Spirochaetaceae

In the *L. pauciflorum* dataset, 6 ASVs affiliated with Spirochaetes all of which classified to the genus "*Spirochaeta 2*". Merging the dataset with that of other host corals showed that domination by Spirochaetes-affiliated sequences was shared only with the alcyoniid host *Sarcophyton*, together containing 21 ASVs. No ASVs were shared between hosts, probably due to sequencing run bias and differing methodology. However, 7 ASVs account for 98 % of all Spirochaetes-affiliated sequence reads (Table 2.5) which were assigned to 2 distinct clusters in a Bayesian phylogenetic tree (Figure 2.6). Cluster I was comprised of the ASVs Spiro_[1,2,4,5 and 6] as well as 2 strains (HQ288601.1 and

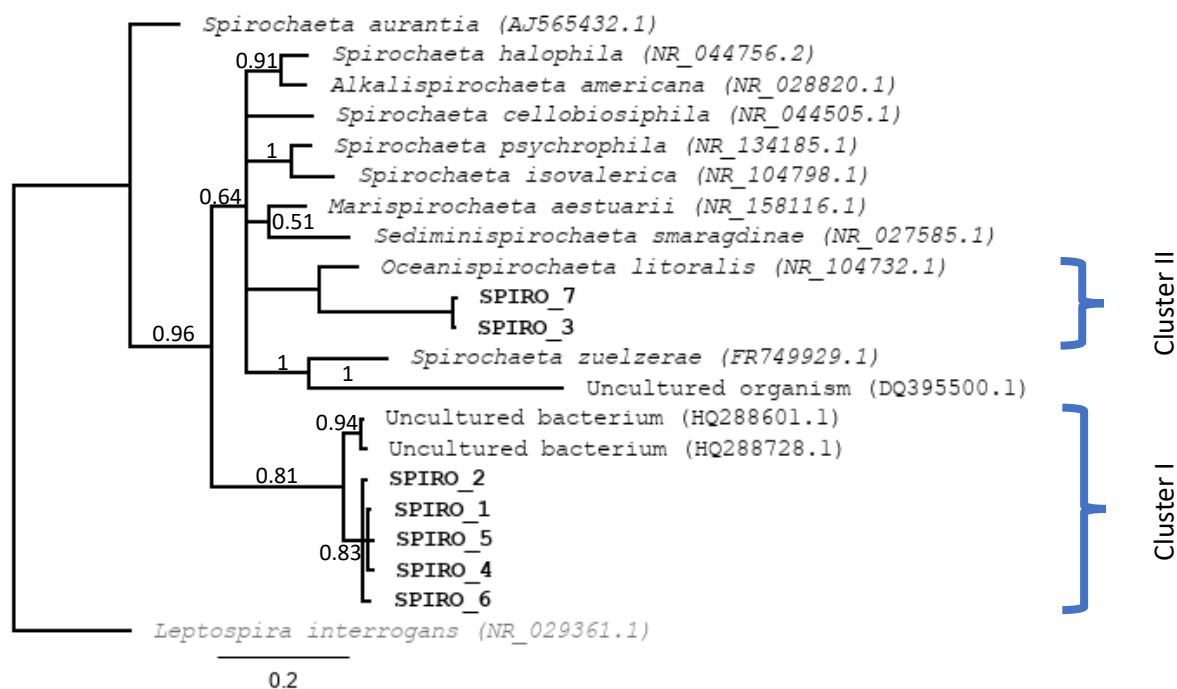


Figure 2.6: Bayesian phylogenetic tree Spirochaetes-affiliated ASVs recovered from Octocorallia hosts (bold) and Spirochaetes type strains from NCBI. The tree was built on a 215 bp extracted region of a MAFFT alignment using the HKY85 substitution model (Hasegawa *et al.* 1985). IQTree Modelfinder recommended several transversion-transition models (TVM, TIM and TPM) which were not executable in Geneious so HKY85 was selected as the next-most-favorable option.

HQ288728.1) isolated from fire corals in the Red Sea (Paramasivam *et al.* 2013). The most dominant Spirochaetes-affiliated ASVs in both *L. pauciflorum* (SPIRO_1) and *Sarcophyton* spp. (SPIRO_[2,4]) were included in Clade I. The remaining 2 ASVs SPIRO_3 and SPIRO_7 were assigned to a second clade positioned near *Oceanispichoeta litoralis* (0.03).

2.4 Discussion

2.4.1 The bacterial community of *L. pauciflorum*

This study profiles the bacterial community of *L. pauciflorum* via 16S rRNA gene amplicon sequencing reporting a diverse bacterial community largely defined by sequences affiliated with Endozoicomonadaceae. The relative abundance of Endozoicomonadaceae-affiliated sequences in *L. pauciflorum* contributed both to differences and similarities with the microbiome of other soft coral host taxa. While Endozoicomonadaceae-affiliated sequences were recovered from all host taxa analysed here, they were recovered in highest relative abundance from the Alcyoniidae and the gorgonian. In Alcyoniidae and Gorgoniidae, more ASVs affiliated with Endozoicomonadaceae aligned

to the genus *Parendozoicomonas* spp. than *Endozoicomonas* spp., a relationship which is inverted in the other host taxa analysed here. Phylogenetic analysis suggests that, while several distinct strains of Endozoicomonadaceae are likely present in the dataset, similar ASVs are also distributed across multiple host taxa.

Close associations with members of *Endozoicomonas* have been identified in many hard and soft corals from around the world (Morrow *et al.* 2012; Bayer *et al.* 2013; Robertson *et al.* 2015; van de Water *et al.* 2016; Neave *et al.* 2016, 2017 b; Ziegler *et al.* 2019). The genus *Endozoicomonas* was only recently recharacterized as the Family Endozoicomonadaceae, and *Parendozoicomonas* described as a genus within (Bartz *et al.* 2018), therefore it is possible that sequences which would now be affiliated with *P. haliclona* were overlooked in previous studies. *Endozoicomonas* had been classified as a genus in the Hahellaceae family and is now considered a family of Oceanospirillales, which is composed of the genera *Endozoicomonas*, *Parendozoicomonas*, *Kistimonas* and *Endonucleobacter* (Bartz *et al.* 2018).

Analyses of the genomes of *Endozoicomonas* spp. are consistent with their adaptation to life as symbionts, as their complements of genes are involved in secretion and transport pathways. Patterns of genomic degradation and repeat patterns identified in *Endozoicomonas* spp. also resemble those of known symbiont strains. The ability to digest glycoproteins may help to bypass the mucus layer (glycoproteins). Likewise the ability to digest testosterone – an animal hormone present in the tissue of *Euphyllia ancora* year round (Twan *et al.* 2006) – may assist in recognizing host tissue. Ephrin-signalling may help to hide the symbiont from the host defences (Ding *et al.* 2016). The genome of *E. acropora* included genes involved in nitrogen, carbon and phosphorus cycling pathways as well as the metabolism of glucose (Sheu *et al.* 2017) and dimethylsulfoniopropionate (Tandon *et al.* 2020). Furthermore, a metanalysis of Bacteria associated with Sclerectinia, Octocorallia and Porifera demonstrated a degree of phyllosymbiosis between Endozoicomonadaceae and Octocorallia, consistent with a close evolutionary relationship (O'Brien *et al.* 2020).

This study indicates that *L. pauciflorum* hosts *Parendozoicomons* spp. in higher abundance than *Endozoicomonas* spp. and in higher abundance than most other host taxa analysed. While the full genome of *P. haliclona* has been analysed for phylogenetic distinction, function and metabolic pathways have not been as comprehensively assessed as in the case of *Endozoicomonas* spp. The initial study (Bartz *et al.* 2018) determined that the *P. haliclona* type strains are mesophilic, facultative anaerobes with optimal growth at 25°-30° C and pH 7-8. Enzyme activity assays suggest the metabolic pathways of *P. haliclona* may also differ from *Endozoicomonas* spp. The type strain for *P.*

haliclona was, however, able to reduce nitrate to nitrite (but not nitrogen), produce indole and esculin but was unable to digest or assimilate glucose. Ding and colleagues (2016) predicted that symbiosis with *Endozoicomonas* spp. would rely on provisions of glucose from the host, which if true suggests the nature of a host-symbiont relationship with *Endozoicomonas* and *Parendoicomonas* may rely on completely different metabolic pathways within the holobiont despite their close phylogenetic relationship.

The majority of sequences associated with the potential core community is attributed to Endozoicomonadaceae but some diversity was still observed. A single ASV related to Lentisphaerae is present throughout all *L. pauciflorum* samples. Lentisphaerae has been found associated with healthy colonies of the hard coral *Mussismilia* spp. (De Castro *et al.* 2010) and juvenile *Coelastrea* (Williams *et al.* 2015) but has not often been reported in abundance in corals. Species related to Shewinellaceae, Enteroplasmatales and Francisellaceae were distributed among most samples in low abundance. *Shewinella* spp. has previously been isolated from corals (Rhower *et al.* 2001, Kellogg 2008, Raina *et al.* 2009). In the alcyoniid *Alcyonium digitatum*, *Shewinella* spp. demonstrated antimicrobial activity against pathogens (Pham *et al.* 2016). Francisellaceae has been reported as a member of the core community in soft corals previously and could suggest a host-symbiont relationship which has not been documented in Scleractinia (Kellogg *et al.* 2016, Holm and Heidelberg 2016, van der Water 2018).

2.4.2 Variability between colonies of *L. pauciflorum*

This study outlined several highly conserved species that may have implications to the health of the host, but some degree of variability was also clear between *L. pauciflorum* colonies. Some ASVs which were ubiquitous among samples in low relative abundance were recovered in high relative abundance from just 1 or 2 colonies. Examples include Alphaproteobacteria and Cyanobacteria in Colony I, and Lentisphaerae in Colony VII. Several samples also harbor a high relative abundance of sequences affiliated with Bacteroidetes, Francisellaceae, Vibrionaceae and other taxa in the rarefaction of other colonies suggesting that the rare members of the community may be opportunistic to an extent. An alternative to opportunism could be interchangeability aligned with function rather than taxonomy, where a variety of bacteria with similar functions may be able to fill the same niche in the holobiont. Variability in bacterial community structure has also been interpreted as potentially reflecting adaptability of the holobiont to changing environmental conditions, with some host species expressing a higher tolerance for variability than others (Ziegler *et al.* 2019).

The relative abundance and distribution of Spirochaetaceae across samples suggests a relationship in which organisms affiliated with Spirochaetaceae may be facultative symbionts of *L. pauciflorum*. Spirochaetaceae are common endosymbionts in a range of hosts from termites (Lilburn *et al.* 2001) to marine sponges (Neulinger *et al.* 2010) and have been recovered from deep-sea Octocorallia (Weiler *et al.* 2018). Free-living and environmental strains of Spirochaetes are both efficient nitrogen fixers (Lilburn *et al.* 2001). Sequences affiliated with Spirochaetes dominated every colony from the previous study (Wessels *et al.* 2017) and half of the colonies in the current study. When these sequences were present in a colony in this study, they were often in similar or greater relative abundance as Endozoicomonadaceae but represented by a much lower number of ASVs. A reduction in Endozoicomonadaceae-affiliated sequences in communities where they normally dominate is a pattern previously been ascribed to disease-related dysbiosis (Gignoux-Wolfsohn *et al.* 2016, Quintanilla *et al.* 2018), however all colonies were visually assessed upon sample collection appeared equally healthy. It should be noted that, while sample location was not a factor being analyzed in this study, 2 of the colonies absent Spirochaetes (I and II) were collected from an outcropping of reef with high cover of living substrate. As the remaining colonies were collected from the reef floor surrounded by a mix of living substrate and coral rubble, the differences between their local surroundings could have influenced the proliferation of Spirochaetaceae and the increased diversity of colony I.

A correlation between host phylogeny and associated microbiota has been identified in corals, indicating phyllosymbiosis and, therefore, a degree of coevolution between the host and symbiont (Zilber-Rosenberg and Rosenberg 2008, O'Brien *et al.* 2019, 2020). Sequences from this study affiliated with Lentisphaerae or Spirochaetaceae do not follow this pattern. Lentisphaerae is a small phylum commonly recovered in low abundance from hard (de Castro *et al.* 2010, Pootakham *et al.* 2017) and soft corals (Correa *et al.* 2013, Kellogg *et al.* 2016, Lawler *et al.* 2016). Sequences affiliated with Spirochaetaceae were abundant in 2 of the 5 Alcyoniidae (*Lobophytum* and *Sarcophyton*) and none of the other host genera. Another study found Spirochaetes-affiliated sequences also dominated (~72.4 %) the microbiome of an alcyoniid *Corallium rubrum* over Endozoicomonadaceae (~3.4 %) (van de Water *et al.* 2016). However, A study of 2 species of *Anthothela* and 1 Alcyoniidae found Spirochaetes absent from the Alcyoniidae (*Alcyonium grandiflorum*) but present in both *Anthothela* species (Lawler *et al.* 2016). The relationship between Octocorallia and Spirochaetes is therefore not restricted to the Alcyoniidae, nor is it widely distributed within the family.

One possible explanation regarding the distribution of Spirochaetes and Lentisphaerae among colonies and host genera is that the metabolic functions of bacterial associates may in some cases be more important than the taxonomic affiliation. Some members may shift in relative abundance to

match metabolic requirements of the host or environmental stressors that arise. Endozoicomonadaceae have previously been proposed to play a regulatory role in the bacterial community structure in corals (Neave *et al.* 2016), but if variation is a result of reduced relative abundance of Endozoicomonadaceae and the respective regulatory influence, it is unknown what would cause this reduction in these colonies. The same pattern was observed in *L. pauciflorum* sampled in 2013 and 2014, a study that also demonstrated the relatively high resiliency of the holobiont community to environmental change (Wessels *et al.* 2017) While we cannot deduce this conclusively from this study, the community characterized here can be described as a diverse array of rare taxa heavily dominated by Endozoicomonadaceae and tolerant of some substantial shifts in community composition and structure.

2.4.3 Conclusion

This study successfully produced a comprehensive characterization of the 16S rRNA community of the model alcyoniid *L. pauciflorum* to serve as a baseline in future studies and provided intriguing insight into intimate and complex host-symbiont relationships. The microbiome of *L. pauciflorum* is dominated by sequences affiliated with the family Endozoicomonadaceae, commonly abundant in soft corals, but is the first to recover dominant sequences aligned with the genus *Parendoziomonas* spp. This study found the bacterial community structure of soft corals to harbor both similarities and differences among one another. The conserved and variable community factions affiliated with *L. pauciflorum* in this study demonstrate the need to understand symbiont function before conclusive deductions can be made on the benefit or detriment of the observed associations. Apparently healthy colonies dominated by Endozociomonadaceae revealed high variability in bacterial community structure indicating that *L. pauciflorum* is a plastic holobiont under the influence of multiple factors shaping the microbiome. These results also highlight an undefined relationship with members of Spirochaetaceae, a group which does not conform to host phylogeny and can be completely absent from or highly abundant in an *L. pauciflorum* colony without causing apparent phenotypic consequences in the holobiont. The relationship between Octocorallia and Spirochaetaceae should be explored further as should the metabolic potential for *Parendoziomonas* spp. as a symbiont in soft corals.

Chapter 3: Bacterial communities in microhabitats of the Alcyoniidae *Lobophytum pauciflorum*

Abstract

The microbiome associated with soft corals is poorly understood compared to other cnidarians. This study characterizes the bacteria associated with inner tissue, outer tissue and mucus layers of the soft leather coral *Lobophytum pauciflorum* using partial 16S rRNA gene amplicon sequencing. While the inner and outer tissue layers host similar communities of bacteria the mucus layer is distinct. Sequences recovered from the tissues affiliated with common coral associated bacterial taxa such as members of Endozoicomonadaceae, Rubritaliaceae, Shewinellaceae and Terasakiellaceae. Phylogenetic analysis of sequences affiliated with Endozoicomonadaceae highlight *Endozoicomonas ascidia*, *Endozoicomonas montiporae* and *Parendozoicomonas* spp. as the dominant members of the community. The mucus layer was characterized by sequences affiliated with Actinobacteria, Cyanobacteria, Planctomycetes, and Verrucomicrobia. Analysis of the putative roles of bacterial communities associated with each microhabitat suggest that they may each perform distinct metabolic functions in the holobiont. This study highlights the need to localize symbionts in Alcyoniidae to address additional mechanisms mediating microbial community structure and to characterize the function of common associates of cnidarian hosts to better understand the host-symbiont relationships.

3.1 Introduction

The coral holobiont refers to a coral host and the diverse assemblage of resident microorganisms (Rhower *et al.* 2001). Some associated microbes appear intimately associated with the host, forming conserved (Turbaugh *et al.* 2007; Ainsworth *et al.* 2015; Hernandez-Agreda *et al.* 2017; van de Water *et al.* 2017), species-specific (Kvennefors *et al.* 2010; Morrow *et al.* 2012; Carlos *et al.* 2013; Chu *et al.* 2016; van de Water *et al.* 2017; Pollock *et al.* 2018) relationships with host corals. However, there are a number of factors influencing the microbiome in addition to host species. The age (Williams *et al.* 2015), depth (Klaus *et al.* 2007; Jensen *et al.* 2019) and location (Littman *et al.* 2009; Pantos *et al.* 2015; Zhang *et al.* 2015) of the host colony as well as environmental stress (Ducklow and Mitchell 1979), pollution (Klaus *et al.* 2007; Zhang *et al.* 2015) and mucus shedding (Glasl *et al.* 2016) are among the many variables found to influence the coral microbiome.

One method for helping to organize and stabilize associated microbiota in animal hosts is through compartmentalization via the provisioning of distinct microhabitats within the host. Studies often do not consider the portions of mucus, tissue layers or skeleton comprising the sample, which all host distinct communities of Bacteria and can also significantly influence the observed community (Pollock *et al.* 2018). In this study we explore distinct bacterial communities in the tissue and mucus layers of *Lobophytum pauciflorum* to better our understanding of microbial community structure in Alcyoniidae, the soft leather corals.

The hydrozoan *Hydra* is a model organism for studying host-bacteria interactions in Cnidaria and has provided insights into the mechanisms mediating the associated community (Augustin *et al.* 2017; Delnes *et al.* 2020). Members of the resident bacterial community are actively selected for and maintained by the host, partly by species-specific antimicrobial peptides (Fraune and Bosch 2007; Franzenberg *et al.* 2013). Compartmentalized microhabitat spaces within the host, along with cooperation with members of the rarefaction, is likely one reason why the two primary bacterial members associated with *Hydra* spp., *Duganella* and *Curvibacter*, cannot coexist outside of the host (Delnes *et al.* 2020). The epithelial mucus layer in *Hydra* spp. also provides a microhabitat for a bacterial community vital to the innate immune function in the host (Bosch *et al.* 2014). When the associated bacteria were removed from the epithelial layer, the host was quickly compromised by a fungal infection (Fraune *et al.* 2015; Shröder and Bosch 2016). Research on *Hydra* has provided evidence that the innate immune system arose in Cnidaria primarily to shape and maintain the resident probiotic microbiome and that the defence against pathogens is part of this maintenance (Augustin *et al.* 2010; Bosch 2014). The efficacy of this system is such that strains of *Hydra* raised in identical laboratory conditions for more than 30 years hosted more similar microbial communities to

the same species sampled in the field than to each other (Fraune and Bosch 2007). The *Hydra* model demonstrates the importance of cooperation between the host and associated bacteria, relying on distinct communities associated with microhabitats for successful holobiont function.

In Scleractinia, the mucus layer has also been shown to help maintain the associated microbiome (Ritchie *et al.* 2006; Glasl *et al.* 2016). The composition of the bacterial community associated with the coral mucus layer is distinct from that in the tissue (Zhang *et al.* 2015; Apprill *et al.* 2016, Engelen *et al.* 2018). While the mucus-associated bacterial community does not reflect passive colonization (Sweet *et al.* 2011a, Sweet *et al.* 2011b), many species, including pathogens, are thought to be transient members acquired from the surrounding environment (Bourne and Munn 2005, Sweet *et al.* 2011; Frade *et al.* 2016). Mechanisms must therefore be in place to restrict access to the host tissue by pathogens from the environment. Indeed, Bacteria isolated from coral mucus have demonstrated a range of powerful antimicrobial peptides which are able to inhibit the growth of known coral pathogens such as *Vibrio* spp. (Ritchie *et al.* 2006; Nissimov *et al.* 2009; Ibrahim *et al.* 2012; Setyaningsih *et al.* 2012; Kvennefors *et al.* 2012; Bharathi *et al.* 2013; Pham *et al.* 2016). Periodic shedding of the mucus layer has also been shown to help regulate the community in *Porites astreoides*, which returns to a healthy state (dominated by members of Endozoicomonadaceae and Oxalobacteraceae) each time an old layer was shed (over time became dominated by members of Verrucomicrobiaceae and Vibrionaceae) and a fresh one produced (Glasl *et al.* 2016).

Distinct communities have been characterized in microhabitats associated with the tissue and skeleton of hard corals, in addition to the mucus layer (Koren and Rosenberg 2006; Sweet *et al.* 2010; Tremblay *et al.* 2011; Pollock *et al.* 2018). Bacteria associated with coral tissue could potentially be involved in shared metabolic pathways in the holobiont (Bourne *et al.* 2016; Hernandez-Agreda *et al.* 2017; Robbins *et al.* 2019). The gastrovascular cavity also hosts a distinct bacterial community (Engelen *et al.* 2018; Bourne *et al.* 2016). Some of the most common associates of coral tissue include members of Endozoicomonadaceae (Bayer *et al.* 2013; Neave *et al.* 2017; Pogoreutz *et al.* 2018; Pollock *et al.* 2018). In the skeleton, endolithic bacteria are also diverse and displayed a high level of co-phylogeny across host Scleractinia, more-so than observed in bacteria associated with tissue or mucus (Pollock *et al.* 2018; Pernice *et al.* 2020). It has been suggested that endolithic microbes may help sustain the host when the overlying tissue has been bleached (Fine and Loya 2002).

The microbiome of Octocorallia has been far less studied than those of *Hydra* or Scleractinia. Fluorescence *in situ* hybridization imaging of the soft coral *Paramuricea clavulata* has shown intracellular bacterial aggregates in the autozooids (La Riviere *et al.* 2016). To date, only one study has characterized the bacterial communities in the tissue and mucus layers as separate microhabitats, in

one family of soft corals, Paragorgiidae, from the deep sea. Members of *Spirochaeta*, *Mycoplasma*, Flavobacteriaceae, Terasakiellaceae, Campylobacteria and Rickettsiales were associated with tissues, while the the Rhodobacteriaceae *Paracoccus* was associated with the mucus (Weiler *et al.* 2018). The distinction of microhabitats in the host has not been examined in Alcyoniidae or in any tropical soft corals, leaving a significant knowledge gap in understanding the structure and function of bacterial symbionts in Octocorallia.

The soft leather coral *Lobophytum pauciflorum* is a thick-encrusting dioecious octocoral and the lobes form simple, unbranched digits (Fabricius and Alderslade 2001). Each digit is lined with polyps and, when cross-sectioned, show porous tissue which is dark brown around the outer surface with a yellowish, slightly firmer center (Figure 3.1). Previous studies on *L. pauciflorum* have characterized the bacterial community, dominated by sequences affiliated with Endozoicomonadaceae and Spirochaetaceae (Wessels *et al.* 2016; *Unpublished data – Chapter 2*). In this study, the basic organizational scheme of the *L. pauciflorum* holobiont is investigated via 16S rRNA gene amplicon-sequencing to determine whether the bacterial community is uniform throughout the tissues of soft corals or whether distinct microhabitats are maintained within the host. This is the first investigation into the potential for a soft coral to maintain distinct microhabitats within the host tissue. Ultimately, the large pool of knowledge gained from studying Scleractinia cannot be applied to Octocorallia if the fundamental similarities and differences in their holobiont structure are not well understood.

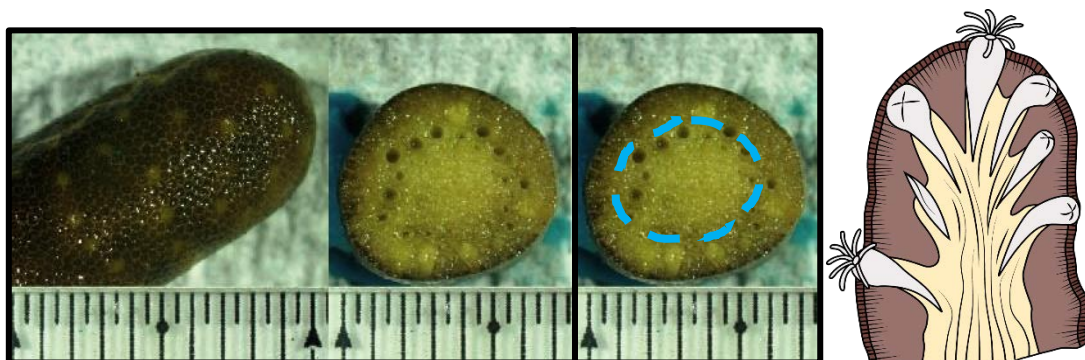


Figure 3.1: Image of inner and outer tissue layers in *Lobophytum pauciflorum* cross-section. The diagram illustrates tissue coloration pattern used to distinguish inner from outer tissue layers.

3.2 Methods

3.2.1 Sample collection

Samples were collected from Little Pioneer Bay, Orpheus Island (18°35'26"S, 146°28'56"E) under the Great Barrier Reef Marine Park Association (GBRMPA) permit number G16/38499.1 in October, 2017. Visually healthy adult colonies of *L. pauciflorum* at 4-6 m depth were sampled via SCUBA for histology and 16S rRNA gene sequencing. For each of 8 colonies (colonies I to VIII), 3 mucus and 4 tissue samples were collected. Mucus was sampled by rubbing a sterile cotton swab along the colony surface until the tip was fully discoloured and then snap-frozen in liquid nitrogen. Tissues were collected by cutting a 2-3 cm digit (one for each of the 3 replicates per colony) with dissection scissors, placed in separate, sterile 15 ml tubes with ambient seawater and kept on ice while returning to the station (~30 min). To reduce mucus contamination of the surface tissue layer, nubbins were gently grazed with a sterile scalpel to remove as much excess mucus as possible and thoroughly rinsed with 0.22 µm-filtered seawater. The inner core tissue and outer surface tissue were dissected via sterile scalpel and distinguished by eye according to colour and texture (Figure 3.1). After the layers were separated, any remaining mismatched tissue was removed and the inner and outer tissue fractions were rinsed again and snap-frozen in liquid nitrogen. The outer layer is soft and dark in colour while the inner layer is firm and pale in comparison. This yielded a total of 9 samples (3x mucus, 3x inner tissue, 3x outer tissue) per colony for each of 8 colonies to compare inner tissue, outer tissue and mucus layers as microhabitats. The remaining tissue sample collected from each colony was processed for histology.

3.2.2 Sample preparation for histology

Upon returning to the station, histological samples were immediately fixed for 10 hours in 4 % paraformaldehyde in 10 mM phosphate-buffered saline solution. The tissues were then rinsed with and kept in a 1:1 solution of 10 mM phosphate-buffered saline and 100% molecular grade ethanol. Dehydration with subsequent baths of Xylene and Ethanol before being embedded in paraffin wax and cut into 200-micron slices. The tissue cross-sections were then mounted and stained with hematoxylin and eosin for imaging.

3.2.3 DNA isolation and 16S rRNA gene amplification

To extract genomic DNA, the PowerPlant DNA Isolation Kit (QIAGEN) was used according to manufacturer's instructions. To homogenize the tissue, 100-150 mg were snap frozen in liquid nitrogen, crushed under a mortar and pestle, horizontal bead-beat for 5 min before 5 min resting on ice. The cotton tips were removed from the mucus swabs and cut up into the lysis buffer to assist

with bead-beating. Universal bacterial primers 27F and 1492R (S-D-Bact-0008-d-S-20 “AGAGTTTGATCMTGGCTCAG” and S*-Univ-1492-a-A-21 “GGTTACCTTGTTACGACTT”, respectively) were used to determine the success of the extraction (Bourne and Munn 2005; Galkiewicz and Kellogg 2008; Klindworth 2013; Zhang *et al.* 2015). Reaction conditions for test amplification were 15 min at 95°C, [1 min at 95°C, 1 min at 54°C, 2 min at 72°C]x31 cycles, 8 min at 72°C and infinite hold at 4°C (Bourne and Munn 2005).

For amplification of 16S V3/V4 the primers 341F and 785R with Illumina adapter overhangs (underlined) (S-D-Bact-0341-b-S-17 “TCGTCGGCAGCGTCAGATGTGTATAAGAGACAGCCTACGGGNGGCWGCAG” and S-D-Bact-0785-a-A-21 “GTCTCGTGGGCTCGGAGATGTGTATAAGAGACAGGACTACHVGGGTATCTAATCC”, respectively) were chosen (Klindworth 2012). Reaction conditions were as follows: 30 sec at 98°C, [10 sec at 98°C, 30 sec at 55°C, 25 sec at 72°C]x32 cycles, 5 min at 72°C and infinite hold at 4°C (manufacturer’s suggestion tweaked according to specific primer T_m). Both primer sets were amplified with 1.25 µl template DNA, 1.25 µl each of 5 µM forward and reverse primers, 6.25 µl Platinum SuperFi PCR MasterMix (Invitrogen, US) totalling 12.5 µl reaction.

3.2.4 Next-generation sequencing of 16S rRNA

Products were cleaned with Sera-Mag Speed Beads (Merk, DE) using ZEPHYR G3 NGS Workstation (PerkinElmer, USA) before and after indexing with Nextera XT DNA Library Prep Kit (Illumina, USA). The Indexing PCR conditions were the same with only 8 cycles. Quantification was carried out on EnSpire multimode plate reader (PerkinElmer, USA) with Quantifluor dsDNA (Promega, USA). Samples were pooled and final libraries normalized to 4 nM, 5 µl from each indexed library so that 6 pM were sequenced together with several other projects. Sequencing for 2 x 300 bp reads was done on a 2x300 Cycles V3 Flow Cell for MiSeq (Illumina, USA). The run was spiked with 15% PhiX v3 Control Kit (Illumina, USA) for quality and calibration control.

3.2.5 Bioinformatics

Post-sequencing sample processing was performed with Qiime2 (Bolyen *et al.* 2019). Data was denoised with the quality control plugin DADA2 (Callahan *et al.* 2016). Sequencing depth was set at 8800 which retained 53 % of the sequences in 80 % samples. To assign taxonomic designations to ASVs, a feature classifier was trained on the SILVA 132 99% database (Quast *et al.* 2013). After classification, statistical analysis was run on microbial communities using the Vegan package (Oksanen *et al.* 2018) in R (R Core Team 2013). Sequences unaffiliated with Bacterial clades (such as archaeal and mitochondrial sequences) were removed and a minimum read threshold of 10 was applied to

each ASV. For visualizing community structure and comparison of relative composition between samples, data was normalized using total sum standardization (TSS) (McKnight *et al.* 2019).

Alpha and Beta diversity were calculated in Qiime2; Shannon Index was used for rarefaction diversity and richness, Bray-curtis dissimilarity index was used to calculate distances for PCoA and PERMANOVA analyses, Faith's PD was used for phylogenetic diversity and Pielou Index for evenness. Qiime2 taxonomy and feature-table files were imported to R for analysis of bacterial community composition (R Core Team 2013). Comparison of community composition between groups was done according to the mean and standard deviation (SD) of relative abundance across groups. The package seqINR was used to work within .fasta format and the package VEGAN was used for community beta diversity analysis (Oksanen *et al.* 2018). Sequence alignments, phylogenetic analysis and BLAST searches to NCBI GenBank (Benson *et al.* 2012) were conducted on Geneious Prime 2019.2.1 (<http://www.geneious.com>). Sequences were aligned with MAFFT and input to IQTree modelfinder (Kalyanamoorthy *et al.* 2017) for prediction of substitution model. Phylogenetic trees were built according to the top suggested model, Hasegawa-Kishino-Yano (1985), with MrBayes in Geneious Prime. Taxonomy-based phenotype assignment was applied for putative prediction of community metabolism and biological characteristics in METAGENassist (Xing *et al.* 2017). The characteristics included in METAGENassist are biotic lifestyle, cell arrangement, cell shape, chromosome shape, flagellated cells, GC content, genome size, gram (positive or negative), habitat affiliation, host affiliation, human pathogens, membrane number, motility, oxygen requirement, plasmid shape, sporulation and temperature range.

3.3 Results

3.3.1 Histology

Histological images reveal distinct morphological patterns between tissue layers (figure 3.2). The outer tissue layer harbors the majority of the polyps and aggregations of the photosynthetic Symbiodiniaceae cells are visible in mesenteries and near the surface tissue layer. The Symbiodiniaceae are likely the cause of visual differentiation between the light inner tissue and darker outer tissue coloration. The inner tissue layer is primarily composed of coenecyeme surrounding many transport canals, some of which contain oocytes. The differences observed between inner and outer tissue layers support the theory that they could provide distinct microhabitats for associated bacteria.

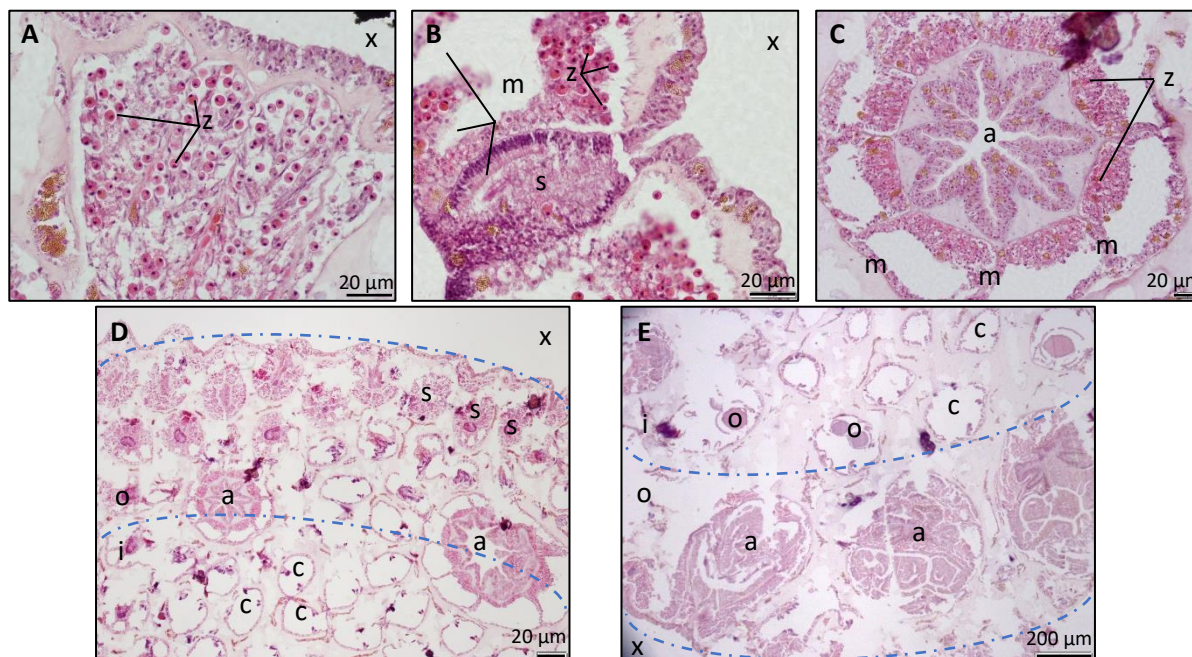


Figure 3.2: Histology of inner and outer tissue layers in *Lobophytum pauciflorum*. The surface layer (A) is densely populated with Symbiodiniaceae (z), which aggregate around mesenteries (m) in siphonozooids (s)(B) and autozooids (a)(C) and give the outer tissue layer the observed pigmentation. The inner tissue layer (i) does not have dense aggregations of Symbiodiniaceae or polyp structures, mostly consisting of transport canals (c), containing visible oocytes (o) and interstitial coenenchymal tissue (D,E). The exterior environment is labelled as 'x'. Scale bars are as shown (20 μm A-D, 200 μm E). Tissues were fixed in 4 % paraformaldehyde, mounted on paraffin wax and stained with hematoxylin and eosin.

3.3.2 Alpha and beta diversity

The sequencing run produced high-quality reads, with 15.8 % PhiX recovery from a 15 % spike. After cleaning and quality filtering, 4,423 ASVs were retained from 50 samples (Table 3.1) across the

Table 3.1: The number of samples across colonies and microhabitats which showed successful amplification and sequencing of the 16S rRNA gene. All samples were originally collected in triplicate, but some replicates were compromised in a liquid nitrogen dewar malfunction.

Colony	I	II	III	IV	V	VI	VII	VIII	
Inner	1	3	3	2	2	3	2	2	18
Outer	1	3	2	2	3	3	2	3	19
Mucus	1	2	1	2	2	2	1	2	13
	3	8	6	6	7	8	5	7	50

3 microhabitats: 1303 from inner tissue samples, 1,541 from outer tissue samples and 2,485 from the mucus layer (Figure 3.3). From both tissue layers combined, a total of 2,475 ASVs were recovered, similar to the number of ASVs in the mucus. Phylogenetic diversity was similar between all samples and the inner and outer tissue layers across all colonies (26.1 ± 16.3 SD and 27.7 ± 13.4 SD, respectively PD), while mucus was 2.5x higher (79.1 ± 20.2 SD PD) (Figure 3.4). Evenness was similar across all samples and layers (mean 0.7 ± 0.1 e for both categories). Alpha rarefaction showed all samples plateaued by the median frequency sampling depth of 13,000 sequence reads, indicating sufficient sampling for maximum diversity in the community. The 3 microhabitats and the 8 colonies showed greater similarity within than between groups based on analysis of similarity ($p = 0.001$ for colony and for microhabitat). In stepwise PERMANOVA with adonis2, microhabitat and colony also both showed statistically distinct groups of sequences ($p = 0.001$), however, the influence of colony ($R^2 = 0.28$) in this dataset was slightly stronger than the influence of microhabitat ($R^2 = 0.11$). Plotting in NMDS showed that the bacterial

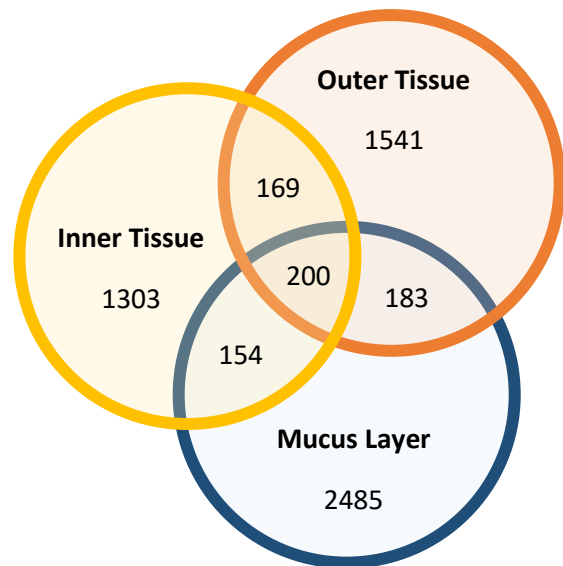


Figure 3.3: Count of ASVs specific to and shared between microhabitats in *Lobophytum pauciflorum*.

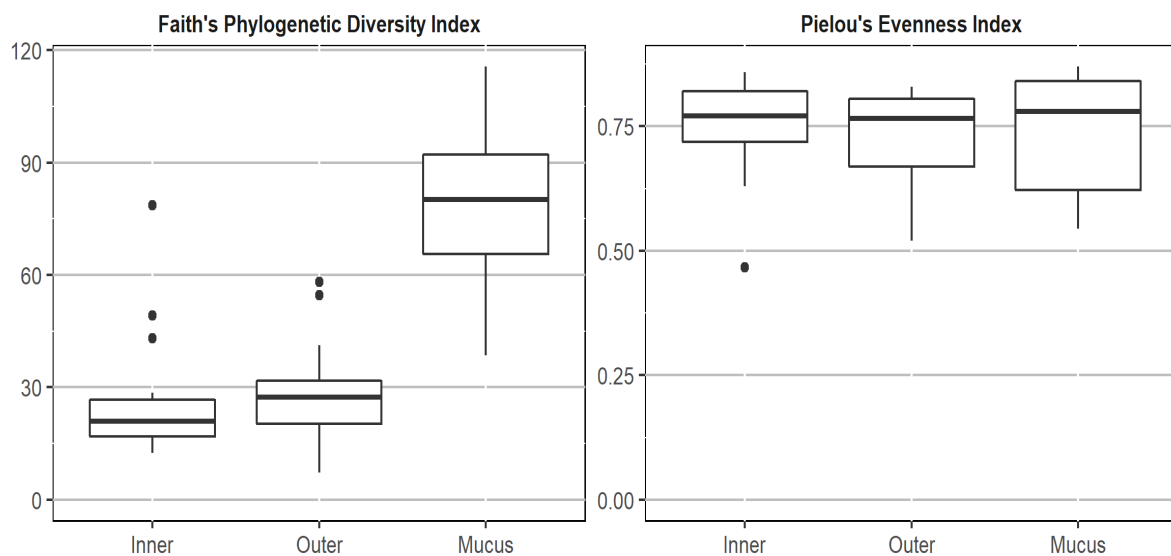


Figure 3.4: Faith's Phylogenetic Diversity (PD) (left) and Pielou's Evenness (right) between the three microhabitats sampled in *Lobophytum pauciflorum* (whiskers denote SD).

community in the tissue layers were similar, but both tissue layers were distinct from the mucus (Figure 3.5).

3.3.3 Bacterial community composition of host microhabitats

There was a high variability between samples and colonies in this study, however, sequences affiliated with the phylum Proteobacteria dominated all three microhabitats at 61.0 ± 27.7 % relative abundance in the inner tissue layer, 55.8 ± 28.4 SD % in the outer tissue and 46.4 ± 25.4 SD % in the mucus layer (Figure 3.6 A).

Sequences affiliated with Bacteroidetes (11.5 ± 20.5 % in the inner tissue, 8.8 ± 21.2 % in the outer tissue and 11.1 ± 5.4 % in the mucus layer) were abundant in all three layers as well as sequences unclassified beyond the level Bacteria (21.9 ± 27.9 %, 22.7 ± 25.6 %, and 23.4 ± 28.6 % recovered from inner tissue, outer tissue and mucus layers, respectively). Sequences affiliated with Tenericutes were abundant in one sample from outer tissue (37.0 % in one sample from outer tissue of colony II) but were otherwise recovered in similar abundance between tissue layers (1.1 ± 1.1 % in inner tissue, 1.4 ± 1.9 % in

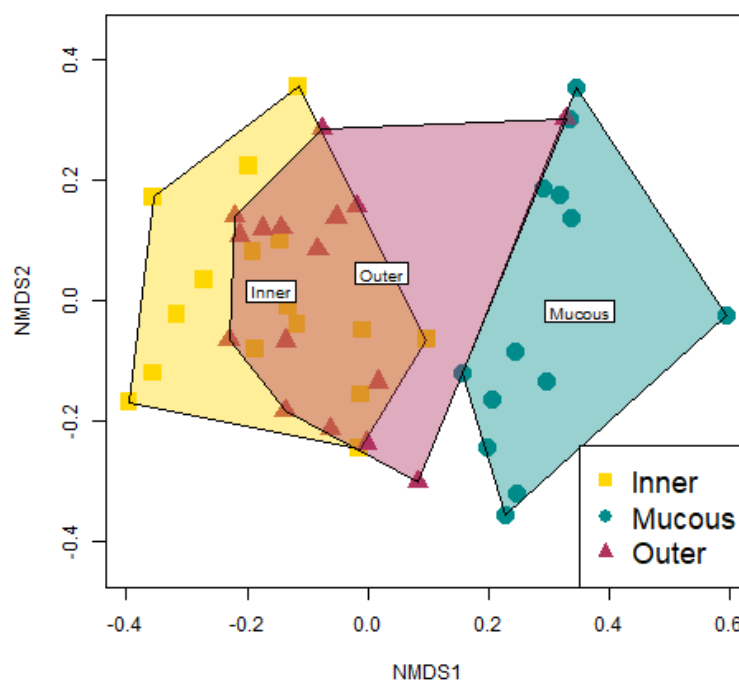


Figure 3.5: Non-metric multi-dimensional scaling (NMDS) plot of Bray-Curtis dissimilarity showing distinct community composition in each of the three microhabitats sampled: Inner tissue (yellow convex hull), outer tissue (red convex hull), and mucus (green convex hull).

outer tissue) but not from the mucus layer (0.1 ± 0.1 %). Spirochaetes-affiliated sequences were recovered in highest relative abundance from the outer tissue (2.2 ± 6.5 %), primarily from one sample each from colony VI (80.2 %) and colony III (8.5 %). The mucus layer was the most diverse microhabitat and sequences affiliated with Cyanobacteria (6.0 ± 3.1 %), Planctomycetes (3.7 ± 2.6 %), Verrucomicrobia (3.7 ± 4.5 %) and Actinobacteria (2.7 ± 2.1 %) were all recovered in highest relative abundance.

Classification of sequences to the family level shows a much greater number of taxa affiliated with or shared between each layer. Sequences affiliated with the Bacteroidetes Flavobacteriaceae (10.2 ± 20.5 %) and the Gammaproteobacteria Vibrionaceae (9.4 ± 9.9 %) were recovered in highest mean relative abundance from the inner tissue. Sequences affiliated with the Alphaproteobacteria families and Rhodobacteraceae (4.5 ± 9.7 %) and Kiloniellaceae (1.3 ± 3.3 %) were also in highest

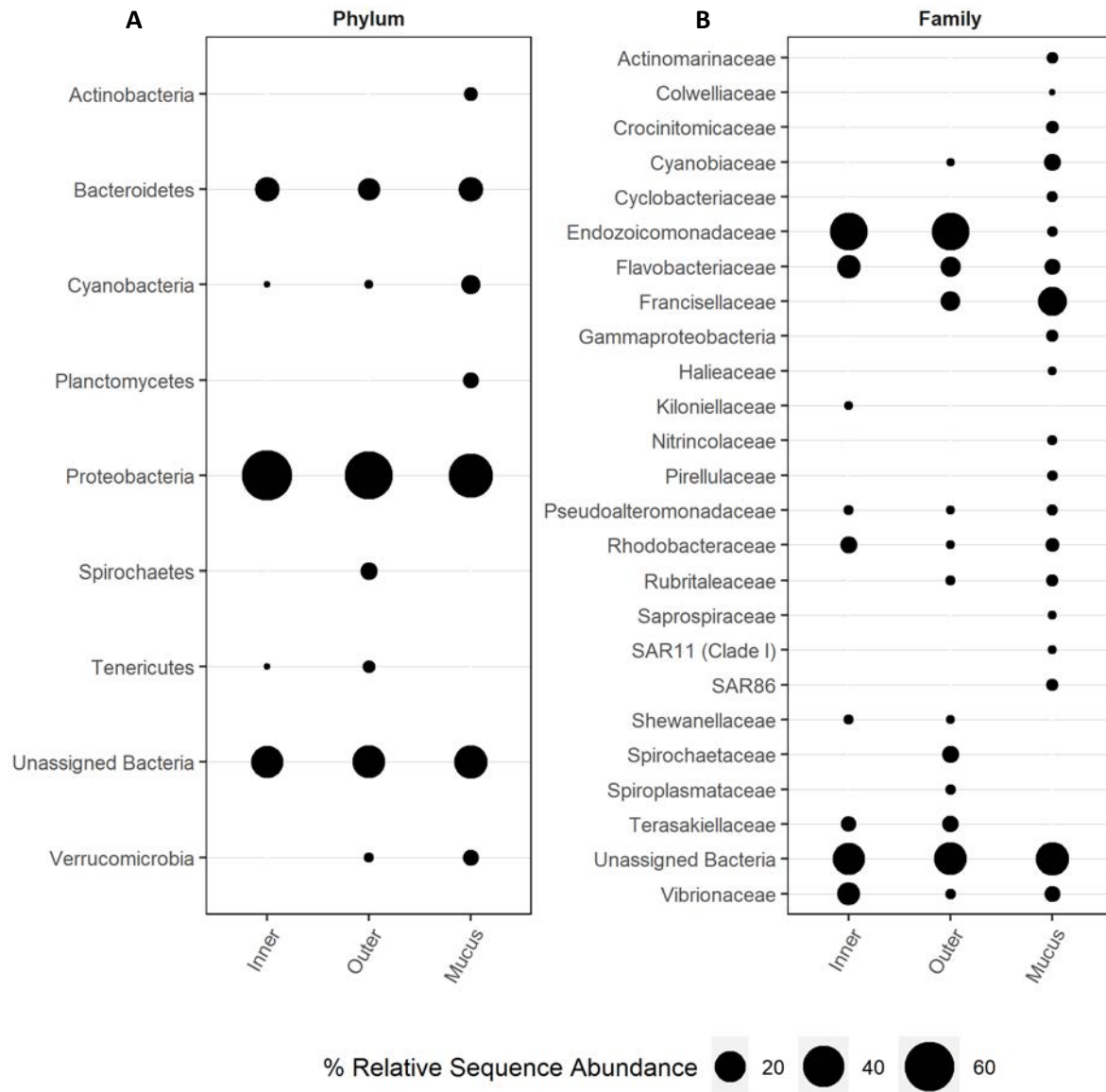


Figure 3.6: Relative abundance of sequences affiliated with Bacterial taxa at phylum (A) and family (B) level across the three microhabitats sampled: inner tissue, outer tissue and mucus layer.

abundance in the inner tissue layer. Recovered from the outer tissue, sequences affiliated with Spirochaetaceae (4.7 ± 18.4 %) and Spiroplasmataceae (1.6 ± 6.7 %), both families of Spirochaetes, were in higher relative abundance than inner tissue or mucus layers. The most dominant sequences in both tissue layers affiliated with the Gammaproteobacteria family Endozoicomonadaceae, recovered at 32.0 ± 26.8 % relative abundance in inner tissue, 31.6 ± 25.1 % in outer tissue but only

1.6 ± 3.6 from the mucus layer. Sequences affiliated with the Alphaproteobacteria Terasakiellaceae (3.5 ± 9.0 % and 4.1 ± 10.8 % in the inner and outer tissue and 0.2 ± 0.2 % in the mucus layer) and the Gammaproteobacteria Shewinellaceae (1.4 ± 2.0 % in inner tissue, 1.3 ± 3.3 % in outer tissue and 0.6 ± 0.9 in the mucus layer) were also in highest relative abundance in the tissue layers and lowest in the mucus.

The number of ASVs were similar between tissue and mucus, but phylogenetic diversity was much higher in sequences recovered from the mucus layer. Sequences affiliated with Francisellaceae dominated the mucus layer ($16.6 \pm 28.6 \%$) but were recovered at only $6.7 \pm 18.2 \%$ and $0.5 \pm 0.8 \%$ in the outer and inner tissue layers, respectively (Figure 3.6 B). Sequences affiliated with the Cyanobacteria Cyanobiaceae ($4.6 \pm 3.0 \%$), the Alphaproteobacteria SAR11 (2.0 ± 1.5), the Gammaproteobacteria SAR86 were all most abundant in the mucus layer. A number of other low-

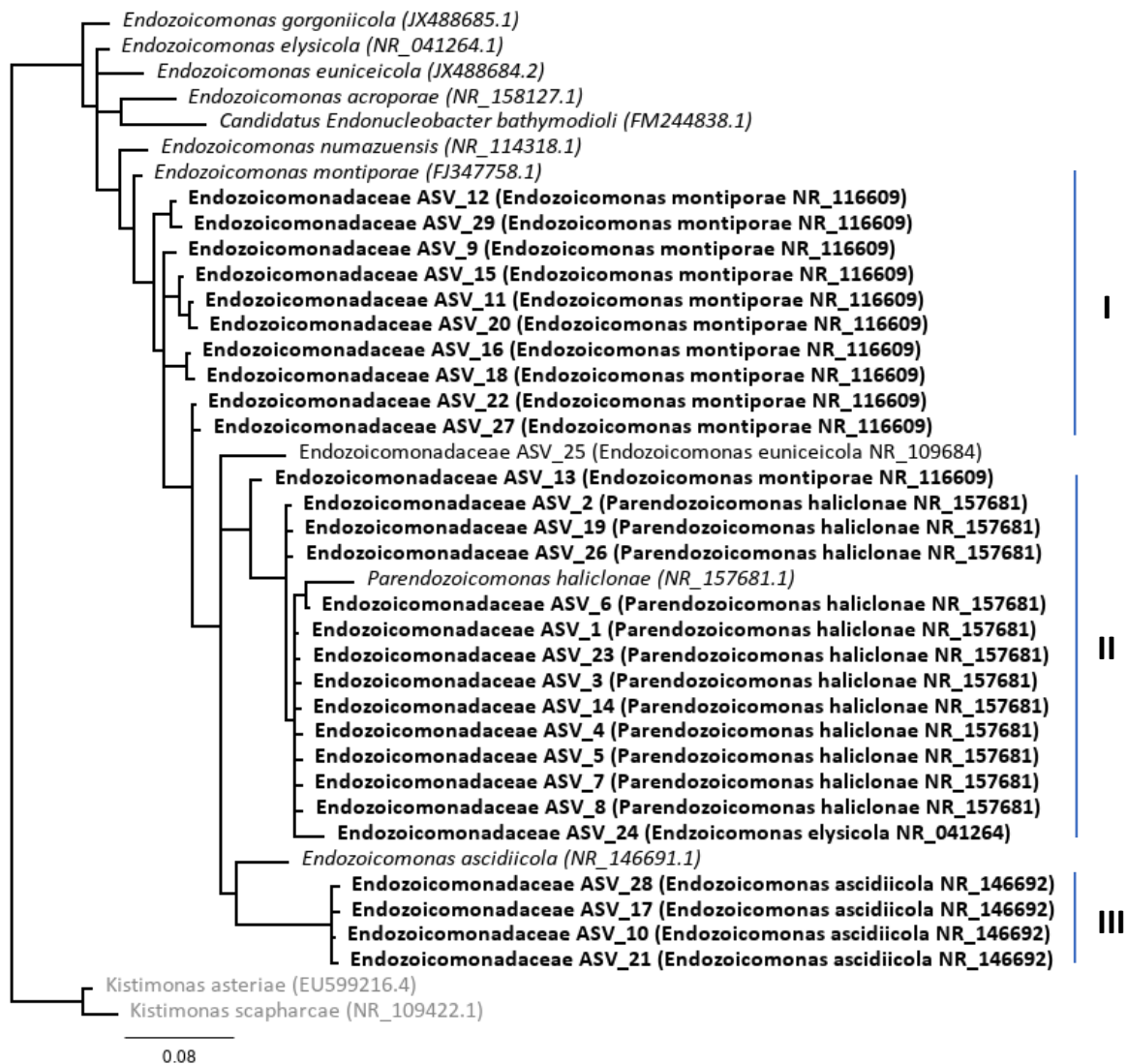


Figure 3.7: Phylogenetic tree displaying the 29 Endozoicomonadaceae-affiliated sequences which received more than 1000 sequence reads. The tree was built with Hasegawa-Kishino-Yano (1985) substitution model (as suggested by IQTree modelfinder) of MAFFT alignment in MrBayes in Geneious Prime 2019.2.1. Type strains were retrieved from NCBI and the Endozoicomonadaceae genus *Kistimonas* was used as an outgroup. ASVs in this study grouped with *Endozoicomonas montiporae* (I), *Parendoziomonas haliclona* (II) and *Endozoicomonas ascidiicola* (III).

abundance taxa were recovered in highest relative abundance from the mucus, including the Bacteroidetes Crocinitomicaceae (2.2 ± 1.9 %) and Cyclobacteriaceae (1.7 ± 1.5 %), the Gammaproteobacteria Nitrospiraceae (1.5 ± 0.7 %) and Colwelliaceae (1.1 ± 1.6 %), Actinobacteria Actinomarinaceae (1.9 ± 1.6 %), and the Planctomycetes Pirellulaceae (1.6 ± 1.3 %) along with many others. Some sequences were also recovered in similar relative abundance from all three microhabitats sampled. Sequences affiliated with the Verrucomicrobia Rubritaleaceae were recovered in higher relative abundance from the outer tissue and mucus layers (1.4 ± 3.0 % and 2.1 ± 3.0 %, respectively) than in the inner tissue layer (0.1 ± 0.2 %). The Gammaproteobacteria Pseudoalteromonadaceae was recovered from all three layers in 1.5 ± 3.0 % (inner tissue), 1.3 ± 3.3 % (outer tissue) and 1.7 ± 2.0 % relative abundance (mucus layer).

3.3.4 Phylogeny of *Endozoicomonadaceae*

A total of 283 ASVs affiliated with the family Endozoicomonadaceae each received more than 10 sequence reads. Only 29 Endozoicomonadaceae-affiliated sequences retrieved more than 1000 reads and these were aligned with 11 type strains representing the Endozoicomonadaceae family for phylogenetic analysis (Figure 3.7). The sequences recovered from this study formed 3 groups according to maximum-likelihood tree-building: two large clusters near *Endozoicomonas montiporae* (NR_FJ347758.1) and *Parendozoicomonas haliclona* (NR_157681.1) and a small cluster near *Endozoicomonas ascidiicola* (NR_146691.1). Some of these ASVs varied slightly in relative abundance between tissue layers but primarily displayed an even distribution between them.

3.3.5 Putative biological characteristics associated with distinct microhabitats

Analysis with metagenAssist (Zing *et al.* 2017) was applied to infer putative biological functions of the bacteria associated with inner tissue, outer tissue and mucus. Sequences recovered from each microhabitat were compared to sequences with known affiliations to various metabolic pathways and biological characteristics (Figure 3.8). Overall, the putative metabolic functions associated with each microhabitat were not distinct (ANOSIM, $p = 0.059$). A significance test on individual metabolic groups, however, showed that some putative metabolic functions associated differently with each microhabitat. Inferred pathways with distinct associations were atrazine metabolizers ($p = 0.04$), an herbicide (Ralebitso *et al.* 2002) and likely an artefact of the analysis, and cellobiose ($p = 0.0001$), chitin ($p = 0.012$) and xylan ($p = 0.041$) degraders, nitrogen fixers ($p = 0.012$) and nitrite reducers ($p = 0.045$) which were all associated in highest relative abundance with sequences recovered from the mucus layer.

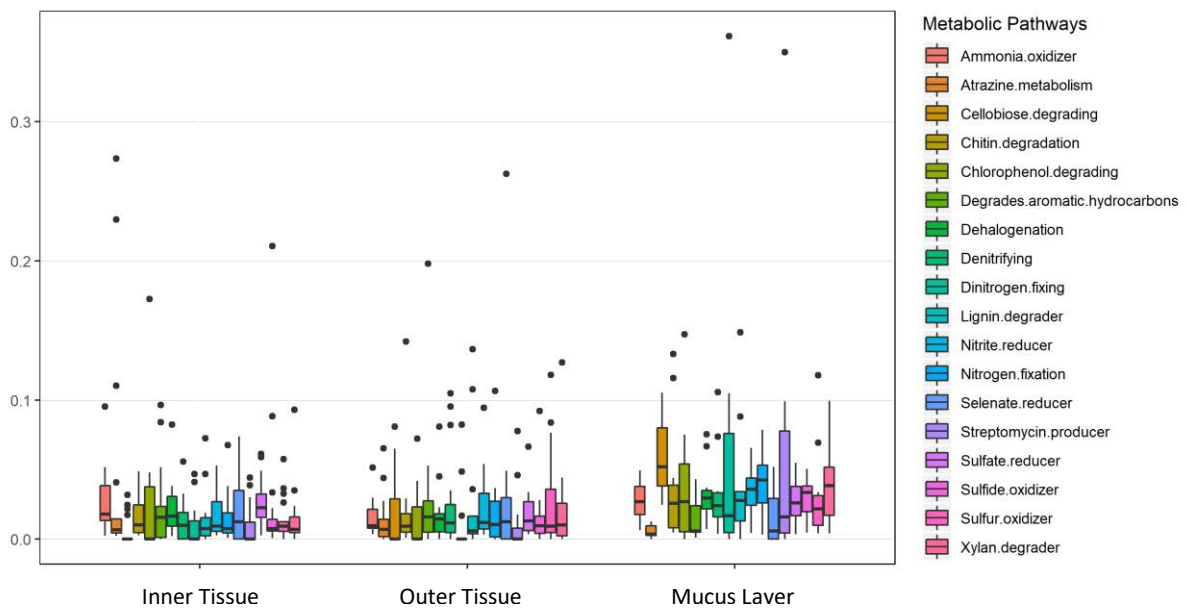


Figure 3.8: Putative metabolic pathways affiliated with sequences recovered from Inner tissue, outer tissue and mucus layers of *Lobophytum pauciflorum* analyzed with metagenAssist. The y-axis represents the relative abundance of sequences associated with each biological function (color guide) recovered from each microhabitat (x-axis).

In addition to metabolism, we compared putative biological characteristics affiliated with the sequence communities of each microhabitat (Figure 3.9). Trophic type, cell shape and sporulation vs non-sporulation were all statistically different between all three microhabitats (ANOSIM, significance = 0.014, 0.002 and 0.001, respectively). The most significant factors related to trophic type were chemoorganotrophs, affiliated with sequences in highest relative abundance in the mucus layer (t.test, $p = 0.003$) and photosynthesizers, affiliated in highest relative abundance in the inner tissue layer (t.test, $p = 0.001$). The only statistically significant difference in cell shape was the high relative abundance of tailed-cells putatively associated with the mucus layer (t.test, $p = 0.022$), but mean relative abundance indicates bacilli-shaped cells are more prevalent in the tissue while cocci, filamentous and tailed all appear higher in the mucus layer. The inference of sporulating vs non-sporulating cells was distinct between microhabitat (ANOSIM, $p = 0.001$) with a much lower relative abundance of sporulating cells in the tissue layers. The characteristics concerning symbiotic vs free-living lifestyles, the number of membranes and the oxygen requirement were not statistically significant between microhabitats. However, the mean relative abundance of putative sequences associated with free-living bacteria was highest in the mucus layer while inferred double-membrane cells and aerobic bacteria were recovered from the tissues in highest mean relative abundance. The remaining inferred characteristics inferred by METAGENassist either did not show differences between microhabitats or were not applicable to this study.

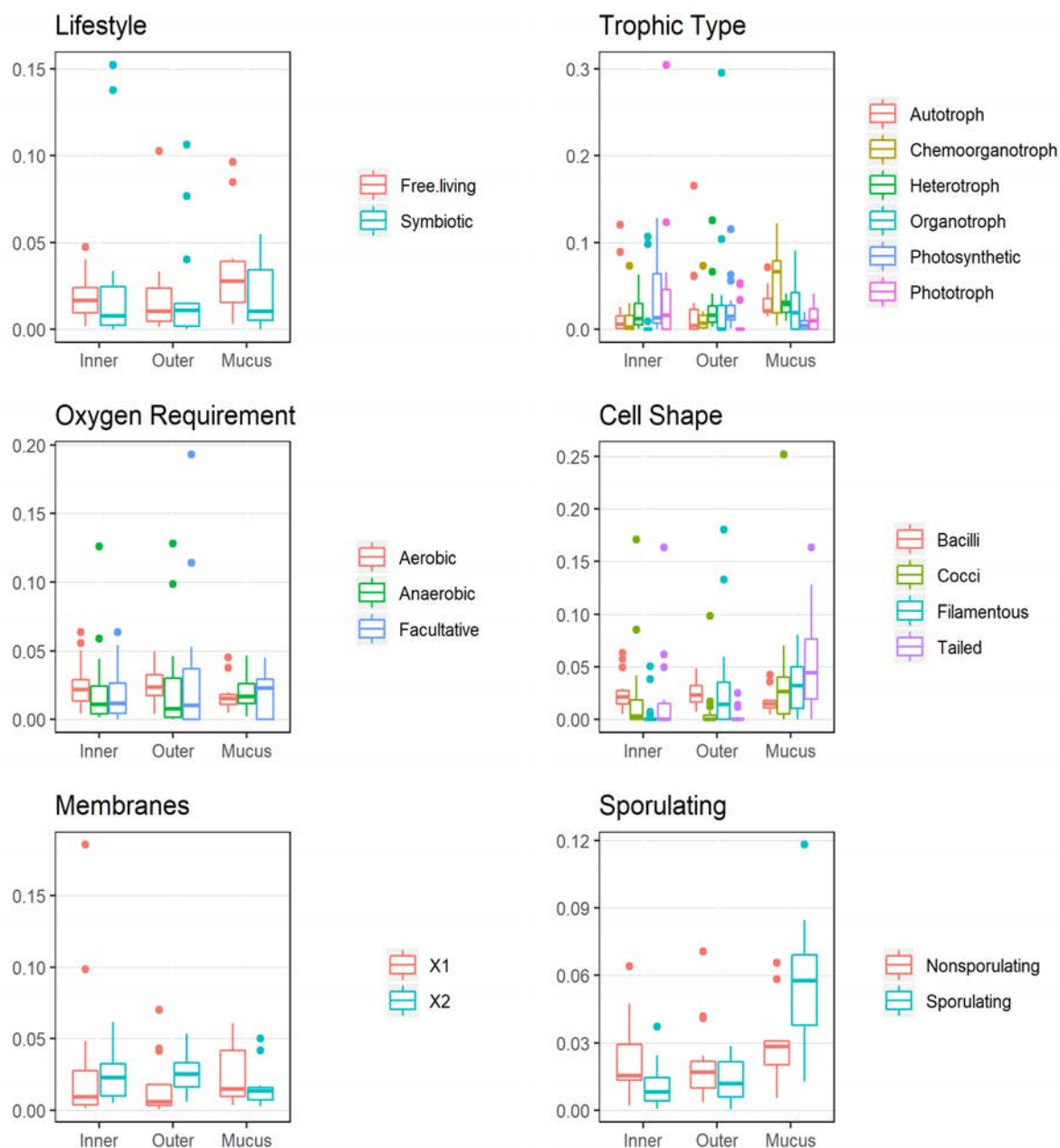


Figure 3.9: Putative biological parameters and preferences of 16S communities in each microhabitat as determined by metagenAssist. The parameters displayed include **A.** lifestyle (symbiotic or free-living), **B.** method of carbon acquisition (autotrophy, chemoautotrophy, heterotrophy, organotrophy, photosynthesis or phototrophy), **C.** Oxygen requirements (aerobic, anaerobic or facultative), **D.** Cell Shape (Bacilli, Cocci, Filamentous or tailed), **E.** Membranes (one or two) and **F.** Sporulation (sporulating or non-sporulating). The y-axis represents the relative abundance of sequences associated with each biological function (color guide) recovered from each microhabitat (x-axis).

3.4 Discussion

This study characterized the bacterial communities associated with the inner tissue, the outer tissue and external mucus layer of *L. pauciflorum*. The tissue layers hosted similar communities that were distinct from that of the mucus layer (summarized in Figure 3.10). The mucus layer was dominated by Cyanobacteria and Francisellaceae, while the tissue layers were dominated by Endozoicomonadaceae. Putative functional profiles of the 16S community recovered from each microhabitat are also similar between tissue layers and distinct from the mucus. High variability was also observed among samples and colonies, despite the significant grouping of both colony and microhabitat. High variability between colonies was also observed in a previous study on *L. pauciflorum*-associated bacteria (*Unpublished data – chapter 2*).

The bacterial community characterized in *L. pauciflorum* shared many similarities with a previous study on the cold-water soft coral *Paragorgia arborea*. The bacterial taxa Campylobacterales, Flavobacteriaceae, Mollicutes (*Mycoplasma*), Spirochaetes (*Spirochaeta*), Rickettsiales and Terasakiellaceae were characterized as ‘biomarkers’ in the tissues of *P. arborea* (Weiler *et al.* 2018).

	Inner Tissue	Outer Tissue	Mucus Layer
Bacteria affiliated with sequences in highest relative abundance			Actinobacteria Colwelliaceae Cyanobacteria Nitrincolaceae Planctomycetes Verrucomicrobia
		Francisellaceae	
		Spirochaetes	
		Endozoicomonadaceae Mollicutes Shewinellaceae Terasakiellaceae	
		Flavobacteriaceae Kiloniellaceae Rhodobacteriaceae Vibrio	
	Pseudoalteromonas		
Putative metabolic pathways	Atrazine metabolizers		Cellobiose degraders Chitin degraders Nitrogen fixers Nitrite reducers
Inferred biological characteristics	Phyotosynthesizers		Chemoorganotrophs Tailed-cells
	Non-sporulating cells		

Figure 3.10: Summary of 16S community taxonomic affiliation and inferred biological characteristics associated with each of the three microhabitats sampled: inner and outer tissue and mucus layers. Only statistically significant inferred biological functions are shown.

All of these taxa were also identified as being associated with one or both tissue layers in *L. pauciflorum* in this study, with the exception of Rickettsiales (Clade I) which was more abundant in the mucus than tissues. The tissues of *P. arborea* were heavily dominated by sequences affiliated Mollicutes, while the tissues of *L. pauciflorum* are dominated by Endozoicomonadaceae-affiliated ASVs.

3.4.1 *The mucus layer hosts a distinct community of associated bacteria*

The mucus layer of *L. pauciflorum* hosted a distinct, species rich community with higher phylogenetic diversity and variability between samples and colonies than the tissue layers. While the number of ASVs in the combined tissue layers was similar to that in the mucus layer (2,475 and 2,485 ASVs, respectively), phylogenetic diversity recovered from the mucus layer was more than twice as high as in the tissues. The only previous study to compare the bacterial community associated with soft coral mucus and tissue layers did not find any significant difference in diversity (Weiler *et al.* 2018). As of now only two phylogenetically distinct soft coral species, a tropical Alcyoniidae (*L. pauciflorum*) and a deep-sea Paragorgiidae (*Paragorgia arborea*), have been characterized by microhabitat rather than as a whole. Before generalizations on the structure of bacterial communities between microhabitats in soft corals can be deduced, additional host taxa should be characterized in this manner.

While variability was observed, Francisellaceae- and Cyanobacteriaceae-affiliated sequences, along with unclassified sequences, were in high mean relative abundance in the tissue layer. Cyanobacteria are common in coral reefs and are involved in nitrogen cycling but can also be pathogenic or free-living (Charpy *et al.* 2012). The mucus layer of the *P. arborea* was also dominated by Cyanobacteria-affiliated sequences (Weiler *et al.* 2018). In *L. pauciflorum*, they were recovered in significantly lower relative abundance in the outer tissue layer and even less so from the inner tissue. The same pattern of decreasing relative abundance toward the inner tissue was observed in ASVs affiliated with Actinobacteria, Planctomycetes and Verucocomicrobia, among others. Previous studies on hard corals have demonstrated antimicrobial activity in the mucus layer, potentially helping to filter out undesirable microbes (Ritchie *et al.* 2006). The significant reduction in diversity observed between the mucus and tissue layers in *L. pauciflorum* indicate that mucus layer of *L. pauciflorum* could also prevent some microbes from colonizing tissue. Indeed, it is well established that *Lobophytum* spp. harbor diverse powerful antimicrobial compounds (Cheng *et al.* 2008; Yan *et al.* 2010 a, b; Ibrahim *et al.* 2012; Zhao *et al.* 2013).

Francisellaceae-affiliated sequences were recovered in high mean relative abundance but also exhibited high variability (16.6 ± 28.6 % in the mucus; 6.7 ± 18.2 % in the outer tissue; 0.5 ± 0.8 % in

the inner tissue). This is more consistent with the patterns observed in Spirochaetaceae-affiliated sequences, also discussed in Chapter 2, raising an interesting question of the nature of these relationships with *L. pauciflorum*. These results highlight the need for research into the function of common coral-associated Bacteria.

3.4.2 *The tissue layers host similar bacterial communities*

The inner and outer tissue layers were initially differentiated by and dissected along their pigmentation pattern. The outer layer is significantly darker in colour, and part of that pigmentation comes from the algal symbionts Symbiodiniaceae (Chalker and Dunlap 1981). Histological analysis of *L. pauciflorum* tissues showed an abundance of Symbiodiniaceae in the outer layer, especially in and around zooid mesenteries. This study also recovered sequences affiliated with the Bacteria family Rubritaleaceae present in the outer tissue and mucus layers. Members of the family Rubritaleaceae are known for their pigmentation, possibly contributing further to the darker hue of the outer tissue layer compared to the pale inner tissue (Rosenberg 2014).

Sequences that were distinct between layers include Fibrobacteraceae, Spirochaetaceae, Francisellaceae and Rubritaleaceae. However, some sequences were recovered in similar abundance from both layers, including those affiliated with Endozoicomonadaceae, Shewinellaceae and Terasakiellaceae – potentially important members of the bacterial community associated with *L. pauciflorum* (Chapter 2). Shewinellaceae is commonly reported in association with the coral microbiomes (Rhower 2001; Raina *et al.* 2009) and has shown antimicrobial activity in association with a scleractinian hosts (Pham *et al.* 2016).

Endozoicomonadaceae-affiliated sequences appear closely associated with host tissue and were approximately 18-fold less abundant in the mucus layer. The association between *L. pauciflorum* and the family Endozoicomonadaceae has been explored in chapter 2. In agreement with those data, the phylogenetic analysis here (Figure 3.7) has characterized the 285 Endozoicomonadaceae-affiliated ASVs into 2 main phylogenetic clades which align most closely to *E. montiporae* and *P. haliclona*. Interestingly, there was very little variation in the distribution of these ASVs between tissue layers. In previous studies of *L. pauciflorum*, Spirochaetaceae-affiliated sequences were the next most abundant following Endozoicomonadaceae-affiliated sequences, dominating about half of the colonies while remaining absent from the rest (Wessels *et al.* 2016, Chapter 2). While only present in a few samples in this study, Spirochaetaceae were in highest abundance in the outer tissue layer.

The inner tissue of *L. pauciflorum* hosted a diverse group of ASVs which were not retrieved or were retrieved in lower abundance from the other layers. The Bacteroidetes Flavobacteriaceae, the

Gammaproteobacteria Vibrionaceae and the Alphaproteobacteria families Rhodobacteriaceae and Kiloniellaceae were all in highest relative abundance in the inner tissue layer. Kiloniellaceae-affiliated sequences were previously recovered from *Anthothela* spp. and found to associated specifically with the tissue layer, as well (Lawler *et al.* 2016). Full genome analysis of symbiotic *Kiloniella* species indicated that they may have a role in sulphur and carbon metabolism, denitrification and the biosynthesis of secondary metabolites (Wiese *et al.* 2019). Many Flavobacteria and *Vibrio* spp., however, are opportunistic pathogens of marine fish and invertebrates (Austin *et al.* 2012). In the deep-sea octocoral genus *Anthothela*, Endozoicomonadaceae (Oceanospirillales), *Spirochaeta* and Kiloniellales were identified as members of the 'core tissue microbiome' (Lawler *et al.* 2016). The bacteria of the inner tissue in *L. pauciflorum* may be beneficial to holobiont fitness or opportunistic pathogens that have successfully bypassed the outer defences. Understanding relationships between host and symbiont however, requires the functional analyses of microbes within the holobiont. The sequences closely associated with host inner tissue highlighted in this study identify putative bacterial species for further study that likely have a strong positive or negative influence on holobiont fitness.

Bacterial communities associated with inner and outer tissue layers displayed both distinct and similar components with one another. The hydroskeletal system may contribute to similarities observed between tissue layers. The hydroskeleton provides structural support to the soft tissue in Octocorallia by maintaining water pressure throughout a series of canals connected to the zooid openings (Fabricius and Alderslade 2001). In doing so, some bacterial aggregates along the gastrovascular canal system may be homogeneously distributed throughout the tissue layers by the flowing water. In contrast, the skeleton of hard corals is strong and static, providing a far more stable central region of the colony in hard corals than is possible in soft corals. The potential homogenizing impact of the hydroskeleton system in soft corals provides further motivation for future research to localize bacterial aggregates in *L. pauciflorum*.

3.4.3 Putative biological characteristics associated with distinct microhabitats

While putative, the biological inferences based on sequences associated with microhabitats in *L. pauciflorum* offer insights into the potentially differentiated functions between microhabitats. As in hard corals, the mucus layer in *L. pauciflorum* is not only a barrier between the host and environment but a microhabitat with a unique associated bacterial community.

Sequences recovered from the mucus layer affiliated with chemoorganotrophs, possibly as a result of organisms in this habitat using the complex carbon rich polysaccharides of the mucus for metabolism. An abundance of putative nitrogen-fixing bacteria were also associated in the mucus layer, which is consistent with the high relative abundance of sequences recovered that affiliated with

cyanobacteria, a common diazotroph (Zehr *et al.* 2012). The inference of the ability to degrade chitin, a polysaccharide component of the cell walls of fungi, in the mucus-associated community of *L. pauciflorum* poses an interesting comparison to the studies in *Hydra*, where Bacteria in the mucus layer help to defend the host from fungal pathogens (Fraune *et al.* 2015). Sequences recovered from the inner tissue affiliated with putative photosynthetic and phototrophic cells. This is particularly interesting because endolithic microalgae have been identified in Scleractinia (Bentis *et al.* 2000; Fine and Loya 2002), suggesting that there could be a benefit to photosynthetic symbionts deep beneath the outer tissues in corals. Fine and Loya (2002) suggest this could supplement the host with photosynthesized energy when overlying tissue is damaged.

The characteristics of single or double membrane, cell shape, tailed or non-tailed, and sporulation were included in the analysis with the idea that these factors could influence the molecular processes of host association and therefore suitability of a symbiont for association with *L. pauciflorum*. Sequences inferred to be tailed or non-sporulating were recovered in highest relative abundance from the mucus layers lower relative abundance of sequences recovered from the tissue layers are inferred to be tailed and non-sporulating cells. Sequences associated with Firmicutes, the primary sporulating phylum, were however higher in the tissue (0.2 %) than in the mucus (0.1 %) and were dominated by Clostridiaceae, recovered in highest relative abundance from the inner tissue layer (0.1 ± 0.1 %; 0,0 % in outer and mucus). The putative association with sporulation in the mucus layer may therefore be an artefact of the sequences available for comparison in the metagenASSIST database.

The presence of a tail implies motility and is therefore not expected to be a characteristic of tissue-associated symbionts. If the bacteria are also endosymbiotic, they may also be enclosed in a symbiosome as a result of the horizontal assimilation process in corals (Neckelmann and Muscatine 1983, Mohamed *et al.* 2016). While not statistically significant, the tissues hosted higher mean relative abundance of sequences putatively affiliated with double membrane and bacilliform cells. Cell shape and membrane number may influence phagocytosis by offering an easy shape for enclosing (as opposed to rod or helical cells) and the double membrane characteristic may provide resistance to digestion by the host before phagocytosis is arrested. It is possible that these characteristics – double membraned, non-tailed, bacilliform cells – potentially contribute to the suitability of bacteria for association with *L. pauciflorum* tissue.

3.4.4 Conclusion

Differentiation of the bacterial community into microhabitats within the host has been shown to contribute toward shaping and maintaining the microbiome in both *Hydra* and Scleractinia. The

purpose of this study was to test the idea that microhabitats might also exist in an Alcyoniidae; the only other soft coral to be analysed in this way was *P. arboraea* from the deep-sea. We show that there is a high degree of dissimilarity between mucus and tissue-associated bacterial communities in *L. pauciflorum*, but that the tissue layers were largely homogeneous. Differences in sequence abundance and inferred function between the microhabitats sampled here indicate that the communities associated with different tissue layers may perform different functions in the holobiont. Future work should focus on localization of bacterial cells within the tissues and structures of soft leather corals through imaging techniques to better understand microhabitat delineation. The high variability between colonies also indicates that further investigation into the Alcyoniid microbiome is needed to better understand natural variability compared to that induced by various stressors. Finally, the recovery of sequences associated with common coral-associated Bacteria such as Endozoicomonadaceae, Shewinellaceae, Francisellaceae and others further highlight the need for investigations into the function of these microbial taxa within the holobiont via stable isotope tracing and metabolomics studies. While we continue to learn about host-symbiont partnerships in corals we still have very little information concerning the symbiont function or mechanisms of community mediation. Understanding these aspects of the host-symbiont relationship should be considered the next objectives in coral microbiome research.

Chapter 4: *Lobophytum pauciflorum* larva-associated bacteria from fertilization to competency

Abstract

The bacteria associated with Metazoa are important for maintaining host health. The timing of bacterial onset and the pattern of community establishment during the early stages of host development can have significant implications for health later in life. While an important component of the coral holobiont, very little is understood concerning the onset and establishment of the associated bacterial community. This study characterizes the bacterial community associated with the soft leather coral *L. pauciflorum* throughout 9 timepoints between fertilization and competency (6, 14, 24, 36, 48, 72, 96, 120 and 210 hours post fertilization) (hpf). Two stages of community succession are highlighted: an early stage (timepoints 6 – 48 hpf) characterized by Pseudoalteromonadaceae and Alteromonadaceae and a late stage (timepoints 72 – 210 hpf) characterized by Sphingomonadaceae and Comamonadaceae. Additionally, sequences affiliated with Francisellaceae are dominant during the transition from early to late stages, and sequences recovered from healthy adult colonies of *L. pauciflorum* – such as Endozocimonadaceae – were recovered from the final timepoint at 210 hpf, when larvae were expressing competency. This novel study enhances our understanding of development and host-symbiont interactions in the Octocorallia. Similarities in *L. pauciflorum* development with that of Scleractinia and *Hydra* also indicate that these findings may contribute to our understanding of development at higher taxonomic levels in the Cnidaria.

4.1 Introduction

The bacterial community associated with corals is predicted to provide many benefits to host physiology (Reshef *et al.* 2006; Peixoto *et al.*, 2017). Some bacteria recovered from coral colonies have demonstrated antimicrobial properties (Ritchie *et al.* 2006; Kvennefors *et al.* 2012) while others may enable the host to better tolerate environmental stress (Ziegler *et al.* 2017) and changes in local environmental conditions (Voolstra and Ziegler 2020). The pattern of colonization on coral larvae, and how the assemblage develops into the complex community observed in mature coral colonies, however, remains a knowledge gap in our understanding of the coral microbiome. The bacterial community structure in mature colonies to some extent correlates with host phylogeny (Pollock *et al.* 2018; O'Brien *et al.* 2020), suggesting that the bacterial community on coral larvae may follow a repeatable pattern of succession during the colonization of each new generation. Even in humans, inhibition of a healthy pattern of community succession during initial colonization of offspring can result in significant physiological conditions later in life (Clarke *et al.* 2014; Tamburini *et al.* 2016). To comprehend the bacterial community structure in a healthy, mature coral colony, we must therefore understand how that community structure is established. As anthropogenic climate change is currently threatening coral reefs on a global scale (Hoegh-Guldberg *et al.* 2007; D'Angelo and Wiedenmann 2014), understanding the interactions between corals and their associated microbes is more important now than ever.

Microbes may initially be introduced to developing larvae either vertically, from the parent, or horizontally by being encountered in the environment. Brooding corals exhibit vertical transmission during internal fertilization and development with horizontal acquisition following their release from the parent colony (Thompson *et al.* 2015; Hartmann *et al.* 2017; Epstein *et al.* 2019; Damjanovic *et al.* 2020 c). Broadcasting corals that release gametes into the water for external fertilization are not sheltered by a parent colony throughout early development and are thought to largely rely on the horizontal acquisition of bacterial associates (Figure 4.1). Local environmental conditions therefore have the potential to significantly influence community composition and structure during initial bacterial colonization of coral larvae. In the brooding scleractinian *Porites astreoides*, increased seawater temperature decreased larval size and Symbiodiniaceae density (Edmunds *et al.* 2005) and increased larval mortality (Serrano *et al.* 2018) and post-settlement recruitment failure (Ross *et al.* 2013). However, rearing larvae in manipulated environments – with water or substrate imported from the reef, in varying concentrations of ambient microbes, and in the vicinity of adult coral colonies – had no impact on the pattern of bacterial community development (Bernasconi *et al.* 2019; Damjanovic *et al.* 2020a). This also supports the hypothesis that coral larvae display preferential

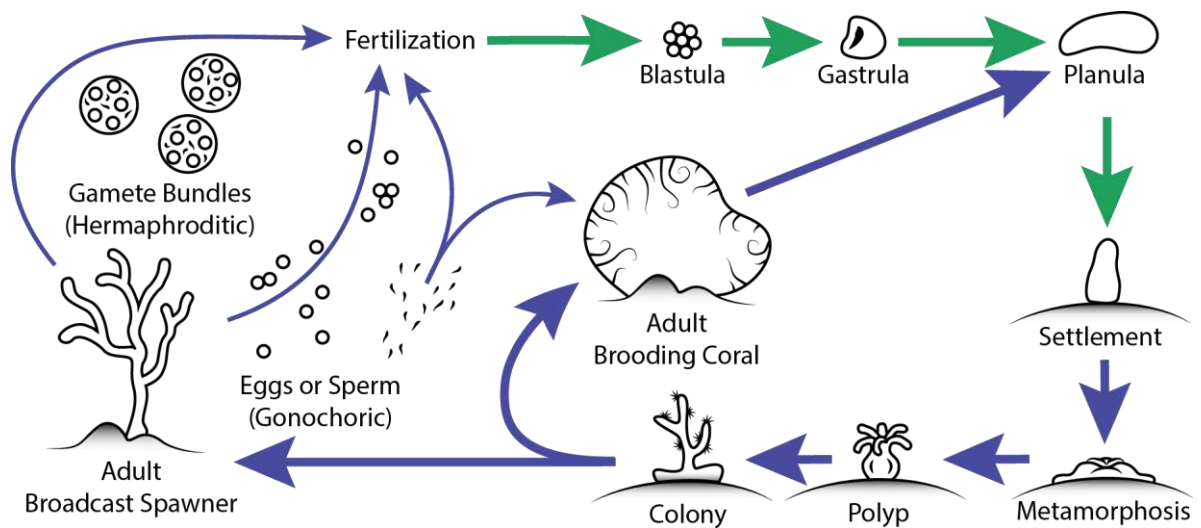


Figure 4.1: Modes of reproduction in corals showing pelagic and benthic stages of development.

Lobophytum pauciflorum is a gonochoric broadcast spawner, releasing unbundled eggs and sperm separately into the water column with external fertilization and development. Developmental stages investigated in this study are represented by green arrows (fertilization to competency) representing the first 210 hours post-fertilization (hpf).

selection of bacteria horizontally acquired from the environment (Aprill *et al.* 2009; Freire *et al.* 2019).

Analysis of the Scleractinian broadcast-spawners *Acropora tenuis* and *Pocillopora meandrina* with FISH found that bacterial cells are not internalized by the host until larvae are fully developed (Aprill *et al.* 2009; Damjanovic *et al.* 2020b). A study of 7 broadcasting corals offered further support to these findings by failing to recover 16S sequences in larvae prior settlement and metamorphosis of the polyp (~120 hpf) (Sharp *et al.* 2010). While bacteria were not internalized until later in larval development, external bacteria on the epithelial surface or mucous layer may still be closely associated with the host. This is supported by a study on *Acropora digitifera* larvae where bacterial community in the mucus layer shifted with development stage of the host (Damjanovic *et al.* 2020 b). Shifts in the bacterial community have been hypothesized to correlate with the changing metabolic requirements of the developing host, though this has not been proven (Bernasconi *et al.* 2019). In *P. meandrina*, however, larvae as early as 18-36 hours post-fertilization (hpf) have been recorded assimilating nitrogen previously metabolized by associated bacteria (Ceh *et al.* 2013 b), leading some credence to the potential for metabolite exchange with the host larvae.

Successful metamorphosis in the brooding octocoral *Rhytisma fulvum* after rearing in sterile seawater indicated that brooding corals may not require horizontal transmission of associated Bacteria for development (Freire *et al.* 2019). Studies on *Pocillopora acuta* and *Pocillopora damicornis*, however, found that vertical transmission likely occurs but that horizontal acquisition still shapes the

community (Epstein *et al.* 2019; Damjanovic *et al.* 2020). Additionally, a metastudy of scleractinian larvae proposed that horizontal acquisition during the planular phase could help larvae tolerate environmental influences and spend more time in the water column selecting an appropriate settlement site. (Hartmann *et al.* 2017).

Sequences affiliated with the Bacteria Rhodobacteraceae (*Roseobacter* spp.) and Alteromonadaceae (*Alteromonas* spp.) have been consistently recovered in high abundance from larvae in Scleractinia (Apprill *et al.* 2009, 2012; Sharp *et al.* 2012; Ceh *et al.* 2013 a; Lema *et al.* 2014, Sharp *et al.* 2015; Damjanovic *et al.* 2020a; Kullapanich *et al.* 2021). *Roseobacter* species have demonstrated antimicrobial properties against coral pathogens and both families have been shown to induce settlement in coral larvae (Webster *et al.* 2004, Sharp *et al.* 2015). The common occurrence of *Roseobacter* and *Alteromonas* across multiple host species and reproductive strategies in these studies suggest that Bacteria may play an important role in the early development of larvae in hard corals.

Studies on microbial community development in coral larvae have thus far focused on scleractinian larvae at a limited number of developmental timepoints. This study will characterize the bacterial community associated with *L. pauciflorum* larvae at 9 timepoints between fertilization and competency (6, 14, 24, 36, 48, 72, 96, 120 and 210 hpf). The soft leather coral *L. pauciflorum* is a gonochoric broadcast-spawner that reproduces sexually during annual mass-spawning events between October and December (Alino 1989, Wessels 2016), as well as asexually through colony fission (Fan *et al.* 2005). The Bacteria associated with mature colonies of *L. pauciflorum* were characterized previously (Chapter 2 and 3) which would be complimented by a better understanding of the initial patterns of colonization and community development. The timeline in this study provides higher resolution sampling points between fertilization and competency than any previous study of this type and is the first to focus on bacteria colonizing on soft coral larvae. Closing these knowledge gaps will improve our understanding of the host-symbiont interactions in cnidarians and in developing metazoans.

4.2 Methods

4.2.1 Spawning of *L. pauciflorum*

Fieldwork was conducted on Orpheus Island, Queensland in 2016. Spawning took place at approximately 20:00 on November 18, 4 days after the full moon. Colonies were selected and sexed based on histology published in a previous study (Wessels *et al.* 2017). Cone-shaped nets were placed over gravid females in the field; eggs are funnelled up the cone toward a collection cup for transport to the wet laboratory. Male colonies were isolated in the wet laboratory thus sperm was retained in

individual buckets for distribution amongst the eggs. Fertilization was carried out at ~22:00 in 60 L tubs and monitored by periodically examining a dozen or so larvae under a dissecting microscope. When more than 75% of the fertilized eggs were successfully dividing, they were gently transferred to tubs of fresh seawater to prevent biofouling from excess sperm. When over 75% of the embryos approached the 16-cell stage, all embryos were transferred to a 500 L flow-through circular rearing tub. The rearing tub was continually fed with seawater pumped in from the reef crest and filtered through a series of 10-, 5- and 1-micron filters. The rearing tubs were kept in a circular current to prevent stagnation or biofouling.

4.2.2 Sample collection

Larvae collected at each time point (6, 14, 24, 36, 48, 72, 96, 120 and 210 hours post fertilization (hpf)) were photographed (Figure 4.2) and sampled in triplicate under Great Barrier Reef Marine Park Association (GBRMPA) permit number G16/38499.1 (Table 4.1). Larvae were sieved from the 500 L rearing tub, transferred to a sterile 15 ml tube and rinsed 3 times by removing the water (touching the pipette tip into the bottom of the tube removed water from beneath the larvae without damaging them) and refilling with 3-5 ml 0.22 μm -filtered seawater. After removing the water to

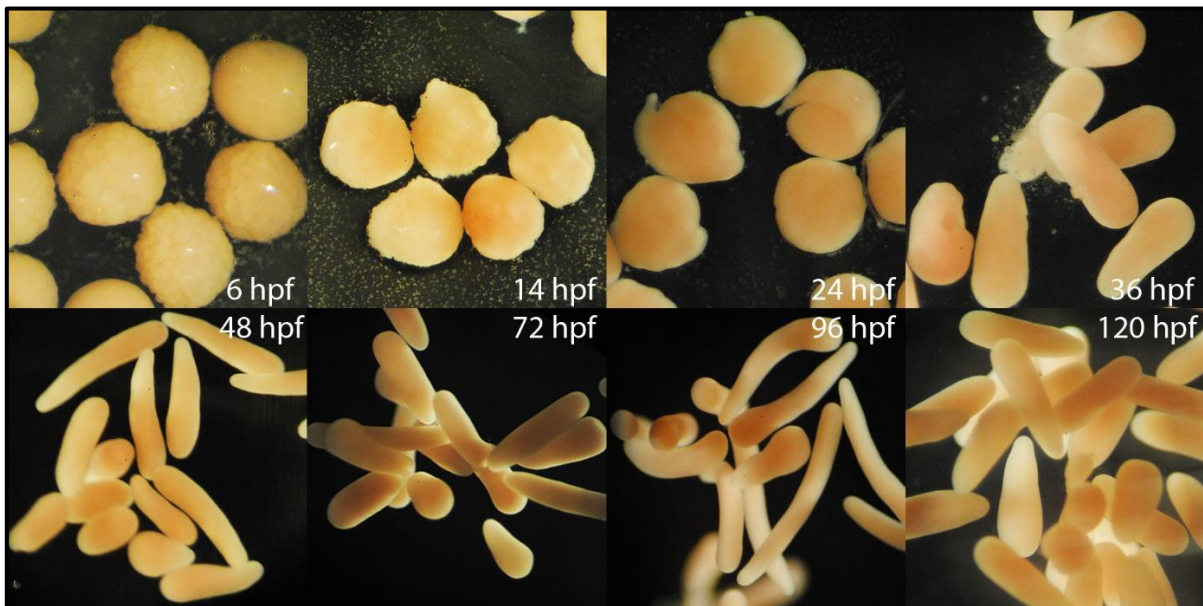


Figure 4.2: *Lobophytum pauciflorum* larvae photographed under a dissection microscope at each timepoint sampled. Photographs were taken absent scale for visualization only, as reproduction and developmental morphology of *L. pauciflorum* have previously been described in detail by Wessels (2016).

Table 4.1: List of samples collected and processed for 16S rRNA gene amplification, sequencing and analysis. Some samples did not yield amplicon products due to insufficient optimization of genomic extraction (Polymerase chain reaction [PCR] run B). Product was also recovered from one negative control (PCR run A) and was therefore included in sequencing. The final samples analyzed in this study were those which exceeded the sampling depth of 7,400 sequence reads, shown on bottom in bold.

	Timepoints sampled (hpf)									controls with product
	6	14	24	36	48	72	96	120	210	
16S samples	3	3	3	3	3	3	3	3	3	
Extracted	3	3	3	3	3	3	3	3	3	
PCR_run (A)	1	1	1	1	1	1	1	1	1	1
PCR run (B)				1						0
PCR run(C)	1	1	1	1	1	1	1	1	1	0
Failed	1	1	1	0	1	1	1	1	1	
Sequenced	2	2	2	3	2	2	2	2	2	1
>7,400 reads	0	1	2	2	2	2	2	2	2	1

concentrate the larvae, ~200 μ l were collected via a sterile 1000 μ l pipette with the tip trimmed so that the opening was large enough to extract larvae without damaging them. Three 200 μ l technical replicates were collected at each time point, snap frozen in liquid nitrogen and maintained at -80°C.

4.2.3 DNA isolation and amplification

Isolation of DNA was done with the PowerPlant DNA Isolation Kit (QIAGEN) according to the manufacturer's instructions. After adding the lysis buffer, phenolic separation solution and Rnase A to the tube containing 200 μ l of larvae, the sample was homogenized via bead-beating on a horizontal vortex at 2500 RPM followed by 5 minutes resting on ice. Three layers were present following centrifugation: The bottom layer of precipitates, an aqueous middle layer and a top 'slime' layer. During extraction of the 8 absent samples in PCR run B, the aqueous layer was collected and did not yield sufficient genomic DNA. In the remaining samples, the slime layer was collected and the extracted DNA was of higher quality and quantity and therefore used for amplification.

Three PCRs were run to prevent confounding batch effects, each composed of a single sample from each of the 9 timepoints plus a positive (*Flavobacteria sp.* culture) and negative (UltraPure water, Invitrogen, US) control reaction. The 16S rRNA target gene (variable regions 3 and 4) was amplified using the bacterial primers 341F and 785R with Illumina adapter overhangs (underlined) (S-D-Bact-0341-b-S-17 "TCGTCGGCAGCGTCAGATGTGTATAAGAGACAGCCTACGGGNGGCWGCAG" and S-D-Bact-0785-a-A-21 "GTCTCGTGGGCTCGGAGATGTGTATAAGAGACAGGACTACHVGGGTATCTAATCC", respectively) (Klindworth 2013). Reaction conditions were as follows: 30 sec at 98°C, [10 sec at 98°C, 30 sec at 55°C, 25 sec at 72°C] x 32 cycles, 5 min at 72°C and infinite hold at 4°C. Both primer sets were amplified with 1.25 μ l template DNA, 1.25 μ l each of 5 μ M forward and reverse primers, 6.25 μ l

Platinum SuperFi PCR MasterMix (Invitrogen, US) totalling 12.5 μ l reaction. An amplicon product was retrieved for 2 complete sets of timepoints (runs A and C). Run B comprised samples extracted prior to proper optimization of the extraction protocols for these larvae, therefore adequate PCR product was only recovered from the sample at 36 hpf. Additionally, the negative control from PCR run A produced an amplicon product while the negative controls from runs B and C did not. Negative control A was therefore sequenced along with the samples and analyzed with the R package microDecon (McKnight *et al.* 2019) aimed at removing potential contaminating 16S rRNA gene amplicons.

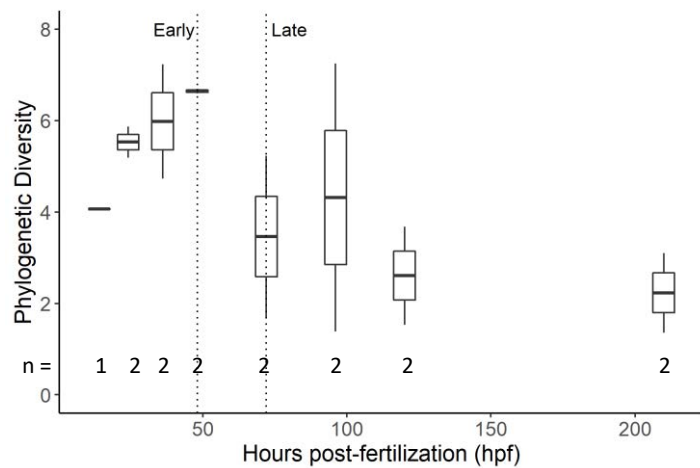


Figure 4.3: Faith's phylogenetic diversity index showing sequentially higher diversity across samples between 6 hours post-fertilization (hpf) and 48 hpf and lower diversity in the samples collected thereafter.

4.2.4 16S rRNA gene sequencing

Before and after indexing with Nextera XT DNA Library Prep Kit (Illumina, USA), products were cleaned with Sera-Mag Speed Beads (Merk, DE) using a Zephyr G3 NGS Workstation (PerkinElmer, USA) to standardize pipetting. The Indexing PCR conditions were the same as above with only 8 cycles. Quantification for library pooling was carried out on Enspire Alpha Plate Reader (PerkinElmer, USA) with Quantifluor dsDNA (Promega, USA). From each sample, 5 μ l were pooled and normalized to 4 nM final library concentration. Sequencing for 2 x 300 bp reads was done on a 2x300 Cycles V3 Flow Cell for MiSeq (Illumina, USA) with a 15% spike of PhiX v3 Control Kit (Illumina, USA) for quality control and calibration.

4.2.5 Analysis of 16S rRNA gene sequences communities

The Qiime2 pipeline (Bolyen *et al.* 2019) was used to sort and filter raw sequence reads, group identical sequences into amplicon sequence variants (ASVs) (Porter and Hajibabaei 2018) and assign taxonomic affiliations (SILVA 99 % database release 132) (Quast *et al.* 2013). Data was denoised with the quality control plugin DADA2 (Callahan *et al.* 2016). Feature data was exported to R and sequences which affiliated with anything other than Bacteria (Archaea, mitochondria or chloroplast) were removed. The filtered feature table was imported back to QIIME2 for alpha and beta diversity metrics

with a sequencing depth of 7,400, retaining 41.6 % of sequences in 80.0 % of samples. Rarefaction was based on Shannon's Diversity Index, total ASV count and Faith's Phylogenetic Diversity index. Measures of community dissimilarity and ordination for Beta diversity metrics were calculated according to Bray-Curtis Index. The Alpha metrics for phylogenetic diversity and evenness were calculated with Faith's Phylogenetic Diversity and Pielou's Evenness indices, respectively.

For analysis of community composition, reads were normalized according to total sum standardization (TSS) (McKnight 2019). For grouped comparisons, mean and standard deviation were based on the relative abundance calculated at the respective taxonomic level. Statistical analysis was run with the Vegan package (Oksanen *et al.* 2020) in R (R Core Team 2013; R Studio Team 2015) and seqinr was used to manipulate fasta formatted sequence files (Charif and Lobry 2007). The differentiation of communities was analyzed with analysis of similarity (ANOSIM) and permutational multivariate analysis of variation (PERMANOVA). For phylogenetic comparison with some sequences, MAFFT alignments and BLAST searches (Altschul *et al.* 1990) were performed in Geneious Prime 2019.2.1 (<http://www.geneious.com>). Contamination of the negative control from amplification run A was explored with the R package microDecon (McKnight *et al.* 2019), considering each time point as a population, and all analyses were applied to both decontaminated and unaltered datasets for comparison.

4.3 Results

4.3.1 16S rRNA gene sequencing and data processing

The sequencing run recovered 304,103 reads from 21 samples (mean 14,481 reads per sample). Fewer sequences were recovered from the samples at 6 hpf (37 and 3,865 reads in the replicates) and 14 hpf (5132 and 8126 reads, respectively). Sampling depth in QIIME2 was set to 7,400 which excluded both replicates from 6hpf, 1 sample from 14 hpf and 1 from 36 hpf. The number of samples per time point included in downstream diversity metrics were therefore $n = 0$ at 6 hpf, $n = 1$ at 14 hpf and $n = 2$ for all remaining time points. Alpha diversity as determined according to Faith's Phylogenetic Diversity index was high in the first few time points (5.8 ± 1.2), highest at 48 hpf (6.6 ± 0.1) and lower in the samples from 72 hpf onward (3.2 ± 2.2) (Figure 4.3). Group evenness was similar across all samples (pielou's 'e' value = 0.8 ± 0.1).

4.3.2 Bacterial community composition during the first 210 hours of life

The bacterial community of developing *L. pauciflorum* larvae was characterized at 9 timepoints between fertilization and competency (Figure 4.4). The first time point sampled at 6 hpf received a low number of sequence reads (3,865) and was therefore excluded from the analyses of

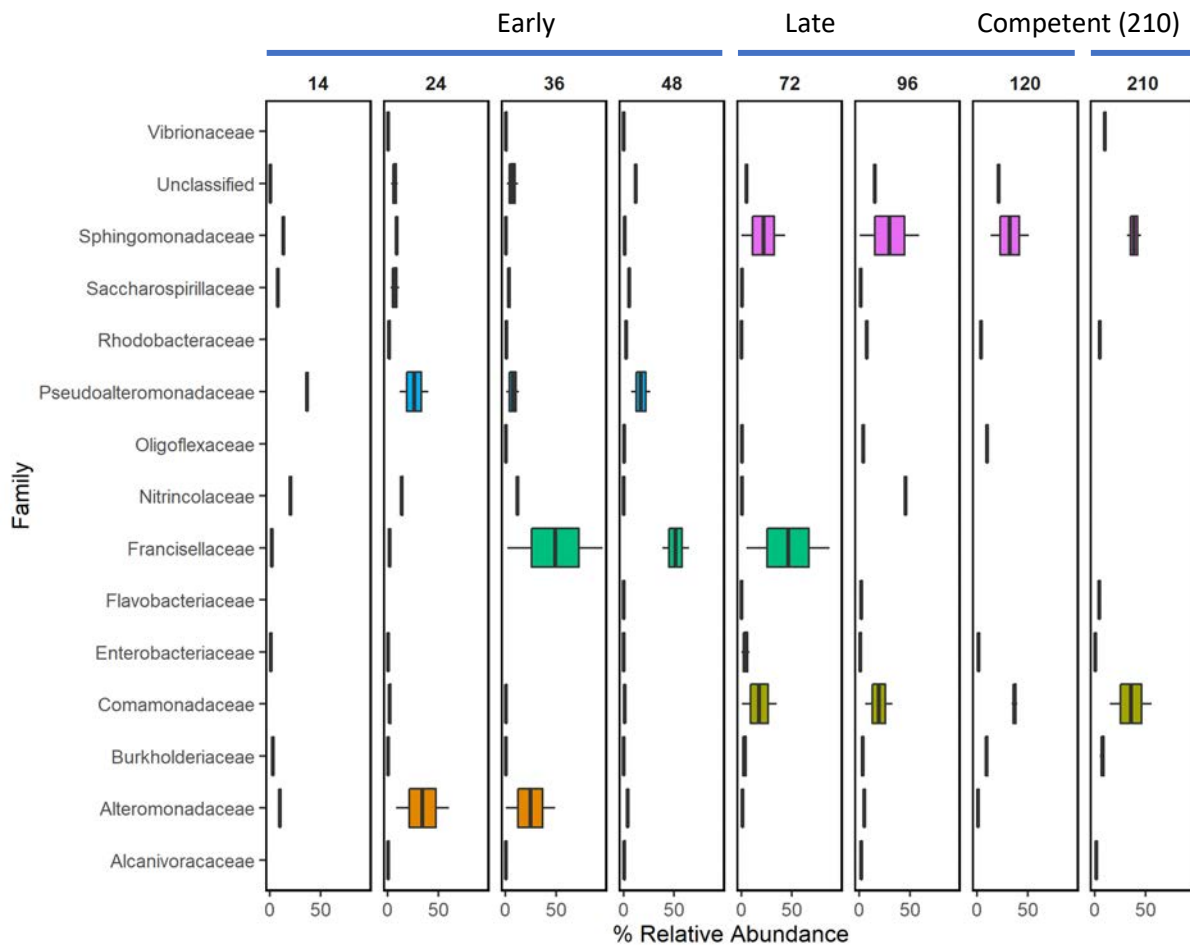


Figure 4.4: Most prominent bacterial families affiliated with sequences recovered from larvae of *Lobophytum pauciflorum* at 9 timepoints: 6, 14, 24, 36, 48, 72, 96, 120, 210 hours post-development (hpf). Only ASVs which contributed more than 5.0 % relative abundance cumulatively across samples are included in this visualization for practicality. The “early” and “late” stages of development, as well as competency at 210 hpf, are noted at the top.

diversity metrics. However, as the community composition of sequences did not appear as an outlier in the dataset, it is presented briefly here for context. Many of the reads recovered from 6 hpf were Unclassified (53.1 % relative abundance) but 27.1 % affiliated with Proteobacteria and 8.9 % affiliated with Saccharospirillaceae. The Proteobacteria-affiliated sequences were classified to the families Pseudoalteromonadaceae (27.1 %) and Saccharospirillaceae (8.7 %).

All of the timepoints sampled between 14 and 210 hpf were dominated by sequences affiliated with Proteobacteria (92.4 ± 7.2 % SD) with a diverse assemblage of low-abundance sequences. The sequences which were not classified beyond the level of Bacteria comprised a mean of 6.0 ± 6.8 % relative abundance with highest abundance in the 48 hpf samples (11.6 ± 0.3 %) and in one replicate from 120 hpf (21.2 %). Sequences affiliated with Dependentiae (1.2 %) and candidate phylum WPS-2 (Eremiobacterota) (0.8 %) were recovered from 14 hpf only. Sequences affiliated with

Bacteroidetes were recovered in low relative abundance from samples at 36 hpf through to 72 hpf (0.2 ± 0.3 %) and were slightly higher in one sample from 96 hpf (4.8 %). Similarly, sequences affiliated with Actinobacteria were recovered in low abundance from all time points from 36 hpf and later (0.5 ± 0.5 %). Sequences affiliated with Chloroflexi were recovered from 72 hpf (1.3 ± 1.8 %), and Firmicutes from 48 (0.4 ± 0.6 %) and 120 hpf (0.5 ± 0.7 %) samples.

Of the Proteobacteria-affiliated sequences, those affiliated with Gammaproteobacteria were recovered in highest relative abundance from samples 14 hpf to 48 hpf (90.3 ± 7.8 %). The time points sampled at 72 hpf and later were dominated by sequences affiliated with Alphaproteobacteria (34.7 ± 21.6 %) and Betaproteobacteria (35.1 ± 23.2 %). Deltaproteobacteria was also affiliated with a low number of sequences recovered from 14 through 72 hpf (0.8 ± 0.5 %) but comprised 7.7 % and 12.5 % in one replicate each from 96 and 120 hpf, respectively.

Sequences classified to the level of family show distinct changes in community structure throughout larval development but also show high variability between replicates. Sequences recovered from 14 hpf affiliated with Pseudoalteromonadaceae (36.8 %), Nitrospiraceae (20.4 %), Sphingomonadaceae (13.5 %), Alteromonadaceae (9.7 %) and Saccharospirillaceae (7.8 %). Showing similar composition, the samples at 24 hpf were dominated by sequences affiliated with Alteromonadaceae (34.3 ± 36.8 %), Pseudoalteromonadaceae (25.9 ± 20.0 %), Nitrospiraceae (13.9 ± 0.7 %) and Saccharospirillaceae (6.9 ± 5.9 %). In the samples collected from 36, 48 and 72 hpf the community is dominated by sequences affiliated with Francisellaceae (48.6 ± 65.9 %, 51.4 ± 18.6 % and 46.1 ± 57.9 %, respectively). The next-most abundant sequences at 36 and 48 hpf are affiliated with Alteromonadaceae (24.4 ± 34.5 %, 4.0 ± 0.8 %, respectively) and Pseudoalteromonadaceae (7.0 ± 8.7 % and 17.2 ± 13.3 %, respectively) as well as Nitrospiraceae at 36 hpf (5.9 ± 8.4 %) and Saccharospirillaceae at 48 hpf (5.6 ± 2.2 %) in low relative abundance. While dominant in these early time points, sequences affiliated with Pseudoalteromonadaceae (72 hpf and later) and Francisellaceae (96 hpf and later) contributed 0.0 % relative abundance in samples from the later time points.

The sequences recovered from the later time points at 72, 96, 120 and 210 hpf affiliated with Sphingomonadaceae (21.8 ± 30.6 %, 30.0 ± 41.4 %, 32.1 ± 26.6 % and 38.7 ± 9.8 %, respectively) and Comamonadaceae (17.7 ± 24.1 %, 29.4 ± 18.6 %, 37.0 ± 3.9 % and 35.7 ± 29.2 %, respectively). In one sample from 96 hpf, sequences affiliated with Nitrospiraceae were in high relative abundance (45.8 %) and 0.0 % in the replicate). Sequences recovered from 120 and 210 hpf affiliated with Burkholderiaceae (9.5 ± 3.0 % and 7.6 ± 3.5 %, respectively). At 210 hpf, sequences in low abundance affiliated with Bacteria families which have previously identified as *L. pauciflorum* associates, including Vibrionaceae (5.1 ± 7.2 %), Flavobacteriaceae (2.1 ± 3.0 %), Shewanellaceae (2.0 ± 0.8 %) and Endozoicomonadaceae (0.8 ± 1.1 %), all of which are absent or in much lower relative abundance in

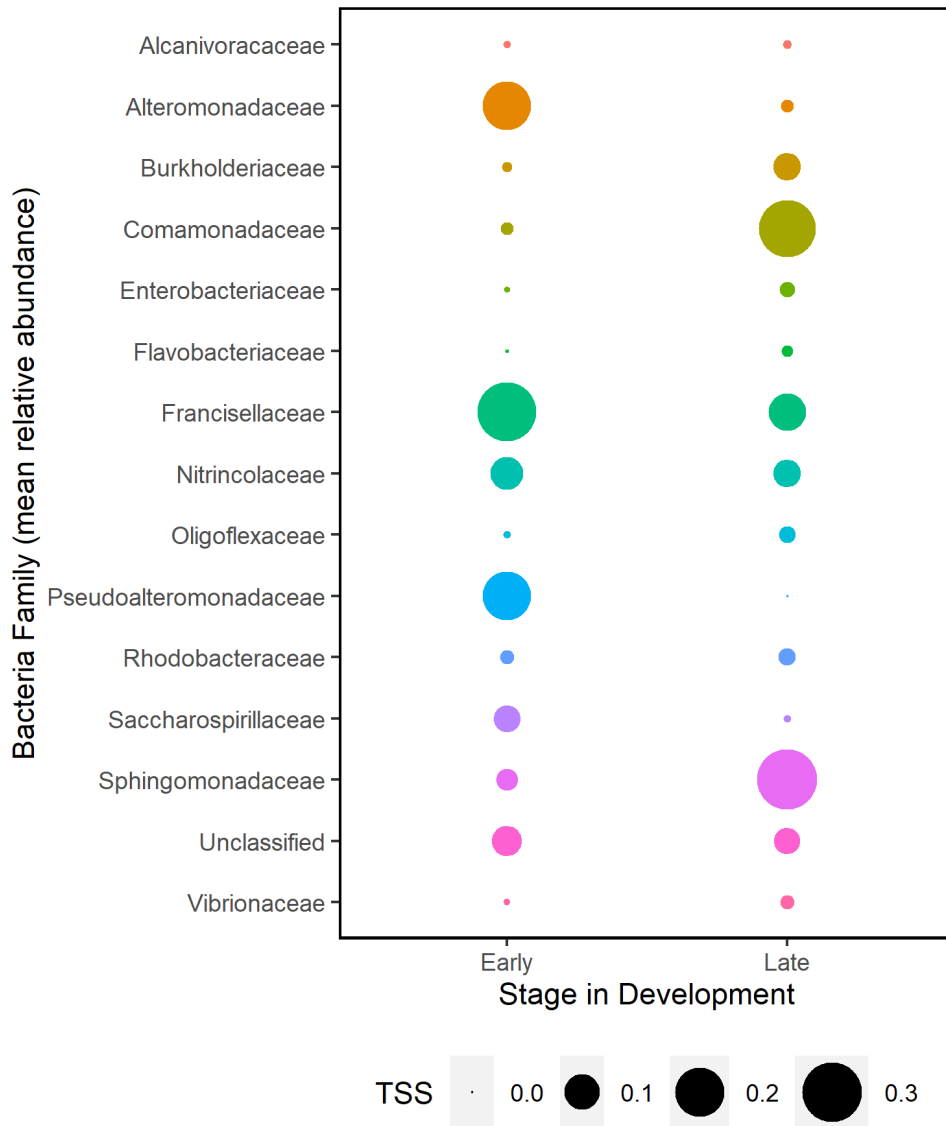


Figure 4.5: Stages of Community Succession showing mean relative abundance of sequences between early (14 to 48 hours post-fertilization [hpf]) and late (72 to 210 hpf) communities. For visualization, only sequences contributing cumulative relative abundance of at least 5 % across samples are shown.

all previous time points sampled. Sequences affiliated with Rhodobacteraceae were present in low abundance across all time points sampled after 14 hpf (1.8 ± 2.3 %).

4.3.3 Stages of community succession

Significant differences were observed in alpha diversity and community composition between samples collected at 48 and 72 hpf. Timepoints were therefore clustered into ‘early’ (14 through 48 hpf) and ‘late’ (72 through 210 hpf) communities (Figure 4.5). By ANOSIM hpf was not a significant variable on its own ($p = 0.123$), but designation of early and late communities was highly significant ($p = 0.001$). The samples at time points 48 and 210 hpf were also tested as distinct communities: 48 hpf

as the transition between early and late stages, dominated by sequences affiliated with Francisellaceae and 210 hpf as the competent phase of the larval life history. These grouping regimes were also significant by ANOSIM ($p = 0.01$ for early, late and competent stages and $p = 0.031$ early, late, a transitional community and competency), but less so than a 2-stage description of early and late communities. PERMANOVA supported the findings from ANOSIM. Early and late ($R^2 = 0.28$, pseudo-F = 0.010), the distinction of competency ($R^2 = 0.31$, pseudo-F = 0.020) and transition plus competency ($R^2 = 0.38$, pseudo-F = 0.038) were all significant descriptors of variability, but none significantly increased the explanatory power in stepwise comparison. These analyses indicate that 2, 3 and 4-stage descriptions of community succession are all statistically significant but that they describe roughly the same variability among communities. We therefore focus on a 2-stage description of early and late successive communities in this discussion.

The early stage was characterized by sequences affiliated with Pseudoalteromonadaceae (21.2 ± 16.1 %), Alteromonadaceae (20.9 ± 26.3 %), Saccharospirillaceae (6.1 ± 3.6 %). While the sample at 6 hpf was excluded from the analyses, the community composition also aligns well with this characterization of the early-stage community. The mean relative abundance of Francisellaceae-affiliated sequences is also higher in the early stage (31.3 ± 40.2 %) than in the late stage (12.1 ± 32.3 %), though they are a better description of the transitional phase between them (36 through 72 hpf), as shown previously. The late stage was characterized by sequences affiliated with Sphingomonadaceae (31.1 ± 22.8 %), Comamonadaceae (28.9 ± 19.8 %) and Burkholderiaceae (6.2 ± 3.9 %). Sequences affiliated with Nitrospiraceae and Rhodobacteraceae were recovered in similar mean relative abundance from the early (9.1 ± 8.8 % and 1.4 ± 1.3 %, respectively) and late (6.8 ± 19.1 % and 2.4 ± 3.5 %, respectively) stages.

Intrinsic factors constitute indicator species driving community distribution as determined by envfit in vegan (max significance for all intrinsic variables = 0.01). The early-stage community shows higher variability in NMDS than the late community and shows intrinsic influence in 2 general directions: Cellvibrionaceae, Francisellaceae and Oleiphilaceae in one direction and Alteromonadaceae, Cellvibrionaceae and Nitrospiraceae in the other. The families Sphingomonadaceae, Comamonadaceae and Burkholderiaceae are the strongest indicator species of the late-stage community. Extrinsic variables supported the previous analysis in that the distinction between early- and late-stage communities was the most significant descriptor of site distribution ($R^2 = 0.40$, pseudo-F = 0.001) followed by early, late and competent ($R^2 = 0.43$, pseudo-F = 0.005) and finally early, transition, late and competent ($R^2 = 0.46$, pseudo-F = 0.016).

4.3.4 Alignment to BLAST hits

Most of the 43 ASVs affiliated with Alteromonadaceae sequences were unassigned at the genus level, but 15.2 % were classified as *Alteromonas* and 2.2 % as *Aestuariibacter*. The consensus identity shared a 92.4 % pairwise identity match and, in BLAST, matched 99.3 % with *Aestuariibacter aggregatus* (NR_116838) and 98.9 % with both *Alteromonas oceani* (NR_159349) and *Alteromonas lypolytica* (NR_156088). There were also 43 ASVs classified to Pseudoalteromonadaceae, 94.5 % of which were classified as *Algicola* spp in the SILVA database but affiliated with members of *Pseudomonas* in BLAST. The consensus identity shared 93.2 % pairwise identity and aligned at 98.0 % identity to more than 10 *Pseudomonas* spp. The dominant ASVs showed 97.9 % sequence identity to both *Pseudomonas piratica* (NR_157758) and *Pseudomonas spongiae* (NR_043172) isolated from the scleractinian (*Montipora capitata*) (Beurmann *et al.* 2017) and the marine sponge *Mycale adhaerens* (Lau *et al.* 2005), respectively.

The 7 Francisellaceae-affiliated ASVs in highest relative abundance shared 99.5 % pairwise identity match and the consensus sequence aligned with a 98.3 % closest identity match in BLAST to the type strain *Cysteiniphilum litorale* (NR_157652), isolated from coastal seawater in Japan (Liu *et al.* 2017). However, BLAST searches of individual Francisellaceae-affiliated sequences aligned each between 94 - 99.9 % sequence identity to Accession numbers FJ202895 and FJ202734, originally retrieved from the scleractinian *Montastraea faveolata* (Sunagawa *et al.*, 2009). The sequences affiliated with Sphingomonadaceae were assigned to *Sphingobium* and *Sphingomonas*. The sphingobium-affiliated sequences shared 99.6 % pairwise identity and matched 100 % to *Sphingobium yanoikuyae* (NR_115524) in BLAST. The sequences affiliated with *Sphingomonas* shared 99.0 % pairwise identity and the consensus sequence identity matched 99.9 % each to *Sphingomonas alpina* (NR_117230), *Sphingomonas echinoides* (NR_113806) and *Sphingomonas oligophenolica* (NR_024685). The 8 *Pelomonas*-affiliated sequences in high relative abundance shared 99.5 % pairwise identity and the consensus sequence had a 99.6 % BLAST closest identity match to *Pelomonas aquatica* (NR_042614) and 99.4 % to *Pelomonas sacharophila* (NR_115053). Both of these type strains were isolated from wastewater (Gomila *et al.* 2007). The 5 *Ralstonia*-affiliated sequences were a 99.5 % pairwise identity match and 99.7 % closest BLAST identity match to *Ralstonia pickettii* (NR_114126), the same species classification as assigned by SILVA. Finally, all 3 ASVs assigned to Endozoicomonadaceae shared 99.3 % pairwise identity and matched most closely to *E. acroporae* (NR_158127) and *E. coralli* (NR_169415) (99.8 % and 99.4 %, respectively).

4.3.5 Analysis of a contaminated blank

Analysis of the negative control sequenced from amplification run A provided evidence that the negative blank was cross contaminated by a sample from 72 or 96 hpf but that the dataset was not contaminated with external sequences (Appendix C). There was no bias apparent in NMDS related to the different amplification runs (A, B or C) (Figure 4.6). The negative control clustered with the late-stage samples while early-stage samples clustered separately. The early and late clusters included the respective samples from both runs A and C, and the 36 hpf sample amplified in run B clustered with

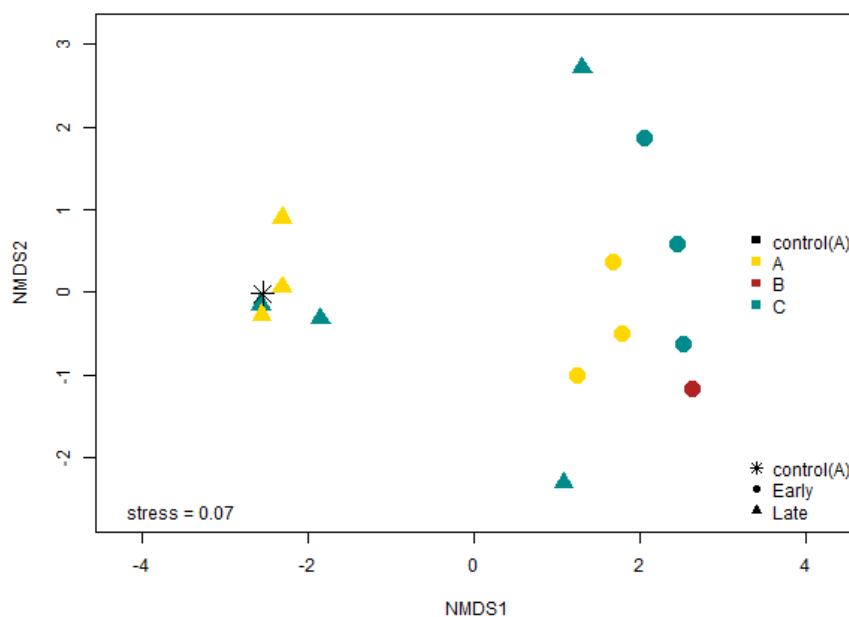


Figure 4.6: Non-metric multi-dimensional scaling (NMDS) plot of all samples analysed including the blank, displayed with color representing the amplification run (A, B or C) and shape representing the stage of community succession (early or late). The negative control from amplification run A is indicated as a black asterisk and clusters strongly with late-stage samples from both runs A and C.

the early-stage community. Analysis with ANOSIM and adonis2 confirmed that PCR run was not a significant descriptor of sample distribution. The package microDecon in R is intended to identify and remove sequences affiliated with contaminated blanks included in the analysis. Of all sequence reads affiliated with Sphingomonadaceae, Burkholderiaceae and Comamonadaceae recovered in this dataset, 39.5 %, 26.4 % and 15.2 %, respectively were identified as potential contamination by microDecon. An additional 4.0 % of Beijerinckiaceae- and 0.1 % of Rhodobacteraceae-affiliated sequences were also identified as possible contaminants. Removing these sequences from the dataset, however, had little influence on mean relative abundance in community composition and had no impact on the statistical significance of characterizing the community succession into early and late stages. Furthermore, these sequences have already been shown to correspond to the late-stage

community and not the early-stage community, and do not differ according to amplification run. This is supported by envfit which highlights sequences affiliated with these taxa as indicator species of the late stage with and without putative contaminant sequences included in the analysis. Extrinsic factors tested by envfit with and without decontamination also show that the distinction between successive stages (early, transition, late, competent) are the most significant drivers of distribution (max = 0.01) included in the analysis, and that PCR run is not a significant extrinsic factor. Community composition of the sequences recovered from the negative control closely resemble the community at 72 and 96 hpf, indicating possible sources of internal cross-contamination.

4.4 Discussion

This study characterized a dynamic pattern of succession in the developing bacterial community at 9 timepoints throughout the first 210 hours of life in *L. pauciflorum*. Based on the pattern of compositional changes and analyses of alpha and beta diversity, the succession of the bacterial community on developing larvae in *L. pauciflorum* can be grouped into distinct phases: “early development”, “late development” and “competency”. Statistical analysis of the community associated with each timepoint showed dramatic changes in structure between 48 hpf and 72 hpf, and between 120 hpf and 210 hpf. Variability within individual timepoints and between development phases is probably partially reflective of the low number of samples and potential variability between the individual planulae pooled for each sample. Furthermore, analysis of the 16S sequences recovered from the blank were determined not to have influenced the tissue samples.

4.4.1 Phases of community development

I Early Stage

The early stage described the bacterial communities associated with time points at 48 hpf and prior and was primarily characterized by sequences affiliated with Alteromonadaceae and Pseudoalteromonadaceae. Members of Alteromonadaceae have been reported as an early-onset member of the bacterial community in Scleractinia (Aprill *et al.* 2009, Ceh *et al.* 2013a, Freire *et al.* 2019). Via stable-isotope tracing, larvae have demonstrated that they take up nutrients previously metabolized by associated members of *Alteromonas* sp. (Ceh *et al.* 2013b). The Alteromonadaceae-affiliated sequences recovered from *L. pauciflorum* matched most closely with *A. aggregatus* (NR_116838) isolated from seawater (Wang *et al.* 2010), *A. oceani* (NR_159349) isolated from deep-sea sediment (Jin *et al.* 2018) and *A. lypolytica* (NR_156088) isolated from surface seawater (Shi *et al.* 2017).

The family Pseudoalteromonadaceae has also been reported in association with larvae of the scleractinian *Acropora humilis* during the first 48 hpf (Kullapanich *et al.* 2021). Members of Pseudoalteromonadaceae are recognized for the production of antimicrobial peptides (Atencio *et al.* 2018) and may in this way participate in helping to shape the early microbial community. Metabolites produced by members of Pseudoalteromonadaceae induce settlement and metamorphosis in some scleractinians (Tebben *et al.* 2011, Sneed *et al.* 2014) and can inhibit the growth of coral pathogens (Nissimov *et al.* 2009). The vast majority of Pseudoalteromonadaceae-affiliated sequences here were assigned to the genus *Algicola*, members of which have previously been associated with ‘stony coral tissue loss disease’ in scleractinians (Meyer *et al.* 2019), though the genus *Algicola* is metabolically versatile and may have some benign and some pathogenic members. This characterization of the bacterial community associated with early-stage coral larvae agrees overall with previous studies while highlighting the need for functional information on commonly recovered sequences such as Pseudoalteromonadaceae.

II Early stage – transition

Sequences affiliated with Francisellaceae became dominant at 36, 48 and 72 hpf, the time points that also show a shift from early to late stage communities. Francisellaceae-affiliated sequences have been recovered previously from adult *L. pauciflorum* (Chapters 1,2) and other octocorals (Holm and Heidelberg 2016). However, members of Francisellaceae are pathogenic in molluscs, fish and land mammals including humans (Rosenberg *et al.* 2014). Members of Francisellaceae were also proposed as opportunists or potential pathogens in a previous study on the bacteria associated with white band disease-infected tissue of *Acropora* spp. (Gignoux-Wolfsohn *et al.* 2016). The 7 ASVs in highest relative abundance shared 99.5 % pairwise identity match and the consensus sequence displayed 98.3 % closest identity match in BLAST to the type strain *Cysteiniphilum litorale* (NR_157652), isolated from coastal seawater of Japan (Liu *et al.* 2017). However, BLAST searches of individual Francisellaceae-affiliated sequences showed high sequence identity (between 94-99.9 %) to Accession numbers FJ202895 and FJ202734, retrieved from the scleractinian *Montastraea faveolata* (Sunagawa *et al.*, 2009). In this previous study the respective *M. faveolata* had spent 23 days in aquaria, so it is possible the proliferation of this strain was an artefact of the environment. However, as sequences were also recovered from adult *L. pauciflorum* collected from the field, it is more likely that Francisellaceae is an opportunist coral associate.

Gastrulation could be a contributing factor to the transition from early to late stages of succession. Gastrulation takes place in *L. pertusa* embryos between 14 and 27 hpf (Wessels 2016). The introduction of an orifice and gastric cavity could be a point of expansion in microbial diversity due to the increase in surface area and habitat heterogeneity. It is also presumed there will be a lag between

what takes place within the host during development and the observed structure of the microbiome. Larvae in this experiment underwent gastrulation in the expected time frame of 14-24 hpf, were elongate by 36 hpf and by 48 hpf they were fully developed, motile planulae. It is therefore possible that the shift in community structure at 48 hpf could be a latent response to gastrulation (~24 to 34-hour delay), but it would need to be studied in greater detail. In addition to changing physiology, Bernasconi *et al.* hypothesized that bacterial community associated with *Acropora digitifera* larvae was shaped by the changing metabolic requirements of the developing host. It is also notable that Apprill *et al.* (2009) determined that bacterial associates on larvae of the brooding coral *Pocillopora meandrina* were present on the surface but were not assimilated into the host tissue until after 48 hpf. The shifts observed in *L. pauciflorum* around this time could therefore also reflect the assimilation of tissue-associated bacteria following colonization on the surface.

III Late Stage – 72 hpf to 210 hpf

The late stage was dominated by sequences affiliated with the Alphaproteobacteria Sphingomonadaceae (*Sphingobium* and *Sphingomonas*). Sequences affiliated with Sphingomonadaceae have been recovered from both healthy (Carlos *et al.* 2013; Li *et al.* 2013; Kellogg *et al.* 2019) and diseased hard corals (Rosenberg and Ben-Haim 2002, Sobhana *et al.* 2019). The Sphingomonadaceae-affiliated sequences here were abundant, diverse and align mostly to strains isolated from environmental samples such as soil. Sequences affiliated with Comamonadaceae were also abundant in the late stage, classified to the genus *Pelomonas*, which has been reported in the core microbiome from the deep-sea coral *Eguschipsammia fistula* (Rothig *et al.* 2017).

Members of the order Burkholderiales also dominated the bacterial community associated with developing *Hydra*, an ancestor to Anthozoa. The community was first dominated by the family Burkholderiaceae and was successively dominated by members of Comamonadaceae (Franzenburg 2013). Host-symbiont interactions between the strains isolated from adult *Hydra* showed that the host physiology (Murillo-rincon *et al.* 2017) and defence against impending fungal infection required the presence of members of Comamonadaceae (genera *Pelomonas*, *Curvibacter* and *Acidovorax*), without which the host died (Fraune *et al.* 2015). Furthermore, the normal frequency of spontaneous body contractions in gnotobiotic *Hydra* was only restored via recolonization by *Pelomonas* sp. and not by other bacterial associates tested (Murillo-Rincon *et al.* 2017). This is particularly interesting considering the late stage of community development in coral larvae is when motility is achieved and they will soon metamorphose into contracting, filter-feeding polyps as well.

Sequences affiliated with another Burkholderiales genus, *Ralstonia*, also become prominent in the later time points, in highest relative abundance at 120 hpf. This is consistent with larvae of the stony coral *Mussismilia hispida* which were dominated by the genera *Burkholderia* and *Ralstonia*, as

well as *Pseudoalteromonas* (Leite *et al.* 2017). A coral microbiome review in 2015 regarded *Ralstonia* as a member of the core microbiome in a number of both hard and soft corals throughout the Caribbean Sea, the Red Sea, the Coral Sea and the Pacific Ocean (Ainsworth *et al.* 2015). The association with *Ralstonia* has been met with scepticism however due to its prevalence as a common laboratory contaminant of DNA isolation kits (Salter *et al.* 2014).

IV Competency – by 210 hpf

The samples at 210 hpf are notable because the planulae at this time are all competent, as evidenced by their obvious motility when in the large rearing tub but assuming a ‘competent’ phenotype (i.e. becoming stationary, assuming a vertical position with the aboral end touching the bottom substrate) when collected and transferred into petri dishes. While no larvae successfully settled or metamorphosed in the timeline of this study, all of those observed did achieve competency. The bacterial community at this timepoint more closely resembles that of an adult colony in the field (Wessels *et al.* 2017; Chapter 2) than any other time point analyzed, indicating that the microbial community succession in this study parallels the natural succession. Morphological development and competency also took place within the same timeframe as outlined in a study of reproduction and development in *L. pauciflorum* (Wessels 2016). Wessels (2016) reported difficulty inducing settlement of competent *L. pauciflorum* larvae even with the application of known settlement clues. In the current study, there were too few larvae remaining by 210 hpf to experiment widely, but application of crustose coralline extract did not successfully induce settlement. It is likely that a separate experiment on *L. pauciflorum* settlement cues will be necessary to study the pre- and post-metamorphosis microbiome.

The taxa affiliated with dominant groups in the earliest time points, Alteromonadaceae, Pseudoalteromonadaceae, Francisellaceae and Saccharospirillaceae, are virtually absent by 210 hpf. Sequences affiliated with Comamonadaceae and Sphingomonadaceae both increased from the other late-stage time points. Sequences affiliated with Endozoicomonadaceae, Shewinellaceae and Vibrionaceae were all present at 210 hpf but absent or nearly absent from earlier timepoints. These 3 taxa are known associates of the bacterial community in adult *L. pauciflorum* in the field (Wessels *et al.* 2017, Chapter 2). The final timepoint most closely resembles the bacterial community of mature colonies indicating that the pattern of community development observed in this study follows the natural course of succession.

4.4.2 Conclusion

The microbiome of mature colonies has been studied for composition, environmental resilience, functional capacity, antimicrobial capacity and more in a variety of corals, but all of this

knowledge should be complemented by understanding how the composition and structure of healthy adult corals is established. During the first 210 hours of life in *L. pauciflorum* larvae, the bacterial community is dominated by Francisellaceae, Sphingomonadaceae and Comamonadaceae and forms 2 distinct stages in composition during development. The observed patterns suggest active manipulation of the developing bacterial community by the host beginning in the first 48 hours post-fertilization. Whether bacterial associates triggered a response in the host (production of antimicrobial compounds) or vice versa (gastrulation) needs to be explored further to understand the role of the host in bacterial community succession during early life history. The study presented in this chapter made a significant step toward characterizing patterns of community succession on octocoral larvae, but future work needs to address symbiont function, to confirm that this pattern is repeatable and to test how resilient the pattern of succession is under predicted future stresses such as increased temperature, acidity, human disturbance, prevalence of pathogens and pharmaceuticals, sedimentation, etc.

Chapter 5: Differential expression of genes encoding AMP and Kazal-domain proteins may influence bacterial community development in *L. pauciflorum* larvae

Abstract

The onset and development of the bacterial community in early life stages has the potential to significantly impact host health later in life. Little is understood about the process of bacterial community development in soft coral larvae, including whether the host plays a role in mediating the succession. Studies on *Hydra* have shown that a host-specific consortium of antimicrobial peptides and Kazal-type serine protease inhibitors helps mediate the bacterial community in offspring throughout development, contributing to the innate immune system of the host. This study analysed the transcription of genes encoding potential homologs of AMP and Kazal-type proteins and throughout the first 183 hours post-fertilization (hpf) in the soft coral *Lobophytum pauciflorum* to explore the potential for antimicrobial mediation of bacterial community development. The R packages AMPiR and Mfuzz were used to predict candidate AMPs and for soft-clustering of differential expression profiles, respectively. Likely AMP and Kazal-type proteins (870) and nucleotide sequences (157) with shared homology in other Cnidaria were obtained from NCBI Genbank and aligned to an assembled *L. pauciflorum* reference transcriptome. Predicted Kazal- and Kunitz-type serine protease inhibitors and other Kazal-domain containing proteins were particularly abundant in *L. pauciflorum* larvae. Likely homologs of the cnidarian AMPs Aurelin, Hydramacin and Periculin were also identified and were differentially expressed in larvae. During development, the differential expression patterns of predicted AMPs and Kazal-type homologs correspond with the distinct stages of bacterial community succession characterized in chapter 4. These analyses imply that AMPs, serine protease inhibitors and Kazal-domain containing proteins may play important roles in modulating bacterial community structure during the development of *L. pauciflorum* larvae.

5.1 Introduction

The bacterial communities associated with corals are thought to influence environmental resilience, disease resistance, nutrient cycling and reproduction in the holobiont (Rosenberg and Rosenberg 2007). Despite the apparent importance to the adult host colony, there is a knowledge gap around the timing of the onset and pattern of development in the bacterial community associated with coral larvae. From the ‘human microbiome project’ we have learned that development of the microbiome during early life history can have life-long consequences for the health of the host (Tanaka and Nakayama 2017). As we continue to learn about the importance of a stable, healthy bacterial community to coral – and thereby coral reef – health and resilience, it is important that we improve our understanding of how bacterial communities are developed during the early life history of coral larvae and, ultimately, how the community succession is mediated to ensure healthy host development in a time of rapidly deteriorating environmental conditions.

Insights into host-symbiont interactions in Cnidaria have been gained from *Hydra* spp. The bacterial community structure of *Hydra* is highly conserved over time and space; two species sampled in the field hosted similar bacterial communities to laboratory-raised members of the same species more-so than to each other, even after more than 30 years of laboratory rearing (Fraune and Bosch 2007). This mediatory capability is due in part to a host-species-specific assemblage of powerful, discriminatory antimicrobial peptides (AMPs) (Franzenburg *et al.* 2013b). The innate immune system in *Hydra*, potentially conserved throughout the Cnidaria, relies on an intimate relationship with associated bacteria to trigger and secrete appropriate AMPs that ward off pathogens and suppress opportunists (Augustin and Bosch 2010; Fraune *et al.* 2015). In addition to AMPs, Kazal-type proteins also contribute to defense and physiology in *Hydra* (Chera *et al.* 2006; Augustin *et al.* 2009). The Kazal-2 serine protease inhibitors are part of the innate immune system in *Hydra magnipapillata*, and are secreted by endodermal gland cells in the epithelium. Kazal-2 inhibited trypsin and subtilisin, resulting in strong *in vitro* antibacterial activity against *Staphylococcus aureus* (Augustin *et al.* 2009).

The development of the bacterial community associated with developing *Hydra* follows a repeatable pattern of succession mediated by a host-specific regime of discriminatory AMPs (Fraune *et al.* 2011; Franzenburg *et al.* 2013), an important one of which is NDA-1 (Augustin *et al.* 2017). This pattern of succession features an early stage of high diversity followed by a late stage at 2 weeks post-hatching that more closely resembles the community associated with adults (Fraune *et al.* 2011; Bosch *et al.* 2012). A similar pattern was observed in developing *L. pauciflorum* (chapter 4) though the transition in the octocoral was observed around 48 hours post-fertilization (hpf). In *Hydra*, some

AMPs, such as Periculin, are maternally inherited and mediate the colonization of offspring by horizontally acquired bacteria in the earliest stages of development before larval transcription of AMPs begins (Fraune *et al.* 2010; Franzenberg *et al.* 2013).

The involvement of AMPs in modulating the microbiome is thought to be an ancient and widespread property among the Metazoa (Pasupuleti *et al.* 2012). In the marine environment, direct interaction with water-borne pathogens occurs constantly and AMPs are a staple of the innate immune system for host defense (Destoumieux-Garzon *et al.* 2016). The mechanisms employed by AMPs typically involve disruption of target cell membranes (Brogden *et al.* 2005). Defensins are a class of cysteine-rich antimicrobial peptides often involved in the innate immune system that have diversified extensively throughout metazoan evolution (Ganz 2003; Machado and Ottolini 2015).

Characterized AMPs associated with other Cnidaria include aurelin, an ShKT domain-containing defensin isolated from *Aurelia aurita* (Ovchinnikova *et al.* 2006) and damicornin. Damicornin was the first AMP isolated from a scleractinian (*Pocillopora damicornis*) and demonstrated antimicrobial activity against fungi and gram-positive bacteria (Vidal-Dupiol *et al.* 2011). In corals, antimicrobial activity has been confirmed in the mucus layer and suggested as a defense mechanism preventing opportunistic and pathogenic microbes in the local environment from colonizing the host tissue (Ritchie 2006; Kvennefors *et al.* 2012). An AMP known as amAMP-1 was recently identified in the scleractinian *Acropora millepora* and shown to be active against a range of bacteria. Although AmAMP-1 homologs are present in many scleractinians, the absence of clear homologs outside this group suggests that it is potentially a coral-specific AMP (Mason *et al.* 2021). Although amAMP-1 and damicornin both contain ShK-domains and are considered to be orthologs, the level of primary sequence similarity is relatively low (53 %). The protein amAMP-1 displayed behavioural similarities to NDA-1 in *Hydra* in that they are both produced in ectodermal cells resembling sensory neurons and that they both appear highly relevant during the developmental stages of host larvae (Mason *et al.* 2021).

It has been suggested that antimicrobial activity helps to stabilize the microbiome in octocorals (van de Water 2018). Potent antimicrobial activity has been documented in extracts of a variety of adult soft corals, including *L. pauciflorum* (Kelmen *et al.* 2009; Ibrahim *et al.* 2012; Nunez-Pons *et al.* 2013). Host-derived compounds are believed to mediate the associated bacterial community in gorgonians by both inhibiting colonizers and stimulating putatively beneficial bacteria (Hunt *et al.* 2012). However, while octocorals have been shown to be rich sources of novel antimicrobial agents, research has focused primarily on potential pharmaceutical properties of these

rather than their biological roles in the host (Hunt *et al.* 2012; Setyaningsih *et al.* 2012; Ledoux and Antunes 2018). The first transcriptomic analysis of an octocoral, *Gorgonia ventalina*, suggested that potential homologs of the AMPs arenicin-2 and royalisin were induced upon exposure to a parasite (Burge *et al.* 2013). Arenicin-2 is a polychaete AMP with antimicrobial activity against gram-negative bacteria (Andra *et al.* 2008), while royalisin is a defensin isolated from honeybees (Fujiwara *et al.* 1990).

Extracts of larvae of the soft coral *Parerythropodium fulvum* displayed strong antimicrobial activity against a range of bacteria and appeared to discriminate against coral pathogens over known coral associates. This activity was present in all developmental stages tested, between 1- and 6-day-old larvae (Kelmen *et al.* 1998). Likewise, larvae of the broadcast-spawning coral *Pocillopora meandrina* displayed preferential acquisition, favouring some bacterial species over others, and bacteria were not internalized until 2 weeks post fertilization (Aprill *et al.* 2009). Chapter 4 of this dissertation also characterized a distinct shift in bacterial community structure in *L. pauciflorum* larvae that was apparent in the 16S community around 48 hpf. While research into this topic is limited, these studies indicate the possibility that octocoral development (as represented by *L. pauciflorum*) may be similar to *Hydra* and Scleractinia in that maternally inherited AMPs protect the externally developing embryo until bacterial associates are internalized and the larvae are able to produce AMPs, at which point the bacterial community composition shifts dramatically.

The study presented here investigates this concept through differential expression analysis of larval transcripts collected throughout the first 183 hours post-fertilization in the soft leather coral *L. pauciflorum*. Applying the predictive R package AMPiR to the transcriptome of *L. pauciflorum* allowed the identification of a number of candidate AMPs and BLAST searching was then used to determine whether *L. pauciflorum* predicted proteins shared homology with known AMPs and defensins. The extent to which differential expression of these potential AMPs corresponded with bacterial community succession was examined through development to investigate the possibility that bacterial community composition may be shaped by AMPs expressed by the host larva.

5.2 Methods

5.2.1 Acquisition of available transcript data

Samples consisting of 100 larvae each, reared at Orpheus Island Research Station, QLD, Australia in 2014, were collected at 16, 27, 36, 48, 96 and 183 hours post-fertilization (hpf) in correspondence with morphological stages of development. Sample collection, RNA extraction, library

preparation and sequencing were carried out in a previous study and are described in detail in Wessels *et al.* (2016). Each sample was sequenced (100 bp; paired-end reads) in 2 separate lanes - treated as technical duplicates - with the Illumina HiSeq2000 platform (Illumina, USA). Samples received a mean of 8.9 million reads assembled into 632,920 contigs of 884 bp mean length and 67.95% mean GC content (Wessels *et al.* 2016). These transcripts were assembled into a *de novo* transcriptome and translated with the Trinity platform (Haas et al. 2013) in Wessels *et al.* (2016), used as references for AMPiR and BLAST analyses. This study will compare the differential gene expression in larvae sampled at these timepoints with 16S rRNA gene community data collected at 14, 24, 36, 48, 72, 96, 120 and 210 hpf (chapter 4) (Figure 5.1).

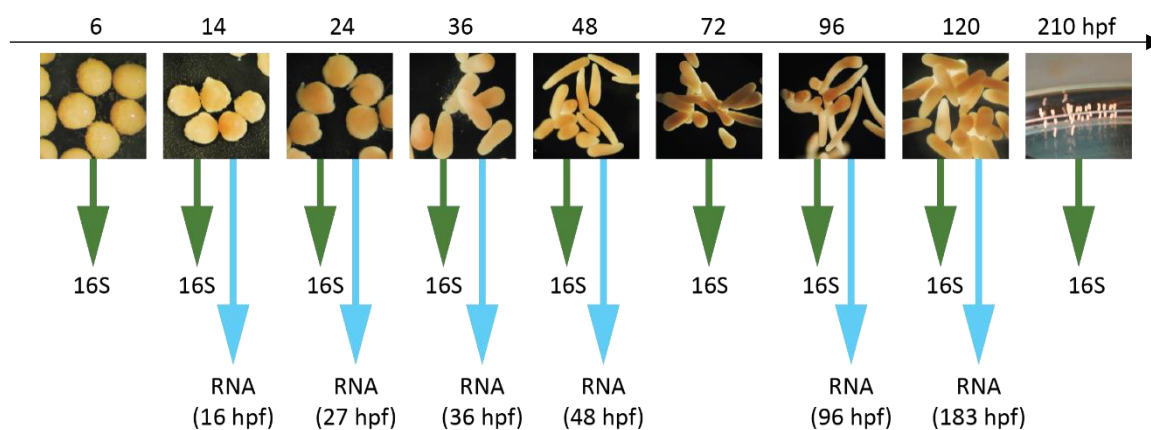


Figure 5.1: Timeline of samples (analyzed here) collected for 16S rRNA gene analysis (green) (chapter 4) and transcriptomics (blue) (Wessels *et al.* 2016) throughout the development of *Lobophytum pauciflorum* larvae. Images taken through dissection scope without scale markers; 210 hours post-fertilization image was taken without microscope, displaying competent larvae standing on end along the edge of a glass petri dish.

5.2.2 Read alignment and quantification

Larval transcripts were mapped to a fully assembled *L. pauciflorum de novo* transcriptome previously using Bowtie2 (Wessels *et al.* 2016). Transcript abundance was estimated from raw sequencing reads from all developmental stages of *L. pauciflorum* larvae in RSEM (Li and Dewey 2011). Sequences were sorted and input to R using the package tximport (Soneson *et al.* 2015). The R package DESeq2 was used to calculate the differential expression of transcripts with more than 10 mapped sequence reads followed by standard variance transformation normalization (Callahan *et al.* 2016).

5.2.3 Predictive package AMPiR

The package AMPiR (Fingerhut *et al.* 2020) was used to predict potential AMPs present in the protein translation of the *L. pauciflorum* transcriptome. Sequences with high predicted probability (90 %, 95 %, 97 % and 99 % probability) of having antimicrobial activity were extracted for further analysis. Differential expression of the strongest candidate AMPs (99% probability) throughout larval development were compared to the developing bacterial community characterized over the same timeline of host development in chapter 3. The R package mFuzz was used to cluster the 99% predicted AMPs based on their expression profiles in developing larvae. Mfuzz produced 6 soft clusters built on an m score of 2.33 as estimated by mfuzz::mestimate (Futschik *et al.* 2016).

5.2.4 Cnidarian AMP homology

Nucleotide and protein sequences for AMPs, defensins and Kazal-types with suspected or identified homology in Cnidaria were retrieved from NCBI Genbank (Clark *et al.* 2016) using the search terms arenicin, arminin, aurelin, damicornin, hydramacin, periculin and royalisin along with “defensin” and “Kazal-type” under taxon:Cnidaria (NCBI:txid6073). This search resulted in 870 protein and 157 nucleotide sequences. Additionally, nucleotide sequences corresponding to the cnidarian AMPs amAMP-1 (Mason *et al.* 2021) and NDA-1 (Augustin *et al.* 2017) were obtained from the respective literature. Sequences of 2 predicted AMPs recovered from adult *L. pauciflorum* in a previous study (*unpublished*) were also included, and are referred to in this analysis as LpAMP-1 and LpAMP-2. All of these sequences were used as a query set to search for homologs in *L. pauciflorum* with BLAST 2.11.0+ (BLASTp for proteins; BLASTn for nucleotides) (Altschul *et al.* 1990).

The full *de novo* assembled transcriptome and translation were used as reference databases for BLASTn and BLASTp, respectively, in this study. These searches were initially performed with a permissive e-value thresholds $1e^{-5}$ to ensure the inclusion of all potential homologs and then with a stringent e-value threshold, $1e^{-50}$ to identify conserved sequences. Potential homologs identified in *L. pauciflorum* were then analyzed for differential expression in larvae.

5.3 Results

5.3.1 Sequencing and assembly

Raw sequences recovered from larvae (232,830) were filtered for low abundance (>10 reads), normalized and transformed (variance stabilizing transformation) in DESeq2 resulting in 138,472 differentially expressed transcripts included in the analysis. Variance stabilised expression values for

all quantifiable transcripts were then used for subsequent analysis with mFuzz. A low membership threshold (30%) was used to visualize the core expression profiles soft-clustered into 30 clusters with the R package mFuzz ($m = 1.70$) (Figure 5.2). The clusters show a wide variety of expression profiles across the sampled timeline. As 67.4 % of the transcripts did not conform to these cluster cores at 30 % membership or higher, the variability in expression profile is even greater than observed (not

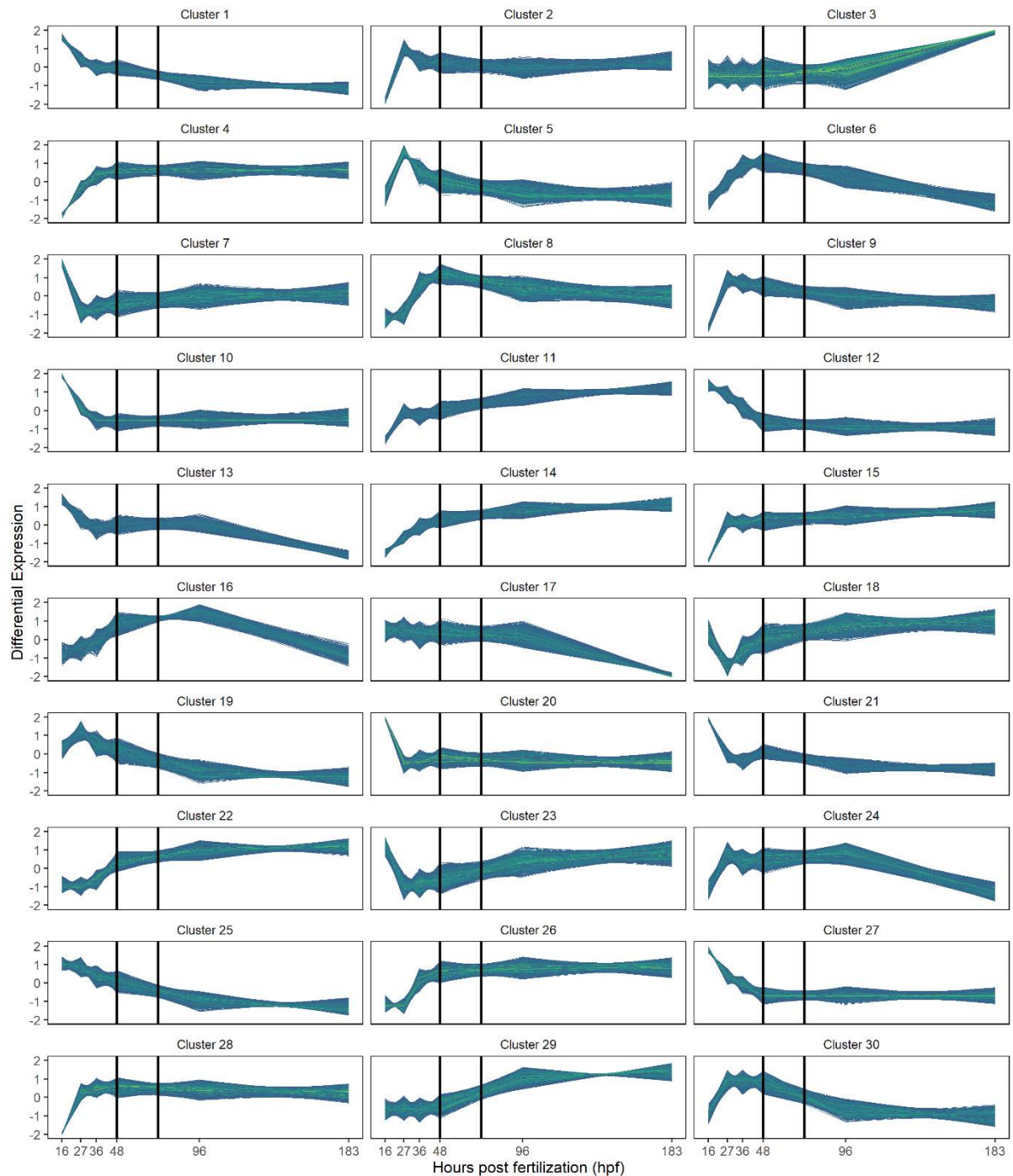


Figure 5.2: Differential expression of *L. pauciflorum* transcripts soft clustered (x30) with mFuzz package in R. A minimum membership threshold of 0.30 was applied, retaining 45,228 (32.6 %) of the 131,957 differentially expressed genes. Vertical lines mark sample points at 48 and 72 hpf.

shown). Differential expression of the larval transcriptome provided a basis for predictive analysis (AMPiR) as well as a reference for the differential expression of potential AMP homologs identified in BLAST analysis.

5.3.2 AMPiR predicted AMPs

The protein translations of the full *de novo* assembled transcriptome was input to the antimicrobial peptide predicting R package AMPiR (Fingerhut *et al.* 2020) with probability thresholds of 99 %, 97 %, 95% and 90 %. A total of 12,262 *L. pauciflorum* sequences were predicted above 90% probability of being AMPs: 108 sequences were predicted at 99%, 1,255 between 97 % and 99 %, 2,686 between 95 % and 97 % and an additional 9,576 between 90 % and 95 % probability.

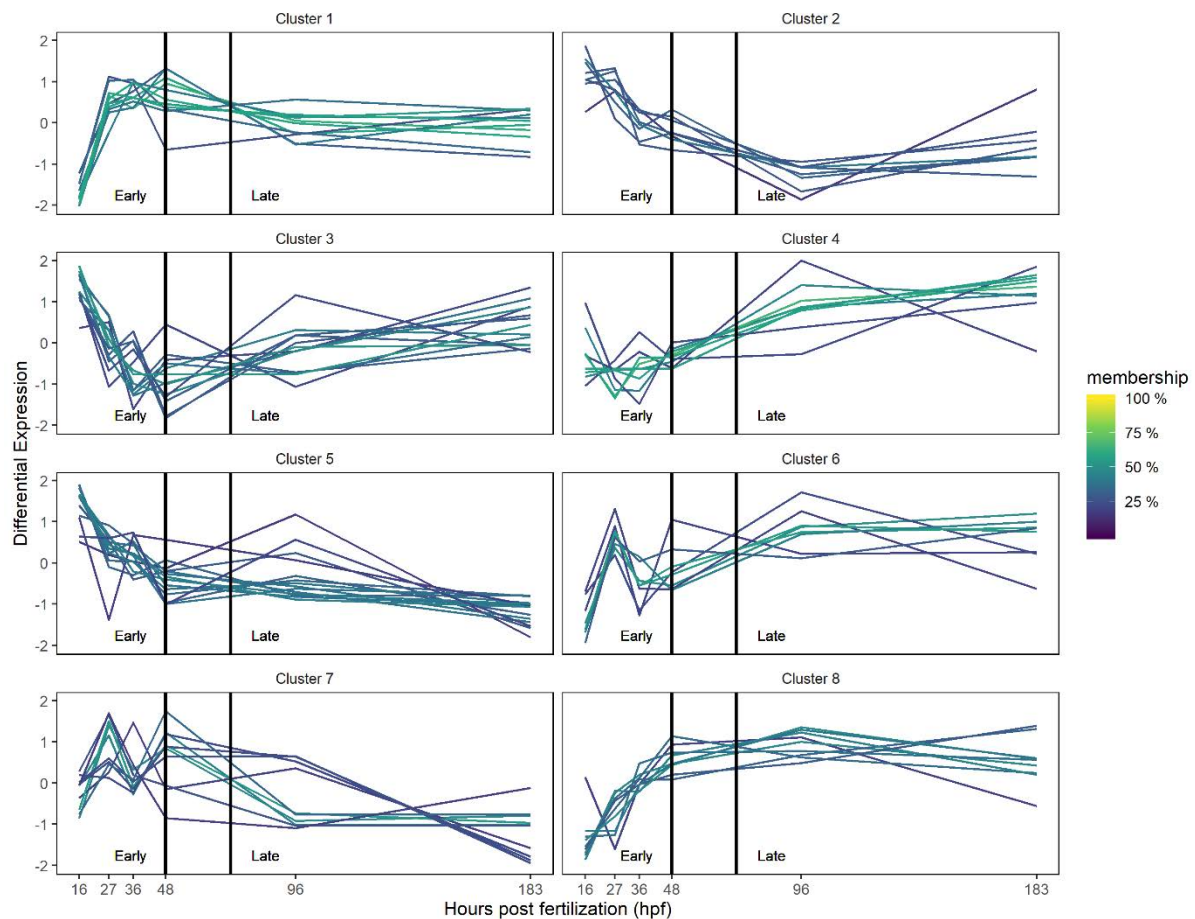


Figure 5.3: Differential expression of *Lobophytum pauciflorum* genes predicted at 99% AMP or higher in the R package AMPiR (Fingerhut *et al.* 2020). High membership value to cluster alpha-cores can indicate higher similarity between the respective genes. Vertical lines indicate 48 and 72 hpf as the end of the late stage and beginning of the late stage in *L. pauciflorum* larval development. Of 82 genes predicted over 99 % AMP and expressed in larvae, clusters 1-8 are represented by n = 11, 8, 13, 9, 14, 8, 10 and 9 genes, respectively.

Of the 108 genes in the translation that were predicted at 99 % or greater probability of antimicrobial activity, 82 were differentially expressed throughout the timeline of larval development samples as calculated by DESeq2. The 82 genes were analyzed via soft clustering with mFuzz to deduce similar differential expression profiles among these most highly predicted AMPs. An 8-cluster regime was applied with an m score of 2.33 (Figure 5.3). Most of the *L. pauciflorum* predicted proteins with high AMP probability clearly displayed large expression differentials between samples taken during the early stage of community development in larvae and far less between samples taken during the late stage, particularly in clusters 1, 3, 4, 6, 7 and 8. The pattern expressed in clusters 2 and 5, with transcript levels consistently decreasing over time, suggests that these might be maternal mRNAs which not zygotically expressed during development.

In soft clustering analysis with mFuzz, cluster membership is based upon similarity of the expression profile to others in the cluster. High membership of genes in the same cluster is also an indication of similarity between the genes themselves (Futschik and Kumar 2013). The soft-clustering of the *L. pauciflorum* genes predicted at 99 % here showed low overall membership to core clusters (minimum = 0.02 %, maximum = 65.4 % and mean = 0.13), thus indicating high diversity in both sequence and expression profiles among the potential AMPs.

5.3.3 Homology of cnidarian AMPs and defensins from literature

Homologs of cnidarian AMPs, defensins and Kazal-types were identified in the *L. pauciflorum* *de novo* assembled transcriptome and trinity protein translation with BLASTn and BLASTp, respectively. Analyses were run on both nucleotide and protein query sequences to incorporate a more encompassing diversity of sequences associated with cnidarian antimicrobial agents available in NCBI (Table 5.1).

5.3.3.1 Protein homologs in *L. pauciflorum*

At a significance cutoff of 1×10^{-5} in BLASTp, 244 *L. pauciflorum* predicted proteins were identified as potential homologs of Kazal-type serine protease inhibitors, AMPs and defensin query protein sequences obtained from NCBI and the literature. Potential homologs in *L. pauciflorum*

Table 5.1: Summary of BLAST hits received between *Lobophytum pauciflorum* genes and known AMP and Kazal-type genes from NCBI. At a significance of e^{-5} (left), 244 potential homologs were identified in *L. pauciflorum*, 226 of which were expressed in larvae. At a significance of e^{-50} (right), 115 potential homologs were identified in *L. pauciflorum*, 110 of which were expressed in larvae.

	Protein sequences						Nucleotide sequences											
	Sequences from NCBI	BLAST hits > e-5		Potential homologs in <i>L. pauciflorum</i> Homologs differentially expressed in larvae		BLAST hits > e-50		Potential homologs in <i>L. pauciflorum</i> Homologs differentially expressed in larvae		Sequences downloaded from NCBI	BLAST hits > e-5		Potential homologs in <i>L. pauciflorum</i> Homologs differentially expressed in larvae		BLAST hits > e-50		Potential homologs in <i>L. pauciflorum</i> Homologs differentially expressed in larvae	
Sequences from NCBI:	870	691				396				157	28				13			
Number of HSPs:		17,730				3,148				0	146				43			
Potential homologs in <i>L. pauciflorum</i> :			244	226			115	110				84	72			32	27	
Protein	Organism																	
AmAMP-1	<i>Acropora millepora</i>	1																
Arenicin	<i>Arenicola</i> spp.	16	6	4						4								
Arenicin	<i>Komagataella pastoris</i>	0								2								
Arminin	<i>Hydra oligactis</i>	6								0								
Arminin	<i>Hydra viridissima</i>	4								0								
Arminin	<i>Hydra vulgaris</i>	19								0								
Aurelin	<i>Actinia tenebrosa</i>	0								1	4	4	4					
Aurelin	<i>Aurelia aurita</i>	3								1								
Aurelin	<i>Pocillopora damicornis</i>	0								3	6	5	5					
Aurelin	<i>Stylophora pistillata</i>	0								1	5	2	1					
Damicornin	<i>Pocillopora damicornis</i>	1								1								
defensins	<i>Anemonia sulcata</i>	27								0								
defensins	<i>Anemonia viridis</i>	12								0								
defensins	<i>Antheopsis maculata</i>	2								0								
defensins	<i>Anthopleura elegantissima</i>	8								0								
defensins	<i>Bunodosoma granuliferum</i>	4								0								
defensins	<i>Bunodosoma</i> spp.	10								0								
defensins	<i>Edwardsia elegans</i>	1								0								
defensins	<i>Heteractis crispa</i>	4								0								
defensins	<i>Heteractis magnifica</i>	4	16	8	8					0								
defensins	<i>Oulactis muscosa</i>	5								5								
defensins	<i>Oulactis</i> sp.	0								25								
defensins	<i>Oulactis</i> sp.	25								0								
defensins	<i>Phymanthus crucifer</i>	1								0								
defensins	<i>Rhodactis</i> sp.	0								3								
defensins	<i>Rhodactis</i> sp.	3								0								
defensins	<i>Urticina crassicornis</i>	1								1								
defensins	<i>Urticina eques</i>	1								0								
Hydramacin	<i>Folsomia candida</i>	0								3	9	5	4					
Hydramacin	<i>Hydra magnipapillata</i>	0								1								
Hydramacin	<i>Hydra vulgaris</i>	4								1								
Hydramacin	<i>Orbicella faveolata</i>	0								1	17	5	3	3	2	2		
Hydramacin	<i>Ruditapes philippinarum</i>	0								1								
Kazal-type	<i>Acropora digitifera</i>	82	1855	78	75	305	32	31		3	5	5	5	2	2	2		
Kazal-type	<i>Acropora millepora</i>	79	2322	80	78	185	19	19		5	6	5	4	2	1	0		
Kazal-type	<i>Actinia tenebrosa</i>	4	32	11	10	4	2	2		7	8	8	8					
Kazal-type	<i>Anemonia sulcata</i>	1	13	5	5					0								
Kazal-type	<i>Cyanea capillata</i>	1	14	5	5					1								
Kazal-type	<i>Dendronephthya gigantea</i>	83	3109	77	70	1117	51	49		4	16	13	10	14	12	9		
Kazal-type	<i>Exaiptasia diaphana</i>	123	2882	97	92	606	42	38		3	10	10	6					
Kazal-type	<i>Exaiptasia pallida</i>	0								10	10	10	6					
Kazal-type	<i>Hydra magnipapillata</i>	0								10								
Kazal-type	<i>Hydra vulgaris</i>	39	600	57	54	64	17	17		9	1	1	1					
Kazal-type	<i>Malithaea caledonica</i>	1	14	5	5					0								
Kazal-type	<i>Nematostella vectensis</i>	58	706	66	61	97	21	20		8	17	10	10	7	5	5		
Kazal-type	<i>Orbicella faveolata</i>	58	2252	91	87	156	24	24		6	12	9	8	2	1	1		
Kazal-type	<i>Pocillopora damicornis</i>	39	1196	90	88	137	23	22		2	2	2	2					
Kazal-type	<i>Stylophora pistillata</i>	116	2686	124	119	475	48	48		4	10	7	6	8	4	4		
Kazal-type	<i>Thelohanelus kitauei</i>	4	20	9	7	1	1	1		0								
LpAMP-1	<i>Lobophytum pauciflorum</i>	0	2	2	2					1	2	2	2	2	2	2		
LpAMP-2	<i>Lobophytum pauciflorum</i>	0	5	4	4	1	1	1		1	3	2	1	2	2	1		
NDA-1	<i>Hydra</i> spp.	0								1								
Periculin	<i>Hydra magnipapillata</i>	0								5								
Periculin	<i>Hydra vulgaris</i>	17								19	1	1	1	1	1	1		
Royalisin	<i>Apis</i> spp.	3								2								

included 4 of arenicin, 226 of Kazal-type proteins, 2 of LpAMP-1, and 4 of LpAMP-2. A Kunitz-type

serine protease-inhibitor defensin ((NCBI Accession COHK72.1, COHK73.1, COHK74.1) also matched with 8 potential homologs in *L. pauciflorum*.

Of the 226 potential AMP and Kazal-type protein homologs in *L. pauciflorum*, 81 were also identified as probable AMPs in AMPiR. Predictions included 26 homologs were above 50% probability and 12 homologs were over 90 % probability of being AMPs. In BLASTp, The 12 potential homologs predicted over 90 % matched with 99 distinct Kazal-type protein sequences and 1 homolog also matched with 2 defensin query sequences. These sequences were isolated from 13 different source Cnidaria including *A. digitifera* (4 sequences), *A. millepora* (8), *A. tenebrosa* (2), *C. capillata* (1), *D. gigantea* (19), *E. diaphana* (7), *H. magnifica* (2), *H. vulgaris* (18 sequences), *M. caledonica* (1 sequence), *N. vectensis* (12 sequences), *O. faveolata* (6 sequences), *P. damicornis* (7 sequence) and *S. pistillata* (14 sequences). The defensins that shared homology with *L. pauciflorum* transcripts in BLAST and were highly predicted as AMPs were two of the Kunitz-type serine protease inhibitors isolated from *H. magnifica* (NCBI Accession COHK73.1 and COHK74.1).

To focus on only the highest confidence *L. pauciflorum* homologs of AMPs, defensins and Kazal-type serine proteases, the significance threshold in BLASTp was increased to $1e^{-50}$. This resulted

Table 5.2: BLASTn results (e^{-50}) of AMP and Kazal-type homologs in *Lobophytum pauciflorum*.

Identity matches are automatically rounded to 0 if the e-value is lower than $1e^{-180}$.

Protein	Source organism	NCBI accession	<i>L. pauciflorum</i> gene	e-value	Description
Hydramacin	Orbicella faveolata	NW_018149766.1	c219005_g1_i1	4.86E-132	Whole genome shotgun sequence scaffold
Hydramacin	Orbicella faveolata	NW_018149766.1	c219005_g1_i1	1.06E-123	Whole genome shotgun sequence scaffold
Hydramacin	Orbicella faveolata	NW_018149766.1	c65095_g1_i1	5.44E-52	Whole genome shotgun sequence scaffold
Kazal-type	Acropora digitifera	NW_015441130.1	c237117_g1_i1	9.05E-111	Whole genome shotgun sequence scaffold
Kazal-type	Acropora digitifera	NW_015441130.1	c253609_g1_i3	2.74E-51	Whole genome shotgun sequence scaffold
Kazal-type	Acropora millepora	NW_021126546.1	c38497_g1_i1	1.81E-140	Whole genome shotgun sequence scaffold
Kazal-type	Acropora millepora	NW_021126546.1	c38497_g1_i1	6.61E-130	Whole genome shotgun sequence scaffold
Kazal-type	Dendronephthya gigantea	NW_021163010.1	c252353_g1_i4	0	Whole genome shotgun sequence scaffold
Kazal-type	Dendronephthya gigantea	NW_021163010.1	c252353_g1_i4	1.06E-63	Whole genome shotgun sequence scaffold
Kazal-type	Dendronephthya gigantea	NW_021163010.1	c257398_g1_i3	0	Whole genome shotgun sequence scaffold
Kazal-type	Dendronephthya gigantea	NW_021163010.1	c242279_g1_i2	0	Whole genome shotgun sequence scaffold
Kazal-type	Dendronephthya gigantea	NW_021163010.1	c256697_g1_i2	0	Whole genome shotgun sequence scaffold
Kazal-type	Dendronephthya gigantea	NW_021163010.1	c242896_g1_i2	0	Whole genome shotgun sequence scaffold
Kazal-type	Dendronephthya gigantea	NW_021163143.1	c226015_g1_i2	0	Whole genome shotgun sequence scaffold
Kazal-type	Dendronephthya gigantea	NW_021163143.1	c241802_g1_i1	0	Whole genome shotgun sequence scaffold
Kazal-type	Dendronephthya gigantea	NW_021163143.1	c257157_g1_i4	0	Whole genome shotgun sequence scaffold
Kazal-type	Dendronephthya gigantea	NW_021163143.1	c220426_g1_i1	0	Whole genome shotgun sequence scaffold
Kazal-type	Dendronephthya gigantea	NW_021163143.1	c287482_g1_i1	0	Whole genome shotgun sequence scaffold
Kazal-type	Dendronephthya gigantea	NW_021163143.1	c287482_g1_i1	6.40E-81	Whole genome shotgun sequence scaffold
Kazal-type	Dendronephthya gigantea	XM_028550715.1	c255893_g3_i9	0	Predicted kazal motif (LOC114528966), mRNA
Kazal-type	Dendronephthya gigantea	XM_028550715.1	c255893_g3_i1	0	Predicted kazal motif (LOC114528966), mRNA
Kazal-type	Nematostella vectensis	NW_001834375.1	c252583_g2_i1	0	Whole genome shotgun sequence scaffold
Kazal-type	Nematostella vectensis	NW_001834375.1	c246648_g4_i4	0	Whole genome shotgun sequence scaffold
Kazal-type	Nematostella vectensis	NW_001834375.1	c246648_g4_i4	3.12E-171	Whole genome shotgun sequence scaffold
Kazal-type	Nematostella vectensis	NW_001834375.1	c246648_g4_i4	7.79E-68	Whole genome shotgun sequence scaffold
Kazal-type	Nematostella vectensis	NW_001834375.1	c255754_g1_i2	1.93E-148	Whole genome shotgun sequence scaffold
Kazal-type	Nematostella vectensis	NW_001834375.1	c252583_g2_i7	1.51E-144	Whole genome shotgun sequence scaffold
Kazal-type	Nematostella vectensis	NW_001834375.1	c246614_g1_i1	1.23E-105	Whole genome shotgun sequence scaffold
Kazal-type	Orbicella faveolata	NW_018150037.1	c224252_g1_i1	2.57E-66	Whole genome shotgun sequence scaffold
Kazal-type	Orbicella faveolata	NW_018150037.1	c224252_g1_i1	2.60E-56	Whole genome shotgun sequence scaffold
Kazal-type	Stylophora pistillata	LSMT01000323.1	c246051_g2_i4	0	Whole genome shotgun sequence scaffold
Kazal-type	Stylophora pistillata	LSMT01000323.1	c246051_g2_i1	0	Whole genome shotgun sequence scaffold
Kazal-type	Stylophora pistillata	LSMT01000323.1	c197615_g1_i1	0	Whole genome shotgun sequence scaffold
Kazal-type	Stylophora pistillata	LSMT01000323.1	c192248_g1_i1	1.80E-69	Whole genome shotgun sequence scaffold
Kazal-type	Stylophora pistillata	NW_019218106.1	c246051_g2_i4	0	Whole genome shotgun sequence scaffold
Kazal-type	Stylophora pistillata	NW_019218106.1	c246051_g2_i1	0	Whole genome shotgun sequence scaffold
Kazal-type	Stylophora pistillata	NW_019218106.1	c197615_g1_i1	0	Whole genome shotgun sequence scaffold
Kazal-type	Stylophora pistillata	NW_019218106.1	c192248_g1_i1	1.80E-69	Whole genome shotgun sequence scaffold
LpAMP-1	Lobophytum pauciflorum	LpAMP-1	c256188_g2_i8	0	Predicted AMP
LpAMP-1	Lobophytum pauciflorum	LpAMP-1	c243416_g3_i1	8.85E-75	Predicted AMP
LpAMP-2	Lobophytum pauciflorum	LpAMP-2	c236356_g1_i3	0	Predicted AMP
LpAMP-2	Lobophytum pauciflorum	LpAMP-2	c384694_g1_i1	6.66E-107	Predicted AMP
Periculin	Hydra vulgaris	NW_004167108.1	c249451_g2_i2	4.20E-149	Whole genome shotgun sequence scaffold

in a total of 115 *L. pauciflorum* transcripts identified as potential homologs of 396 query sequences from Kazal-type (395) and LpAMP-2 (1) proteins.

5.3.3.2 Nucleotide sequence homologs in *L. pauciflorum*

A total of 84 *L. pauciflorum* transcripts were identified as potential homologs of 28 (out of 157 obtained from NCBI) nucleotide query sequences in BLASTn at e^{-5} . The query sequences that received BLASTn hits were affiliated with aurelin (11 homologs in *L. pauciflorum*), hydramacin (10 homologs), kazal-type (80 homologs) LpAMP-1 (2 homologs), LpAMP-2 (2 homologs) and periculin (1 homolog). Of these potential homologs, 12 had a higher than 50% predicted probability of antimicrobial activity (via ampir) and for 3 of these the predicted probability was higher than 90%. These three sequences are potential homologs of Kazal-domain containing regions in the genomes of *Orbicella faveolata* (NW_018150037.1) ($2.06e^{-42}$), *Exaiptasia diaphana* (LJWW01000109.1) ($6.62e^{-27}$) and *Exaiptasia*

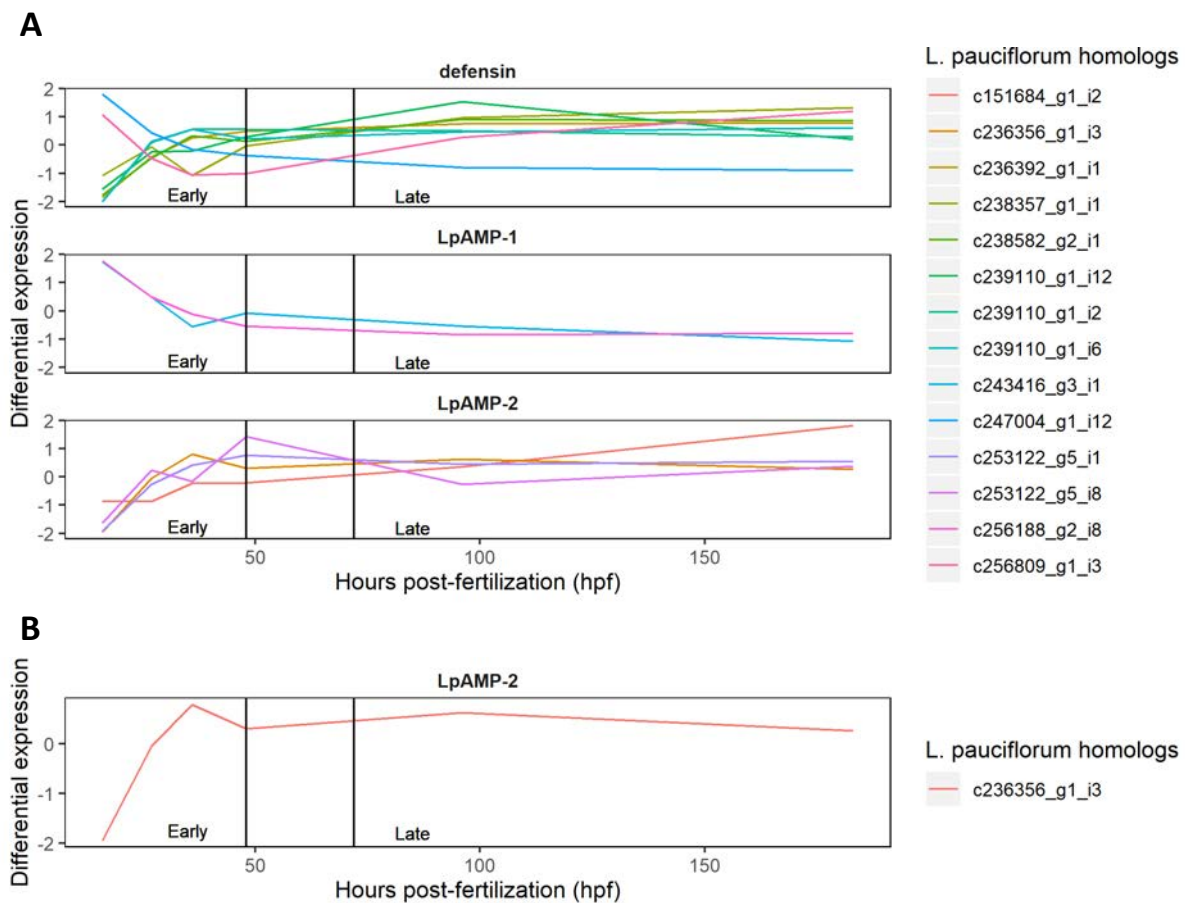


Figure 5.4: Differential expression of AMP protein homologs in developing *Lobophytum pauciflorum* larvae. Homologs are shown separately at significance thresholds of $1e^{-5}$ (A) and $1e^{-50}$ (B). Vertical lines at 48 and 72 hpf indicate the last sample period of the early stage and the first sample period of the late stage of community development, respectively (Chapter 4).

pallida (NW_018384202.1) ($6.62e^{-27}$). At a significance threshold of e^{-50} in BLASTn, 32 *L. pauciflorum* transcripts were identified as potential homologs of 13 query sequences affiliated with the same diversity of proteins as at e^{-5} : aurelin (10 homologs), hydramacin (7 homologs), Kazal-type (25 homologs), LpAMP-1 (2 homologs), LpAMP-2 (2 homologs) and periculin (1 homolog) (Table 5.2). The nucleotide sequences with homology in *L. pauciflorum* are associated with cysteine-rich protein encoding regions in the full genome assemblies of Cnidaria, mostly from other corals.

5.3.4 Differential expression of homologs in *L. pauciflorum* larvae

At both e^{-5} and e^{-50} minimum significance thresholds, most of the potential homologs expressed in the *L. pauciflorum* transcriptome were differentially expressed between the early and late stages. The early stage was generally characterized by higher expression differentials than the late stage in all analyses.

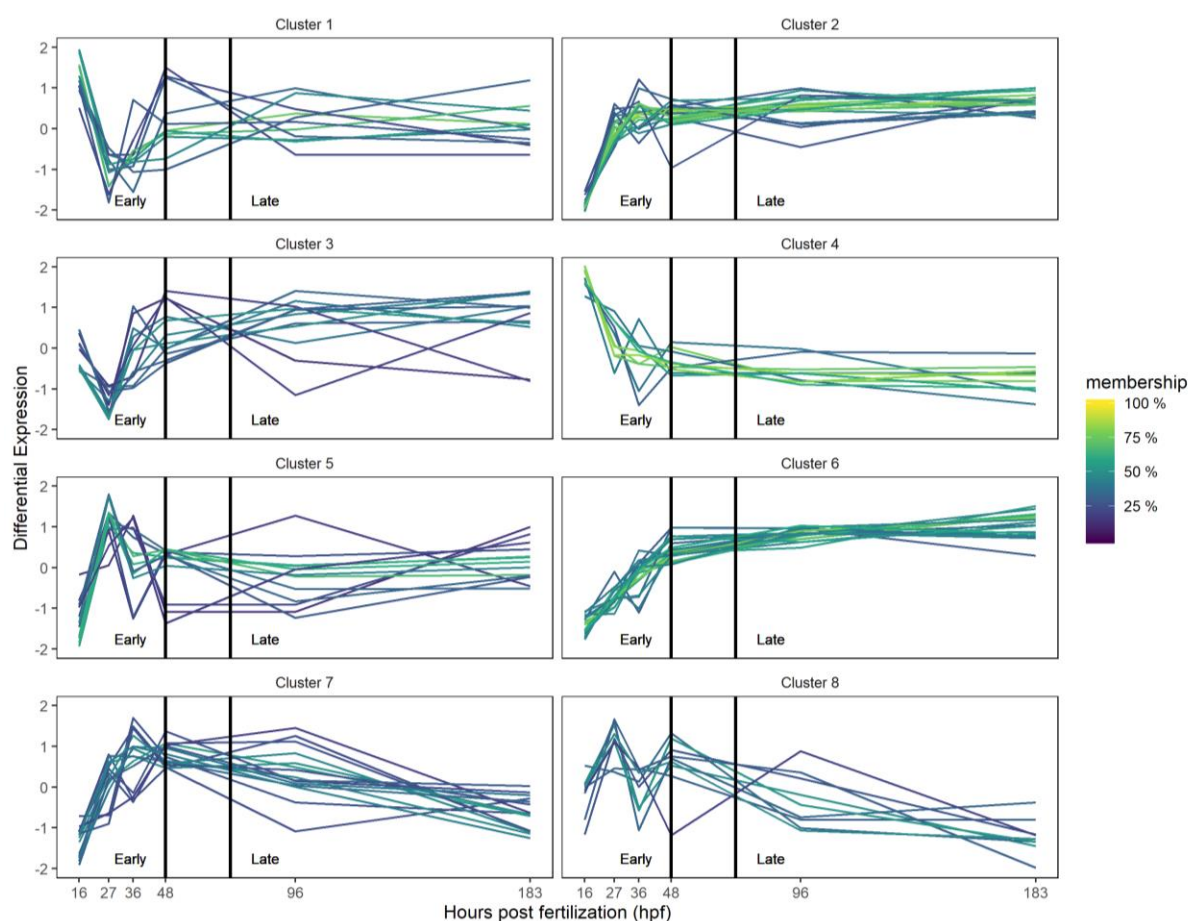


Figure 5.5: Differential expression of Kazal-type homologs of nucleotide sequences in developing *Lobophytum pauciflorum* larvae. Vertical lines represent 48 and 72 hours post-fertilization (hpf) as the end of the early stage and beginning of the late stages of development, respectively.

Homologs of defensin-related protein sequences (8 homologs) and LpAMP-1 (2 homolog) at e^{-5} (Figure 5.4 A) and LpAMP-2 (1 homolog) at e^{-50} (Figure 5.4 B) were differentially expressed between the early and late stages of development in larvae. Due to the high number of homologs affiliated with Kazal-type protein sequences differentially expressed in larvae (109), soft-clustering with mFuzz was applied to determine common expression profiles of the homologs (BLASTp e^{-50}) (Figure 5.5). All of the 8 clusters show large expression differential in the early stage. Clusters 1, 3, 5, 7 and 8 also vary in their level of expression differential in the late stage. Clusters 2,4 and 6, however, show high expression differential between early-stage samples with low differential between late-stage samples. Clusters 2 and 6 are also the largest clusters with 20 and 19 *L. pauciflorum* homologs respectively, and high membership to the alpha core indicating high similarity within clusters.

Of the 84 *L. pauciflorum* homologs of nucleotide sequences, 72 were differentially expressed in developing larvae (Figure 5.6). Differentially expressed sequences shared homology with the antimicrobial peptides aurelin (NCBI Accession NW_019217875.1, NW_020847569.1 and NW_022258714.1), hydramacin (LNIX01000005.1 and NW_018149766.1) and periculin

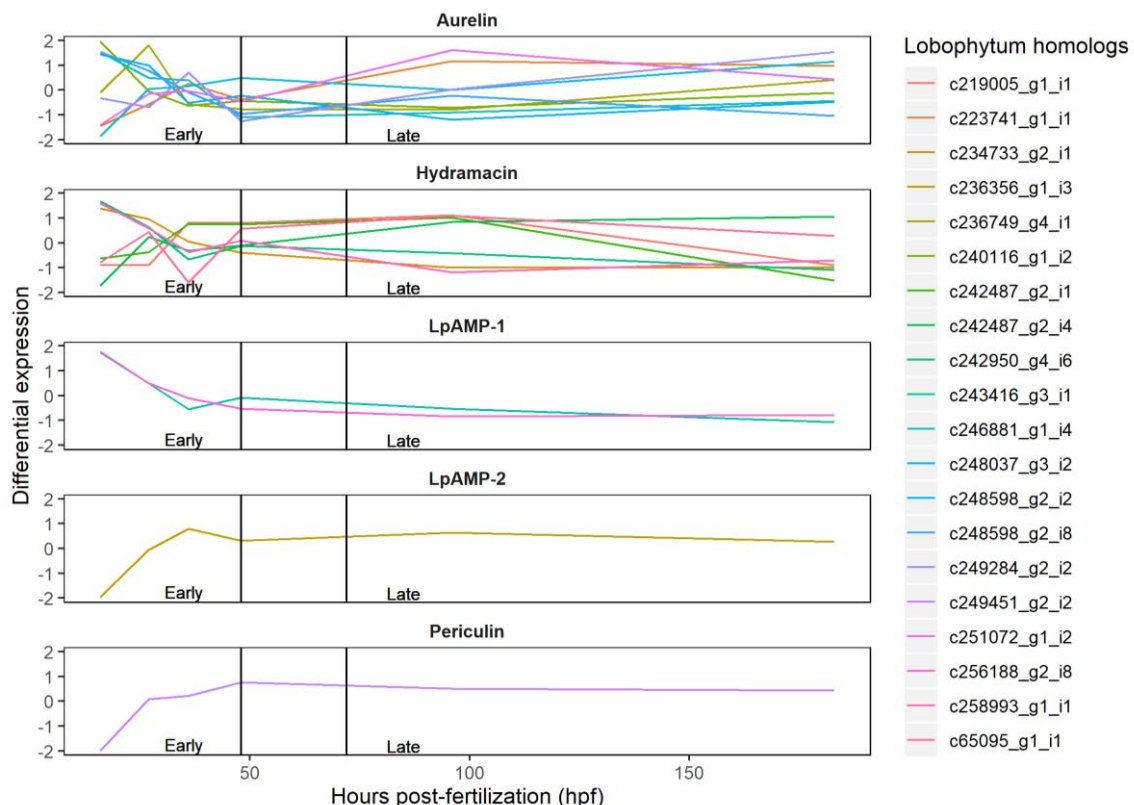


Figure 5.6: Differential expression of antimicrobial peptide nucleotide homologs to Cnidarian antimicrobial peptides (e^{-5}) in *Lobophytum pauciflorum* larvae. Vertical lines at 48 and 72 hours post-fertilization (hpf) indicate the end of the early stage and the beginning of the late stage of community succession, respectively.

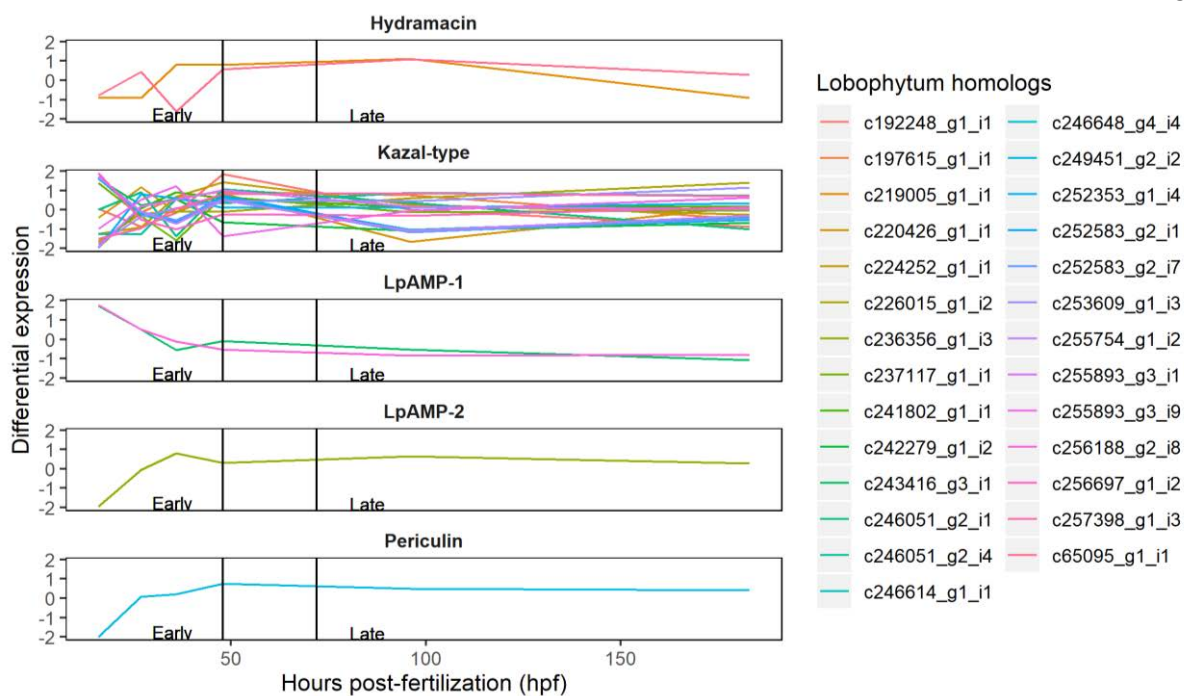


Figure 5.7: Differential expression of antimicrobial peptide and Kazal-type nucleotide sequence homologs (e^{-50}) differentially expressed in *Lobophytum pauciflorum* larvae. Vertical lines denote 48 hours post fertilization (hpf) as the end of the early community and 72 hpf as the beginning of the late-stage community (Chapter 4).

(NW_004167108.1) as well as LpAMP-1 and -2. An additional 58 sequences differentially expressed in *L. pauciflorum* larvae shared homology with 20 kazal-type proteins isolated from 11 organisms and were further filtered to e^{-50} to characterize differential expression. At a threshold of $1e^{-50}$, 27 homologs were identified in *L. pauciflorum* matching with 12 query nucleotide sequences of hydrumacin (2 homologs), Kazal-type (21 homologs), LpAMP-1 (2 homologs), LpAMP-2 (1 homolog) and periculin (1 homolog) (Figure 5.7).

5.4 Discussion

This study identified homologs of AMPs and Kazal-domain containing proteins in *L. pauciflorum* based on BLAST searches to query sequences that were either isolated from or homologous to known AMPs and Kazal-domain containing proteins in other cnidarian hosts. Many of the putative homologs identified in *L. pauciflorum* were differentially expressed throughout the development of larvae between fertilization and competency. The expression patterns observed show

distinct patterns before 48 hpf and after 72 hpf, in parallel with the patterns of bacterial community succession in *L. pauciflorum* larvae characterized in Chapter 4 (Figure 5.8).

5.4.1 AMPs in *L. pauciflorum* predicted by AMPiR

The identification of 82 differentially expressed, predicted proteins with high ($p > 99\%$) probability of having AMP activity by AMPiR in our analysis implies that AMPs are likely to be present in *L. pauciflorum* larvae. In addition, the gene expression profiles of these AMP-like proteins were different between the early and late stages of community development. The largest expression differentials were recorded in samples from the early stage, either significantly increasing or decreasing in differential expression, while remaining comparatively stable across time points sampled in the late stage. While this type of predictive analysis cannot point to AMPs with absolute certainty, the high number (12,262) of protein translations from *L. pauciflorum* predicted above 90% is a strong indication that, even with a high margin of error, AMPs are present in the dataset. The differential expression of predicted genes also coincides with shifts in the bacterial community between early and late stages of development (figure 5.6), in agreement with the hypothesis that changes in the AMP regime may influence the associated bacterial community development during larval development. Previous studies in *Hydra* determined that AMPs are a major factor in shaping the bacterial community of hatchling *Hydra*, thereby impacting the physiological development and health

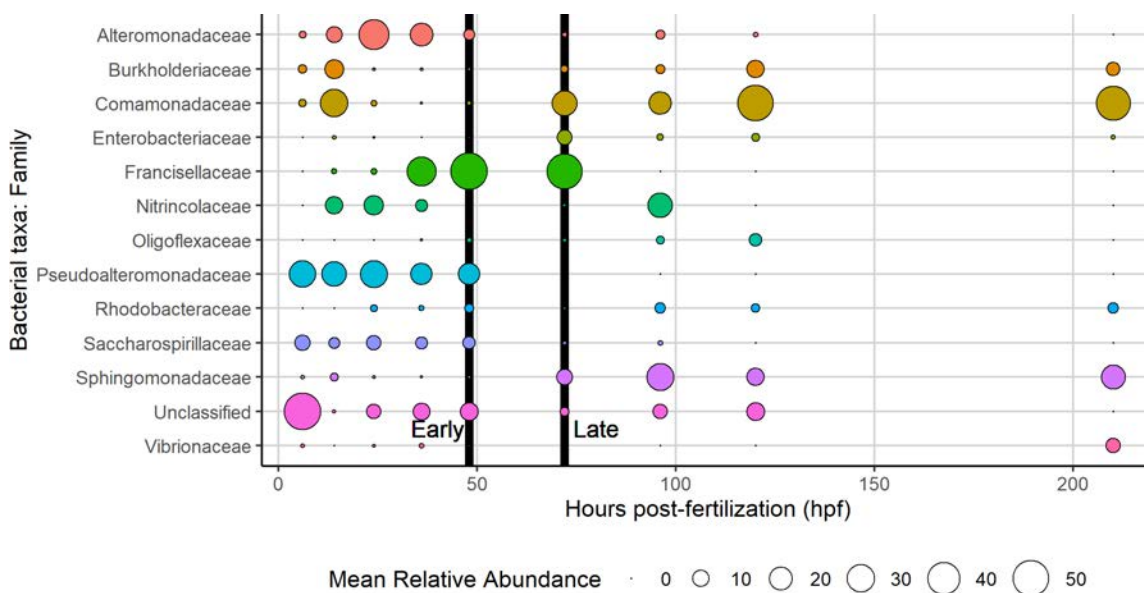


Figure 5.8: Composition of the bacterial community during larval development in *Lobophytum pauciflorum*. As outlined in chapter 4, two distinct communities are formed prior to and post 48 hours post-fertilization (hpf) (early stage) and 72 hpf (late stage), respectively. Dominant bacterial families (y-axis) are presented over the first 210 hpf (x-axis); vertical lines indicate 48 and 72 hpf.

of the host (Fraune *et al.* 2011, Franzenberg *et al.* 2013, Augustin and Bosch 2017). Similar biological interactions maybe occurring during the development of *L. pauciflorum*.

5.4.2 Candidate homologs of antimicrobial peptides

The AMPs arminin, hydramacin and periculin, homologs of which were identified and expressed in *L. pauciflorum* larvae, here, have been reported as important components of the innate immune system in *Hydra* spp. Hydramacin is a potent AMP which causes bacterial cells to aggregate before initiating spontaneous cell death and may also play a role in secondary repair functions in the host (Jung *et al.* 2008, 2012), while periculin expresses discriminatory, taxon-specific antimicrobial properties in *Hydra* spp. (Augustin and Bosch 2010). However, homology was not found between all Cnidarian AMPs analyzed here, such as aurelin, damicornin and royalisin. Homologs of the jellyfish AMP aurelin (Ovchinnikova *et al.* 2006) were identified in the scleractinian *P. damicornis* along with a novel AMP damicornin (Vidal-dupiol *et al.* 2011), while homologs of arenicin-2 and royalisin were isolated from the gorgonian *Gorgonia ventalina* (Burge *et al.* 2013). These AMPs are suggested to play important roles in the immune system of the respective hosts. The findings from this analysis agree with other studies in that Cnidaria host species-specific consortia of AMPs, some of which are host-specific.

5.4.3 Kazal-type protein homologs

In addition to AMPs, a large number and diversity of predicted proteins with homology to the Kazal-type serine protease inhibitors were also identified in the transcriptome of *L. pauciflorum* in this study. Furthermore, these Kazal-domain containing proteins were differentially expressed between early and late stages of community development in larvae. Kazal-domain containing proteins are diverse and have been recovered from a wide variety of animal hosts (Rimphanitchayakit and Tassanakajon 2010). Genes encoding Kazal-type proteins often contain multiple Kazal domains due to alternative splicing and duplication, thus a single gene may produce multiple distinct proteins. These characteristics may contribute to the high number of high-scoring segment pairs (HSPs) identified in this study. The serine protease inhibitors, such as Kazal- and Kunitz-types, are families that have been characterized in a wide variety of animals, performing functions as diverse as blood coagulation in blood-sucking insects and the protection of cocoons from biodegrading bacteria, in addition to antimicrobial activity and defense in cnidarians (Rimphanitchayakit and Tassanakajon 2010). Inhibition of serine proteases impacts bacterial cell functions such as host colonization, proliferation, pathogenesis and fitness, rendering these types of proteins effective as means of defence against a

wide range of bacterial pathogens (Supuran *et al.* 2002). As such, protease inhibition is a leading method of fighting human diseases in modern medicine (Angbowuro *et al.* 2018).

In *H. magnipapillata*, silencing the Kazal-1 gene resulted in excessive autophagy and a failure to regenerate (Chera *et al.* 2006), thus some Kazal-type proteins identified in Cnidaria may have functions other than antimicrobial activity. Five Kazal-2 serine protease inhibitor homologs, however, demonstrated both inhibitory and lethal antimicrobial characteristics in *Hydra* spp. These genes were expressed in the endodermal gland cells along the body column, save the ends (both oral and aboral), as a component of the innate immune system (Augustin *et al.* 2009). A suggested role is that serine protease inhibitors are expressed after feeding to prevent colonization by newly acquired environmental bacteria coming into the gastric column with the food. Kazal proteins could potentially play similar roles in coral larvae by affording protection to vulnerable larval tissue cells from bacteria acquired from the environment. However, to confirm this hypothesis tissue-specific localization of the transcripts and immunolocalization of the corresponding proteins are required.

The defensin identified in *D. gigantea* (NCBI acc. XP_028406516.1) has been characterized as a Kunitz-type serine protease inhibitor, and members of this family of toxins are involved in defense in sea anemones (Frazao *et al.* 2012). The candidate Kunitz- and Kazal-type serine protease inhibitor homologs expressed in *L. pauciflorum* larvae suggest that these specialized proteins with defensive functions are likely to be present in *L. pauciflorum*. Furthermore, the expression patterns of these candidate genes indicate that serine protease inhibition may be important in shaping the development of the bacterial community in *L. pauciflorum* larvae.

5.4.4 Differential expression in *L. pauciflorum* larvae

Clustering the differential expression profiles of the full *L. pauciflorum* larval transcriptome (Figure 5.2) provided a reference to compare with the differential expression of potential AMP homologs. As the fertilized egg developed into a planula it was expected that many genes would be differentially expressed with the formation of new anatomical features and biological processes, especially following gastrulation. Gastrulation in *L. pauciflorum* takes place between 14 and 27 hpf and is assumed to correspond to the initiation of zygotic expression of many genes (Wessels 2016). Gastrulation could also contribute to a shift in bacterial community structure by increasing larval surface area and microhabitat heterogeneity. However, while many of the transcriptome clusters do display a high expression differential between time points in the early stage, there is a much higher variability in expression profile between clusters of the full transcriptome than observed in the identified and predicted AMP homologs.

In addition to Kazal-type homologs that were expressed in *L. pauciflorum* larvae, the homologs in cluster 4 show differential expression patterns reflective of maternally inherited transcripts (Figure 5.5). At the earliest timepoint (16 hpf) the levels of these transcripts were at their highest. At each subsequent timepoint the transcripts were at lower levels and at no time during development did they increase. These patterns are characteristic of maternal mRNAs which appear not to be expressed zygotically.

The homologs of Kazal-domain proteins identified in this study showed very different expression patterns during the early and late stages of *L. pauciflorum* development. Differential expression profiles also show that the early and late stage are characterized by distinct assemblages of expressed homologs that correspond with the distinct bacterial communities associated with early and late stages of development. Considered together, these analyses suggests that antimicrobial agents play important roles in shaping the bacterial community structure in developing *L. pauciflorum* larvae.

5.4.5 Conclusion

Two main conclusions can be drawn from the analyses included in this study. The first is that homologs of AMPs and Kazal-domain containing proteins are abundant and differentially expressed throughout development in *L. pauciflorum* larvae, between fertilization and competency. The second is that the parallels observed between the differential expression of candidate AMPs and protease inhibitors and bacterial community succession over time suggest that the former influence microbiome composition and structure during early larval development. While putative, these findings provide a new perspective on the development of the bacterial community associated with coral larvae and the potential mediatory interplay between animal host and bacterial symbiont – current knowledge gaps in the field of cnidarian microbiology. Future work should explore the roles of serine protease inhibition in mediating the coral microbiome and in larval development. The findings from this study imply that serine protease inhibition may be an important process in cnidarians in general, especially during the early life stages when other AMPs may not yet be expressed. A metastudy characterizing specific octocorallian AMPs and the level of shared homology among the Cnidaria would also help to extrapolate on these results and to better understand the role of AMPs in cnidarian health and development.

**Chapter 6: Development and structure of the bacterial community associated
with the soft leather coral *Lobophytum pauciflorum***

This dissertation characterizes the baseline bacterial community of the common GBR Alcyonacea *L. pauciflorum* (Chapter 2), investigates how these communities are distributed across microhabitats within the host (Chapter 3), and describes the bacterial communities associated with different early life stages of developing larvae (Chapter 4). The findings from this thesis enhance our understanding of the bacteria associated with soft corals and contributes to establishing *L. pauciflorum* as a model species for soft corals. Chapter 5 explores the potential for host mediation of larval colonization by bacteria through the production of antimicrobial compounds, an important aspect of coral microbiology which has remained a knowledge gap in the field. This chapter synthesizes these accumulated findings into the broader understanding of cnidarian-symbiont interactions to explore what the bacterial community associated with *L. pauciflorum* as a model Alcyoniidae means to the field of coral microbiology.

6.1 The holobiont *L. pauciflorum*: community structure

6.1.1 Bacteria associated with soft corals

The microbiomes of corals demonstrate a degree of species-specificity and are composed of both conserved and variable community fractions. The core microbiome theory, first proposed in connection with the human genome project (Turnbaugh *et al.* 2007), has been explored previously in hard corals (Ainsworth *et al.* 2015; Hernandez-Agreda *et al.* 2017) and characterized in some soft corals (van de Water *et al.* 2018). The core microbiome is conserved among its host species over space and time and is therefore suggested to be important in maintaining holobiont health. The larger, more diverse and variable fraction is influenced by local and regional environmental factors, though may have equally important roles in underpinning host health (Ainsworth *et al.* 2015; Hernandez-Agreda *et al.* 2017).

A similar community structure comprised of conserved and variable fractions was also observed here, in samples derived from *L. pauciflorum* and collected from reefs surrounding Orpheus Island in the central GBR. The community was dominated by Endozoicomonadaceae, with members of Lentisphaeraceae, Shewinellaceae, Francisellaceae among other affiliated taxa recovered in lower relative abundance from 16S rRNA gene amplicon sequencing libraries. Members of Endozoicomonadaceae, particularly *Parendozoicomonas* spp. and *Endozoicomonas* spp. were dominant and conserved throughout *L. pauciflorum* samples and colonies (Chapter 2). The Endozoicomonadaceae-affiliated sequences were almost exclusively recovered from host tissue, with few affiliated sequences derived from the external mucus layer of the soft coral (Chapter 3). This is in agreement with previous studies that used FISH to visualize *Endozoicomonas* spp. aggregations in the tissue layer of Scleractinia (Bayer *et al.* 2013; Neave *et al.* 2017 b).

The association with *Parendozoicomonas* is of interest due to its relatively new classification as a genus (Bartz *et al.* 2018). Sequences affiliated with *Parendozoicomonas* spp. were recovered in high relative abundance in specific association with the tissue layers of *L. pauciflorum*. Sequences affiliated with this new taxon were also detected across the range of soft coral hosts analyzed in chapter 2, suggesting that this may constitute a previously unrecognized relationship that is conserved among soft corals. It is likely that previous studies included the then undescribed *Parendozoicomonas*-affiliated sequences with other *Endozoicomonas*-affiliated sequences, thus overlooking the correlation. The findings from chapter 2 warrant a meta-study of *Endozoicomonas*-affiliated sequences recovered from hard and soft corals to determine how widely distributed is the association with *Parendozoicomonas*.

Some of the other Endozoicomonadaceae-affiliated sequences observed in this study were also recovered from multiple soft coral hosts, but the overall community composition and structure of *L. pauciflorum* was distinct (Chapter 2). Endozoicomonadaceae are commonly recovered in association with coral hosts, though a study with Scleractinia showed that not all host corals share the same degree of species-specificity with *Endozoicomonas* spp. symbionts (Neave *et al.* 2017b). Metagenomics and full genome analyses of *Endozoicomonas* spp. suggest involvement in numerous metabolic pathways and show enrichment in transportation genes encoding transport proteins (Tringe *et al.* 2005; Neave *et al.* 2014, 2017a, 2017b; Ding *et al.* 2016; Tandon *et al.* 2020). They may therefore contribute to integrated metabolic pathways within the coral holobiont host (Robbins *et al.* 2019).

6.1.2 *The baseline community of L. pauciflorum is flexible*

The bacterial community associated with *L. pauciflorum* was characterized in Chapter 2 and was supported by additional 16S rRNA gene sequencing of microhabitat-associated communities in Chapter 3. Along with analyzing conserved members of the community, variability among and between colonies was also investigated, especially concerning the distribution of Endozoicomonadaceae- and Spirochaetaeaceae-affiliated bacterial sequences (Chapter 2). The implications of the observed variability (Figure 6.1) on our understanding of the coral-associated bacterial community structure are discussed here.

6.1.2.1 *The Endozoicomonadaceae-Spirochaetaeaceae dynamic in L. pauciflorum*

Spirochaetaeaceae-affiliated sequences were abundant in 3 of the 7 *L. pauciflorum* colonies analyzed in chapter 2, in agreement with a previous study carried out at the same location (Pelorus Island, QLD) (Wessels *et al.* 2017). The previous study also found that the abundance of Spirochaetes-

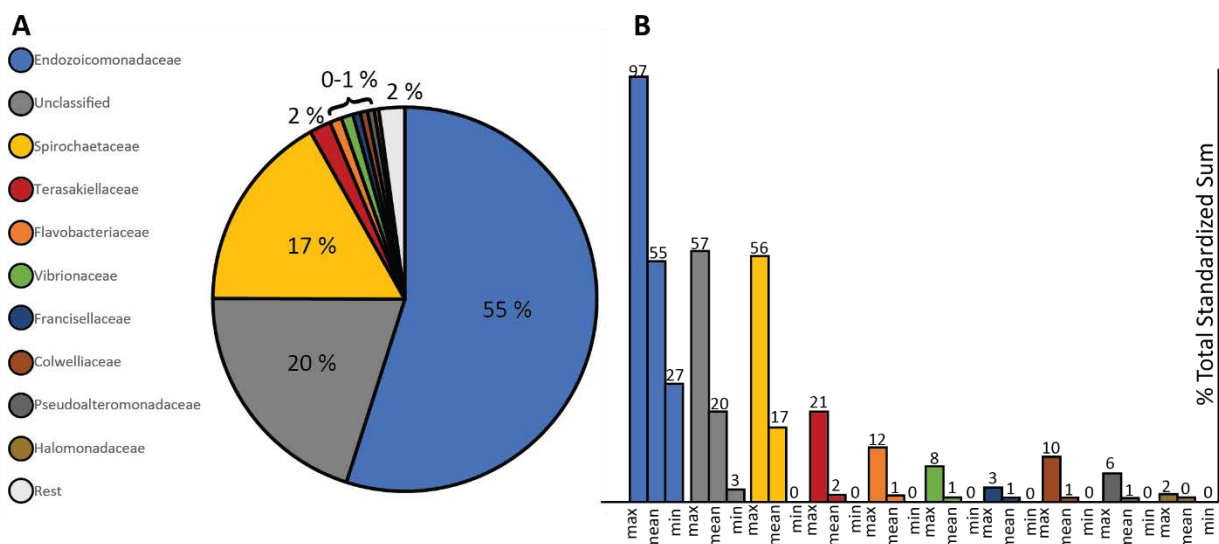


Figure 6.1: The baseline community of *Lobophytum pauciflorum* as represented by the 10 most dominant bacterial families by mean total sum standardization across all 7 colonies (**A**). **B** shows the same 10 families as represented by the mean (center bar) as well as maximum (dodge left) and minimum (dodge right) total sum standardized mean relative abundance between each of the 7 colonies.

related sequences was influenced by sample location and differed between samples collected on different reefs. Differences between location and habitat of sampled colonies on the reef at a local scale may also have influenced the variability observed in Chapters 2 and 3.

The recovery of Spirochaetes-affiliated sequences from tissue samples in the Cnidarian *Hydra* has been associated with tumor formation in the host (Rathje *et al.* 2020). Additionally, some studies determined that a decrease in relative abundance of dominant *Endozoicomonas* spp. can result from disease in the host (Gignoux-wilson *et al.* 2016; Quintanilla *et al.* 2018). However, while the Spirochaetes-affiliated sequences recovered from *L. pauciflorum* were most closely associated with the outer tissue layer (Chapter 3), no visible signs of compromised health were apparent in any of the *L. pauciflorum* colonies sampled. Furthermore, no significant shift in the bacterial community composition associated with *L. pauciflorum* was detected following environmental stress of increased temperature and decreased pH (Wessels *et al.* 2017), indicating the *L. pauciflorum* holobiont structure is resilient to external influences.

Members of Spirochaetes have also been associated with the core microbiome in some soft corals, such as *Corallium rubrum* (van de Water *et al.* 2016; 2018). In *L. pauciflorum*, however, no Spirochaetes-affiliated sequences were recovered from 3 of the 7 colonies, excluding the taxa as a member of the traditionally defined “core” community (Chapter 2). This is an example of variability in the community which confounds previous studies on the baseline community of corals. Additionally,

while high phylogenetic diversity was observed between many ASVs affiliated with Endozoicomonadaceae, few ASVs affiliated with Spirochaetes and they were phylogenetically similar (Chapter 2 and 3). This indicates that the recovered sequences are affiliated with a specific Spirochaetes population which is forming the association observed in *L. pauciflorum* colonies from Pelorus island, QLD. Future studies should investigate if this association is beneficial, commensal or parasitic for the host coral.

6.1.2.2 High flexibility in the coral holobiont

Flexibility in the associations formed with horizontally acquired bacteria could be an advantage in the holobiont's ability to respond to changes in its environment. Transplantation of *Acropora hemprichii* to thermally distinct habitats was followed by a shift in the microbiome, which reverted when transplanted back to the original location (Ziegler *et al.* 2017; 2019). In *Acropora hyacinthus*, the host response to thermal stress was predicted by the bacterial community composition (Ziegler *et al.* 2017). In *Pocillopora verrucosa*, however, the bacterial community did not shift following transplantation (Ziegler *et al.* 2019) and *Endozoicomonas* remained dominant throughout bleaching and mortality (Pogoreutz *et al.* 2018), demonstrating that not all coral holobionts are equally flexible.

A link between flexibility in the associated bacterial community composition and the ability of the coral host to respond to environmental change has several larger implications. Ongoing research is investigating the potential for artificial manipulation of the coral microbiome as a means of increasing the thermal tolerance of the host, hopefully to aid reefs in overcoming bleaching events and other effects of climate change (van Oppen *et al.* 2015; Peixoto *et al.* 2019; Blackall *et al.* 2020). While the mechanisms by which associated bacteria influence the host thermal tolerance are unknown, using this technique as a long-term solution to climate change relies somewhat on unproven yet often presumed probiotic hypotheses. These hypotheses draw on the accumulated research in coral microbiology to suggest that coral-associated bacteria actively play beneficial roles in host physiology, metabolism, defense or other putative functions (Reshef *et al.* 2006; Peixoto *et al.* 2017).

In contrast, the theory of metaorganismal neutrality posits that host species provide microhabitats which are distinct from one another and from their environment but are otherwise colonized according to the same stochastic dynamics as a free-living community (Sieber *et al.* 2018). Under this scenario, the bacteria present in corals are not necessarily providing any benefit to the coral or vice-versa. Mechanisms such as bacterial AMPs, which are antagonistic to pathogens, are then a consequence of inter-bacterial competition and independent of the impact on host health. To achieve the variability observed in *L. pauciflorum* under the neutral theory of metaorganisms,

Endozoicomonadaceae and Spirochaetaceae must only outcompete each other without compromising host health. The distribution and high relative abundance of Endozoicomonadaceae and Spirochaetaceae among host coral taxa and the relationship observed with *L. pauciflorum* in chapters 2 and 3 highlight the need for research into the function and potential interplay between common components of the coral holobiont.

Direct competition between Endozoicomonadaceae and Spirochaetaceae, however, requires co-occurrence of the bacterial cells within the host. Potential probiotic functions of associated bacteria also depend on the localization of symbionts in relation to host anatomy such as the gastrovascular system or epidermal layer. Chapter 3 showed that Endozoicomonadaceae affiliated sequences were routinely retrieved from both the tissue layers in *L. pauciflorum* and Spirochaetes affiliated sequences with the outer tissue layer, more specifically. In the scleractinian corals *Pocillopora verrucosa* and *Stylophora pistillata*, *Endozoicomonas* spp. were visualized with FISH deep within the host endoderm, forming dense aggregates (Bayer et al 2013b; Neave et al. 2017b). The variability in community structure reported in this dissertation may also have been influenced by symbiont localization if bacterial aggregates are not homogeneously distributed throughout the host tissue. Future work must explore the localization of these taxa within the host *L. pauciflorum* tissue using FISH, SEMS or similar imaging techniques.

Previous studies have determined that some corals are more tolerant of changes in the bacterial community than others (Ziegler et al. 2019). The flexibility of the bacterial community associated with *L. pauciflorum* is apparent in the distribution of Spirochaetes across samples and colonies observed in this study and highlights that *L. pauciflorum* may be among the more flexible hosts, expressing a level of variability other host corals may not be able to tolerate. Understanding the degree of tolerable variability within the coral holobiont is important in identifying and thereby predicting the effect of environmental disturbances on bacterial community composition and structure.

Furthermore, Conservation, restoration and management strategies often depend on predicting the impact of variables such as habitat destruction and warming ocean temperatures to succeed in preserving coral reef health and biodiversity. Recognizing host corals that have particularly high or low flexibility will also assist in the identification of species that are more vulnerable to the impacts of climate change. Increasing our understanding of the factors influencing microbiome stability and variability in host corals and how the corals will respond is crucial to improve our efficacy in these fields, especially during the current and predicted climate changes.

6.2 Bacterial community development in larvae

The current understanding of coral-associated bacteria suggests that they may play important roles in maintaining the health of the holobiont (Peixoto *et al.* 2017). However, there is a poor understanding of the timing of onset and pattern of succession in the bacterial community colonizing developing coral larvae. The studies on coral larvae have thus far been conducted across a range of different host species, most of which were Scleractinia. Chapters 4 and 5 in this dissertation address this knowledge gap by compiling comprehensive bacterial community characterization and transcriptomic analysis of larvae in *L. pauciflorum* between fertilization and competency.

The most comprehensive study to date on bacteria associated with developing larvae in Cnidaria focuses on the *Hydra*. In *Hydra*, Bacteria are acquired horizontally and mediated by maternally inherited AMPs (Fraune *et al.* 2010). When the neural system has formed by 2-3 weeks post fertilization, the antimicrobial neuropeptide NDA-1 is produced in the larvae and plays a pivotal role in shaping bacterial community structure throughout the rest of development (Augustin *et al.* 2017). The production of AMPs in developing *Hydra* is accompanied by a major shift in bacterial community structure and composition (Fraune *et al.* 2010; Franzenburg *et al.* 2013). This transition defines distinct “early” and “late” stages of community succession during larval development. The early stage is characterized by high variability, while the late stage exhibited higher stability and composition more closely resembling the community assemblage recovered from healthy adults.

The pattern of community development in *L. pauciflorum* larvae characterized in this dissertation (Chapter 4 and 5) shares similarities with *Hydra* and is consistent with previous studies on coral larvae (Table 6.1). A distinct change in the bacterial community structure at early life stages occurred in planula of *L. pauciflorum* between 48 and 72 hpf. In developing *Hydra*, a distinct change occurred at 2 weeks when the hatchlings had settled (Franzenburg *et al.* 2013). In *L. pauciflorum*, the differential expression of antimicrobial compounds corresponded to the distinct stages of bacterial community composition. The expression of AMP and Kazal-type serine protease inhibitor noted in *L. pauciflorum* could contribute to this observed shift in bacterial community composition. If the development of associated bacterial communities in cnidarian larvae is mediated by antimicrobial compounds secreted by the host, it is inconsistent with the neutral model of metaorganisms (Sieber *et al.* 2018).

In *L. pauciflorum* larvae, sufficient quantity and quality 16S rRNA gene sequences could not be recovered from samples collected at 6 hpf. Few studies have examined the bacterial community associated with larvae prior to the planula stage, but some studies in Scleractinia have reported that bacterial associations are not formed with the host until later in development. A study across

Table 6.1: Overview of the current understanding of the timing of bacterial community onset and succession throughout early life history in Cnidarian Octocorallia (green), Scleractinia (yellow) and *Hydra* (gray).

	Octocorallia	Scleractinia	Hydra
Release	<ul style="list-style-type: none"> The differential expression of AMP and Kazal-type homologs in <i>L. pauciflorum</i> larvae reflects maternal inheritance (Chapter 5). 	Bacteria released into the water column with gametes/larvae for uptake (Ceh <i>et al.</i> 2013b).	Maternally inherited AMPs mediate early onset of Bacteria (Fraune <i>et al.</i> 2010; Franzenburg <i>et al.</i> 2013)
Fertilization		Vertical transmission of Bacteria reported in brooding corals (Sharp <i>et al.</i> 2010; Pollock <i>et al.</i> 2018; Bernasconi <i>et al.</i> 2019; Damjanovic <i>et al.</i> 2020).	
1 day	<ul style="list-style-type: none"> Very strong antimicrobial activity detected in larval extracts from 6 species of soft coral in all samples days 1-6 (Kelman <i>et al.</i> 1998). "Early Stage" bacterial community in <i>L. pauciflorum</i> dominated by diverse Gammaproteobacteria (Chapter 4) 	<ul style="list-style-type: none"> Little to no antimicrobial activity detected in larval extracts of 6 hard corals days 1-6 (Kelman <i>et al.</i> 1998). First 48 hpf dominated by Alpha- and Gammaproteobacteria (Damjanovic <i>et al.</i> 2020; Kullapanich <i>et al.</i> 2021). 	
2 days	<ul style="list-style-type: none"> Early-to-late stage transition phase dominated by the family Francisellaceae (Chapter 4). Gastrulation takes place in <i>L. pauciflorum</i> (Wessels <i>et al.</i> 2017). 		
3 days	"Late Stage" bacterial community in <i>L. pauciflorum</i> dominated by Betaproteobacteria (Chapter 4).	Bacterial cells taken up horizontally are detected (FISH) internally within tissue cells of <i>Pocillopora meandrina</i> (Apprill <i>et al.</i> 2009).	
4 days		Diverse Alpha- and Gammaproteobacteria present but not internalized in <i>Acropora tenuis</i> (Damjanovic <i>et al.</i> 2020).	
5 days	AMP and Kazal-type homologs expressed in <i>L. pauciflorum</i> during the "Late Stage" form a consortium distinct from that in the Early Stage (Chapter 5).	Bacteria were not detected (FISH and 16S rRNA gene sequencing) until after settlement and metamorphosis in <i>Montastraea</i> (3 species), <i>Acropora</i> (3 species) and <i>Diploria strigosa</i> (Sharp <i>et al.</i> 2010).	"Early Stage" bacterial community characterized by high diversity (Fraune <i>et al.</i> 2010).
polyp		Bacterially metabolized N15 taken up by <i>Acropora</i> larvae (Ceh <i>et al.</i> 2013a).	
3 weeks			<ul style="list-style-type: none"> "Late Stage" bacterial community characterized by lower diversity and dominated by the betaproteobacteria <i>Curvibacter</i> spp. (Fraune <i>et al.</i> 2010). Late stage community succession mediated by AMPs such as NDA-1 (Augustin <i>et al.</i> 2017).

broadcast-spawning Scleractinia did not recover bacterial sequences from larvae prior to settlement and metamorphosis (Sharp *et al.* 2010). In the broadcast spawner *Acropora tenuis* and the brooding coral *Pocillopora meandrina*, bacterial cells were detected but not internalized by the larvae (as

determined by FISH) prior to 5 and 6 days post-fertilization, respectively (Aprill *et al.* 2009; Damjanovic *et al.* 2020). This may infer a difference between development in hard and soft corals or by species. It also further warrants the use of FISH in future studies on developing larvae to determine when Bacteria are assimilated by the tissue in addition to colonizing the surface.

6.3 *L. pauciflorum* as a model Alconiid

The studies presented in this dissertation provide a robust characterization of the bacterial community of *L. pauciflorum* (Figure 6.2). The baseline community is similar to that of other soft corals, though differs from them at high taxonomic resolution (Chapter 2). The communities associated with mucus and tissue layers were distinct within each colony of *L. pauciflorum* with the most abundant and conserved members associated with the tissue layers (Chapter 3). The onset and development of the bacterial community, studied here for the first time in soft corals, shares some similarities to developmental patterns observed in *Hydra* (Chapter 4 and 5). Finally, I provide strong evidence that genes encoding likely antimicrobial proteins, including AMPs and serine protease inhibitors, are

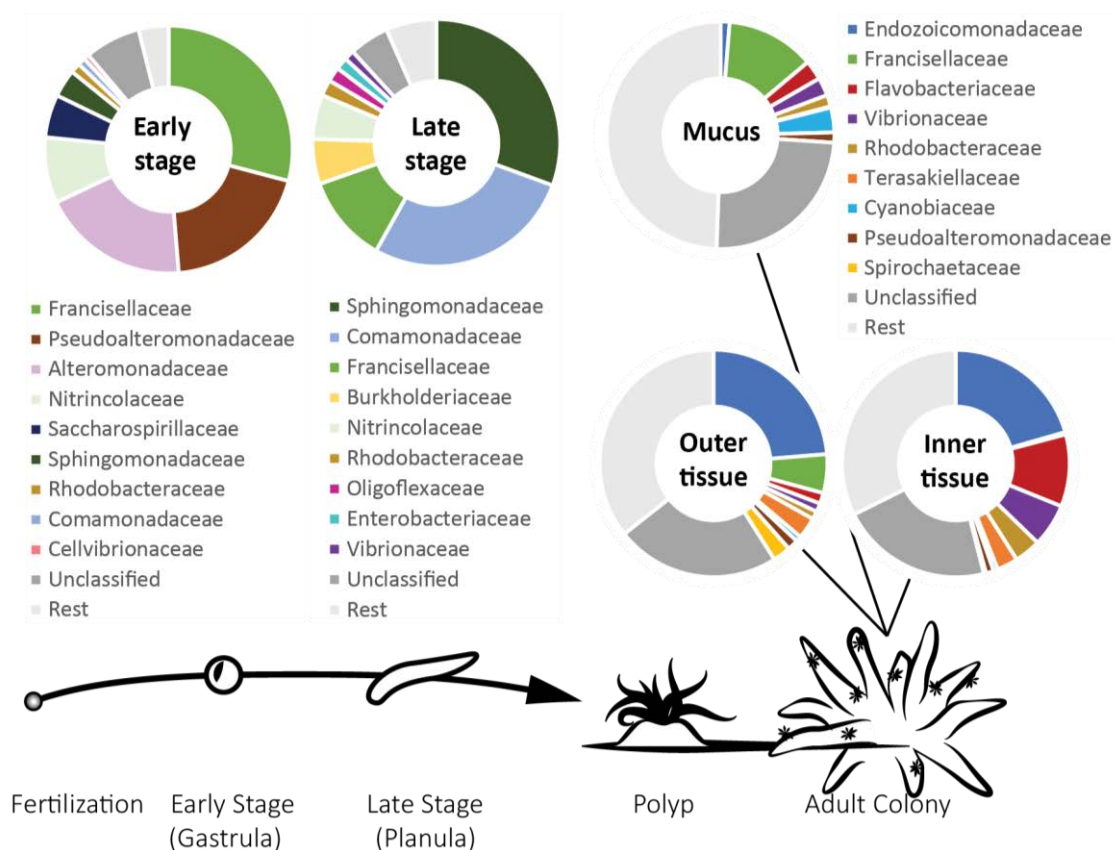


Figure 6.2: Bacterial community of early and late stage larvae and the adult microhabitats in the mucus layer, outer tissue and inner tissue of *Lobophytum pauciflorum*. Only the top 10 most dominant bacterial families associated with each community are included, as characterized in the analyses of chapters 3 and 4).

expressed in larvae and potentially contribute towards shaping the developing bacterial community. Cumulatively, these studies provide the context to develop a deeper understanding of the bacterial communities associated with *L. pauciflorum* and the soft corals more generally.

Model organisms possess qualities that allow for the comprehensive study of specific characteristics that can be extrapolated to improve our broader understanding of other organisms (Leonelli and Ankeny 2013). The Octocorallia were proposed as good models for complex host-symbiont interactions in marine invertebrates and for studying holobiont structure, assembly and function by van de Water *et al.* (2018). The body of research that exists on *L. pauciflorum* across the fields of chemistry, genetics, transcriptomics and now microbiology position this species as an effective model Alcyoniid. Prior to the studies presented in this dissertation, the full genome and transcriptome of *L. pauciflorum* had also been assembled at JCU (Wessels 2016). Transcriptomic analyses have been conducted on *L. pauciflorum* throughout development, metamorphosis and adulthood (Wessels 2016) and during intercolonial competition (Andrade-Rodriguez 2018). As no other soft coral taxa, and few hard coral taxa, have been studied to this extent, *L. pauciflorum* is proposed as a model organism for the study of Alcyoniid and Octocorallia microbiology, transcriptomics and genetics.

One limitation in using *L. pauciflorum* as a model has been the inability to induce settlement and metamorphosis of competent larvae in the laboratory. While breeding and rearing larvae has been optimized at Orpheus Island Research Station, QLD, inducing settlement and metamorphosis with CCA extracts or CsCl has been unsuccessful (*unpublished*). Identifying the settlement cues to successfully induce reared would allow research to fill the knowledge gap in soft coral bacterial community development from competency through metamorphosis and into adulthood. Furthermore, an important knowledge gap in coral microbiology which should be studied in *L. pauciflorum* is how disturbances to the onset and development of the bacterial community in larvae influence microbial community composition, health and physiology in the adult colonies. This would also require successful settlement and metamorphosis techniques to rear larvae through to adulthood.

6.4 Final Conclusions

The studies contained within this dissertation enhance our understanding of the host-symbiont relationship in soft corals with extrapolations to be considered throughout the Cnidaria. As a greatly understudied taxon compared with Scleractinia, this work provides a foundation for future studies into the mechanisms influencing and resulting from Octocorallia-bacteria relationships. Equally vital components to unraveling the host-symbiont dichotomy, the biological function of symbionts and the factors shaping the community must be further elucidated to fully understand

inter-kingdom interactions on coral reefs. Furthermore, degradation of the marine environment due to anthropogenic activity has impacted coral reefs on a global scale, though many efforts are being made to preserve the reefs which remain and to restore life and biodiversity to those that have been lost. As it has become clear that the hosts' response and ability to adapt to a changing environment is directly related to the associated microbiota, a greater comprehension of their relationship is needed for these efforts to succeed.

Appendix

Appendix A: Phylogenetic relationships between host Octocorallia used in this study (Chapter 2)

Phylogeny of host species was analyzed by alignments of the *msh1* gene, a mutS-like mitochondrial sequence specific to octocorals and used to successfully differentiate between taxa at the genus level in McFadden *et al.* (2006). For the host genera used in chapter 2, sequences corresponding to the *msh1* gene were obtained from NCBI GenBank. There were 5 unique entries for *Sarcophyton* spp. (MH040765.1, MH040756.1, MH040759.1, MH040760.1 and MH040760.3), therefore the first 5 entries were also selected from *Briareum* spp. (GU356010.1, GQ342484.1, FJ434352.1, AB763398.1 and AB763397.1) and *Sinularia* spp. (FJ621487.1, FJ621488.1, FJ621489.1, FJ621490.1 and DQ302813.1) although more were returned from the database. Additionally, 3 entries were obtained that were sequenced from *Lobophytum pauciflorum* (DQ280577.1, DQ280576.1 and DQ280575.1). There was only 1 entry for *Clavularia* spp. (DQ302799.1) and *Pinnigorgia* spp. (GQ342498.1) and 2 unique entries for *Xenia* spp. (GQ342529.1 and DQ302842) and *Cladiella* spp. (GU356011.1 and DQ302807.1). There were no entries corresponding to *Isis* spp., however. Therefore, while some host species were underrepresented (and *Isis* spp. absent), 24 sequences were aligned using MUSCLE (Edgar 2004) in Geneious Prime 209.2.1 (<http://www.geneious.com>).

Alignments were run using MUSCLE and a 736 bp region (85.8 % pairwise identity and 56.5 % identical sites) (Figure A.1) was extracted and imported to the modelfinder web server at IQTree (<http://iqtree.cibiv.univie.ac.at/>) to determine the most appropriate model for calculating phylogenetic distance (Kalyaanamoorthy *et al.* 2017). The modelfinder determined that TPM3 and TIM3 were the best models, but that Hasegawa-Kishino-Yano (Hasegawa 1985) was the best model available to run on Geneious Prime 2019.2.1 (<http://www.geneious.com>). Bayesian phylogenetic distance was then calculated in Geneious Prime according to the HKY substitution model with 1.1 million iterations in MrBayes (Figure A.2) (Huelsenbeck and Ronquist 2001, Ronquist and Huelsenbeck



Figure Appendix 1: MUSCLE alignment of sequences corresponding to the *msh1* gene downloaded from NCBI and corresponding to host genera analyzed in this study. The Pennatulacea genus *Pteroeides* spp. was used as an outgroup.

2003). Because *msh1* is specific to octocorals a distant outgroup could not be included as an outgroup, therefore the sea pen *Pteroeides* spp. (DQ302871.1) was used (Order Pennatulacea; txid6133).

Phylogenetic analysis of the host species was consistent with previous studies on the relationship between cnidarian phylogeny and bacterial community composition (O'Brien *et al.* 2020) and all sequences grouped together according to host species. The Alcyoniidae genera *Sinularia*, *Sarcophyton* and *Lobophytum* clustered together in both the phylogenetic tree and an NMDS of Bray-curtis dissimilarity based on community composition (Figure 2.4). The alcyoniid *Cladiella*, however, grouped with *Pinnigorgia* and *Xenia* phylogenetically but not in bacterial community composition NMDS. The genera *Briareum* and *Cavularia* formed the most distant group from *Lobophytum* and other the Alcyoniidae in both phylogeny and community composition NMDS.

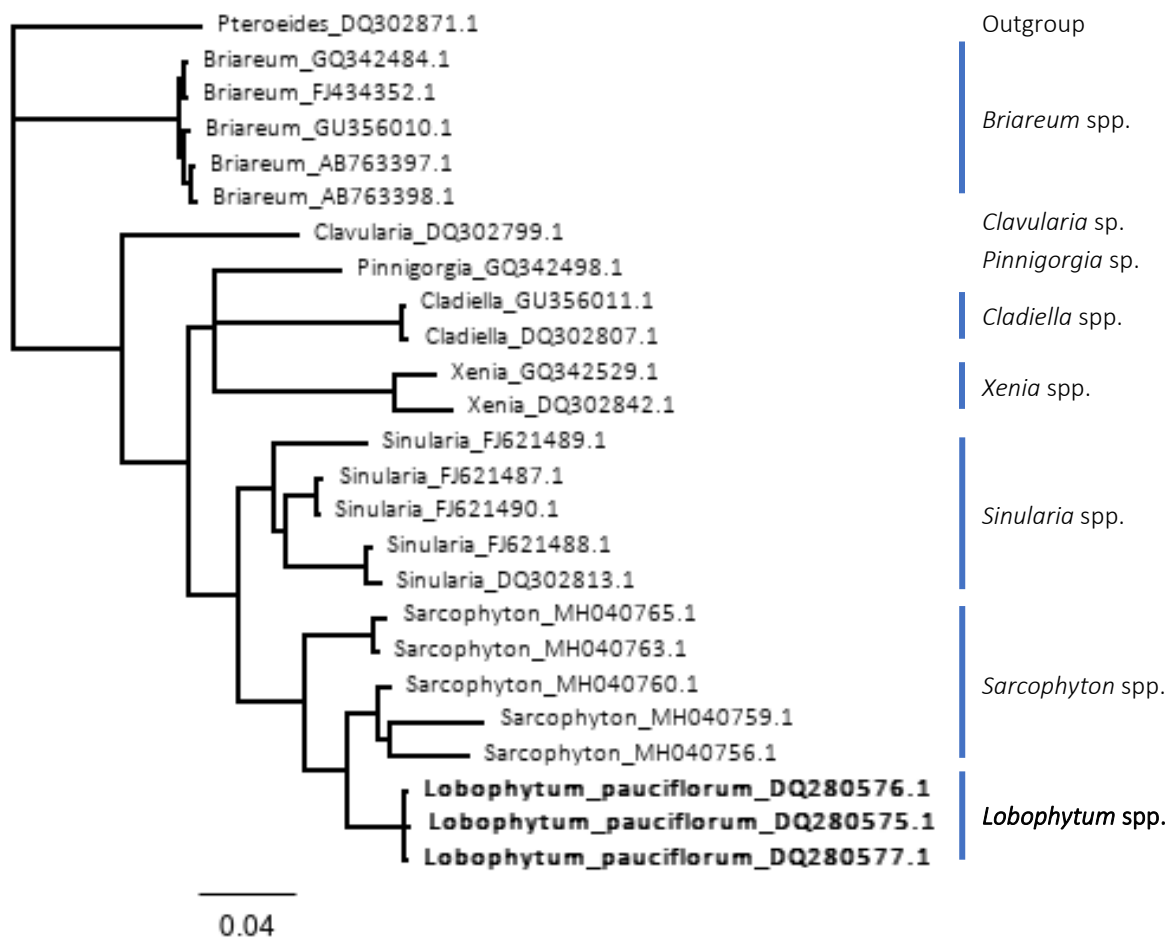


Figure Appendix 2: Phylogenetic tree depicting the relationship between host species built on a MAAFT alignment of the *msh1* gene with MrBayes in Geneious Prime 2019.2.1 using Hasegawa-Kishino-Yano (HKY) model (Hasegawa *et al.* 1985) to calculate Bayesian distance with 1.1 million iterations. The sea pen *Pteroeides* sp. was used as an outgroup.

Appendix B: Putative identification of unclassified ASVs via NCBI BLAST (Chapter 2)

Consistent with previous studies on *Lobophytum pauciflorum* (Wessels *et al.* 2017) and other corals, the bacterial community was characterized by a large number of sequences (22.7 %) which were unclassified by the SILVA database. These sequences were distributed across 44 distinct ASVs which were submitted to NCBI basic local alignment search tool (BLAST) (Altschul *et al.* 1990) and compared against the NCBI SSU 16S/18SBacteria/Archaea sequence database with a cutoff of $1e^{-5}$ (Table A.1). Of these 44 ASVs, 34 received BLAST hits with high sequence identity to sequences attributed with 21 bacterial families (Figure A.3).

The majority of the unclassified sequences were sparsely distributed among colonies and were recovered in low relative abundance. Several were ubiquitous among samples however, including those associated with Phyllobacteriaceae, Rhizobiaceae and Spirochaetaceae. Additionally, several of the previously unclassified ASVs were in high relative abundance in some colonies including those associated with Kiloniellaceae recovered from Colony II, Lentisphaerae and Spirochaetaceae recovered from Colony VII and Rhodospirillaceae recovered from Colonies III-VI. Sequences affiliated with the Rhodospirillaceae *Oceanibaculum nanhaiense* (NR_159190.1) were in high relative abundance in colonies III and IV (27.8 ± 7.4 SD %) but were not associated with ASVs abundant in any colony according to SILVA database. Samples from colony VII were dominated by 2 unclassified ASVs (44.7% and 27.2% relative abundance) that both aligned to sequences derived from the spirochaete *Oceanispirochaeta litoralis* (NR_104732.1) in BLAST.

The putative identification of unclassifiable sequences via BLAST brought additional insight into the community structure of colonies that had a high relative abundance of unclassified sequences (Figure A.4). Sequences identified in this way showed distribution and abundance patterns consistent with the ASVs classified in SILVA database and provide additional support for the conclusions drawn from the baseline bacterial community in *L. pauciflorum*.

Table Appendix 1: Basic local alignment search tool (BLAST) results identifying unclassified sequences recovered from *Lobophytum pauciflorum* with known sequences in the 16S/18S SSU Bacteria/Archaea database at NCBI (<https://blast.ncbi.nlm.nih.gov/Blast.cgi>) at a maximum e-value of $1e^{-5}$.

FeatureID	Genus	Species	NCBI Acc. No	evalue
Unclassified_1	<i>Oceanispirochaeta</i>	<i>litoralis</i>	NR_104732.1	5.00E-91
Unclassified_2	<i>Oceanibaculum</i>	<i>nanhaiense</i>	NR_159190.1	6.00E-120
Unclassified_3	<i>Kiloniella</i>	<i>majae majae</i>	NR_152635.1	6.00E-150
Unclassified_4	<i>Lentisphaera</i>	<i>profundi</i>	NR_145667.1	2.00E-115
Unclassified_5	<i>Lentisphaera</i>	<i>profundi</i>	NR_145667.1	8.00E-119
Unclassified_6	<i>Lentisphaera</i>	<i>profundi</i>	NR_145667.1	4.00E-117
Unclassified_7	<i>Borrelliella</i>	<i>chilensis</i>	NR_125639.1	2.00E-74
Unclassified_8	<i>Pirellula</i>	<i>staleyii</i>	NR_074521.1	2.00E-16
Unclassified_9	<i>Mesorhizobium</i>	<i>thiogangeticum</i>	NR_042358.1	0
Unclassified_10	<i>Mycoplana</i>	<i>ramosa ramosa</i>	NR_113740.1	6.00E-160
Unclassified_11			Unclassified	
Unclassified_12	<i>Luteimonas</i>	<i>arsenica</i>	NR_149301.1	5.00E-81
Unclassified_13	<i>Spiroplasma</i>	<i>mirum</i>	NR_121794.2	6.00E-150
Unclassified_14	<i>Lentisphaera</i>	<i>profundi</i>	NR_145667.1	8.00E-119
Unclassified_15	<i>Streptococcus</i>	<i>sanguinis</i>	NR_111994.1	4.00E-10
Unclassified_16	<i>Spiroplasma</i>	<i>mirum</i>	NR_121794.2	3.00E-148
Unclassified_17	<i>Marispirochaeta</i>	<i>aestuarii</i>	NR_158116.1	9.00E-104
Unclassified_18	<i>Spiroplasma</i>	<i>mirum</i>	NR_121794.2	3.00E-148
Unclassified_19	<i>Sulfurospirillum</i>	<i>multivorans</i>	NR_044868.1	1.00E-106
Unclassified_20	<i>Kangiella</i>	<i>chungangensis</i>	NR_148305.1	4.00E-162
Unclassified_21			Unclassified	
Unclassified_22			Unclassified	
Unclassified_23	<i>Lujinxingia</i>	<i>sediminis</i>	NR_165015.1	8.00E-154
Unclassified_24			Unclassified	
Unclassified_25	<i>Spirochaeta</i>	<i>perfilievii</i>	NR_115202.1	8.00E-119
Unclassified_26			Unclassified	
Unclassified_27	<i>Oceanibaculum</i>	<i>nanhaiense</i>	NR_159190.1	1.00E-121
Unclassified_28	<i>Endozoicomonas</i>	<i>atrinae</i>	NR_134024.1	4.00E-177
Unclassified_29			Unclassified	
Unclassified_30			Unclassified	
Unclassified_31	<i>Spirochaeta</i>	<i>perfilievii</i>	NR_115202.1	5.00E-96
Unclassified_32	<i>Oceanispirochaeta</i>	<i>litoralis</i>	NR_104732.1	2.00E-89
Unclassified_33			Unclassified	
Unclassified_34			Unclassified	
Unclassified_35	<i>Spiroplasma</i>	<i>mirum</i>	NR_121794.2	6.00E-150
Unclassified_36	<i>Pseudomonas</i>	<i>urumqiensis</i>	NR_171524.1	4.00E-157
Unclassified_37	<i>Streptococcus</i>	<i>sanguinis</i>	NR_111994.1	4.00E-10
Unclassified_38	<i>Thiopfundum</i>	<i>lithotropicum</i>	NR_112829.1	0
Unclassified_39	<i>Flexithrix</i>	<i>dorothaeae</i>	NR_113831.1	5.00E-156
Unclassified_40	<i>Sulfurospirillum</i>	<i>cavolei</i>	NR_041392.1	3.00E-113
Unclassified_41	<i>Lentisphaera</i>	<i>profundi</i>	NR_145667.1	2.00E-120
Unclassified_42	<i>Thiohalobacter</i>	<i>thiocyanaticus</i>	NR_116699.1	6.00E-115
Unclassified_43			Unclassified	
Unclassified_44	<i>Eubacterium</i>	<i>nodatum</i>	NR_119311.1	6.00E-14

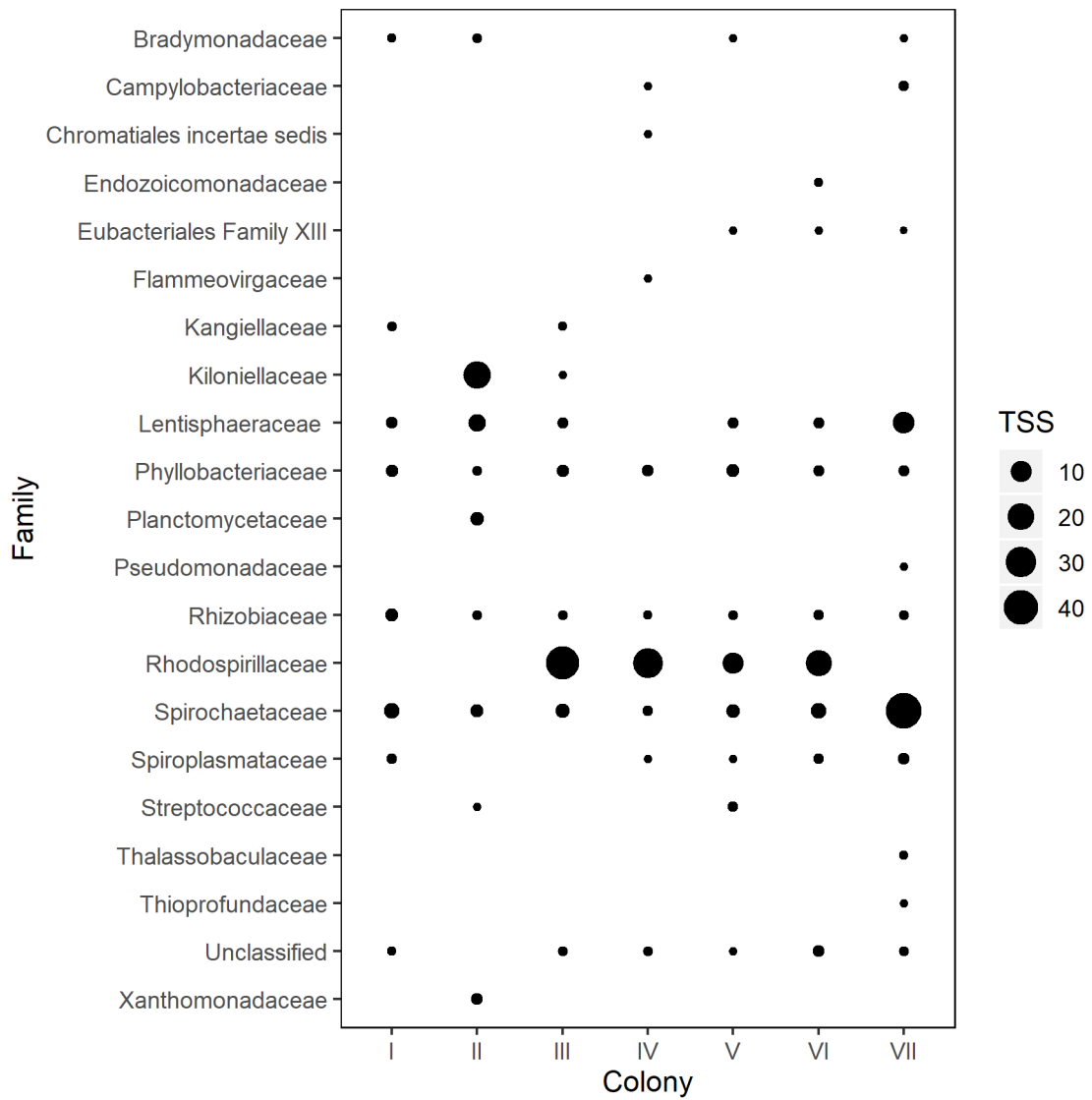


Figure Appendix 3: Distribution of sequences associated with the respective families in NCBI BLAST as they are distributed by relative abundance across colonies of *Lobophytum pauciflorum*.

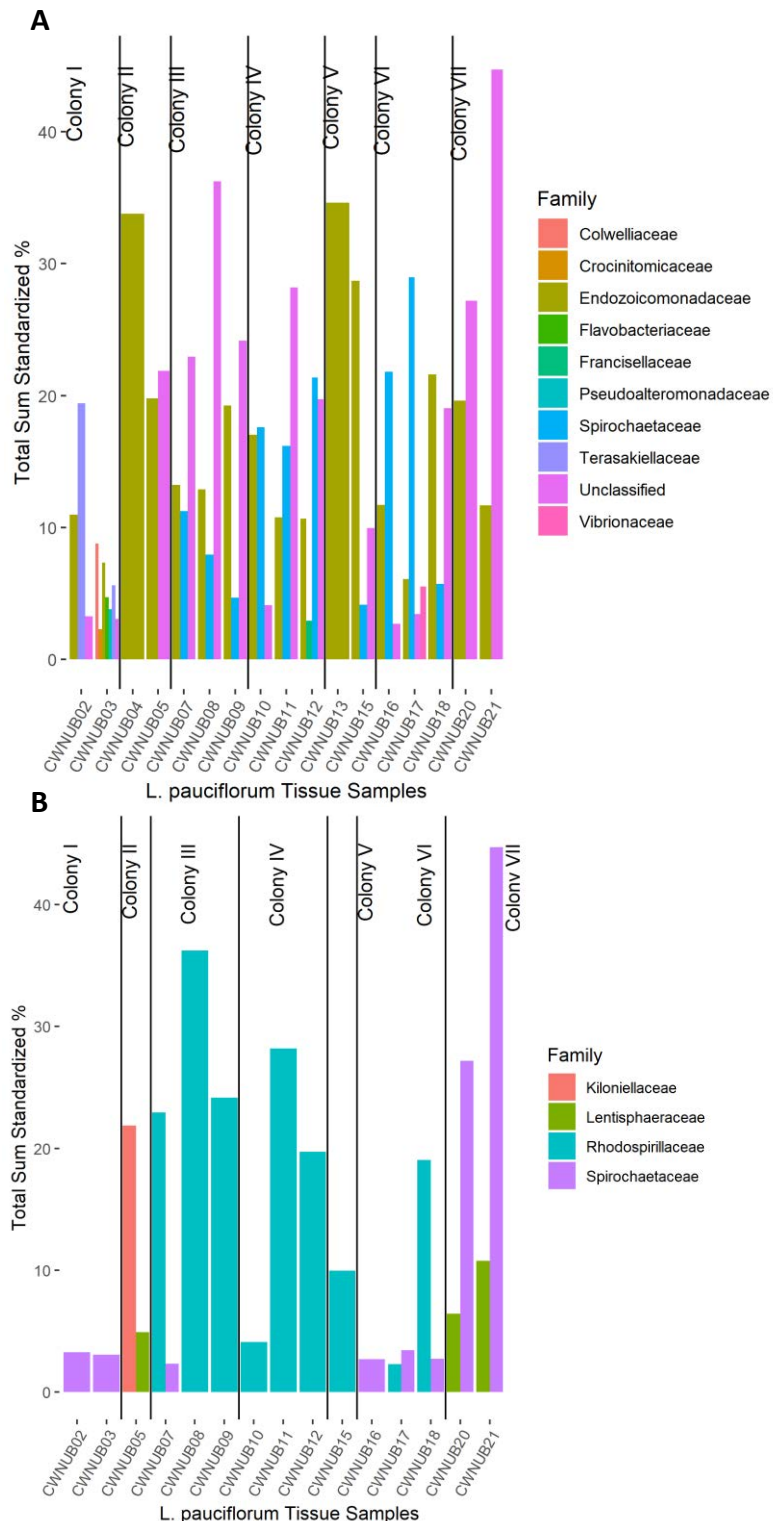


Figure Appendix 4: Composition of the 16S rRNA gene community as classified by SILVA (A) and the unclassified sequences subsequently identified via basic local alignment search tool (BLAST) (B).

Appendix C: Decontamination of 16S community data with the R package microDecon (Chapter 4)

Larval samples (Individuals subsampled in 200 µl aliquots) were collected in triplicate for genomic DNA extraction from 9 timepoints throughout development (6 hours post-fertilization [hpf], 14 hpf, 24 hpf, 36 hpf, 48 hpf, 72 hpf, 96 hpf, 120 hpf and 210 hpf). Complications in the optimization of genomic DNA extraction and 16S gene amplification in PCR resulted in only 2 high quality amplicon samples per time-point, and 3 at 36 hpf, that were submitted for sequencing. The samples were amplified in 3 individual PCR runs (run A, run B and run C), each of which included a positive (Flavomonadaceae sp. culture) and negative (ultrapure water) control reaction. The negative control run A showed an amplicon band during post-PCR quality control in the gel electrophoresis. This positive blank (hereafter 'blankA') is the subject of the following analysis into potential contamination of the PCR run using the R package microDecon (McKnight *et al.* 2019). The designations of early (48

Table Appendix 2: Samples of developing *Lobophytum pauciflorum* larvae collected at each time point and included in extraction, amplification and sequencing. 1 sample from each time point was also preserved at -80°C.

	Timepoints sampled (hpf)									Negative controls with PCR product
	6	14	24	36	48	72	96	120	210	
Sampled	4	4	4	4	4	4	4	4	4	
Extracted	3	3	3	3	3	3	3	3	3	
Failed	1	1	1	0	1	1	1	1	1	
PCR_run (A)	1	1	1	1	1	1	1	1	1	1
PCR run (B)				1						0
PCR run(C)	1	1	1	1	1	1	1	1	1	0
Sequenced	2	2	2	3	2	2	2	2	2	1

hpf and before) and late (72 hpf and later) stages of community succession refer to the conclusions of chapter 4.

Sequencing and bioinformatics analysis (results detailed in chapter 4) classified sequences recovered from the blank as members of the bacterial families Sphingomonadaceae (Alphaproteobacteria), Comamonadaceae and Burkholderiaceae (Betaproteobacteria). Sequences associated with Burkholderiaceae were from the genera *Ralstonia* and *Pelomonas*. While *Ralstonia* spp. have been reported previously as common contaminants of DNA extraction kits (Salter *et al.* 2014), members of the genus have also been reported as core members of the microbiome in some Scleractinia (Ainsworth *et al.* 2015). Furthermore, all of these bacterial families are commonly recovered from corals, therefore sequencing did not inform if the amplicon sequences recovered from blankA were contaminants or cross-contamination from PCR reactions.

To provide further insight into the potential for contamination, the R package microDecon was applied to the dataset (McKnight *et al.* 2019). MicroDecon identified contaminant sequences in blankA based on the distribution and abundance of ASVs across populations and removed them from the dataset. The following presentation compares the 16S rRNA gene community associated with developing larvae prior to and post ‘decontamination’ with microDecon. Based on these analyses, it was concluded that the sequences were cross-contaminants from a sample in the ‘late stage’ of community development and not external contamination from the laboratory or DNA extraction kits.

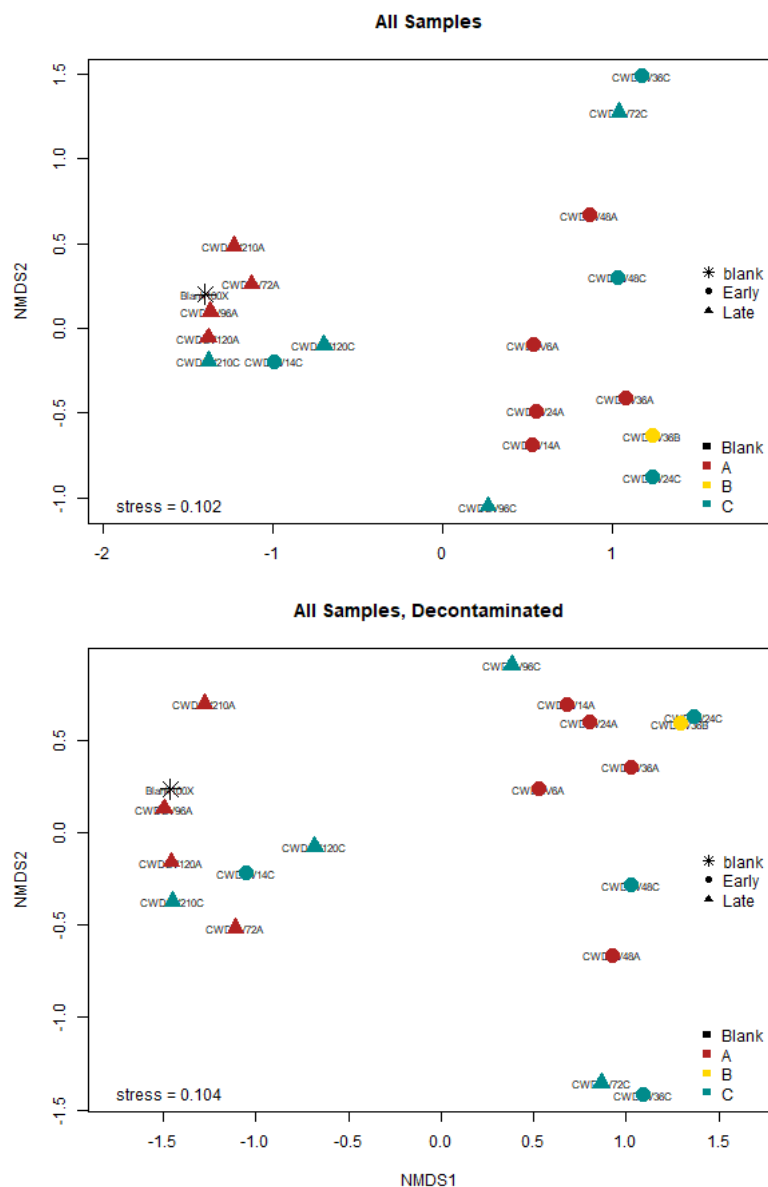


Figure Appendix 5: NMDS of all samples - including blankA - prior to (top) and below (bottom) decontamination. The clustering and grouping of samples with and without ‘contaminant’ sequences is almost identical, though aesthetically the orientation of the samples is inverted. Shapes depict early (circle) and late (triangle) stages of community development while color depicts sequencing run (red = A, yellow = B and cyan = C).

Table Appendix 3: Analysis of significant extrinsic variables influencing community composition in developing larvae. Both before and after decontamination, the most significant factors were 2- and 3-stage descriptions of development. 2-stage considers early (48 hours post-fertilization [hpf] and prior) and late (72 hpf and later) stages, 3-stage considers 210 hpf samples as a distinct stage of larval competency, and 4-stages includes also the samples at 48hpf as a separate ‘transitional’.

Extrinsic variable	Before Decontamination			After Decontamination		
	R2	Pseudo-R	significance	R2	Pseudo-R	significance
Sample	1	1		1	1	
Run	0.1574	0.521	.	0.1786	0.351	.
hpf	0.6682	0.067	.	0.6819	0.074	.
2-stage	0.4002	0.001	***	0.4209	0.002	**
3-stage	0.4299	0.005	**	0.456	0.004	**
4-stage	0.4627	0.16	*	0.4815	0.011	*

The following data includes samples 14c and 36a which were removed from the chapter dataset as outliers, and samples from 6 hpf which ultimately did not have enough sequence reads to include in the chapter analysis and may therefore vary slightly from figures presented in Chapter 4.

Sample clusters and positions relative to one another were not influenced by the removal of ‘contaminant’ sequences, forming 2 primary clusters of early- and late-stage communities (Figure A.5). In both cases, blankA clusters with samples from the late stage of community development. If blankA was reflective of external contamination in the amplification run, samples would be expected to cluster according to PCR run, instead.

The early- and late-stage clusters were further explored using the envfit function in the R package Vegan (Oksanen *et al.* 2018). The envfit function determines the most influential internal (intrinsic) and external (extrinsic) variables driving community composition. The extrinsic variables found to be significant drivers of community distribution were 2-stage (pseudo-F = 0.001) and 3-stage (pseudo-F = 0.005) models of community development and not amplification run. These conclusions were further supported by ANOSIM (table A.3).

Table Appendix 4: Results of analysis of similarity (ANOSIM) indicating the 2-stage model (early/late) as the best description of distinct communities in developing *L. pauciflorum* larvae.

Extrinsic variable	Before Decontamination		After Decontamination	
	R	P	R	P
Run	0.044	0.261	-0.037	0.923
hpf	0.221	0.127	0.276	0.079
2-stage	0.434	0.002	0.497	0.001
3-stage	0.338	0.006	0.429	0.001

The intrinsic variables constitute indicator species driving community distribution (max significance = 0.01). The late cluster, including the blank and samples post 48 hpf from both runs A and C, was driven by sequences affiliated with members of Burkholderiales (families Burkholderiaceae and Comamonadaceae) and Sphingomonadales (family Sphingomonadaceae) (Figure A.5). These sequences were considered contamination in the analysis with microDecon even though they were not exclusive to amplification run A. The same ASVs drive sample distribution before and after decontamination. This includes the 4 main taxa removed by microDecon driving the late-stage cluster (*Sphingobium*, *Sphingomonas*, *Pelomonas* and *Ralstonia*), composed of samples from both runs A and C. Furthermore, these sequences dominated the late community but were not dominant in the early community, even in amplification run A. This is also apparent in the community composition which depicts the community in blankA as a subset of the community associated with the late-stage of development (Figure A.6).

The analysis of blank A is indicative in all cases that the blank was contaminated by some of the amplicon products dominating the adjacent late-stage community samples. The main supporting factors are that i) the 'late' and 'early' designation applies to both amplification runs A and C and is therefore not an artefact of the contamination and ii) The community associated with blank A resembles the late stage, not the early stage, thus contamination is likely from late-stage amplicon products entering the negative control (blank A) rather than external contamination entering the dataset. Following this analysis, the dataset was analyzed for chapter 4 using the full, non-decontaminated sequence communities under the conclusion that contamination was not present.

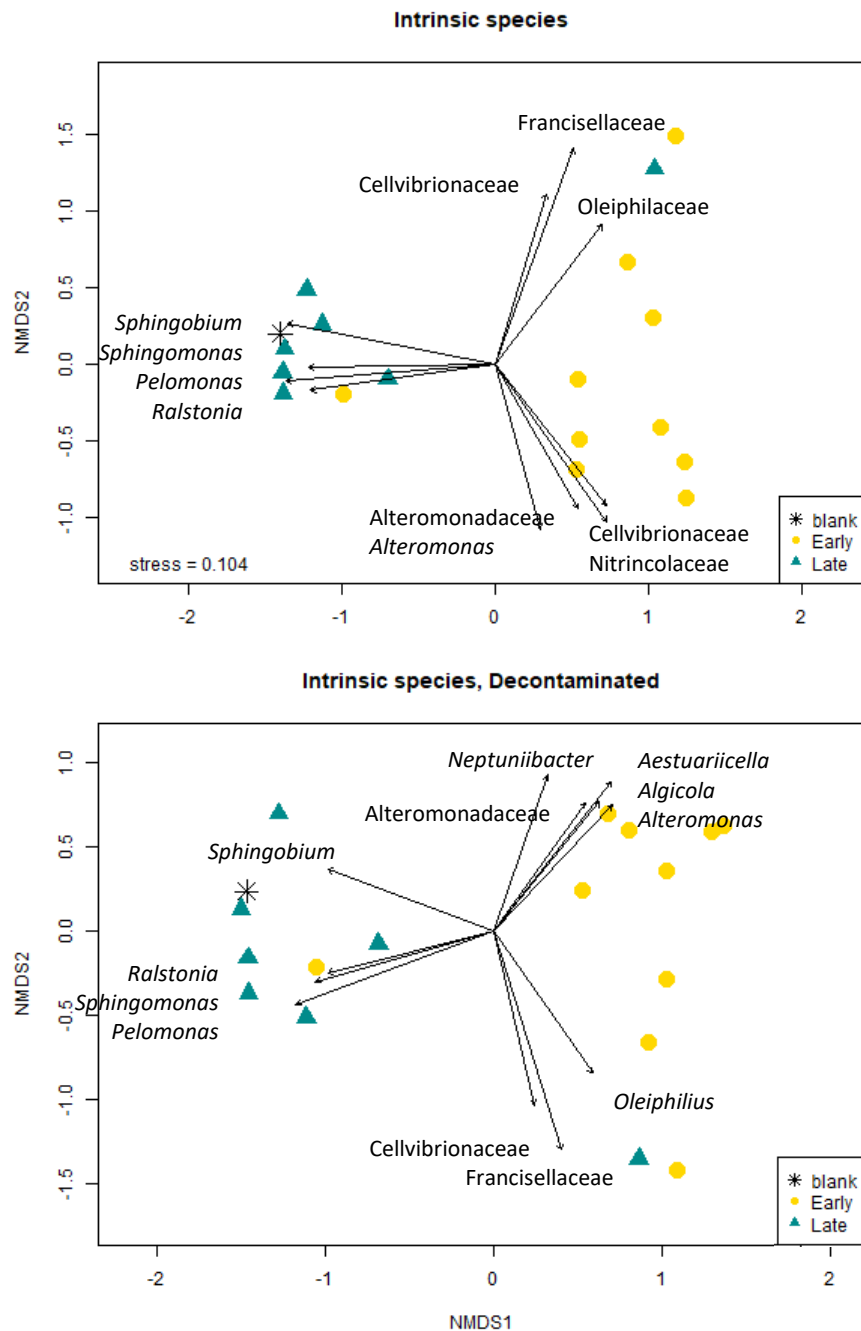


Figure Appendix 6: Bacteria driving the dissimilarity between samples and clusters before (top) and after (bottom) decontamination with microDecon. Intrinsic species as determined by envfit in the R package Vegan. Symbols indicate early (yellow circle) and late (cyan triangle) stages of community development.

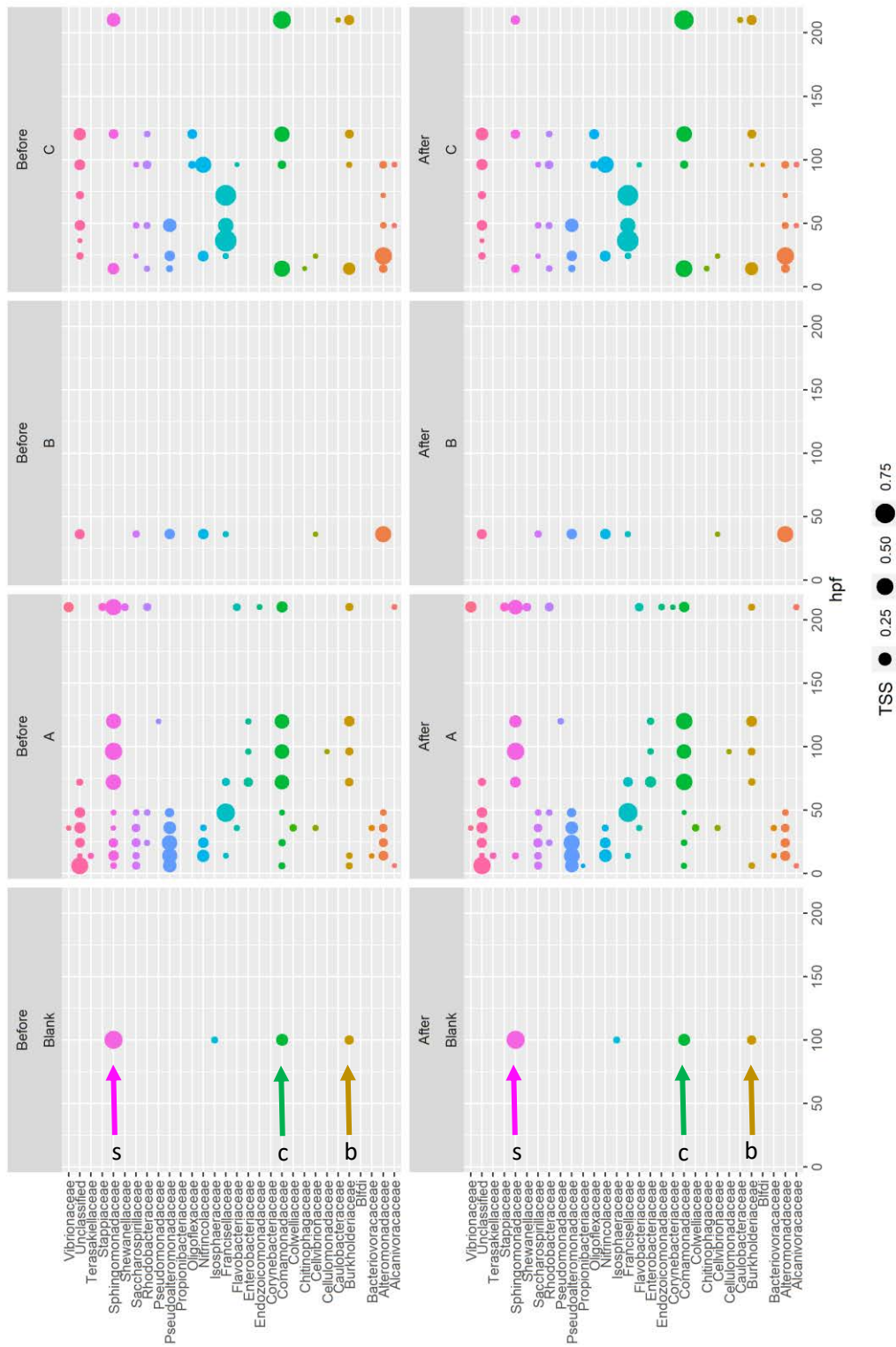


Figure Appendix 7: community composition of each sample faceted according to blankA and PCR runs A, B and C (columns) as well as before and after decontamination with microDecon (rows). The main groups targeted in decontamination were Burkholderiaceae (b), Comamonadaceae (c) and Spingomonadaceae (s).

References

- Agbowuro AA, Huston WM, Gamble AB, Tyndall JD (2018) Proteases and protease inhibitors in infectious diseases. *Medicinal Research Reviews* 38:1295-1331
- Agostini S, Suzuki Y, Higuchi T, Casareto B, Yoshinaga K, Nakano Y, Fujimura H (2012) Biological and chemical characteristics of the coral gastric cavity. *Coral Reefs* 31:147-156
- Ainsworth TD, Gates RD (2016) Corals' microbial sentinels. *Science* 352:1518-1519
- Ainsworth TD, Thurber RV, Gates RD (2010) The future of coral reefs: a microbial perspective. *Trends in Ecology & Evolution* 25:233-240
- Ainsworth T, Fine M, Blackall L, Hoegh-Guldberg O (2006) Fluorescence in situ hybridization and spectral imaging of coral-associated bacterial communities. *Applied and Environmental Microbiology* 72:3016-3020
- Ainsworth TD, Krause L, Bridge T, Torda G, Raina J-B, Zakrzewski M, Gates RD, Padilla-Gamiño JL, Spalding HL, Smith C (2015) The coral core microbiome identifies rare bacterial taxa as ubiquitous endosymbionts. *The ISME Journal* 9:2261-2274
- Alino PM, Coll JC (1989) Observations of the synchronized mass spawning and post settlement activity of octocorals on the Great Barrier Reef, Australia: biological aspects. *Bulletin of Marine Science* 45:697-707
- Altschul SF, Gish W, Miller W, Myers EW, Lipman DJ (1990) Basic local alignment search tool. *Journal of molecular biology* 215:403-410
- Andrä J, Jakovkin I, Grötzinger J, Hecht O, Krasnosdembskaya AD, Goldmann T, Gutschmann T, Leippe M (2008) Structure and mode of action of the antimicrobial peptide arenicin. *Biochemical Journal* 410:113-122
- Andrade Rodríguez NA (2018) Non-contact competition between soft and hard corals: a transcriptomic perspective. James Cook University,
- Anjay A (2012) national center for Biotechnology information (ncBi). Bethesda, Maryland, USA
- Apprill A, Weber LG, Santoro AE (2016) Distinguishing between Microbial Habitats Unravels Ecological Complexity in Coral Microbiomes. *mSystems* 1
- Apprill A, Marlow HQ, Martindale MQ, Rappé MS (2009) The onset of microbial associations in the coral *Pocillopora meandrina*. *The ISME Journal* 3:685-699
- Atencio LA, Dal Grande F, Young GO, Gavilán R, Guzmán HM, Schmitt I, Mejía LC, Gutiérrez M (2018) Antimicrobial-producing *Pseudoalteromonas* from the marine environment of Panama shows a high phylogenetic diversity and clonal structure. *Journal of Basic Microbiology* 58:747-769
- Augustin R, Bosch TC (2010) Cnidarian immunity: a tale of two barriers. *Invertebrate Immunity*:1-16

- Augustin R, Siebert S, Bosch TC (2009) Identification of a kazal-type serine protease inhibitor with potent anti-staphylococcal activity as part of Hydra's innate immune system. *Developmental & Comparative Immunology* 33:830-837
- Augustin R, Fraune S, Bosch TC (2010) How Hydra senses and destroys microbes. *Seminars in Immunology* 22:54-58
- Augustin R, Schröder K, Rincón APM, Fraune S, Anton-Erxleben F, Herbst E-M, Wittlieb J, Schwentner M, Grötzinger J, Wassenaar TM (2017) A secreted antibacterial neuropeptide shapes the microbiome of Hydra. *Nature Communications* 8:1-9
- Austin B, Austin DA, Austin B, Austin DA (2012) *Bacterial fish pathogens*. Springer
- Babcock R, Heyward A (1986) Larval development of certain gamete-spawning scleractinian corals. *Coral Reefs* 5:111-116
- Bartz J-O, Blom J, Busse H-J, Mvie JB, Hardt M, Schubert P, Wilke T, Goessmann A, Wilharm G, Bender J (2018) *Parendoziomonas haliclona* gen. nov. sp. nov. isolated from a marine sponge of the genus *Haliclona* and description of the family *Endoziomonadaceae* fam. nov. comprising the genera *Endoziomonas*, *Parendoziomonas*, and *Kistimonas*. *Systematic and Applied Microbiology* 41:73-84
- Bayer T, Arif C, Ferrier-Pagès C, Zoccola D, Aranda M, Voolstra CR (2013 b) Bacteria of the genus *Endoziomonas* dominate the microbiome of the Mediterranean gorgonian coral *Eunicella cavolini*. *Marine Ecology Progress Series* 479:75-84
- Bayer T, Neave MJ, Alsheikh-Hussain A, Aranda M, Yum LK, Mincer T, Hughen K, Apprill A, Voolstra CR (2013) The microbiome of the Red Sea coral *Stylophora pistillata* is dominated by tissue-associated *Endoziomonas* bacteria. *Applied and Environmental Microbiology* 79:4759-4762
- Benson DA, Cavanaugh M, Clark K, Karsch-Mizrachi I, Lipman DJ, Ostell J, Sayers EW (2012) GenBank. *Nucleic Acids Research* 41:D36-D42
- Berg G, Rybakova D, Fischer D, Cernava T, Vergès M-CC, Charles T, Chen X, Cocolin L, Eversole K, Corral GH (2020) Microbiome definition re-visited: old concepts and new challenges. *Microbiome* 8:1-22
- Beurmann S, Ushijima B, Svoboda CM, Videau P, Smith AM, Donachie SP, Aeby GS, Callahan SM (2017) *Pseudoalteromonas piratica* sp. nov., a budding, prosthecate bacterium from diseased *Montipora capitata*, and emended description of the genus *Pseudoalteromonas*. *International Journal of Systematic and Evolutionary Microbiology* 67:2683-2688
- Bevins CL, Salzman NH (2011) The potter's wheel: the host's role in sculpting its microbiota. *Cellular and Molecular Life Sciences* 68:3675-3685

- Bharathi S, Nithya B, Saravanan D, Radhakrishnan M, Balagurunathan R (2013) In-vitro antibacterial activity of coral reef associated bacteria and optimization of bioactive metabolite production. *In-vitro* 3
- Blackall LL, Wilson B, van Oppen MJ (2015) Coral—the world's most diverse symbiotic ecosystem. *Molecular Ecology* 24:5330-5347
- Blackall LL, Dungan AM, Hartman LM, van Oppen MJ (2020) Probiotics for corals. *Microbiology Australia* 41:100-104
- Bolyen E, Rideout JR, Dillon MR, Bokulich NA, Abnet CC, Al-Ghalith GA, Alexander H, Alm EJ, Arumugam M, Asnicar F (2019) Reproducible, interactive, scalable and extensible microbiome data science using QIIME 2. *Nature Biotechnology* 37:852-857
- Bosch TC (2012) Understanding complex host-microbe interactions in Hydra. *Gut Microbes* 3:345-351
- Bosch TC (2013) Cnidarian-microbe interactions and the origin of innate immunity in metazoans. *Annual Review of Microbiology* 67:499-518
- Bosch TC (2014) Rethinking the role of immunity: lessons from Hydra. *Trends in Immunology* 35:495-502
- Bosch TC, McFall-Ngai MJ (2011) Metaorganisms as the new frontier. *Zoology* 114:185-190
- Bosch TC, Rosenstiel P (2016) The innate immune system in cnidarians. *Diseases of Coral*:125
- Bosch TC, Augustin R, Anton-Erxleben F, Fraune S, Hemmrich G, Zill H, Rosenstiel P, Jacobs G, Schreiber S, Leippe M (2009) Uncovering the evolutionary history of innate immunity: the simple metazoan Hydra uses epithelial cells for host defence. *Developmental & Comparative Immunology* 33:559-569
- Bourne DG, Munn CB (2005) Diversity of bacteria associated with the coral *Pocillopora damicornis* from the Great Barrier Reef. *Environmental Microbiology* 7:1162-1174
- Bourne DG, Morrow KM, Webster NS (2016) Insights into the coral microbiome: underpinning the health and resilience of reef ecosystems. *Annual Review of Microbiology* 70:317-340
- Bourne DG, Garren M, Work TM, Rosenberg E, Smith GW, Harvell CD (2009) Microbial disease and the coral holobiont. *Trends in Microbiology* 17:554-562
- Brandt ME, McManus JW (2009) Disease incidence is related to bleaching extent in reef-building corals. *Ecology* 90:2859-2867
- Brogden KA (2005) Antimicrobial peptides: pore formers or metabolic inhibitors in bacteria? *Nature Reviews Microbiology* 3:238-250

- Brück TB, Brück WM, Santiago-Vázquez LZ, McCarthy PJ, Kerr RG (2007) Diversity of the bacterial communities associated with the azooxanthellate deep water octocorals *Leptogorgia minimata*, *Iciligorgia schrammi*, and *Swiftia exertia*. *Marine Biotechnology* 9:561-576
- Brune A, Ohkuma M (2010) Role of the termite gut microbiota in symbiotic digestion *Biology of termites: a modern synthesis*. Springer, pp439-475
- Burge CA, Mouchka ME, Harvell CD, Roberts S (2013) Immune response of the Caribbean sea fan, *Gorgonia ventalina*, exposed to an *Aplanochytrium* parasite as revealed by transcriptome sequencing. *Frontiers in Physiology* 4:180
- Callahan BJ, McMurdie PJ, Rosen MJ, Han AW, Johnson AJ, Holmes SP (2016) DADA2: High-resolution sample inference from Illumina amplicon data. *Nature Methods* 13:581-583
- Carlos C, Torres TT, Ottoboni LM (2013) Bacterial communities and species-specific associations with the mucus of Brazilian coral species. *Scientific Reports* 3:1624
- Ceh J, van Keulen M, Bourne DG (2013) Intergenerational transfer of specific bacteria in corals and possible implications for offspring fitness. *Microbial Ecology* 65:227-231
- Ceh J, Kilburn MR, Cliff JB, Raina JB, van Keulen M, Bourne DG (2013 b) Nutrient cycling in early coral life stages: *Pocillopora damicornis* larvae provide their algal symbiont (Symbiodinium) with nitrogen acquired from bacterial associates. *Ecology and Evolution* 3:2393-2400
- Chalker BE, Dunlap WC (1981) Extraction and quantitation of endosymbiotic algal pigments from reef-building corals. *Proceedings of the 4th International Coral Reef Symposium* 2:47-50
- Charif D, Lobry JR (2007) SeqinR 1.0-2: a contributed package to the R project for statistical computing devoted to biological sequences retrieval and analysis *Structural Approaches to Sequence Evolution*. Springer, pp207-232
- Charpy L, Casareto B, Langlade M-J, Suzuki Y (2012) Cyanobacteria in coral reef ecosystems: a review. *Journal of Marine Biology* 2012
- Chen W-M, Moulin L, Bontemps C, Vandamme P, Béna G, Boivin-Masson C (2003) Legume symbiotic nitrogen fixation by β -proteobacteria is widespread in nature. *Journal of Bacteriology* 185:7266-7272
- Cheng S-Y, Wen Z-H, Chiou S-F, Hsu C-H, Wang S-K, Dai C-F, Chiang MY, Duh C-Y (2008) Durumolides A-E, anti-inflammatory and antibacterial cembranolides from the soft coral *Lobophytum durum*. *Tetrahedron* 64:9698-9704
- Chera S, De Rosa R, Miljkovic-Licina M, Dobretz K, Ghila L, Kaloulis K, Galliot B (2006) Silencing of the hydra serine protease inhibitor *Kazal1* gene mimics the human SPINK1 pancreatic phenotype. *Journal of Cell Science* 119:846-857

- Cho JC, Hedlund BP (2015) Lentisphaeraceae fam. nov. *Bergey's Manual of Systematics of Archaea and Bacteria*:1-1
- Chu ND, Vollmer SV (2016) Caribbean corals house shared and host-specific microbial symbionts over time and space. *Environmental Microbiology Reports* 8:493-500
- Claar DC, McDevitt-Irwin JM, Garren M, Vega Thurber R, Gates RD, Baum JK (2020) Increased diversity and concordant shifts in community structure of coral-associated Symbiodiniaceae and bacteria subjected to chronic human disturbance. *Molecular Ecology* 29:2477-2491
- Clark K, Karsch-Mizrachi I, Lipman DJ, Ostell J, Sayers EW (2015) GenBank. *Nucleic Acids Research* 44:D67-D72
- Clarke G, O'Mahony S, Dinan T, Cryan J (2014) Priming for health: gut microbiota acquired in early life regulates physiology, brain and behaviour. *Acta Paediatrica* 103:812-819
- Correa H, Haltli B, Duque C, Kerr R (2013) Bacterial communities of the gorgonian octocoral *Pseudopterogorgia elisabethae*. *Microbial Ecology* 66:972-985
- D'Angelo C, Wiedenmann J (2014) Impacts of nutrient enrichment on coral reefs: new perspectives and implications for coastal management and reef survival. *Current Opinion in Environmental Sustainability* 7:82-93
- Damjanovic K, Blackall LL, Menéndez P, van Oppen MJ (2020 a) Bacterial and algal symbiont dynamics in early recruits exposed to two adult coral species. *Coral Reefs* 39:189-202
- Damjanovic K, Menéndez P, Blackall LL, van Oppen MJ (2020 b) Early life stages of a common broadcast spawning coral associate with specific bacterial communities despite lack of internalized bacteria. *Microbial Ecology* 79:706-719
- Damjanovic K, Menéndez P, Blackall LL, van Oppen MJ (2020 c) Mixed-mode bacterial transmission in the common brooding coral *Pocillopora acuta*. *Environmental Microbiology* 22:397-412
- De Castro AP, Araújo SD, Reis AM, Moura RL, Francini-Filho RB, Pappas G, Rodrigues TB, Thompson FL, Krüger RH (2010) Bacterial community associated with healthy and diseased reef coral *Mussismilia hispida* from eastern Brazil. *Microbial Ecology* 59:658-667
- Deines P, Hammerschmidt K, Bosch TC (2020) Microbial species coexistence depends on the host environment. *MBio* 11:e00807-00820
- Destoumieux-Garzón D, Rosa RD, Schmitt P, Barreto C, Vidal-Dupiol J, Mitta G, Gueguen Y, Bachere E (2016) Antimicrobial peptides in marine invertebrate health and disease. *Philosophical Transactions of the Royal Society B: Biological Sciences* 371:20150300
- Ding J-Y, Shiu J-H, Chen W-M, Chiang Y-R, Tang S-L (2016) Genomic insight into the host–endosymbiont relationship of *Endozoicomonas montiporae* CL-33T with its Coral Host. *Frontiers in Microbiology* 7:251

Dinsdale EA, Pantos O, Smriga S, Edwards RA, Angly F, Wegley L, Hatay M, Hall D, Brown E, Haynes M (2008) Microbial ecology of four coral atolls in the Northern Line Islands. *PLOS One* 3:e1584

Ducklow HW, Mitchell R (1979) Bacterial populations and adaptations in the mucus layers on living corals 1. *Limnology and Oceanography* 24:715-725

Edgar RC (2004) MUSCLE: multiple sequence alignment with high accuracy and high throughput. *Nucleic acids research* 32:1792-1797

Edmunds PJ, Gates RD, Leggat W, Hoegh-Guldberg O, Allen-Requa L (2005) The effect of temperature on the size and population density of dinoflagellates in larvae of the reef coral *Porites astreoides*. *Invertebrate Biology* 124:185-193

Engelen AH, Aires T, Vermeij MJ, Herndl GJ, Serrao EA, Frade PR (2018) Host differentiation and compartmentalization of microbial communities in the azooxanthellate cupcorals *Tubastrea coccinea* and *Rhizopsammia goesi* in the Caribbean. *Frontiers in Marine Science* 5:391

Epstein HE, Kingsford MJ (2019) Are soft coral habitats unfavourable? A closer look at the association between reef fishes and their habitat. *Environmental Biology of Fishes* 102:479-497

Epstein HE, Smith HA, Torda G, van Oppen MJ (2019) Microbiome engineering: enhancing climate resilience in corals. *Frontiers in Ecology and the Environment* 17:100-108

Fabricius K, Alderslade P (2001) Soft corals and sea fans: a comprehensive guide to the tropical shallow water genera of the central-west Pacific, the Indian Ocean and the Red Sea. Australian Institute of Marine Science

Fan T-Y, Chou Y-H, Dai C-F (2005) Sexual reproduction of the alcyonacean coral *Lobophytum pauciflorum* in southern Taiwan. *Bulletin of Marine Science* 76:143-154

Fang Z, Martin J, Wang Z (2012) Statistical methods for identifying differentially expressed genes in RNA-Seq experiments. *Cell & Bioscience* 2:1-8

Fernando SC, Wang J, Sparling K, Garcia GD, Francini-Filho RB, de Moura RL, Paranhos R, Thompson FL, Thompson JR (2015) Microbiota of the major South Atlantic reef building coral *Mussismilia*. *Microbial Ecology* 69:267-280

Fine M, Loya Y (2002) Endolithic algae: an alternative source of photoassimilates during coral bleaching. *Proceedings of the Royal Society of London, Series B: Biological sciences* 269:1205-1210

Fingerhut LC, Miller DJ, Strugnell JM, Daly NL, Cooke IR (2020) ampir: an R package for fast genome-wide prediction of antimicrobial peptides. *Bioinformatics*

Finn RD, Bateman A, Clements J, Coggill P, Eberhardt RY, Eddy SR, Heger A, Hetherington K, Holm L, Mistry J (2014) Pfam: the protein families database. *Nucleic Acids Research* 42:D222-D230

- Frade PR, Roll K, Bergauer K, Herndl GJ (2016) Archaeal and bacterial communities associated with the surface mucus of Caribbean corals differ in their degree of host specificity and community turnover over reefs. *PLOS One* 11:e0144702
- Franzenburg S, Fraune S, Altmann PM, Künzel S, Baines JF, Traulsen A, Bosch TC (2013) Bacterial colonization of Hydra hatchlings follows a robust temporal pattern. *The ISME Journal* 7:781-790
- Franzenburg S, Walter J, Künzel S, Wang J, Baines JF, Bosch TC, Fraune S (2013 b) Distinct antimicrobial peptide expression determines host species-specific bacterial associations. *Proceedings of the National Academy of Sciences* 110:E3730-E3738
- Fraune S, Bosch TC (2007) Long-term maintenance of species-specific bacterial microbiota in the basal metazoan Hydra. *Proceedings of the National Academy of Sciences* 104:13146-13151
- Fraune S, Bosch TC (2010) Why bacteria matter in animal development and evolution. *Bioessays* 32:571-580
- Fraune S, Augustin R, Bosch TC (2011) Embryo protection in contemporary immunology: Why bacteria matter. *Communicative & Integrative Biology* 4:369-372
- Fraune S, Anton-Erxleben F, Augustin R, Franzenburg S, Knop M, Schröder K, Willoweit-Ohl D, Bosch TC (2015) Bacteria–bacteria interactions within the microbiota of the ancestral metazoan Hydra contribute to fungal resistance. *The ISME Journal* 9:1543-1556
- Frazão B, Vasconcelos V, Antunes A (2012) Sea anemone (Cnidaria, Anthozoa, Actiniaria) toxins: an overview. *Marine Drugs* 10:1812-1851
- Freire I, Gutner-Hoch E, Muras A, Benayahu Y, Otero A (2019) The effect of bacteria on planula-larvae settlement and metamorphosis in the octocoral *Rhytisma fulvum fulvum*. *PLOS One* 14:e0223214
- Fu P, Kong F, Wang Y, Wang Y, Liu P, Zuo G, Zhu W (2013) Antibiotic Metabolites from the Coral-Associated Actinomycete *Streptomyces* sp. OUCMDZ-1703. *Chinese Journal of Chemistry* 31:100-104
- Fujiwara S, Imai J, Fujiwara M, Yaeshima T, Kawashima T, Kobayashi K (1990) A potent antibacterial protein in royal jelly. Purification and determination of the primary structure of royalisin. *Journal of Biological Chemistry* 265:11333-11337
- Futschik M, Futschik MM, TimeCourse P (2016) Package ‘Mfuzz’
- Galkiewicz JP, Kellogg CA (2008) Cross-kingdom amplification using bacteria-specific primers: complications for studies of coral microbial ecology. *Applied and Environmental Microbiology* 74:7828-7831

- Ganz T (2003) Defensins: antimicrobial peptides of innate immunity. *Nature reviews immunology* 3:710-720
- Geffen Y, Rosenberg E (2005) Stress-induced rapid release of antibacterials by scleractinian corals. *Marine Biology* 146:931-935
- Gignoux-Wolfsohn S, Vollmer SV, Aronson FM (2016) Temporal Sampling of White Band Disease Infected Corals Reveals Complex and Dynamic Bacterial Communities. *AGUOS 2016:ME44C-0869*
- Gilbert SF, Sapp J, Tauber AI (2012) A symbiotic view of life: we have never been individuals. *The Quarterly Review of Biology* 87:325-341
- Glasl B, Herndl GJ, Frade PR (2016) The microbiome of coral surface mucus has a key role in mediating holobiont health and survival upon disturbance. *The ISME Journal* 10:2280-2292
- Gochfeld DJ, Aeby GS (2008) Antibacterial chemical defenses in Hawaiian corals provide possible protection from disease. *Marine Ecology Progress Series* 362:119-128
- Golberg K, Pavlov V, Marks RS, Kushmaro A (2013) Coral-associated bacteria, quorum sensing disrupters, and the regulation of biofouling. *Biofouling* 29:669-682
- Golberg K, Eltzov E, Shnit-Orland M, Marks RS, Kushmaro A (2011) Characterization of quorum sensing signals in coral-associated bacteria. *Microbial Ecology* 61:783-792
- Golubic S, Radtke G, Le Campion-Alsumard T (2005) Endolithic fungi in marine ecosystems. *Trends in Microbiology* 13:229-235
- Gomila M, Bowien B, Falsen E, Moore ER, Lalucat J (2007) Description of *Pelomonas aquatica* sp. nov. and *Pelomonas puraquae* sp. nov., isolated from industrial and haemodialysis water. *International Journal of Systematic and Evolutionary Microbiology* 57:2629-2635
- Grabherr MG, Haas BJ, Yassour M, Levin JZ, Thompson DA, Amit I, Adiconis X, Fan L, Raychowdhury R, Zeng Q (2011) Full-length transcriptome assembly from RNA-Seq data without a reference genome. *Nature Biotechnology* 29:644-652
- Gray MA, Stone RP, McLaughlin MR, Kellogg CA (2011) Microbial consortia of gorgonian corals from the Aleutian islands. *FEMS Microbiology Ecology* 76:109-120
- Guindon S, Dufayard J-F, Lefort V, Anisimova M, Hordijk W, Gascuel O (2010) New algorithms and methods to estimate maximum-likelihood phylogenies: assessing the performance of PhyML 3.0. *Systematic Biology* 59:307-321
- Gutner-Hoch E, Fine M (2011) Genotypic diversity and distribution of *Ostreobium quekettii* within scleractinian corals. *Coral Reefs* 30:643-650

- Haas BJ, Papanicolaou A, Yassour M, Grabherr M, Blood PD, Bowden J, Couger MB, Eccles D, Li B, Lieber M (2013) De novo transcript sequence reconstruction from RNA-seq using the Trinity platform for reference generation and analysis. *Nature Protocols* 8:1494-1512
- Harder T, Lau SC, Dobretsov S, Fang TK, Qian P-Y (2003) A distinctive epibiotic bacterial community on the soft coral *Dendronephthya* sp. and antibacterial activity of coral tissue extracts suggest a chemical mechanism against bacterial epibiosis. *FEMS Microbiology Ecology* 43:337-347
- Harrison PL, Babcock RC, Bull GD, Oliver JK, Wallace CC, Willis BL (1984) Mass spawning in tropical reef corals. *Science* 223:1186-1189
- Harrison HB, Álvarez-Noriega M, Baird AH, Heron SF, MacDonald C, Hughes TP (2019) Back-to-back coral bleaching events on isolated atolls in the Coral Sea. *Coral Reefs* 38:713-719
- Hartmann AC, Baird AH, Knowlton N, Huang D (2017) The paradox of environmental symbiont acquisition in obligate mutualisms. *Current Biology* 27:3711-3716. e3713
- Hasegawa M, Kishino H, Yano T-a (1985) Dating of the human-ape splitting by a molecular clock of mitochondrial DNA. *Journal of Molecular Evolution* 22:160-174
- Hattori M, Taylor TD (2009) The human intestinal microbiome: a new frontier of human biology. *DNA Research* 16:1-12
- Heijtz RD (2016) Fetal, neonatal, and infant microbiome: perturbations and subsequent effects on brain development and behavior. *Seminars in Fetal and Neonatal Medicine* 21:410-417
- Hernandez-Agreda A, Gates RD, Ainsworth TD (2017) Defining the core microbiome in corals' microbial soup. *Trends in Microbiology* 25:125-140
- Hoegh-Guldberg O, Mumby PJ, Hooten AJ, Steneck RS, Greenfield P, Gomez E, Harvell CD, Sale PF, Edwards AJ, Caldeira K (2007) Coral reefs under rapid climate change and ocean acidification. *Science* 318:1737-1742
- Holm JB, Heidelberg KB (2016) Microbiomes of *Muricea californica* and *M. fruticosa*: comparative analyses of two co-occurring eastern Pacific octocorals. *Frontiers in Microbiology* 7:917
- Huang Q, Cheng W, Long H, Liu H, van Ofwegen L, Lin W (2015) Subergane-Type Sesquiterpenes from Gorgonian Coral *Subergorgia suberosa* with Antibacterial Activities. *Helvetica Chimica Acta* 98:1202-1209
- Huelsenbeck JP, Ronquist F, Nielsen R, Bollback JP (2001) Bayesian inference of phylogeny and its impact on evolutionary biology. *Science* 294:2310-2314
- Hughes TP, Kerry JT, Baird AH, Connolly SR, Dietzel A, Eakin CM, Heron SF, Hoey AS, Hoogenboom MO, Liu G (2018) Global warming transforms coral reef assemblages. *Nature* 556:492-496

- Hunt LR, Smith SM, Downum KR, Mydlarz LD (2012) Microbial regulation in gorgonian corals. *Marine Drugs* 10:1225-1243
- Ibrahim HA, Mohamed SZ, El-Regal MA, Farhat AZ (2012) Antibacterial activity of some Red Sea soft corals, Egypt. *Blue Biotechnology Journal* 1:497
- Jari Oksanen F, Friendly M, Kindt R, Legendre P, McGlenn D, Minchin PR, O'Hara R, Simpson GL, Solymos P, Stevens MHH (2018) *Vegan: community ecology package*. R Package Version 2
- Jensen S, Hovland M, Lynch MD, Bourne DG (2019) Diversity of deep-water coral-associated bacteria and comparison across depth gradients. *FEMS Microbiology Ecology* 95:fiz091
- Jin Q-w, Hu Y-h, Sun L (2018) *Alteromonas oceani* sp. nov., isolated from deep-sea sediment of a hydrothermal field. *International Journal of Systematic and Evolutionary Microbiology* 68:657-662
- Jung S, Dingley AJ, Augustin R, Anton-Erxleben F, Stanisak M, Gelhaus C, Gutschmann T, Hammer MU, Podschun R, Bonvin AM (2009) Hydramacin-1, structure and antibacterial activity of a protein from the basal metazoan Hydra. *Journal of Biological Chemistry* 284:1896-1905
- Kalyaanamoorthy S, Minh BQ, Wong TK, von Haeseler A, Jermiin LS (2017) ModelFinder: fast model selection for accurate phylogenetic estimates. *Nature Methods* 14:587-589
- Kellogg CA (2004) Tropical Archaea: diversity associated with the surface microlayer of corals. *Marine Ecology Progress Series* 273:81-88
- Kellogg CA (2008) Microbial ecology of *Lophelia pertusa* in the Northern Gulf of Mexico. Characterization of Northern Gulf of Mexico Deepwater Hard Bottom Communities with Emphasis on *Lophelia* Coral–*Lophelia* Reef Megafaunal Community Structure, Biotopes, Genetics, Microbial Ecology, and Geology (2004–2006): USGS Open-File Report 1148:2008-2015
- Kellogg CA (2019) Microbiomes of stony and soft deep-sea corals share rare core bacteria. *Microbiome* 7:90
- Kellogg CA, Ross SW, Brooke SD (2016) Bacterial community diversity of the deep-sea octocoral *Paramuricea placomus*. *PeerJ* 4:e2529
- Kelman D, Kushmaro A, Loya Y, Kashman Y, Benayahu Y (1998) Antimicrobial activity of a Red Sea soft coral, *Parerythropodium fulvum fulvum*: reproductive and developmental considerations. *Marine Ecology Progress Series* 169:87-95
- Kelman D, Kashman Y, Hill RT, Rosenberg E, Loya Y (2009) Chemical warfare in the sea: The search for antibiotics from Red Sea corals and sponges. *Pure and Applied Chemistry* 81:1113-1121

- Kimes NE, Johnson WR, Torralba M, Nelson KE, Weil E, Morris PJ (2013) The *Montastraea faveolata* microbiome: ecological and temporal influences on a Caribbean reef-building coral in decline. *Environmental Microbiology* 15:2082-2094
- Kimura M (1980) A simple method for estimating evolutionary rates of base substitutions through comparative studies of nucleotide sequences. *Journal of Molecular Evolution* 16:111-120
- Klaus JS, Janse I, Heikoop JM, Sanford RA, Fouke BW (2007) Coral microbial communities, zooxanthellae and mucus along gradients of seawater depth and coastal pollution. *Environmental Microbiology* 9:1291-1305
- Klindworth A, Pruesse E, Schweer T, Peplies J, Quast C, Horn M, Glöckner FO (2013) Evaluation of general 16S ribosomal RNA gene PCR primers for classical and next-generation sequencing-based diversity studies. *Nucleic Acids Research* 41:e1-e1
- Knowlton N, Rohwer F (2003) Multispecies microbial mutualisms on coral reefs: the host as a habitat. *The American Naturalist* 162:S51-S62
- Koren O, Rosenberg E (2006) Bacteria associated with mucus and tissues of the coral *Oculina patagonica* in summer and winter. *Applied and Environmental Microbiology* 72:5254-5259
- Kushmaro A, Rosenberg E, Fine M, Loya Y (1997) Bleaching of the coral *Oculina patagonica* by *Vibrio* AK-1. *Marine Ecology Progress Series* 147:159-165
- Kvennefors ECE, Sampayo E, Ridgway T, Barnes AC, Hoegh-Guldberg O (2010) Bacterial communities of two ubiquitous Great Barrier Reef corals reveals both site- and species-specificity of common bacterial associates. *PLOS One* 5:e10401
- Kvennefors ECE, Sampayo E, Kerr C, Vieira G, Roff G, Barnes AC (2012) Regulation of bacterial communities through antimicrobial activity by the coral holobiont. *Microbial Ecology* 63:605-618
- La Riviere M, Garrabou J, Bally M (2015) Evidence for host specificity among dominant bacterial symbionts in temperate gorgonian corals. *Coral Reefs* 34:1087-1098
- LaJeunesse TC, Parkinson JE, Gabrielson PW, Jeong HJ, Reimer JD, Voolstra CR, Santos SR (2018) Systematic revision of Symbiodiniaceae highlights the antiquity and diversity of coral endosymbionts. *Current Biology* 28:2570-2580. e2576
- Lau SC, Tsoi MM, Li X, Dobretsov S, Plakhotnikova Y, Wong P-K, Qian P-Y (2005) *Pseudoalteromonas spongiae* sp. nov., a novel member of the γ -Proteobacteria isolated from the sponge *Mycale adhaerens* in Hong Kong waters. *International Journal of Systematic and Evolutionary Microbiology* 55:1593-1596

- Lawler SN, Kellogg CA, France SC, Clostio RW, Brooke SD, Ross SW (2016) Coral-associated bacterial diversity is conserved across two deep-sea *Anthothela* species. *Frontiers in Microbiology* 7:458
- Ledoux J-B, Antunes A (2018) Beyond the beaten path: improving natural products bioprospecting using an eco-evolutionary framework—the case of the octocorals. *Critical Reviews in Biotechnology* 38:184-198
- Lee W-J, Hase K (2014) Gut microbiota-generated metabolites in animal health and disease. *Nature Chemical Biology* 10:416-424
- Lee OO, Yang J, Bougouffa S, Wang Y, Batang Z, Tian R, Al-Suwailem A, Qian P-Y (2012) Spatial and species variations in bacterial communities associated with corals from the Red Sea as revealed by pyrosequencing. *Applied and Environmental Microbiology* 78:7173-7184
- Lehnert EM, Burriesci MS, Pringle JR (2012) Developing the anemone *Aiptasia* as a tractable model for cnidarian-dinoflagellate symbiosis: the transcriptome of aposymbiotic *A. pallida*. *BMC genomics* 13:1-10
- Leite DC, Leão P, Garrido AG, Lins U, Santos HF, Pires DO, Castro CB, van Elsas JD, Zilberberg C, Rosado AS (2017) Broadcast spawning coral *Mussismilia hispida* can vertically transfer its associated bacterial core. *Frontiers in Microbiology* 8:176
- Lema KA, Bourne DG, Willis BL (2014) Onset and establishment of diazotrophs and other bacterial associates in the early life history stages of the coral *Acropora millepora*. *Molecular Ecology* 23:4682-4695
- Leonelli S, Ankeny RA (2013) What makes a model organism? *Endeavour* 37:209-212
- Lesser MP, Falcón LI, Rodríguez-Román A, Enríquez S, Hoegh-Guldberg O, Iglesias-Prieto R (2007) Nitrogen fixation by symbiotic cyanobacteria provides a source of nitrogen for the scleractinian coral *Montastraea cavernosa*. *Marine Ecology Progress Series* 346:143-152
- Ley RE, Lozupone CA, Hamady M, Knight R, Gordon JI (2008) Worlds within worlds: evolution of the vertebrate gut microbiota. *Nature Reviews Microbiology* 6:776-788
- Ley RE, Hamady M, Lozupone C, Turnbaugh PJ, Ramey RR, Bircher JS, Schlegel ML, Tucker TA, Schrenzel MD, Knight R (2008) Evolution of mammals and their gut microbes. *Science* 320:1647-1651
- Li B, Dewey CN (2011) RSEM: accurate transcript quantification from RNA-Seq data with or without a reference genome. *BMC Bioinformatics* 12:1-16
- Li J, Zhong M, Lei X, Xiao S, Li Z (2014) Diversity and antibacterial activities of culturable fungi associated with coral *Porites pukoensis*. *World Journal of Microbiology and Biotechnology* 30:2551-2558

- Li J, Chen Q, Zhang S, Huang H, Yang J, Tian X-P, Long L-J (2013) Highly heterogeneous bacterial communities associated with the South China Sea reef corals *Porites lutea*, *Galaxea fascicularis* and *Acropora millepora*. *PLOS One* 8:e71301
- Lilburn T, Kim K, Ostrom N, Byzek K, Leadbetter J, Breznak J (2001) Nitrogen fixation by symbiotic and free-living spirochetes. *Science* 292:2495-2498
- Littman R, Willis BL, Bourne DG (2011) Metagenomic analysis of the coral holobiont during a natural bleaching event on the Great Barrier Reef. *Environmental Microbiology Reports* 3:651-660
- Littman RA, Willis BL, Pfeffer C, Bourne DG (2009) Diversities of coral-associated bacteria differ with location, but not species, for three acroporid corals on the Great Barrier Reef. *FEMS Microbiology Ecology* 68:152-163
- Liu L, Salam N, Jiao J-Y, Shun-Mei E, Chen C, Fang B-Z, Xiao M, Li M, Li W-J, Qu P-H (2017) *Cysteiniphilum litorale* gen. nov., sp. nov., isolated from coastal seawater. *International Journal of Systematic and Evolutionary Microbiology* 67:2178-2183
- Loya Y, Sakai K, Yamazato K, Nakano Y, Sambali H, Van Woesik R (2001) Coral bleaching: the winners and the losers. *Ecology letters* 4:122-131
- Lozupone CA, Knight R (2008) Species divergence and the measurement of microbial diversity. *FEMS Microbiology Reviews* 32:557-578
- Machado LR, Ottolini B (2015) An evolutionary history of defensins: a role for copy number variation in maximizing host innate and adaptive immune responses. *Frontiers in Immunology* 6:115
- Mason B, Cooke I, Moya A, Augustin R, Lin M-F, Satoh N, Bosch T, Bourne D, Hayward D, Andrade N (2021) AmAMP1 from *Acropora millepora* and damicornin define a family of coral-specific antimicrobial peptides related to the Shk toxins of sea anemones. *Developmental & Comparative Immunology* 114:103866
- Massé A, Domart-Coulon I, Golubic S, Duché D, Tribollet A (2018) Early skeletal colonization of the coral holobiont by the microboring Ulvophyceae *Ostreobium* sp. *Scientific Reports* 8:1-11
- Massé A, Tribollet A, Meziane T, Bourguet-Kondracki ML, Yéprémian C, Sève C, Thiney N, Longeon A, Couté A, Domart-Coulon I (2020) Functional diversity of microboring *Ostreobium* algae isolated from corals. *Environmental Microbiology* 22:4825-4846
- McDevitt-Irwin JM, Baum JK, Garren M, Vega Thurber RL (2017) Responses of coral-associated bacterial communities to local and global stressors. *Frontiers in Marine Science* 4:262
- McFall-Ngai M, Hadfield MG, Bosch TC, Carey HV, Domazet-Lošo T, Douglas AE, Dubilier N, Eberl G, Fukami T, Gilbert SF (2013) Animals in a bacterial world, a new imperative for the life sciences. *Proceedings of the National Academy of Sciences* 110:3229-3236

- McKnight DT, Huerlimann R, Bower DS, Schwarzkopf L, Alford RA, Zenger KR (2019) Methods for normalizing microbiome data: an ecological perspective. *Methods in Ecology and Evolution* 10:389-400
- Medina M, Sachs J (2010) Symbiont genomics, our new tangled bank. *Genomics* 95:129-137
- Meistertzheim A-L, Lartaud F, Arnaud-Haond S, Kalenitchenko D, Bessalam M, Le Bris N, Galand PE (2016) Patterns of bacteria-host associations suggest different ecological strategies between two reef building cold-water coral species. *Deep Sea Research Part I: Oceanographic Research Papers* 114:12-22
- Meyer JL, Castellanos-Gell J, Aeby GS, Häse CC, Ushijima B, Paul VJ (2019) Microbial community shifts associated with the ongoing stony coral tissue loss disease outbreak on the Florida Reef Tract. *Frontiers in Microbiology* 10:2244
- Michalek-Wagner K, Bourne D, Bowden B (2001) The effects of different strains of zooxanthellae on the secondary-metabolite chemistry and development of the soft-coral host *Lobophytum compactum*. *Marine Biology* 138:753-760
- Miller MB, Bassler BL (2001) Quorum sensing in bacteria. *Annual Review of Microbiology* 55:165-199
- Miller J, Muller E, Rogers C, Waara R, Atkinson A, Whelan K, Patterson M, Witcher B (2009) Coral disease following massive bleaching in 2005 causes 60% decline in coral cover on reefs in the US Virgin Islands. *Coral Reefs* 28:925
- Mohamed A, Cumbo V, Harii S, Shinzato C, Chan C, Ragan M, Bourne D, Willis B, Ball E, Satoh N (2016) The transcriptomic response of the coral *Acropora digitifera* to a competent *Symbiodinium* strain: the symbiosome as an arrested early phagosome. *Molecular Ecology* 25:3127-3141
- Morrow KM, Moss AG, Chadwick NE, Liles MR (2012) Bacterial associates of two Caribbean coral species reveal species-specific distribution and geographic variability. *Applied and Environmental Microbiology* 78:6438-6449
- Murillo Rincon A (2018) Modulation of neuronal activity by symbiotic bacteria in the early-branching metazoan Hydra.
- Murillo-Rincon AP, Klimovich A, Pemöller E, Taubenheim J, Mortzfeld B, Augustin R, Bosch TC (2017) Spontaneous body contractions are modulated by the microbiome of Hydra. *Scientific Reports* 7:1-9
- Muscatine L (1990) The role of symbiotic algae in carbon and energy flux in reef corals. *Coral Reefs* 25:75-87
- Muscatine L, R. McCloskey L, E. Marian R (1981) Estimating the daily contribution of carbon from zooxanthellae to coral animal respiration 1. *Limnology and Oceanography* 26:601-611

- Neave MJ, Michell CT, Apprill A, Voolstra CR (2014) Whole-genome sequences of three symbiotic *Endozoicomonas* strains. *Genome Announcements* 2
- Neave MJ, Apprill A, Ferrier-Pagès C, Voolstra CR (2016) Diversity and function of prevalent symbiotic marine bacteria in the genus *Endozoicomonas*. *Applied Microbiology and Biotechnology* 100:8315-8324
- Neave MJ, Michell CT, Apprill A, Voolstra CR (2017) *Endozoicomonas* genomes reveal functional adaptation and plasticity in bacterial strains symbiotically associated with diverse marine hosts. *Scientific Reports* 7:40579
- Neave MJ, Rachmawati R, Xun L, Michell CT, Bourne DG, Apprill A, Voolstra CR (2017) Differential specificity between closely related corals and abundant *Endozoicomonas* endosymbionts across global scales. *The ISME Journal* 11:186-200
- Neckelmann N, Muscatine L (1983) Regulatory mechanisms maintaining the Hydra-Chlorella symbiosis. *Proceedings of the Royal Society of London, Series B: Biological sciences* 219:193-210
- Neulinger SC, Stöhr R, Thiel V, Schmaljohann R, Imhoff JF (2010) New phylogenetic lineages of the Spirochaetes phylum associated with *Clathrina* species (Porifera). *The Journal of Microbiology* 48:411-418
- Nguyen L-T, Schmidt HA, Von Haeseler A, Minh BQ (2015) IQ-TREE: a fast and effective stochastic algorithm for estimating maximum-likelihood phylogenies. *Molecular Biology and Evolution* 32:268-274
- Nissimov J, Rosenberg E, Munn CB (2009) Antimicrobial properties of resident coral mucus bacteria of *Oculina patagonica*. *FEMS Microbiology Letters* 292:210-215
- Núñez-Pons L, Carbone M, Vázquez J, Gavagnin M, Avila C (2013) Lipophilic defenses from *Alcyonium* soft corals of Antarctica. *Journal of Chemical Ecology* 39:675-685
- O'Brien PA, Webster NS, Miller DJ, Bourne DG (2019) Host-microbe coevolution: applying evidence from model systems to complex marine invertebrate holobionts. *MBio* 10
- O'Brien PA, Tan S, Yang C, Frade PR, Andreakis N, Smith HA, Miller DJ, Webster NS, Zhang G, Bourne DG (2020) Diverse coral reef invertebrates exhibit patterns of phylosymbiosis. *The ISME Journal*:1-12
- O'Hara AM, Shanahan F (2006) The gut flora as a forgotten organ. *EMBO Reports* 7:688-693
- Oksanen J, Blanchet F, Friendly M, Kindt R, Legendre P, Mcglinn D, Minchin P, Hara R, Simpson G, Solymos P (2020) Package—vegan: Community Ecology Package. R package version 2.5-6
- Ovchinnikova TV, Balandin SV, Aleshina GM, Tagaev AA, Leonova YF, Krasnodembsky ED, Men'shenin AV, Kokryakov VN (2006) Aurelin, a novel antimicrobial peptide from jellyfish *Aurelia aurita*

- with structural features of defensins and channel-blocking toxins. *Biochemical and Biophysical Research Communications* 348:514-523
- Pantos O, Bongaerts P, Dennis PG, Tyson GW, Hoegh-Guldberg O (2015) Habitat-specific environmental conditions primarily control the microbiomes of the coral *Seriatopora hystrix*. *The ISME Journal* 9:1916-1927
- Paramasivam N, Ben-Dov E, Arotsker L, Kramarsky-Winter E, Zvuloni A, Loya Y, Kushmaro A (2013) Bacterial consortium of *Millepora dichotoma* exhibiting unusual multifocal lesion event in the Gulf of Eilat, Red Sea. *Microbial Ecology* 65:50-59
- Pasupuleti M, Schmidtchen A, Malmsten M (2012) Antimicrobial peptides: key components of the innate immune system. *Critical Reviews in Biotechnology* 32:143-171
- Peixoto RS, Sweet M, Bourne DG (2019) Customized medicine for corals. *Frontiers in Marine Science* 6:686
- Peixoto RS, Rosado PM, Leite DCdA, Rosado AS, Bourne DG (2017) Beneficial microorganisms for corals (BMC): proposed mechanisms for coral health and resilience. *Frontiers in Microbiology* 8:341
- Pendleton LH, Hoegh-Guldberg O, Langdon C, Comte A (2016) Multiple stressors and ecological complexity require a new approach to coral reef research. *Frontiers in Marine Science* 3:36
- Pernice M, Raina J-B, Rådecker N, Cárdenas A, Pogoreutz C, Voolstra CR (2020) Down to the bone: the role of overlooked endolithic microbiomes in reef coral health. *The ISME Journal* 14:325-334
- Pham TM, Wiese J, Wenzel-Storjohann A, Imhoff JF (2016) Diversity and antimicrobial potential of bacterial isolates associated with the soft coral *Alcyoniumdigitatum* from the Baltic Sea. *Antonie Van Leeuwenhoek* 109:105-119
- Pike RE, Haltli B, Kerr RG (2013) Description of *Endozoicomonas euniceicola* sp. nov. and *Endozoicomonas gorgoniicola* sp. nov., bacteria isolated from the octocorals *Eunicea fusca* and *Plexaura* sp., and an emended description of the genus *Endozoicomonas*. *International Journal of Systematic and Evolutionary Microbiology* 63:4294-4302
- Pogoreutz C, Rådecker N, Cárdenas A, Gärdes A, Wild C, Voolstra CR (2018) Dominance of. *Ecology and Evolution* 8:2240-2252
- Pollock FJ, McMinds R, Smith S, Bourne DG, Willis BL, Medina M, Thurber RV, Zaneveld JR (2018) Coral-associated bacteria demonstrate phylosymbiosis and cophylogeny. *Nature Communications* 9:1-13
- Pootakham W, Mhuantong W, Yoocha T, Puchim L, Sonthirod C, Naktang C, Thongtham N, Tangphatsornruang S (2017) High resolution profiling of coral-associated bacterial

- communities using full-length 16S rRNA sequence data from PacBio SMRT sequencing system. *Scientific Reports* 7:1-14
- Porter TM, Hajibabaei M (2018) Scaling up: A guide to high-throughput genomic approaches for biodiversity analysis. *Molecular Ecology* 27:313-338
- Quast C, Pruesse E, Yilmaz P, Gerken J, Schweer T, Yarza P, Peplies J, Glöckner FO (2012) The SILVA ribosomal RNA gene database project: improved data processing and web-based tools. *Nucleic Acids Research* 41:D590-D596
- Quast C, Pruesse E, Yilmaz P, Gerken J, Schweer T, Yarza P, Peplies J, Glöckner FO (2013) The SILVA ribosomal RNA gene database project: improved data processing and web-based tools. *Nucleic Acids Research* 41:D590-596
- Quintanilla E, Ramírez-Portilla C, Adu-Oppong B, Walljasper G, Glaeser SP, Wilke T, Muñoz AR, Sánchez JA (2018) Local confinement of disease-related microbiome facilitates recovery of gorgonian sea fans from necrotic-patch disease. *Scientific Reports* 8:1-11
- Rädecker N, Pogoreutz C, Voolstra CR, Wiedenmann J, Wild C (2015) Nitrogen cycling in corals: the key to understanding holobiont functioning? *Trends in Microbiology* 23:490-497
- Raina J-B, Tapiolas D, Willis BL, Bourne DG (2009) Coral-associated bacteria and their role in the biogeochemical cycling of sulfur. *Applied and Environmental Microbiology* 75:3492-3501
- Raina J-B, Tapiolas DM, Forêt S, Lutz A, Abrego D, Ceh J, Seneca FO, Clode PL, Bourne DG, Willis BL (2013) DMSP biosynthesis by an animal and its role in coral thermal stress response. *Nature* 502:677-680
- Ralebitso TK, Senior E, Van Verseveld HW (2002) Microbial aspects of atrazine degradation in natural environments. *Biodegradation* 13:11-19
- Ransome E (2013) The effects of environmental conditions on quorum sensing and community interactions in coral-associated bacteria
- Ransome E, Munn CB, Halliday N, Cámara M, Tait K (2014) Diverse profiles of N-acyl-homoserine lactone molecules found in cnidarians. *FEMS Microbiology Ecology* 87:315-329
- Rathje K, Mortzfeld B, Hoepfner MP, Taubenheim J, Bosch TC, Klimovich A (2020) Dynamic interactions within the host-associated microbiota cause tumor formation in the basal metazoan Hydra. *PLOS Pathogens* 16:e1008375
- Rees T, Bosch T, Douglas AE (2018) How the microbiome challenges our concept of self. *PLOS Biology* 16:e2005358
- Reshef L, Koren O, Loya Y, Zilber-Rosenberg I, Rosenberg E (2006) The coral probiotic hypothesis. *Environmental Microbiology* 8:2068-2073

- Richmond RH (1993) Coral reefs: present problems and future concerns resulting from anthropogenic disturbance. *American Zoologist* 33:524-536
- Rimphanitchayakit V, Tassanakajon A (2010) Structure and function of invertebrate Kazal-type serine proteinase inhibitors. *Developmental & Comparative Immunology* 34:377-386
- Ritchie KB (2006) Regulation of microbial populations by coral surface mucus and mucus-associated bacteria. *Marine Ecology Progress Series* 322:1-14
- Ritchie KB, Smith GW (2004) Microbial communities of coral surface mucopolysaccharide layers. *Coral Health and Disease*. Springer, pp259-264
- Robbins SJ, Singleton CM, Chan CX, Messer LF, Geers AU, Ying H, Baker A, Bell SC, Morrow KM, Ragan MA (2019) A genomic view of the reef-building coral *Porites lutea* and its microbial symbionts. *Nature Microbiology* 4:2090-2100
- Robertson V, Haltli B, McCauley EP, Overy DP, Kerr RG (2016) Highly variable bacterial communities associated with the octocoral *Antilloorgia elisabethae*. *Microorganisms* 4:23
- Rohwer F, Seguritan V, Azam F, Knowlton N (2002) Diversity and distribution of coral-associated bacteria. *Marine Ecology Progress Series* 243:1-10
- Rohwer F, Breitbart M, Jara J, Azam F, Knowlton N (2001) Diversity of bacteria associated with the Caribbean coral *Montastraea franksi*. *Coral Reefs* 20:85-91
- Ronquist F, Huelsenbeck JP (2003) MrBayes 3: Bayesian phylogenetic inference under mixed models. *Bioinformatics* 19:1572-1574
- Rosado PM, Leite DC, Duarte GA, Chaloub RM, Jospin G, da Rocha UN, Saraiva JP, Dini-Andreote F, Eisen JA, Bourne DG (2019) Marine probiotics: increasing coral resistance to bleaching through microbiome manipulation. *The ISME Journal* 13:921-936
- Rosenberg E (2014) The Family Rubritaleaceae. *The Prokaryotes*. Springer,
- Rosenberg E, Ben-Haim Y (2002) Microbial diseases of corals and global warming. *Environmental Microbiology* 4:318-326
- Rosenberg E, Koren O, Reshef L, Efrony R, Zilber-Rosenberg I (2007) The role of microorganisms in coral health, disease and evolution. *Nature Reviews Microbiology* 5:355-362
- Ross C, Ritson-Williams R, Olsen K, Paul V (2013) Short-term and latent post-settlement effects associated with elevated temperature and oxidative stress on larvae from the coral *Porites astreoides*. *Coral Reefs* 32:71-79
- Röthig T, Roik A, Yum LK, Voolstra CR (2017) Distinct bacterial microbiomes associate with the deep-sea coral *Eguchipsammia fistula* from the Red Sea and from aquaria settings. *Frontiers in Marine Science* 4:259

- Ruby E, Henderson B, McFall-Ngai M (2004) We get by with a little help from our (little) friends. *Science* 303:1305-1307
- Salter SJ, Cox MJ, Turek EM, Calus ST, Cookson WO, Moffatt MF, Turner P, Parkhill J, Loman NJ, Walker AW (2014) Reagent and laboratory contamination can critically impact sequence-based microbiome analyses. *BMC Biology* 12:87
- Sato Y, Willis BL, Bourne DG (2013) Pyrosequencing-based profiling of archaeal and bacterial 16S rRNA genes identifies a novel archaeon associated with black band disease in corals. *Environmental Microbiology* 15:2994-3007
- Sayers EW, Agarwala R, Bolton EE, Brister JR, Canese K, Clark K, Connor R, Fiorini N, Funk K, Hefferon T (2019) Database resources of the national center for biotechnology information. *Nucleic Acids Research* 47:D23
- Schröder K, Bosch TC (2016) The origin of mucosal immunity: lessons from the holobiont Hydra. *MBio* 7
- Sekar R, Mills DK, Remily ER, Voss JD, Richardson LL (2006) Microbial communities in the surface mucopolysaccharide layer and the black band microbial mat of black band-diseased *Siderastrea siderea*. *Applied and Environmental Microbiology* 72:5963-5973
- Serrano XM, Miller MW, Hendee JC, Jensen BA, Gapayao JZ, Pasparakis C, Grosell M, Baker AC (2018) Effects of thermal stress and nitrate enrichment on the larval performance of two Caribbean reef corals. *Coral Reefs* 37:173-182
- Setyaningsih I, Nurhayati T, Nugraha R, Gunawan I (2012) Comparative evaluation of the antibacterial activity of soft corals collected from the water of Panggang Island, Kepulauan Seribu. *Pharmacie Globale* 3:1
- Sharp KH, Distel D, Paul VJ (2012) Diversity and dynamics of bacterial communities in early life stages of the Caribbean coral *Porites astreoides*. *The ISME Journal* 6:790-801
- Sharp KH, Ritchie KB, Schupp PJ, Ritson-Williams R, Paul VJ (2010) Bacterial acquisition in juveniles of several broadcast spawning coral species. *PLOS One* 5:e10898
- Sharp KH, Sneed J, Ritchie K, Mcdaniel L, Paul VJ (2015) Induction of larval settlement in the reef coral *Porites astreoides* by a cultivated marine Roseobacter strain. *The Biological Bulletin* 228:98-107
- Shashar N, Cohen Y, Loya Y, Sar N (1994) Nitrogen fixation (acetylene reduction) in stony corals: evidence for coral-bacteria interactions. *Marine Ecology Progress Series*:259-264
- Sheu S-Y, Lin K-R, Hsu M-y, Sheu D-S, Tang S-L, Chen W-M (2017) *Endozoicomonas acroporae* sp. nov., isolated from *Acropora* coral. *International Journal of Systematic and Evolutionary Microbiology* 67:3791-3797

- Shi X-L, Wu Y-H, Jin X-B, Wang C-S, Xu X-W (2017) *Alteromonas lipolytica* sp. nov., a poly-beta-hydroxybutyrate-producing bacterium isolated from surface seawater. *International Journal of Systematic and Evolutionary Microbiology* 67:237-242
- Shnit-Orland M, Kushmaro A (2009) Coral mucus-associated bacteria: a possible first line of defense. *FEMS Microbiology Ecology* 67:371-380
- Siboni N, Ben-Dov E, Sivan A, Kushmaro A (2008) Global distribution and diversity of coral-associated Archaea and their possible role in the coral holobiont nitrogen cycle. *Environmental Microbiology* 10:2979-2990
- Sieber M, Pita L, Weiland-Bräuer N, Dirksen P, Wang J, Mortzfeld B, Franzenburg S, Schmitz RA, Baines JF, Fraune S (2018) The neutral metaorganism. [bioRxiv:367243](https://doi.org/10.1101/367243)
- Silveira CB, Gregoracci GB, Coutinho FH, Silva GG, Haggerty JM, de Oliveira LS, Cabral AS, Rezende CE, Thompson CC, Francini-Filho RB (2017) Bacterial community associated with the reef coral *Mussismilia braziliensis*'s momentum boundary layer over a diel cycle. *Frontiers in Microbiology* 8:784
- Simpson A (2009) Reproduction in octocorals (Subclass Octocorallia): a review of published literature. *Deep-Sea Corals Portal*
- Sneed JM, Sharp KH, Ritchie KB, Paul VJ (2014) The chemical cue tetrabromopyrrole from a biofilm bacterium induces settlement of multiple Caribbean corals. *Proceedings of the Royal Society of London, Series B: Biological sciences* 281:20133086
- Sobhana K, George RM, Jasmine S, Vinod K, Kingsly HJ, Surendran K, Manisseri MK (2019) Disease prevalence and bacterial diversity in stony corals. *Stony Corals, Sponges and Reef Fishes Off Enayam to Kollam*
- Sunagawa S, DeSantis TZ, Piceno YM, Brodie EL, DeSalvo MK, Voolstra CR, Weil E, Andersen GL, Medina M (2009) Bacterial diversity and White Plague Disease-associated community changes in the Caribbean coral *Montastraea faveolata*. *The ISME Journal* 3:512-521
- Supuran CT, Scozzafava A, Clare BW (2002) Bacterial protease inhibitors. *Medicinal Research Reviews* 22:329-372
- Sweet M, Croquer A, Bythell J (2011) Bacterial assemblages differ between compartments within the coral holobiont. *Coral Reefs* 30:39-52
- Sweet MJ, Croquer A, Bythell JC (2011 b) Development of bacterial biofilms on artificial corals in comparison to surface-associated microbes of hard corals. *PLOS One* 6:e21195
- Tait K, Hutchison Z, Thompson FL, Munn CB (2010) Quorum sensing signal production and inhibition by coral-associated vibrios. *Environmental Microbiology Reports* 2:145-150

- Tamburini S, Shen N, Wu HC, Clemente JC (2016) The microbiome in early life: implications for health outcomes. *Nature Medicine* 22:713-722
- Tanaka M, Nakayama J (2017) Development of the gut microbiota in infancy and its impact on health in later life. *Allergology International* 66:515-522
- Tandon K, Lu C-Y, Chiang P-W, Wada N, Yang S-H, Chan Y-F, Chen P-Y, Chang H-Y, Chiou Y-J, Chou M-S (2020) Comparative genomics: Dominant coral-bacterium *Endozoicomonas acroporae* metabolizes dimethylsulfoniopropionate (DMSP). *The ISME Journal* 14:1290-1303
- Team RC (2013) R: A language and environment for statistical computing. Vienna, Austria
- Team R (2015) RStudio: integrated development for R. RStudio. Inc, Boston, MA 700
- Tebben J, Tapiolas DM, Motti CA, Abrego D, Negri AP, Blackall LL, Steinberg PD, Harder T (2011) Induction of larval metamorphosis of the coral *Acropora millepora* by tetrabromopyrrole isolated from a *Pseudoalteromonas* bacterium. *PLOS One* 6:e19082
- Thompson JR, Rivera HE, Closek CJ, Medina M (2015) Microbes in the coral holobiont: partners through evolution, development, and ecological interactions. *Frontiers in Cellular and Infection Microbiology* 4:176
- Tremblay P, Grover R, Maguer JF, Legendre L, Ferrier-Pagès C (2012) Autotrophic carbon budget in coral tissue: a new ¹³C-based model of photosynthate translocation. *Journal of Experimental Biology* 215:1384-1393
- Tremblay P, Weinbauer MG, Rottier C, Guérardel Y, Nozais C, Ferrier-Pagès C (2011) Mucus composition and bacterial communities associated with the tissue and skeleton of three scleractinian corals maintained under culture conditions. *Journal of the Marine Biological Association of the United Kingdom* 91:649-657
- Turnbaugh PJ, Ley RE, Hamady M, Fraser-Liggett CM, Knight R, Gordon JI (2007) The human microbiome project. *Nature* 449:804-810
- Twan W-H, Hwang J-S, Lee Y-H, Wu H-F, Tung Y-H, Chang C-F (2006) Hormones and reproduction in scleractinian corals. *Comparative Biochemistry and Physiology Part A: Molecular & Integrative Physiology* 144:247-253
- Valentine JW (2004) *On the origin of phyla*. University of Chicago Press
- Van De Water JA, Melkonian R, Junca H, Voolstra CR, Reynaud S, Allemand D, Ferrier-Pagès C (2016) Spirochaetes dominate the microbial community associated with the red coral *Corallium rubrum* on a broad geographic scale. *Scientific Reports* 6:1-7
- van de Water JA, Melkonian R, Voolstra CR, Junca H, Beraud E, Allemand D, Ferrier-Pagès C (2017) Comparative assessment of Mediterranean gorgonian-associated microbial communities reveals conserved core and locally variant bacteria. *Microbial Ecology* 73:466-478

- van de Water JA, Voolstra CR, Rottier C, Cocito S, Peirano A, Allemand D, Ferrier-Pagès C (2018) Seasonal stability in the microbiomes of temperate gorgonians and the red coral *Corallium rubrum* across the Mediterranean Sea. *Microbial Ecology* 75:274-288
- van Oppen MJ, Blackall LL (2019) Coral microbiome dynamics, functions and design in a changing world. *Nature Reviews Microbiology* 17:557-567
- Van Oppen MJ, Oliver JK, Putnam HM, Gates RD (2015) Building coral reef resilience through assisted evolution. *Proceedings of the National Academy of Sciences* 112:2307-2313
- Vezzulli L, Pezzati E, Huete-Stauffer C, Pruzzo C, Cerrano C (2013) 16SrDNA pyrosequencing of the Mediterranean gorgonian *Paramuricea clavata* reveals a link among alterations in bacterial holobiont members, anthropogenic influence and disease outbreaks. *PLOS One* 8:e67745
- Vidal-Dupiol J, Ladrière O, Destoumieux-Garzón D, Sautière P-E, Meistertzheim A-L, Tambutté E, Tambutté S, Duval D, Fouré L, Adjeroud M (2011) Innate immune responses of a scleractinian coral to vibriosis. *Journal of Biological Chemistry* 286:22688-22698
- Voolstra CR, Ziegler M (2020) Adapting with Microbial Help: Microbiome flexibility facilitates rapid responses to environmental change. *Bioessays* 42:2000004
- Wada N, Pollock FJ, Willis BL, Ainsworth T, Mano N, Bourne DG (2016) In situ visualization of bacterial populations in coral tissues: pitfalls and solutions. *PeerJ* 4:e2424
- Wang Y, Wang H, Liu J, Lai Q, Shao Z, Austin B, Zhang X-H (2010) *Aestuariusbacter aggregatus* sp. nov., a moderately halophilic bacterium isolated from seawater of the Yellow Sea. *FEMS Microbiology Letters* 309:48-54
- Webster NS, Smith LD, Heyward AJ, Watts JE, Webb RI, Blackall LL, Negri AP (2004) Metamorphosis of a scleractinian coral in response to microbial biofilms. *Applied and Environmental Microbiology* 70:1213-1221
- Weiler BA, Verhoeven JT, Dufour SC (2018) Bacterial communities in tissues and surficial mucus of the cold-water coral *Paragorgia arborea*. *Frontiers in Marine Science* 5:378
- Wessels W (2016) Molecular bases of soft coral reproduction. James Cook University,
- Wessels W, Sprungala S, Watson S-A, Miller DJ, Bourne DG (2017) The microbiome of the octocoral *Lobophytum pauciflorum*: minor differences between sexes and resilience to short-term stress. *FEMS Microbiology Ecology* 93
- Wiese J, Imhoff JF, Horn H, Borchert E, Kyrpidis NC, Göker M, Klenk H-P, Woyke T, Hentschel U (2019) Genome analysis of the marine bacterium *Kiloniella laminariae* and first insights into comparative genomics with related *Kiloniella* species. *Archives of Microbiology*:1-10
- Wild C, Huettel M, Klueter A, Kremb SG, Rasheed MY, Jørgensen BB (2004) Coral mucus functions as an energy carrier and particle trap in the reef ecosystem. *Nature* 428:66-70

- Williams AD, Brown BE, Putschim L, Sweet MJ (2015) Age-related shifts in bacterial diversity in a reef coral. *PLOS One* 10:e0144902
- Woyke T, Teeling H, Ivanova NN, Huntemann M, Richter M, Gloeckner FO, Boffelli D, Anderson IJ, Barry KW, Shapiro HJ (2006) Symbiosis insights through metagenomic analysis of a microbial consortium. *Nature* 443:950-955
- Xing X, Liu JS, Zhong W (2017) MetaGen: reference-free learning with multiple metagenomic samples. *Genome Biology* 18:1-15
- Yan P, Deng Z, Van Ofwegen L, Proksch P, Lin W (2010) Lobophytone H—N, Biscembranoids from the Chinese Soft Coral *Lobophytum pauciflorum*. *Chemical and Pharmaceutical Bulletin* 58:1591-1595
- Yan P, Deng Z, Ofwegen Lv, Proksch P, Lin W (2010) Lobophytone O—T, new biscembranoids and cembranoid from soft coral *Lobophytum pauciflorum*. *Marine Drugs* 8:2837-2848
- Yang C-S, Chen M-H, Arun A, Chen CA, Wang J-T, Chen W-M (2010) *Endozoicomonas montiporae* sp. nov., isolated from the encrusting pore coral *Montipora aequituberculata*. *International Journal of Systematic and Evolutionary Microbiology* 60:1158-1162
- Zanotti AA, Gregoracci GB, Capel KCC, Kitahara MV (2020) Microbiome of the Southwestern Atlantic invasive scleractinian coral, *Tubastraea tagusensis*. *Animal microbiome* 2:1-8
- Zehr JP (2011) Nitrogen fixation by marine cyanobacteria. *Trends in Microbiology* 19:162-173
- Zhang Y-Y, Ling J, Yang Q-S, Wang Y-S, Sun C-C, Sun H-Y, Feng J-B, Jiang Y-F, Zhang Y-Z, Wu M-L (2015) The diversity of coral associated bacteria and the environmental factors affect their community variation. *Ecotoxicology* 24:1467-1477
- Zhao M, Yin J, Jiang W, Ma M, Lei X, Xiang Z, Dong J, Huang K, Yan P (2013) Cytotoxic and antibacterial cembranoids from a South China Sea soft coral, *Lobophytum* sp. *Marine Drugs* 11:1162-1172
- Ziegler M, Seneca FO, Yum LK, Palumbi SR, Voolstra CR (2017) Bacterial community dynamics are linked to patterns of coral heat tolerance. *Nature Communications* 8:1-8
- Ziegler M, Roik A, Porter A, Zubier K, Mudarris MS, Ormond R, Voolstra CR (2016) Coral microbial community dynamics in response to anthropogenic impacts near a major city in the central Red Sea. *Marine Pollution Bulletin* 105:629-640
- Ziegler M, Grupstra CG, Barreto MM, Eaton M, BaOmar J, Zubier K, Al-Sofyani A, Turki AJ, Ormond R, Voolstra CR (2019) Coral bacterial community structure responds to environmental change in a host-specific manner. *Nature Communications* 10:1-11
- Zilber-Rosenberg I, Rosenberg E (2008) Role of microorganisms in the evolution of animals and plants: the hologenome theory of evolution. *FEMS Microbiology Reviews* 32:723-735

Zimmer BL, May AL, Bhedi CD, Dearth SP, Prevatte CW, Pratte Z, Campagna SR, Richardson LL (2014)
Quorum sensing signal production and microbial interactions in a polymicrobial disease of
corals and the coral surface mucopolysaccharide layer. PLOS One 9:e108541